MECHANISMS OF LIGNOCELLULOSIC CONVERSION BY THE BROWN ROT FUNGUS *Serpula lacrymans*

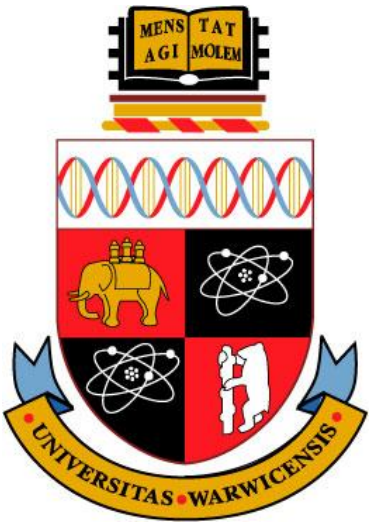

By

IRNIA NURIKA

A thesis submitted to
The University of Warwick
For the degree of

DOCTOR OF PHILOSOPHY

University of Warwick, School of Life Sciences
United Kingdom

2013

Abstract

Cost effective processing of wheat straw using solid state fermentation (SSF) would provide a source for value added chemicals from agricultural waste biomass. Fungi natural breakdown lignocellulosic biomass hence could have received a lot of attention. In this study the ability of *S. lacrymans* to convert straw waste was compared with other Basidiomycetes (*Postia placenta*, *Phanerochaete chrysosporiom*, and *Schizophyllum commune). S. lacrymans* out performed the other Basidiomycetes both in its growth (as measured by ergosterol and fatty acid production (linoleic acid);18:2n6c) , and in the comounds released which included; total soluble phenols, total reducing sugars, and low molecular organic chemicals (MW<400).

Non-enzymatic breakdown requiring the presence of Fe^{2+} was also demonstrtated and influenced by the production of quinone and low molecular organic acid. The amount of the fungal extract used and the concentration of chelator/reducing agents also affected the production of Fe^{2+}. Changes in the lignocellulose structure was also detected as key functional group, such as the pyranose ring and aromatic skeletal vibration were significantly reduced following culture with *S. lacrymans* and a significant reduction in mass was measured.

Iron reductase genes IR1 and IR2 suspected to be involved in the lignocellulose degradation were cloned. It seems that these genes are more closely related to the cellulose binding module (CBM) family instead of cellobiose dehydrogenase (CDH) genes as first suspected. IR1 has an open reading frame of 774 bp which encoding 258 amino acid (55 kDa), whilst IR2 642 bp encoding 214 amino acid (49 kDa). The IR1 gene contains a CBM1 domain which is lacking in IR2. Gene expression analysis using qRT-PCR showed that in the early stage of fungal growth, the level of IR2 genes expression was higher than IR1 while IR1 became more dominant in the latter stages of culture. The time at which these genes are highly expressed correlated with the release of soluble and aromatic phenolic compounds.

The functionality of the recombinant IR1 and IR2 on the decomposition of lignocellulose was shown using several assays including; iron reductases, nitrated lignin and the reduction of electron acceptor (DCPIP). In addition, using both synthetic and nature sources of cellulose or lignocellulose (Avicel and wheat straw powder) the recombinant IR proteins were shown to break down cellulose. This suggested that these enzymes represent a significant addition to those currently used within biomass based biorefineries

Acknowledgments

I would firstly like to thank my supervisors, Dr. Guy C Barker and Prof. Tim DH. Bugg for their continued encouragement and guidance over the years and the University of Warwick for funding the project. I would also like to thanks to Dan Eastwood for his willing advice comment to improve the thesis, and Kerry Burton for giving me the chance to do a PhD and for his help at the beginning of my P.hD.

I would also like to thank Andy Jukes and Matt Matthew for setting up on LC-MS and HPLC machines and Jeanette Selby for helping on the genomic analysis. Also I would like to thanks to Volkan Cevik who taught me about the Gateway system for the cloning genes. I am grateful to all people in Lab 108, Wellesbourne campus, Tim Buggs group in Chemistry Departement and people in Lab C.46, School of Life Sciences-Gibbet Hill campus for all the discussions.

I would also like to thank to all my colleagues and friends at School of Life Sciences, University of Warwick-United Kingdom, my family especially my husband Cahyo Prayogo and my parent who always giving me support during my PhD life. Finally I would like to thank to Directorate General of Higher Education (DIKTI) - Ministry of National Education, Indonesia for providing a studentship.

Declaration

The work presented in this thesis is original, and has not been published or presented for any other degree**.**

Contents

Chapter 3 : Selecting potential fungal lignocellulosic degrader in solid-state fermentation.

Chapter 4: Evidence for the mechanism involved in the degradation of wheat straw by *Serpula lacrymans*

Chapter 5: The identification and expression of iron reductases genes in *Serpula lacrymans*.

Chapter 6: The expression and functional characterisation of recombinant protein from iron reductase encoding genes of brown rot fungus *Serpula lacrymans*

List of Figures

List of Table

List of Abbreviation

AAO	:	aryl alcohol oxidase
AOX	:	alternative oxidase
6-APA	:	aminopenicillanic acid
BLAST	:	basic local alignment search tool
C	:	carbon
CAZy	:	carbohydrate-active enzymes
CBD	:	cellulose binding domain
CBH	:	cellobiohydrolase
CBM	:	cellulose binding module
CDH	:	cellobiose dehydrogenase
cDNA	:	complementary deoxyribonucleid acid
CMC	:	carboxymethyl cellulose agar
CP	:	crossing point
CVA	:	canonical variate analysis
DCPIP	:	dichlorophenolindophenol
DEPC	:	diethylpyrocarbonate
2,3-DHBA	:	2,3-dihydroxybenzoic acid
2,5/4.5-DMBQ	:	2,5/4,5-dimethoxybenzoquinone
4,5 -DMC	:	4,5-dimethoxycatecol
2,5/4.5-DMHQ	:	2,5/4,5-dimetoxyhydroquinone
DNA	:	deoxyribonucleid acid
DNS	:	dinitrosalicylic acid
DMSO	:	dymetyl sulfoxide
EDTA	:	ethylenediaminetetraacetic acid
FAD	:	flavin adenine dinucleotida
FAME	:	fatty acid methyl ester
$FeCl_3$	:	iron chloride
FT-IR spectroscopy	:	fourier transform infra red spectrocopy
GC-MS	:	gas chromatography mass spectrometry
GFA	:	glass fibre
GH	:	glycosyl hydrolase
GLyOX	:	glyoxal oxidase

GOI	:	gene of interest
GST	:	glutathione S tranferase
Gt chelator	:	*Gloeophyllum trabeum* chelator
HCL	:	hydrochloric acid
HQ·	:	hydroquinone radical
H_2O_2	:	hydrogen peroxide
H_2SO_4	:	sulphuric acid
HGS	:	p-hydrixyphenyl-guaiacyl-sryngyl
HMF	:	hydroxymethylfurfural
HPLC	:	high performance liquid chromatography
IGS	:	region intergenic spacer
IPTG	:	isopropyl-β-D-thiogalactopiranocide
IR	:	infrared spectroscopy
IR	:	iron reductase
ITS	:	internal transcribed spacer
KAN	:	kanamycin
MEA	:	malt extract agar
LC-MS	:	liquid chromatography mass spectropmetry
LiP	:	lignin peroxidase
LMW	:	low molecular weight
LSU	:	large sub unit
MnP	:	manganese peroxidase
mRNA	:	messenger ribonucleid acid
MW	:	molecular weight
N	:	nitrogen
NMR	:	nuclear magnetic resonance
OD	:	optical density
·OH	:	hydroxyl radicals
·OOH	:	perhydroxy radical
PBST	:	Phosphate buffer saline tween20
PCR	:	polymerase chain reaction
PDA	:	potato dextrose agar
PEG	:	polyethylene glycol
PLFA	:	phospolipid fatty acid
PMSF	:	phenyl methyl sulfonyl flouride

PS	:	polystrene
QRT-PCR	:	quantitative real time polymerase chain reaction
RAPD	:	random amplification of polymorphic DNA
RNA	:	ribonucleid acid
RT-PCR		real time polymerase chain reaction
SDS-PAGE	:	sulphate dodecyl sulphate-polyacrylamide gel electrophoresis
SSF	:	solid state fermentation
SU	:	sub unit
TAG	:	triacylglycerol
TCA	:	trycarboxylic acid
TCEP	:	tris 2 carboxymethil phospine
UV-VIS spectroscopy	:	ultra violet visible spectroscopy

Chapter 1. General Introduction

1.1 Agricultural Waste Biomass

1.1.1 Total production and the distribution

The world is currently reliant on the use of fossil fuels (e.g oil, coal and natural gas) to produce both its energy and the chemicals we need however these resources are non-renewable (Uihlein and Schebek, 2009). The use of fossil fuels is also thought to be the cause for increasing levels of greenhouse gasses in the atmosphere (Ballesteroos et al., 2006 ; Talebnia et al., 2010). Although alternative energy sources are avaliable (e.g wind, water, sun, geothermal, heat), biomass can provide a source of transport fuels, such as ethanol and bio-diesel, and also offers an opportunity to deliver basic chemical feedstocks (e.g starch, oil, cellulose, lactic acid, amino acid etc) (Uihlein and Schebek, 2009). Biomass has been estimated to contribute 9-13% of the global energy needs (Kim and Dale, 2004) mostly through the use of fire wood for cooking.

The continuing development of the agroindustrial sector has resulted in an increase in the production of waste biomass such as sugar cane baggase, maize straw, rice straw, etc, along with residue from wood (e.g poplar); herbaceous (e.g. switchgrass); forestry (sawdust, wood thinning, mill waste) and municipal solid waste (e.g waste paper) (Table 1). Agricultural wastes are recognized as potential sources of energy as well as for biorefining (Kaparaju et al., 2009). It is predicted that current plant waste production is approximately 1.5 trillion tons per year and includes several types of raw material including wheat straw, rice straw, palm, corncobs, corn stems and husk. The amount of agricultural waste available differs

depending on the crop type, however all could potentially be converted for chemical feedstock production or for the manufacture of biofuel (Kumar et al., 2008).

Table 1. Global annual production of agricultural plant waste (Sanchez, 2009)

Lignocellulosic residue	**Ton x 10^6 $year^{-1}$**
Sugar cane baggase	317 – 380
Maize straw	159 – 191
Rice shell	157 – 188
Wheat straw	**154 – 185**
Soja straw	54 – 65
Yuca straw	40 – 48
Barley straw	35 – 42
Cotton fibre	17 – 20
Sorghum straw	15 – 18
Banana waste	13 – 15
Mani shell	9.2 – 11.1
Sunflower straw	7.5 – 9.0
Bean straw	4.9 – 5.9
Rye straw	4.3 – 5.2
Pine waste	3.8 – 4.6
Coffe straw	1.6 – 1.9
Almond straw	0.4 – 0.49
Hazelnut husk	0.2 – 0.24
Sisal a henequen straw	0.07 – 0.09

Bio-energy crops, wood and plant waste are recognized as the three main sources of sustainable biomass (Talebnia et al., 2010 ; Lin and Tanakan, 2006). Table 1 shows that the largest source of agricultural plant wastes is sugar cane baggase at 317- 380 ton x 10^6 $year^{-1}$, followed by maize straw (159 – 191 ton x 10^6 $year^{-1}$), rice shell (157 – 188 ton x 10^6 $year^{-1}$) and wheat straw (154 – 185 ton x 10^6 $year^{-1}$) (Sanchez, 2009). Among these resources wheat straw biomass is ranked in the first placed in Europe (Talebnia et al., 2010 ; Kim and Dale, 2004). Wheat straw is known as a potential feedstock for producing ethanol (Talebnia et al., 2010) and also as raw material for paper and pulp industry (Sun and Tomkinson, 2002). In 2000, wheat

straw production in Europe reached 184 million tons. The global wheat straw biomass was 354.35Tg, which was lower than rice straw (731.34Tg), but higher than corn stover (203.62Tg) and baggase (180.73Tg) (Table 2).

Furthermore, wheat straw was mainly produced in Asia (145.20Tg) followed by Europe (132.59 Tg) and North America (50.05Tg). Average yield production of wheat varies between 1.7 and 4.1 dry Mg ha^{-1}. In China, yields were reported to be 3.4 dry Mg ha^{-1}, which contributed 18% of global wheat production. In comparison, India produces 2.4 dry Mg ha^{-1} of wheat which represents 12% of total wheat production. In general about 4% global wheat production is recognised as a waste (Kim and Dale, 2004). In 2008, world wide wheat production reached over 650Tg and approximately 850Tg of wheat residue were produced (Talebnia et al., 2010 ; Atwell, 2001).

Generally, the yield of cereal straw in the UK varies from 2.75 to 4 tons ha^{1}, depending on the type of crops. Currently cereal straw comes from several crops in the UK, these are wheat (54%), oilseed rape (21%), barley (20%), oats (4%), other cereals (1%) and linseed (0.1%) (Figure 1) (Copeland and Turley, 2008).

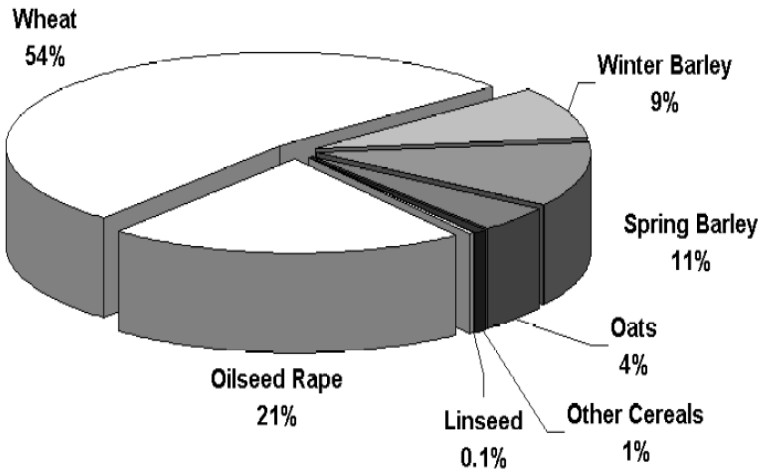

Figure 1. Distribution of cereal straw by crop types in the United Kingdom (Copeland and Turley, 2008)

Regional production of cereal straw is shown in Table 2. 93.5 % of total wheat straw in the UK is produced in England compared to Scotland (5.6%) and Wales (0.7%). The majority is grown in the Eastern part of the UK. The total UK straw production was 11.88 millions tonnes in 2007.

Table 2. Distribution of UK cereal straw production by region (Copeland and Turley, 2008)

Region	Wheat	Winter Barley	Spring Barley	Oats	Other Cereals	Linseed	Oilseed Rape
North East Region	229,865	69,379	29,616	24,812	1,952	*	111,636
North West Region	104,999	39,651	57,641	20,526	7,628	*	17,006
Yorkshire and Humber Region	794,980	184,893	96,815	27,034	7,313	*	320,205
East Midlands Region	1,201,806	116,899	72,157	49,843	9,544	2,457	582,097
West Midlands Region	536,523	81,431	49,792	76,566	7,821	*	179,585
Eastern Region	1,645,860	208,703	149,353	40,364	17,198	2,086	544,949
South East Region	802,254	65,408	104,431	84,928	9,982	2,422	386,005
South West Region	602,158	110,416	149,948	85,772	29,389	2,365	219,144
	5,918,444	**876,780**	**709,753**	**409,844**	**90,828**	**10,720**	**2,360,627**
North West Scotland	13,495	4,270	64,424	11,070	600	*	7,433
North East Scotland	56,474	62,538	241,156	19,354	1,385	*	57,734
South East Scotland	270,004	61,775	243,384	42,951	2,379	*	84,022
South West Scotland	19,630	16,135	72,588	10,097	2,204	*	3,414
	359,603	**144,719**	**621,553**	**83,472**	**6,567**	**356**	**152,602**
Carmarthenshire	392	464	2,276	857	1,167	0	*
Ceredigion	1,189	520	3,464	1,164	778	0	*
North East Wales	7,099	3,953	4,303	1,923	1,388	0	*
North West Wales	794	476	4,420	1,634	441	0	*
Pembrokeshire	7,798	4,915	12,747	2,311	2,648	0	2,592
Powys	10,052	3,075	3,527	3,984	870	0	*
South Wales	18,137	5,159	4,367	4,200	4,088	0	6,049
	45,462	**18,563**	**35,104**	**16,072**	**11,380**	**0**	**11,811**
Total	6,323,508	1,040,061	1,366,409	509,388	108,775	11,076	2,525,040
			Total Cereals			Total Oilseeds	
			9,348,142			2,536,117	
Total GB Straw	11,884,259						

Up to 1993, 50% of wheat straw was burnt in the field until this practice was banned (Horne et al., 1996). Nowadays much of the wheat straw is applied back to the soil with animal manure as a compost application. Straw is also used for animal bedding, feed, mushroom production and the protection of crops. After accounting for such uses the net surplus cereal straw including wheat straw in the UK was 4.9 million tons in 2007. Therefore, surplus straw is potentially a source of abundant biomass and offers a great opportunity for use in renewable energy production. It can also be viewed as a cheap material for use in a biorefinery (Copeland and Turley, 2008).

These studies have shown that wheat straw is the major source of renewable biomass for the UK and for this reason has been chosen as feedstock for this current study.

1.1.2 Characteristics, chemical composition and structure of plant waste biomass

Wheat straw is under normal conditions abundant, cheap and has a complex structure, being composed of cellulose, hemicellulose and lignin (Talebnia et al., 2010). The cellulose, hemicellulose and lignin content of wheat straw ranges between 29-35%, 26-32% and 16-21%, respectively. This is similar to other plant waste such as barley straw, oat straw and rye straw, but very distinct from corn cobs, hardwood, softwood, nut shells and bamboo (Table 3).

Table 3. Composition of wheat straw compared to other lignocellulosic plant waste biomass (Sanchez, 2009).

Lignocelulosic residue	**Lignin (%)**	**Hemicellulose (%)**	**Cellulose (%)**	**Ash (%)**
Hardwood stems	18-25	24-40	40-55	NA
Softwood stems	25-35	25-35	45-50	NA
Nut shells	30-40	25-30	25-30	NA
Corn cobs	15	35	45	1.36
Paper	0-15	0	85-99	1.1-3.9
Rice straw	18	24	32.1	NA
Sorted refuse	20	20	60	NA
Leaves	0	80-85	15-20	NA
Cotton seed hair	0	5-20	80-95	NA
Newspaper	18-30	25-40	40-55	8.8-1.8
Waste paper from chemical pulps	5-10	10-20	60-70	NA
Primary waste water solid	24-29	NA	8-15	NA
Swine waste	NA	28	6	NA
Solid cattle manure	2.7-5.7	1.4-3.3	1.6-4.7	NA
Coastal bermuda grass	6.4	35.7	25	NA
Switchgrass	12.0	31.4	45	NA
S32 rye grass (early leaf)	2.7	15.8	21.3	NA
S32 rye grass (seed setting)	7.3	25.7	26.7	NA
Orchard grass (medium maturity)	4.7	40	32	NA
Grasses (average value for grasses)	10-30	25-50	25-40	1.5
Sugar cane baggasse	19-24	27-32	32-44	4.5-9
Wheat straw	**16-21**	**26-32**	**29-35**	**NA**
Barley straw	14-15	24-29	31-44	5-7
Oat straw	16-19	27-38	31-37	6-8
Rye straw	16-19	27-30	33-35	2-5
Bamboo	21-31	15-26	26-43	1.7-5
Grass Esparto	17-19	27-32	33-38	6-8
Grass Sabai	22.0	23.9	NA	6.0
Grass Elephant	23.9	24	22	6
Bast fiber Seed flax	23	25	47	5
Bast fiber Kenaf	15-19	22-23	31-39	2-5
Bast fiber Jute	21-26	18-21	45-53	0.5-2
Bast fiber Abaca	8.8	17.3	60.8	1.1
Bast fiber Sisal (Agave)	7-9	21-24	43-56	0.6-1.1
Bast fiber Henequen	13.1	4-8	77.6	0.6-1
Coffee pulps	18.8	46.3	35	8.2
Banana waste	14	14.8	13.2	11.4
Yuca waste	NA	NA	NA	4.2

Like many other lignocellulosic residues, wheat straw cellulose and hemicellulose is comprised from different sugars unlike lignin which is an aromatic polymer synthesized from phenylpropanoid (Sanchez, 2009). An illustration of the arrangements of lignocellulosic material in wood is shown in Figure 2.

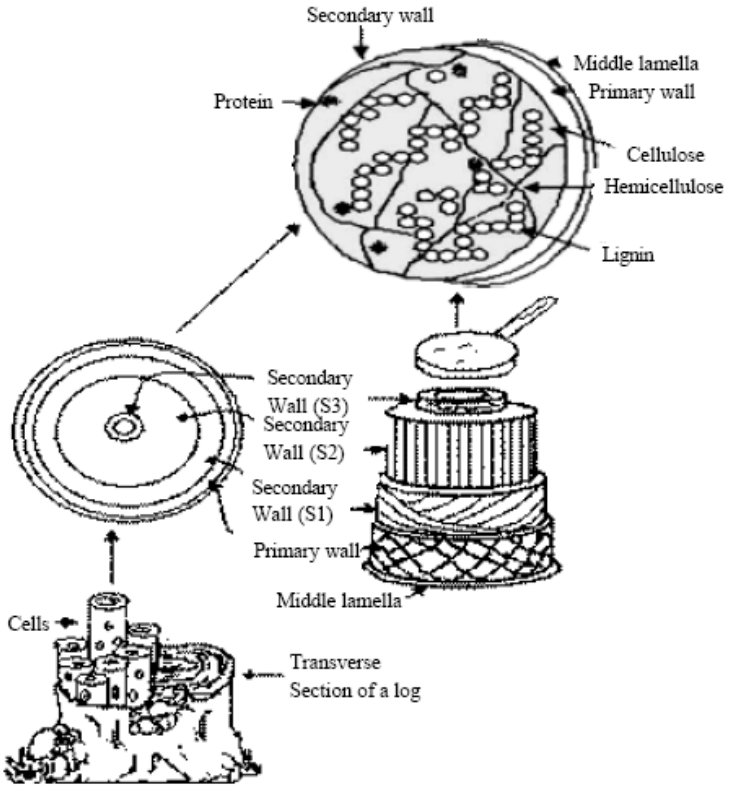

Figure 2. Structure of wood showing its lignocellulosic composition (Sanchez, 2009)

Cellulose is a linear polymer of D-glucose subunits connected via a β-1.4 glycosidic bond creates the polymer of cellobiose (Figure 3). The chains of cellobiose are joined together to form cellulose by the hydrogen bonds and van der Waals forces (Sanchez, 2009).

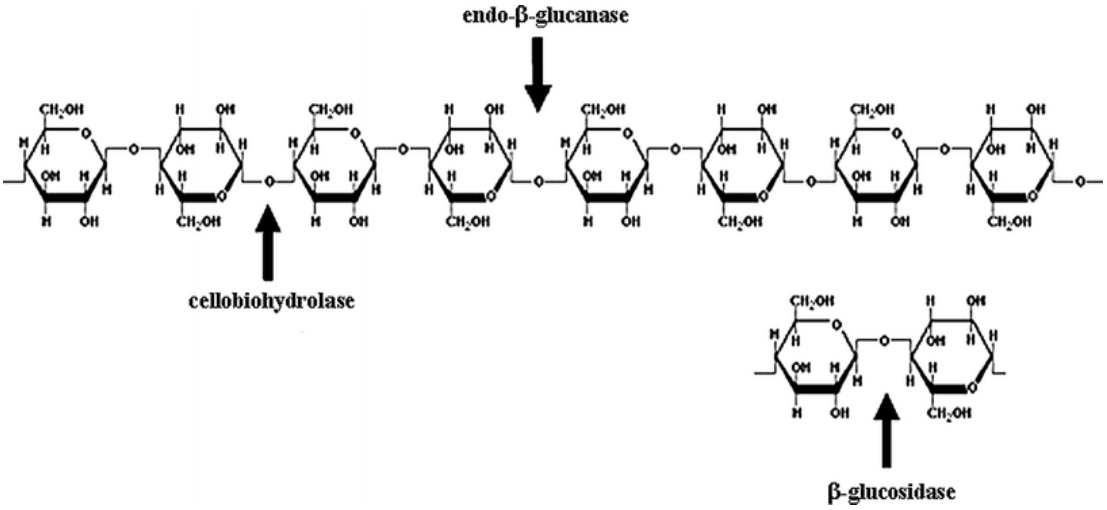

Figure 3. **S**tructure of cellulose and the sites of cellulases during cellulose breakdown (Kumar et al., 2008)

Cellulolysis is the process of deformation of cellulose into smaller polysaccharides called cellodextrins or into glucose units, via a hydrolysis reaction. Cellulolysis is relatively difficult to perform compared to the breakdown of other polysaccharides (David and Roy, 2008). Its microcrystalline structure, comprised of crystalline and amorphous regions (Yang et al. 2011) is very difficult to hydrolyze under natural conditions without involving any pressure and chemical reaction during degradation (Malherbe and Cloete, 2002). The rates of hydrolysis of cellulose is effected by this mycrocrystalline structure (Arantes and Saddler, 2010).

Like cellulose, hemicellulose is also an important source of fermentable sugars for biorefining applications. Hemicellulose, as the second most largest component of lignocellulosic biomass, representing 25–35%, are heterogeneous polymers constructed by pentoses (D-xylose, D-arabinose), hexoses (D-mannose, D-glucose, D-galactose) and

sugar acids (Kumar et al., 2008). The hemicellulose component is connected to both lignin and cellulose fibers which can easily be broken down with acid, base and/or enzymes (Loreano-Perez et al., 2005 ; Talebnia et al., 2010). Compared to cellulose, hemicellulose consists of smaller sugar molecules, predominantly D-xylose, D-mannose, D-galactose, D-glucose, L-arabinoe, 4-0-methyl-glucoronic, D-galacturonic and D-glucoronic acids. The sugars are connected by β-1-4 or 1-3 glycosidic bonds (Sanchez, 2009). The chemical structure of hemicellulose is presented in Figure 4.

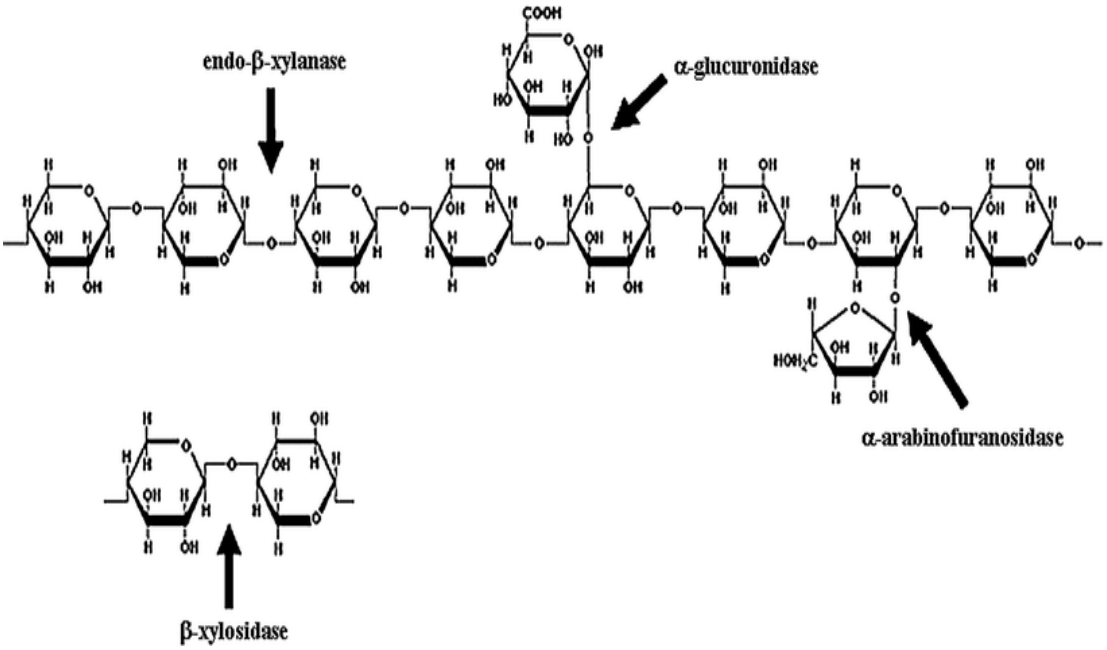

Figure 4. Polymeric chemical structure of hemicellulose showing the targets of hydrolytic enzymes involved in hemicellulosic polymer degradation (Kumar et al., 2008)

It has been believed that to allow access to cellulose by enzymes the hemicellulose needs to be disrupted (Yang B., 2011) .

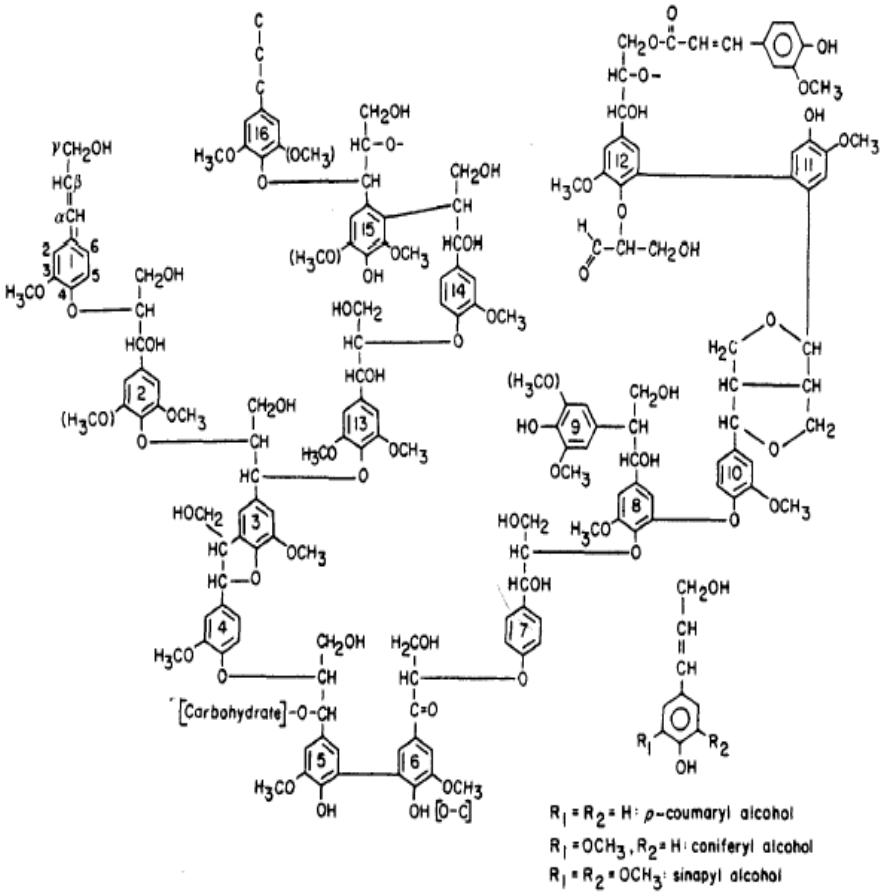

Figure 5. Schematic showing the linkages found in spruce lignin (Cullen and Kersten, 1996).

The third component of plant cell walls is lignin. This is an insoluble polymer which is covalently associated with hemicelluloses through a number of different types of linkages (Sanchez, 2009; Malherbe and Cloete, 2002). These include coupling of monolignols (lignin monomer, monomeric precursor) and three primarily hydrocinnamyl alcohols: (ρ-coumaryl, coniferyl and synapyl alcohols) (Wong, 2009 ; Cullen and Kersten, 1996) (Figure 5). Lignin is often categorised into three types : (1) softwood lignin (gymnospermae), (2) hardwood (angiospermae) and (3) grasses lignin (non woody

or herbaceous). The lignin content determines enzymatic digestability of plant waste biomass for producing biofuels or bioproduct such as vanillin, ferulic acid, vinyl guaiacol, etc. Wheat straw lignin, known as p-hydroxyphenyl-guaiacyl-syringyl (H-G-S) lignin, has a proportion of H-G-S units of 5, 49 and 46% respectively, whilst wood lignin mainly contains guaiacyl and syringyl. In herbaceous plant including wheat, hydroxycynamic acids (p-coumaric and ferrulic acids) are linked to lignin and hemicellulose through ether and ester bonds to create lignin phenolic carbohydrate complex (Figure 6). The most important are the bonds between benzylic carbon of lignin and the carbohydrate moiety and the ester bonds between the benzylic carbon of lignin and uronic carbon residue and lignin glucosidic bonds (Ahmad et al., 2010 ; Wong, 2009 ; Sigh and Cheng, 2008). In lignin, the aryglycerol-β-aryl ether subunit is the most predominant (50-80%), followed by biphenyl (25%), phenylcoumaran (10%) and biphenyl ether subunits (4%) (Wong, 2009). Aryglycerol-β-aryl ether bonds are the easiest linkage to breakdown while the biphenyl ether bond is the strongest. The difficulty in breaking down lignin is due to its complex structure (Buranov and Massa, 2008 ; Sun et al, 2002 ; Sun et al, 1997).

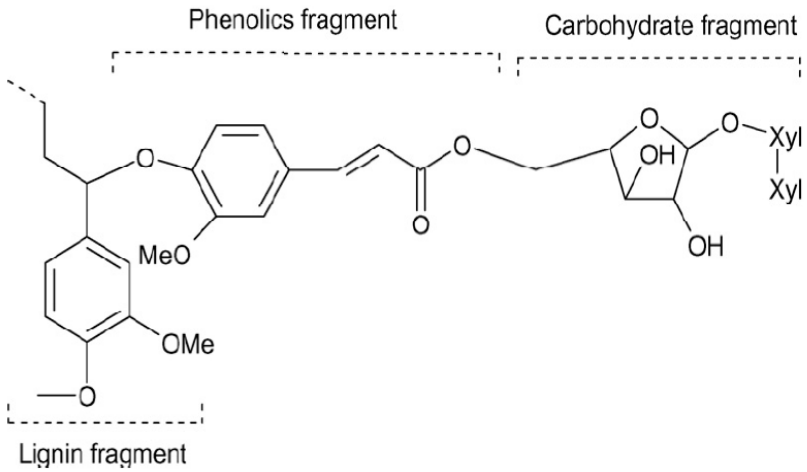

Figure 6. Schematic showing the chemical structure of lignin – carbohydrate complex found in wheat straw (Buranov and Massa , 2008; Sun et al., 1997)

1.2 Development of biorefineries

A biorefinery should mimic a petrochemical refinery as the concept is based on utilising a multistep process that integrates biomass conversion to produce energy, heat, power, and chemicals (Clark, 2007). This process involves three phases (Figure 7). First, raw material is needed, which could be supplied by different agricultural waste products such as wood, corn, weed, straw, etc. In the second phase, these materials are separated into different types of biopolymer, eg. cellulose, hemicellulose, sugar, aromatic, lignin, hydrocarbon, etc. The final phase is the conversion of the products into more valuable compounds.

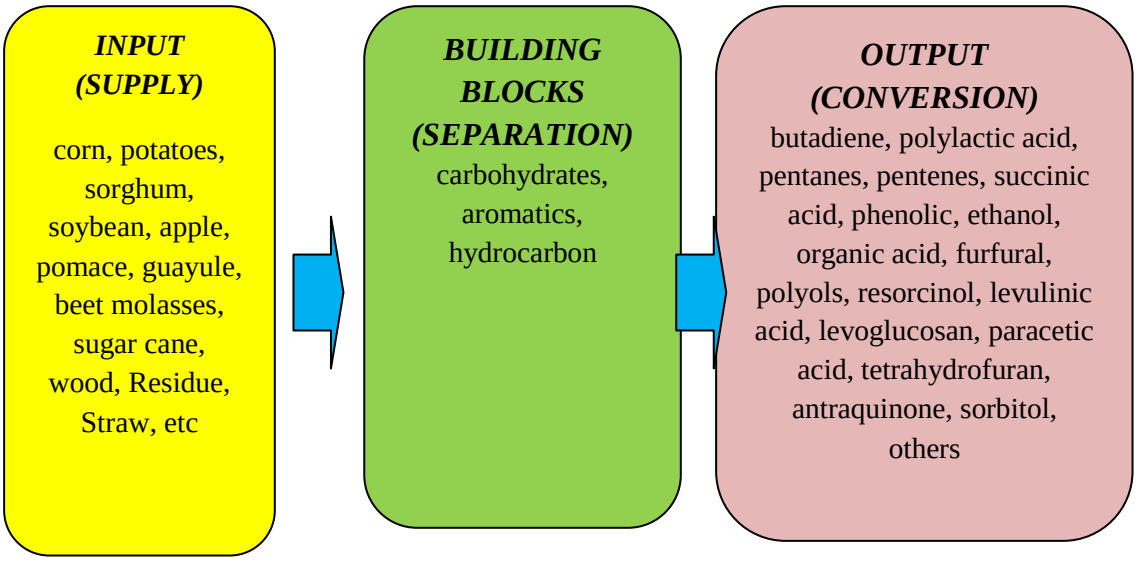

Figure 7. The three major phases of the biorefinery process
(adapted and modified from Bozell, 2006)

Lignocellulosic based biorefinery are considered the most promising for development on a large scale due to availability of the feedstock and a high demand for the products which can be produced in both petrochemical and biobased market sectors (Kamm and Kamm, 2004). The three major components of lignocellulosic material (lignin, cellulose and hemicellulose) can be used to generate a range of derivative products (Figure 8). For example, furfural as derivative product from xylose can be used for Nylon 6 production which has a huge market. Other products derived from cellulose such as 5-hydroxymethyl-furfural can be as a raw material for producing softener, solvent, lubricant, chemicals and polymers (Kamm and Kamm, 2004).

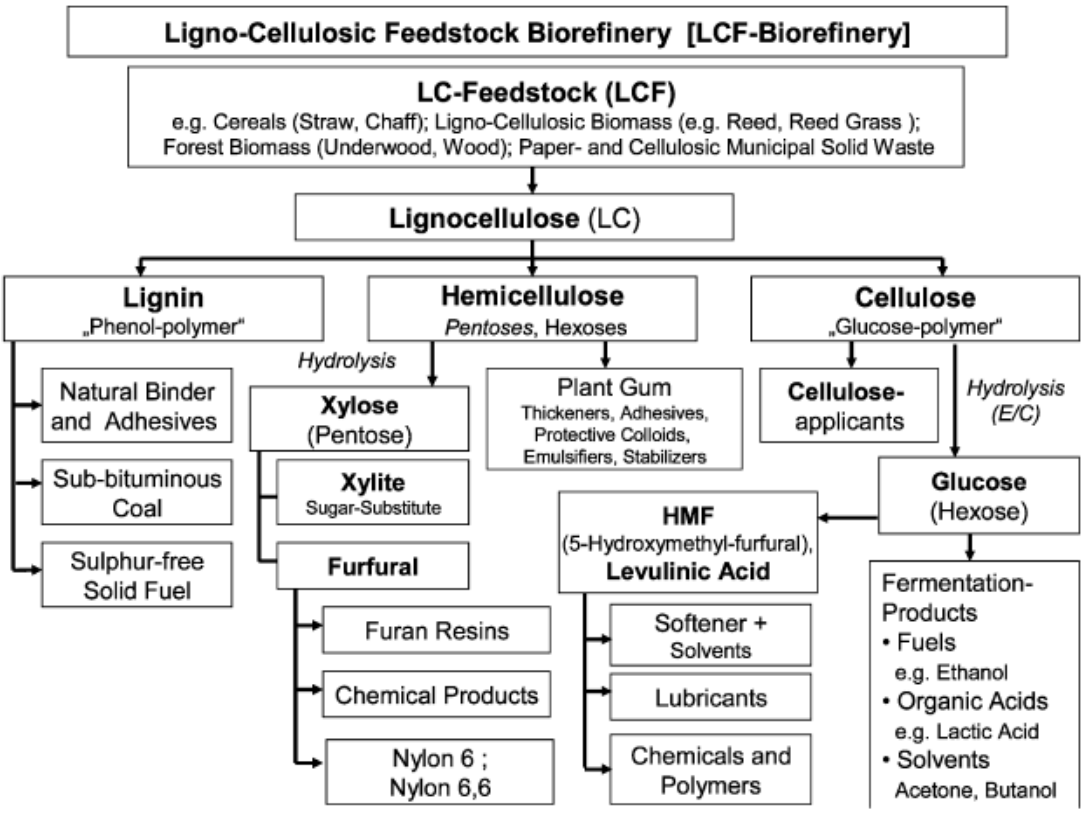

Figure 8. Derivative products obtained from lignocellulosic feedstock biorefinery (Kamm and Kamm, 2004)

Bozell (2006) and Carvalheiro et al. (2008) listed some of the most promising chemicals which could be isolated from cellulose (hemicelluloses) and lignin (Table 4). The products produced from cellulose and hemicellulose have simple structures and lower molecular weights compared to the products that can be derived from lignin. Aromatic and polyaromatic compounds can be produced through the conversion of lignin such as benzaldehyde and vanillin (de Jong et al., 1994).

Table 4. Chemicals that could be produced from cellulose, hemicellulose, and lignin (modified from Bozell, 2006 and Carvalheiro et al. 2008)

Product from cellulose and hemicelluloses	**Product from lignin**
a. Succinic acid	a. Thermochemical products (gasification, pyrolysis, combustion)
b. 2.5 – Furandicarboxylic acid	b. Macro molecule (Carbon fibre, polymer, resin, adhesive)
c. 3-Hydropropionic acid	c. BTX (mixed of Benzene, Toluene and Xylene)
d. Aspartic acid, Fumaric acid	d. Phenols
e. Glucaric acid, Malic acid	e. Substituted coniferols (propylenol, eugenol, aryl ester)
f. Glutamic acid,	f. Oxidized lignin monomer (Vanillin, syringaldehyde)
g. Itaconic acid, Levulinic acid	g. Diacids from chemical transformation
h. Glucaric acid, 2.5 furan dicarboxylic acid	h. Diacids from biochemical transformation
i. 3-Hydroxybutyrolactone	i. Aromatic polyols (cresol, cathecol)
j. Glycerol, Arabitol	j. Cyclohexane and substitute cyclohexane
k. Sorbitol, Xylitol	k. Quinones
l. Xylitol/arabinitol	

The first step for wheat straw pretreatment are through chopping, grinding and milling which will increase the surface area available for digestion. Cost effective pretreatment of wheat straw is important for the developent of a biorefinery. This has been reviewed by Talebnia et al. (2010), who evaluated and compared existing pretreatment methods. These can be classified into 4 major types of pretreatments which are : (1) physical, (2) physico-chemical, (3) chemical and (4) biological process. A schematic diagram of the approach is presented in Figure 9. The commercial application may involve more complex processes or use a combination of more than one process.

For example, a mechanical pretreatmemt followed by thermal or chemical processes (Talebnia et al., 2010).

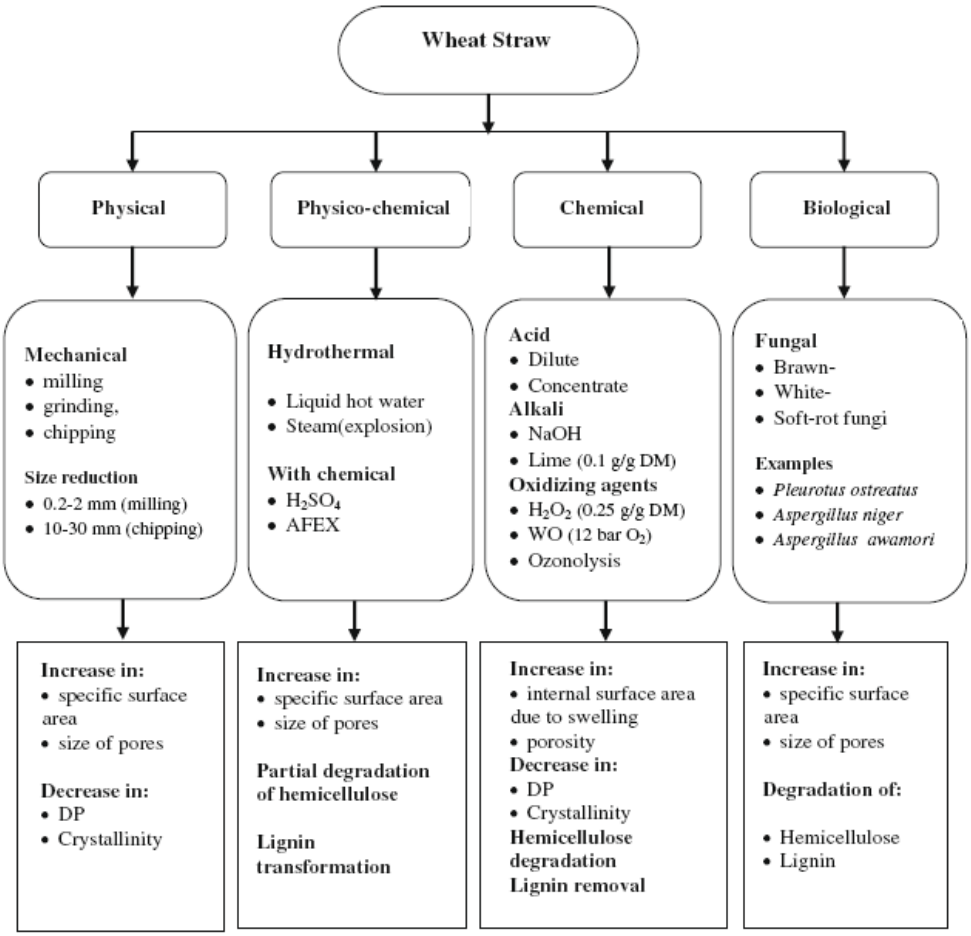

Figure 9. Schematic diagram of a possible biorefinery based on wheat straw pretreatment (Talebnia et al., 2010)

Sun et al. (2005) developed a method for extraction and characterization of original lignin and hemicelluloses from wheat straw using chemical extraction (e.g. toluene, HCl, ethanol and dymetyl sulfoxide (DMSO)). These can be extracted as platform chemicals on an industrial scale in order to synthesise further valuable products. The predominant products of lignin decomposition are vanillin (24.50%) and

syringaldehyde (31.50%), and minor quantities of coumaric acid and ferulic acid were also obtained. Hemicellulose can be broken down to release sugars. Different methods have had varying success e.g. 80% dioxane with 0.05M HCl released 53.58% of the xylose, while 100% dimethylsulfoxide extraction for 5 hours at 85°C released 68.34% of the avaliable xylose. Other sugars were released by the two methods in differing amounts such as arabinose (14.84 or 9.37%) and glucose (13.45 or 14.42%).

Biorefineries that break down lignocellulose feedstock using diluted acid hydrolysis at high temperature have been developed, but this is an expensive method (Uihlen and Schebek, 2009). Wet oxidation or steam explosion are alternative procedures for the release of chemical constituents from wheat straw (Panagiotou and Olsson, 2007) and can complement organo-solvent and alkali treatments (Buranov and Mazza, 2008 ; Jorgensen et al., 2007). It has been noted that wet oxidation is an effective way to extract hemicellulose and cellulose for futher enzymatic hydrolysis and fermentation processes. This can recover up to 96% cellulose and 67% of the available glucose. Ideal conditions for alkaline wet oxidation is considered to be 10 minutes at 195^{o}C under 12 bar oxygen and 6.5 g l^{-1} Na_2CO_3. 100 g of wheat straw, alkali wet oxidation yielded hemicellulose (16 g), carboxylic acid (11 g), phenol (0.48 g), 2-furoic acid (0.01 g), formic acid and acetic acid (8.5 g) and vanillic acid and syringic acid at between 0.04 to 0.12 g (Klinke et al., 2002). However these methods are costly in terms of energy consumption and often produce toxic waste chemicals (Ward and Singh, 2002). The expense increases if pressure equipment is used which allows recovery of

high yields of monosaccharides along with greater production of carboxylic acid and low yield of furan aldehyded and phenolic aldehyde (Carvalheiro et al., 2008)

Often several processes are used in conjunction, for example, the use of steam and acetic acid and/or ethanol on wheat straw pre-treatment. This combination is more effective than steam explosion alone for sugar release as a transitional product for the manufacture of ethanol. This hydrothermal processes may employ liquid hot water and steam explosion at the temperature of 150^{o}C to 230^{o}C. No effect on the material is found when the treatment is below 100^{o}C. Autohydrolisis at 200^{o}C along with pressure can recover hemicellulose in high quantity, but the lignin remains intact (Carvalheiro et al., 2008). Steam explosion has been applied to various feedstock such as mixed hardwood chips, rice hulls, corn stalk, and sugar cane baggase (Schultz et al., 1984). Treatment with steam explosion alone, at 210^{o}C for 10 minutes yielded sugar at 177.3 g kg^{-1} dry solid basis, whilst by steam with acetic acid treatment and steam with ethanol, sugar was produced at the level of 244.1 g kg^{-1} and 264.3 g kg^{-1}, respectively (Zabihi et al., 2010).

Other pretreatment process use alkali treatment to increase cellulose solubility and can in turn be separated into 2 different groups, depending on the type of chemical used : (1) pretreatments which employed sodium, pottasium or calcium hydroxide, and (2) pretreatments using ammonia. Both processes may digest lignin but have less of an effect on the solubility of cellulose and hemicellulose (Carvalheiro et al., 2008). The application of alkali pretreatment (1 M NaOH at 30^{o}C for 18 hours) was used to identify chemical, structural features, physico-chemical and thermal characterization of the lignin, hemicellulose and cellulose from maize stem, rye straw and rice straw. The

results showed that this process can recover lignin from maize stem, rye straw and rice straw at the level of 78.0, 68.8, and 82.1 %, whilst 72.1, 72.6 and 84.6 % was recovered for hemicellulose, respectively (Xiao et al, 2001).

Comparing to such current and expensive biorefining technology, biological delignification has some potential advantages such as: low capital cost and energy input, high yield and reduction in pollutants. Thus, developing a low input method using microorganisms to degrade lignocellulosic biomass for producing sugar or chemicals is important. The use of microorganisms, e.g. fungi, to degrade lignocellulose potentially provides a low input alternative to the use of chemical or high pressure techniques, but requires further study to optimize the process and reduce the cost of production. Technologically, lignocellulosic degradation is not an easy task because of its complex structure. Various microorganisms have the ability to breakdown and utilize cellulose and hemicelluloses as carbon and energy sources using enzymatic degradation processes but fungi are the dominant degraders of lignocelluloses in nature (Kumar et al., 2008; Sanchez, 2009). Therefore, recent works by many groups have focused on the genetic engineering of microorganisms to deliver more efficient lignocellulolytic enzymes.

1.3 Biological degradation of lignocellulosic plant waste biomasss

Biodegradation of lignocellulose material has been recognised as an important research topic for many years (Hatakka, 1994; Singh and Chen, 2008). Lignocelluloses are highly resistant to decay by microorganisms (Lee et al., 2004) and could offer an alternative to grain as a feedstock for future biorefineries, that will not compete with the

food supply chain (Singh and Chen, 2008). The decomposition of lignocellulosic material (wood) in the environment is mostly carried out by white and brown rot fungi from the Basidiomycota (Hatakka,1994 ; Highley and Dashek, 1998). They contain enzymes to degrade lignocellulose as a source of carbon and other important nutrients such as nitrogen to enable mycelial growth. Two different classes of enzymes are recognized as being important, which are : (1) hydrolytic enzymes which enable breakdown of polysaccharide and (2) oxidative enzymes that act extracellularly to degrade lignin and phenyl rings (Hammel, 1997 ; Sanchez, 2009). A list of enzymes produced by both white and brown rot cultured on different substrates is presented in Table 5.

Lignocelluloses waste materials are produced from various sources such as agriculture, forestry, food and pulp and paper, all of which can be degraded by the synergistic action of fungal enzymes. This involves the breakdown of long chained polysaccharides from cellulose, hemicelluloses and lignin (Dashtban et al., 2010). Lignocellulosic degradation by white rot fungi has been intensively studied, for example; *P.chrysosporium* (Singh and Chen, 2008; Martinez et al., 2005; Tanaka et al., 2007; Moredo et al., 2003); *Physisporinus rivulosus* (Hilden et al., 2007); *Tremetes versicolor* (Tanaka et al., 1999); *Ceriporiopsis subvermispora* (Blancette et al., 1992); *Cerrena unicolor* (Michniewicz et al., 2006), however only limited studies of brown rot fungus are available such as: *Coniophora puteana* (Lee et al., 2004); *Fomitopsis palustris* (Yoon et al., 2007); *Gloeophyllum trabeum* (Wang et al., 2006; Enoki et al., 1992).

Tabel 5. Enzyme produced by white and brown rot fungi (Sanchez, 2009)

Fungus	Groups	Type of fungus	Substrates	Enzymes
Strobilurus ohshimae	Basidiomycetes	White rot	Sugar,woods	LiP, MnP
Phanerochaeta chrysosporium	Basidiomycetes	White rot	Grape seed, barley brand and wood shaving	LiP, MnP
Trametes versicolor	Basidiomycetes	White rot	Wood shaving, carozo maize, and compost of gardening wheat straw	Lacasse
Trametes versicolor	Basidiomycetes	White rot	Grape seed, barley brand and wood shaving	Lacasse, xylanase, MnP, cellobio dehydrogenase
Trametes versicolor	Basidiomycetes	White rot	Sugar cane baggase	Laccase, MnP, glucose oxidase, glyoxal oxidase, quinone oxidoreductase, Cellobiose
Pleurotus ostreatus	Basidiomycetes	White rot	Bagase of cane maize straw	Xylanases, Cellulases, Laccase, MnP
Pleorotus ostreatus, Pleorotus	Basidiomycetes	White rot	Coffee pulp, used nappy, grass residue, cleaned coffee (substrate analyzed and in mixture), wheat straw, industrial cotton fiber.	Endoglucanase, cellobiohydrolase, Laccase, MnP
Aspergilus niger	Ascomycetes	Brown rot	Sugar cane baggase	Xylanase, cellulase
Bjerkandera adusta	Basidiomycetes	White rot	Shaving of wood, carozo maize, and compost of gardening wheat straw	MnP, LiP
Clonostachys rosea	Ascomycetes	White rot	Clavel leaves, young plant leaves (from Aster genus) lamella from oats and maize plants	Endopolygalacturonases galactosidase, endo-xylanase, cellulases, arabinofuranosidase, acetylesterase, xylosidase, galactosidase
Fusarium oxysporum	Ascomycetes	Brown rot	young plant leaves (from Aster genus) lamella from oats and maize plants	Endopolygalacturonases galactosidase
Fusarium merismoides	Ascomycetes	Brown rot	Clavel leaves, young plant leaves (from Aster genus) lamella from oats and maize plants	Endo-xylanase, cellulases, arabino furanosidase, acetylesterase, xylosidase
Streptomyces	Actonomycetes (bacteria)	White rot	Clavel leaves, young plant leaves (from Aster genus) lamella from oats and maize plants	Cellulases, xylanases, arabino furanosidase xylosidase, acetylesterase
Penicillium sp	Ascomycetes	White rot	Clavel leaves, young plant leaves (from Aster genus) lamella from oats and maize plants	Endo-xylanases, cellulases, arabino furanosidase, acetylesterase, xylosidase
Pycnoporus cinnabarinus	Basidiomycetes	White rot	Soft wood	Laccase, LiP, MnP
Xylaria hypoxylon	Ascomycetes	White rot	Wood	Laccasse. Endoglucanase, glucosidase, esterase, xylanase
Fomitopsis palustris	Basidiomycetes	Brown rot	Microcrystalline structure	Cellulase (exoglucanases, endoglucanase, β-glucosidase

1.3.1 White rot fungi

The white rot fungi are a heterogeneous group of fungi classified in the basidiomycota that mainly breakdown of lignin and hemicellulose through the release of extracellular enzymes. These are categorized as laccase, lignin peroxidase and manganese peroxiase (Hatakka, 1994). The pathways used by white rot fungi for degradation of lignocellulosic material have been described by Martinez et al., (2005) (Figure 10). These enzymes act to (a) oxidize lignin and release aromatic radicals, (b) followed by further non-enzymatic reactions, including C-4 ether breakdown, (c) aromatic ring cleavage, (d) Cα-Cβ breakdown, (e) demethoxylation, (f ,g) release of aromatic aldehydes, (h) lignin polymer degradation, and (i) the release of phenolic compound, (j) oxidized phenolic compound, (k) phenoxyl radical production and (l,m) yielding in quinone. Release of several monomers from lignin has been shown such as conversion of ρ-coumaryl alcohol to phenol and sinapyl alcohol to syringol (Kleiner and Bath, 2008)

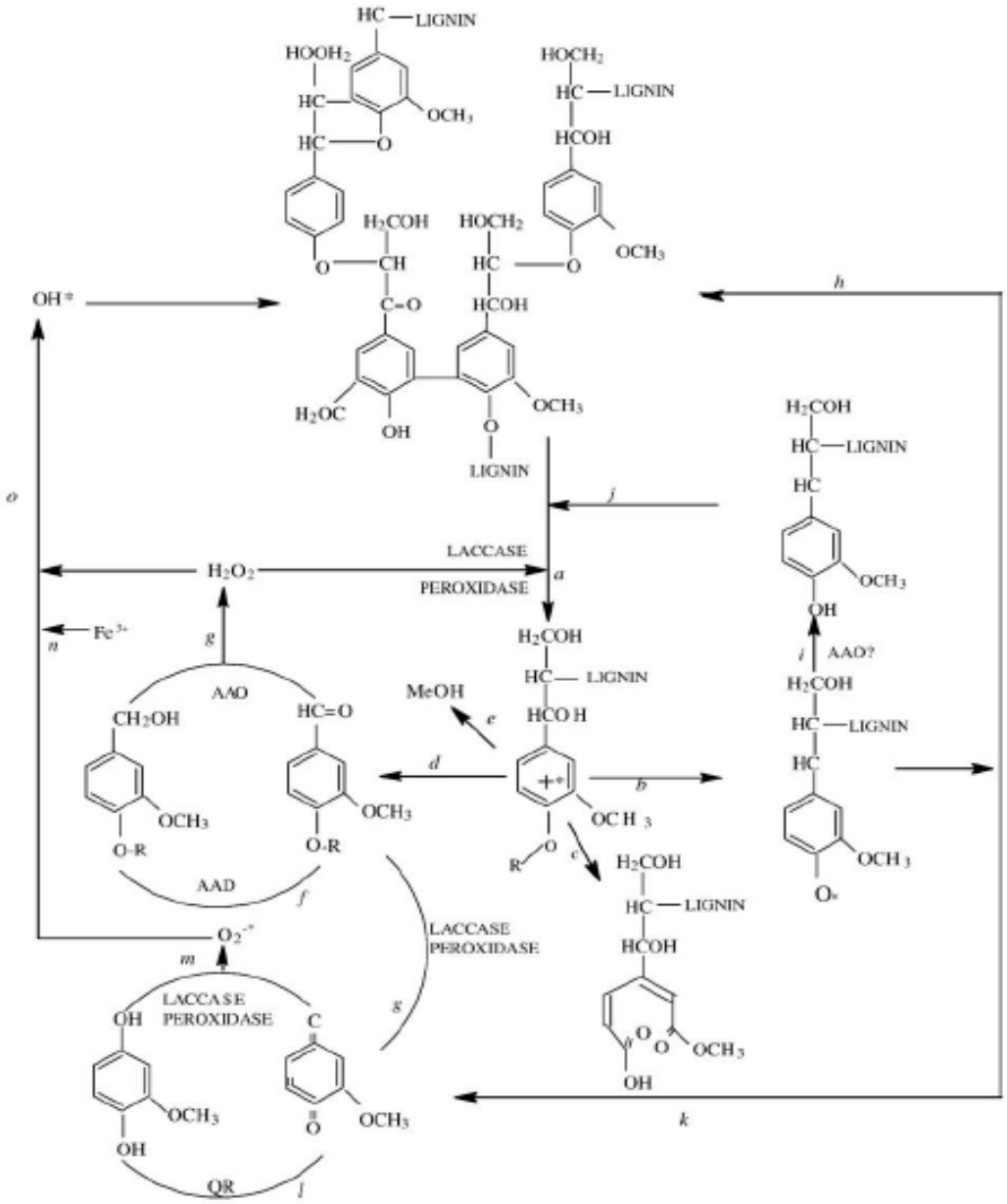

Figure 10. The pathway of lignocellulotic degradation by white rot fungi (Martinez et al., 2005)

The white rot fungus, *Phanerochaete chrysosporium*, is a lignocellulolytic microorganism which produces extracellular lignin-modifying enzymes such as lignin peroxidises (LiPs) and manganese peroxidises (MnPs), but lacks laccase genes (Eriksson et al., 1990; Hatakka 1994) that is intensively produced by other white rot fungi, e.g. *Trametes versicolor*. Thus, the addition of external enzymes, e.g. cellulase

and hemicellulase to *P. chrysosporium* cultures has been used to enhance the substrate breakdown (Tabka et al., 2006). Since physiological conditions for lignin degradation vary between fungal species, it is important to evaluate enzyme combinations which are responsible for lignin degradation by each species (Vares and Hattaka, 1995). The main cofactors and substrates of the principle reaction of each enzyme are presented in Table 6 (Hattaka, 2001). The other lignocellulolytic enzymes produced by white rot fungi (Ascomycota groups) are endopolygalacturonase, galactosidase, endoxylanase, cellulase, arabifuranodiase, acetylesterase (Sanchez, 2009).

Table 6. Main cofactors, substrates and principle reaction conditions for lignin degrading enzymes (Hattaka, 2001).

Enzyme activity	**Cofactor or substrate**	**Main effect or Reaction**
Lignin peroxsidase (LiP)	H_2O_2, veratryl alcohol	Aromatic ring oxidized to cation radical
Manganese peroxidase (MnP)	H_2O_2, Mn, organic acid as chelator, thiols, unsaturated lipids	Mn (II) oxidized to Mn (III) ; chelated Mn(III) oxidized phenolic compound to phenoxyl radical ; other reactions in the presence of additional compounds
Laccase (Lac)	O_2 mediator e.g. hydroxybenzotriazole or ABTS	Phenols are oxidized to phenoxyl radicals ; other reactions in the presence of mediator (e.g ABTS)
Glyoxal oxidase (GLOX)	Glyoxal, metyl glyoxal	Glyoxal oxidized to glyoxylic acid ; H_2O_2 production
Aryl alcohol oxidase (AAO)	Aromatic alcohol (anisyl, veratryl alcohol	Aromatic alcohols oxidized to aldehydes ; H_2O_2 production
Other H_2O_2 producing enzyme	Many organic compound	O_2 reduced to H_2O_2

The first step in cellulose degradation occurs through the production of cellulases resulting in a product called cellobiose which is subsequently hydrolyzed by β-glucosidase to glucose. The enzymes that degrade hemicellulose are more complex due to the heterogeneity of sugar moieties and bonds. Hemicellulose chains are initially targeted by endo-acting enzymes (mananase, xylanase), the products are hydrolyzed to simple sugars by glycosidases (mannosidases, xylosidases, glucosidases) (Highley and Dashek, 1998).

Lignin degradation by the white rot fungi is variable because different fungi produce unique combinations of peroxidases and oxidases (Perie and Gold, 1991). Numerous enzymes play a role in lignin depolymerisation, but the exact number of enzymes, their structure and location of action remain unclear. Lignin and manganese peroxidases produced by the basidiomycete *P. chrysosporium* catalyze the oxidation of a large number of organic or inorganic compounds in combination with hydrogen peroxide and substituted peroxides (Cai and Tien, 1993). The possible pathway of lignin break down by white rot fungi (Figure 11) was also described by Dashtban et al., (2010).

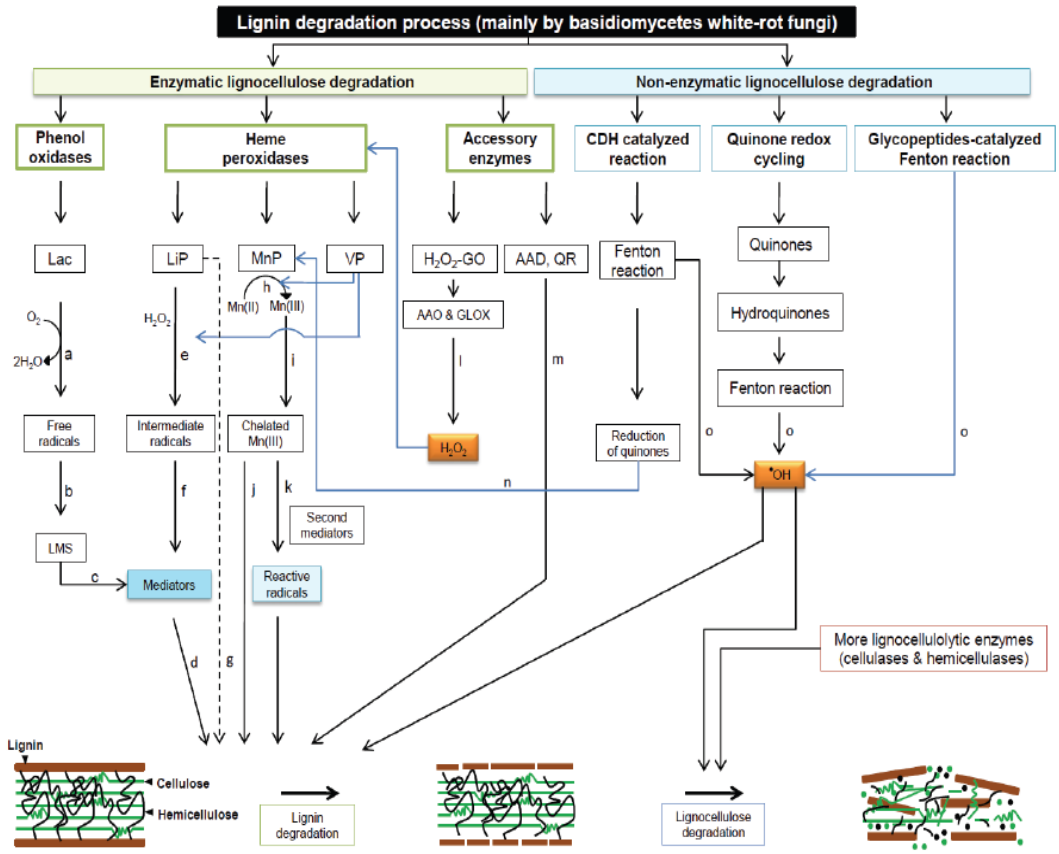

Lac: laccase, LMS: laccase-mediator system, LiP: lignin peroxidase, MnP: manganese peroxidase, VP: versatile peroxidase, H_2O_2-GO: H_2O_2-generating oxidases, AAO: aryl-alcohol oxidase, GLOX: glyoxal oxidase, H_2O_2: hydrogen peroxide AAD: aryl-alcohol dehydrogenases, QR: quinone reductases and $^{\bullet}OH$: free hydroxyl radicals.

Figure 11. Schematic diagram of lignin degradation by basidiomycete white rot fungi (Dashtban et al., 2010)

Figure 11 shows that the degradation of lignin by the white rot fungi involves several extracellular lignocellulolytic enzymes, known as lignin-modifying enzymes, including phenol oxidases (laccase) and hame peroxidases (LiP,MnP and VP). The generation of H_2O_2 is required by the peroxidases. It is produced by aryl-alcohol oxidase and quinone reductase. The different routes shown indicate different radical production steps that could degrade the lignocellulose. Non enzymatic pathways

have also been recognised to play a role in the lignocellulose degradation by the white rot through the Fenton reaction which involves CDH catalysed reactions, quinone redox cycling and the catalysis of glycopetides.

1.3.2 Brown rot fungi

Research on the mechanism of lignin degradation and enzymes produced in basidiomycetes has predominantly focused on the white rot rather than brown rot fungi (Vares et al., 1995). In temperate regions brown rot fungi play a significant role in wood degradation however, the processes involved are poorly understood (Hattaka, 2001). Unlike the white rot fungi, the brown rot fungi do not typically produce ligninolytic enzymes such as laccase, lignin peroxidase and manganese peroxidase which would allow direct decay of lignin and its aromatic structure. Brown rot fungi preferentially attack dead coniferous wood, timber and wooden structure, in which they cause destructive types of decay and rapid degradation of cellulose (Kuhad et al., 1997; Goodell, 2003). All the brown rot fungi are thought to use the same mechanism for lignocellulose decay; this involves a Fenton-type catalytic system producing hydroxyl radicals that attack lignocellulose. The initial stages lignocellulose breakdown by brown rot fungi are believed to involve Fenton chemistry (Fe^{2+} + H_2O_2). Among the brown rot fungi, *Gloeophyllum trabeum* has been studied the most (Hattaka, 2001). This fungus potentially produces several extracellular enzymes, e.g. cellobiose dehydrogenase (CDH) and alcohol oxidase (Ritschkoff et al., 1995).

Brown rot decay is characterised by massive disruption where fungal hyphae rapidly attack wood cellulose (Espejo and Agosin, 1991; Fahr et al., 1999). Hammel

et al., (2002) reported how hydroxyl radicals (OH•) attacks the sub units of lignin (Figure 12), destroying Cα bonds and the aromatic rings, followed by different processes of oxidation (demethoxylation, β-0-4-cleveage, hydroxylation, and Cα-oxidation).

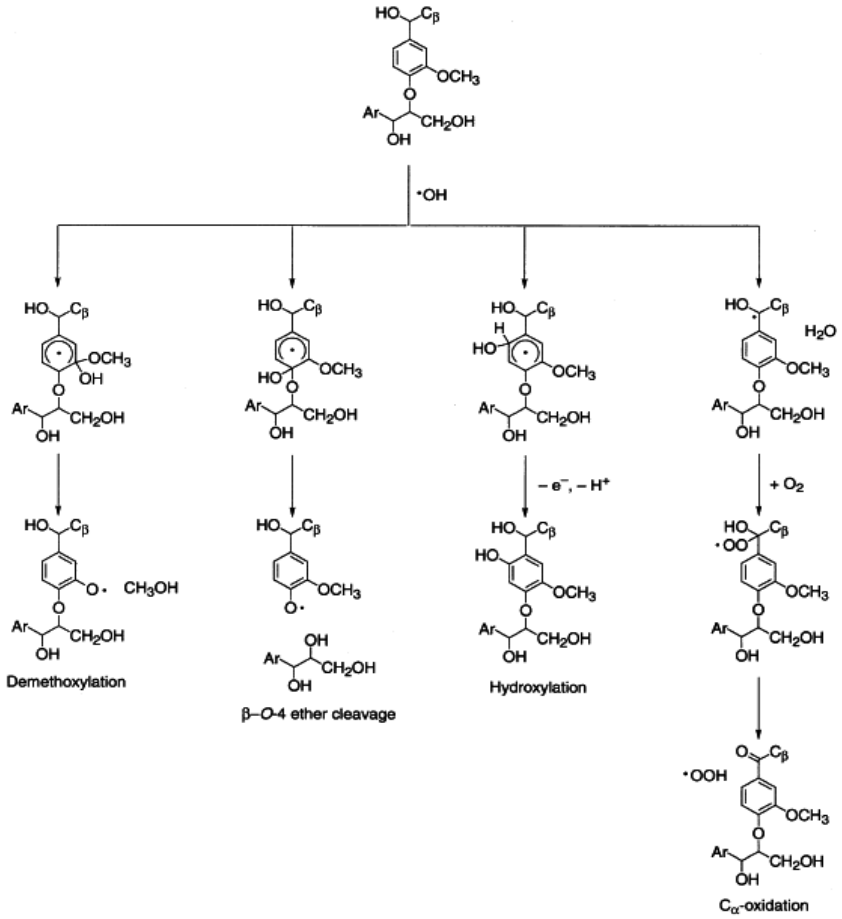

Figure 12. The pathway of lignocellulose degradation by the brown rot fungi (Hammel et al., 2002)

A large number of carbonyl and carboxyl acids are released during decomposition of wood through anoxidative system initiated by brown rot fungi and low molecular weight quinone and oxalic acid are produced which participate in the decomposition of cellulose. Suzuki et al., (2006) proved that oxalic acid chelates the Fe^{3+} into soluble complexes, whereas the iron can be derived from these

Fe^{3+} complexes back to Fe^{2+} promoting the continuation of the Fenton reaction (Xu and Goodel, 2001; Jensen et al., 2001). Espejo and Agosin, (1991) successfully indentified the role of oxalic acid during cellulose depolymerisation by *P. placenta* and *Wolfiporia cocos*. Large amounts of this organic acid is however believed to suppress the Fenton reaction (Shimada et al., 1994 ; 1997). Since the ability of brown fungi to degrade cellulose in wheat straw and the production of low molecular compound such as oxalic acid is still unclear further assessment on how this organic acid is involved in lignocelluloses degradation is required.

The production of oxalic acid is hypothesised to be involved in the fungal breakdown of lignocellulose. It is thought to act in conjunction with some low molecular weight compounds (quinone, hydroquinone and benzoic acid derivative) and specific enzymes (e.g CDH = cellobiose dehydrogenase), to reduce Fe^{3+} to Fe^{2+}. Fe^{2+} then will react with hydrogen peroxide (H_2O_2) to generate OH radicals, which attack both lignin and cellulose (Ray et al., 2010). These degradation concepts has been reviewed by Baldrian and Valaskova, (2008) and are presented in Figure 13.

Another pathway that could produce the OH radical for lignocellulosic degradation by the brown rot fungi is quinone redox cycling (Figure 14). The production of extracellular quinones of brown rot fungi *Gloeophyllum trabeum* which underlie this process (e.g. 2,5 dimethoxybenzoquinone/2,5-DMBQ) and 4,5-dimethoxycatecol/4,5 DMC) could also reduce Fe^{3+} to Fe^{2+} (Baldrian and Valaskova, 2008). Several catechol-type compounds such as 2,3-dihydroxybenzoic acid (2,3-DHBA), 3,4-dihydroxybenzoic acid, and 1,2-dihydroxybenzene (catechol) have been tested to control the concentration of hydroxyl radicals in wood degradation (Rodriguez et al., 2001 ; Contreras et al., 2006), whereas 2,3-DHBA has been

reported to accelerate cellulose degradation when Fe^{3+} was present in excess of the chelator (Xu and Goodell, 2001).

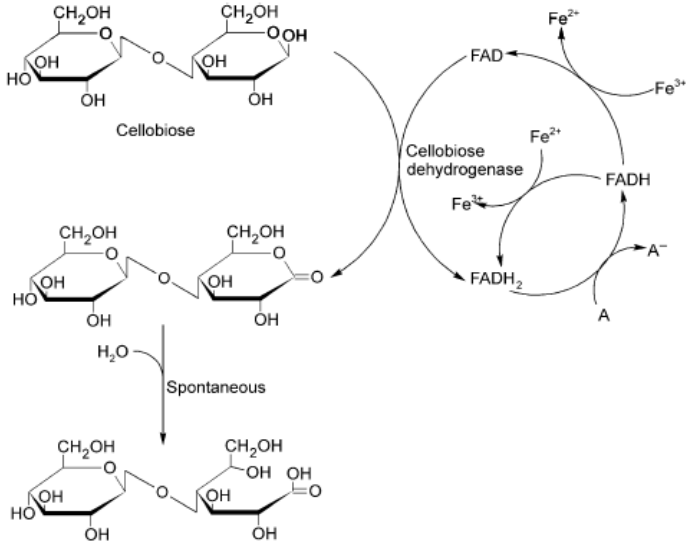

Figure 13. Mechanism of Cellobiose dehydrogenase (CDH) within the Fenton reaction.(Baldrian and Valaskova, 2008)

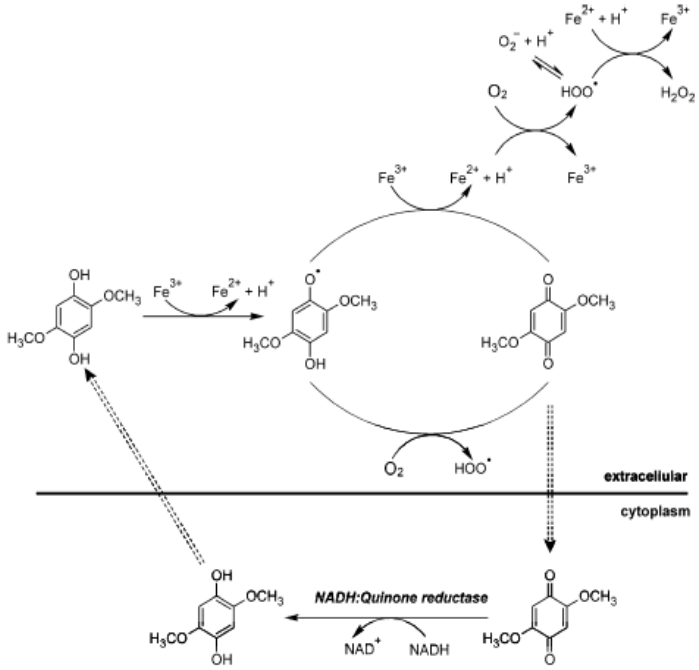

Figure 14. The pathway of quinone redox cyling in the brown rot fungus *Gloeophyllum trabeum* (Baldrian and Valaskova, 2008)

Research on lignin degradation by the white and brown rot fungi has relevance to many subjects such as the pulping industry (Eriksson and Kirk, 1985), biorefinery (Jeffries et al., 2007), organo pollutant degradation (Hammel et al., 1995) and the pharamaceutical industry (Joo et al., 2008). Lignin linked to both hemicellulose and cellulose creating a strong bond which is difficult to dissolve by any solution or enzymes (Hong et al., 2012). During lignin degradation, the complex structure of lignin can be altered by oxidation, demethylation, or depolymerization, whilst polysaccharide complex is used by the fungus for energy and released as CO_2 and fungal metabolites following degradedation (Figure 15) (Filley et al., 2002)

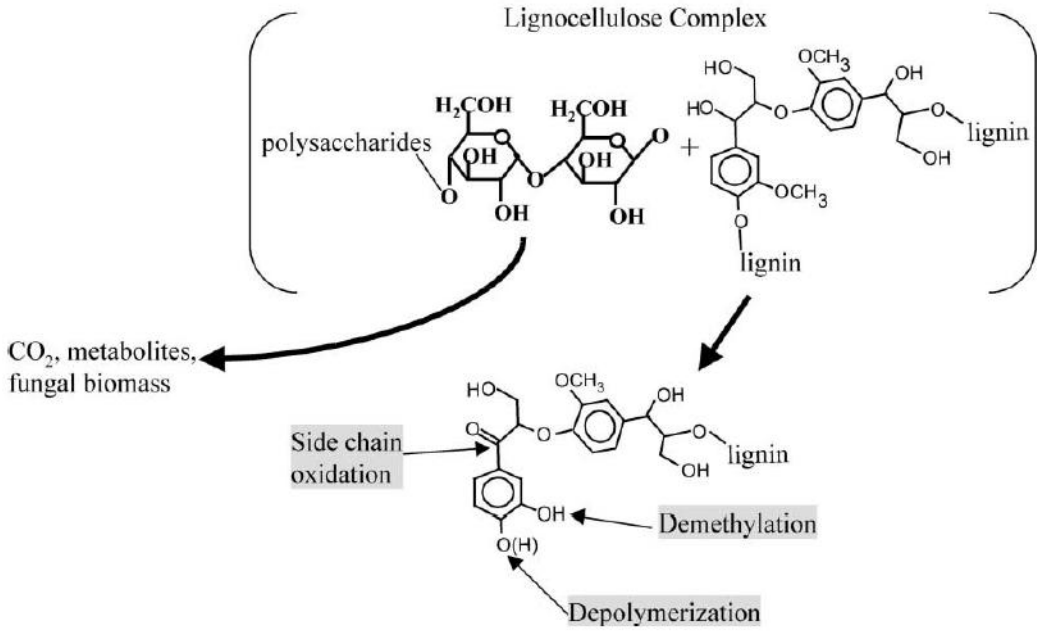

Figure 15. A schematic showing the principles of chemical modification of lignin by brown rot fungi (Filley et al., 2002)

In fungi, different types of celullosic enzymes can have a complementary relationship. Cellulases hydrolyze cellulose through the cleavage of the β-1.4-glycosidic bond. Three major enzyme activities have been recognized, which are: (1)

endoglucanases, commonly named as carboxymethylcellulase or endo-1-4-β-glucanase, (2) cellobiohydrolase, known as exoglucanase, which comprised 40-70% of total cellulase protein and is capable of degrading crystaline cellulose or removing monomer and dimers from the end of glucan chains (3) β-glucanase, which is capable of hydrolizing glucose or cellulose oligosacharides to glucose (Sanchez, 2009 : Rabinovich et al., 2002).

Kumar et al. (2008) noted that cellobiose is the smallest structure of cellulose and the endoglucanases attacked the cellulose chain, while cellobiohydrolases breakdown the chain ends, releasing cellobiose. β-glucosidases can be active when cello-oligosaccharides and cellobiose are present, and release glucose monomers units from the cellobiose (Figure 15). Similar enzymes can participate in both hemicellulose and cellulose degradation, which allows the final completion of lignocellulosic degradation (Malherbe and Cloete, 2002 ; Sanchez, 2009). Hemicellulose can be degraded into monomeric sugars and acetic acid along with xylan as the predominant carbohydrate compounds which entails various hydrolytic enzymes for breakdown into a more simple structure. Several hemicellulases have been reported by Sanchez, (2009) such as : endo-1.4-β-xylanase, 1.4-β-xylosidase, xylanesterase, fereulic and ρ-coumaric esterase, α-1-arabinofuranosidase, α-4-0-methyl glucuronosidase, β-mannosidase and β-glycosidase.

1.4 Biotechnological application of lignocellulose bio-conversion

Identification of the products released as a result of fungal activity following incubation with lignocellulosic biomass could help us to determine the mechanisms involved in its breakdown by non ezymatic or enzymatic processes. The potential of

the enzymes or the process involved to convert lignin offers biotechnological solutions which might effectively be utilised within a biorefinery. This includes the use of recombinant gene technology for enhancing the bioconversion of lignocellulose to value added and industrially significant products and reducing the energy costs of pretreatment processes currently used. This thesis attempts to provide the background knowledge required and offers some potential biotechnological solutions.

1.5 The Aims/Objectives

- To quantify the products released from different fungi (e.g. total reducing sugar, soluble phenolic compounds, Fatty Acid Methyl Ester (FAME)) and establish the relationship between fungal growth and lignocellulose conversion.
- To elucidate the biochemical mechanism of lignocellulose degradation by *Serpula lacrymans* through determination of the effects of pH, oxalic acid and quinone produced
- To identify and characterize genes encoding iron reductase enzymes in *S. lacrymans,* thought to regulate lignocellulose degradation
- To determine the expression level of iron reductase genes by quantification of relative transcription of iron reductase (IR-1 and IR-2) from *S. lacrymans* cultured on wheat straw Solid State Fermentation (SSF)
- To purify the recombinant *S. lacrymans* iron reductases and to verify their function.

Chapter 2. General Methods

2.1. Material

2.1.1 Microorganisms and culture preparation

White rot (*Phanerochaete chrysosporium* and *Schizophyllum commune*) and brown rot basidiomycetes (*Serpula lacrymans* and *Postia placenta*) were grown on malt extract agar (MEA). Agar plugs of mycelia were added to rye grain and grown to produce inocula (grain spawn) for the solid state fermentation (SSF) as follows. 2 kg dry rye grain (locally grown) was added to 2 litres boiling water and left for an hour to soften the husks. This was then simmered for 20 minutes and before being left to cool for 1 hour. 20 mg of Agricultural gypsum and 5 mg of calcium carbonate was then added and mixed into the grain as this encourages quick mycelial growth.

The mixture was added to 300 ml honey jars before being autoclaved twice (121^{o}C) for an hour to sterilise the contents. Five plugs of each fungal species with 1 cm diameters, which had been grown on agar previously to ensure purity was then used to inoculate the grain. The jars were then left to incubate at the optimum temperature for mycelium growth (Table 7). Within approximately one week the grain spawn became well colonised and was transferred to a 4°C cold room ready for use. Fungal isolates were maintained via routine culture on MEA at 20ºC.

Table 7. The optimum temperature (°C) for each fungus during the incubation period.

Species of fungus	Type of fungus	Optimum temperature (°C)
Phanerochaete chrysosporium	White rot	37
Schizophyllum commune	White rot	25
Postia placenta	Brown rot	25
Serpula lacrymans	Brown rot	20

2.1.2 **Solid state fermentation (SSF) of wheat straw**

Wheat straw was obtained locally (Warwick Life Sciences farm) and chopped using a food processor (Moulinex) into small pieces (about 1-2 cm length). 10 g of wheat straw was placed into honey jars (250 ml) and 13 ml of water was added before undergoing a double sterilization of 121°C for 1 hour. The prepared straw was then inoculated with 1 g of grain spawn of the appropriate fungal species and incubated at the optimal temperatures (Table 8) for differing time courses of 0, 7, 14, 21, 28 and 35 days. Four replicates using each of the species of fungus listed in 2:1:1 (two white rot and two brown rot) were grown on wheat straw. This method is known as solid state fermentation (SSF). Additionally four jars of each substrate were left without inoculation as blank samples to provide a baseline for subsequent analysis.

2.2 **Methods**

Both aqueous and organic extraction was used within a two-step process on the samples derived from the time course described above.

2.2.1 Aqueous Extraction

The first stage of extraction used an aqueous solution to remove any sugars and water-soluble phenolics. This involved several steps as follows: (1) 150 ml of purified water was measured into each beaker and boiled to a temperature of 80°C, (2) Each of the sample jars which was to be extracted was then weighed without the lid and the result noted, (3) The boiled water was then poured onto each of the samples. (4) These were mixed at 100 rpm for 15 minutes in an orbital shaker (New Brunswick Scientific-Innova) heated to 40°C, (5) The jars were removed from the

orbital shaker and contents emptied separately into fine muslin netting held in 250 ml beakers. This allowed for the large biomass to be separated from the aqueous extract sample, (6) the biomass was squeezed by hand within the muslin netting trapping the liquid produced in a separate beaker. The cake was retained for subsequent solvent extraction, (7) the aqueous filtrate from the muslin netting was poured into centrifuge test tubes and centrifuged at 18,000 rpm for 10 minutes, (8) The centrifuged extract of each sample was passed, separately, through a 7 μm glass fibre filter using a Buchner funnel and flask attached to a vacuum pump. A glass fibre (GFA) filter was used to prevent the contamination of cellulose from paper-based filters, (8) A second stage of filtration was then applied to each sample, this time at 0.65μm, (9) The filtrate was placed into labelled 50 ml tubes and frozen at -20°C until analysis, to prevent further enzymatic degradation.

2.2.2 Solvent extraction

The purpose of the solvent extraction was to remove any phenolic products released from the biomass samples. This extraction was conducted on the biomass cake post the aqueous extraction described above. The steps involved were: (1) The squeezed cake from the aqueous extract was placed into centrifuge test tubes and centrifuged at 11,000 rpm for 5 minutes, (2) The filtrate then had the liquid section carefully removed leaving the solid precipitate in order to minimise the interference of water in the solvent interaction with the biomass and ensure the maximum solubility of the phenolic fraction, (3) The resulting sample cake was placed into a clean 500 ml conical flask and weighed to obtain the pre-extraction weight, (4) A

mixture of dichloromethane (CH_2Cl_2) and ethanol in a 3:1 ratio was added to the biomass cake and 200 ml of solvent mixture was added to each sample. Ethanol was included in order to encourage the movement of phenolics in the remaining aqueous fraction into the dichloromethane solvent, (5) The flasks were sealed with parafilm to prevent solvent evaporation and the samples left overnight in the fume cupboard on an orbital shaker (Heidolph-Unimax, 2010) at 100 rpm, (6) In a fume cupboard a Buchner flask and funnel with a 7µm GFA filter was set up and attached to a vacuum pump, (7) The sample was then passed through this filter. Once all of the filtrate had been passed through the filter, the biomass was removed from the funnel and placed into labelled aluminium foil. This was dried in an oven to obtain a final post-extraction dry-weight. (8) The solvent filtrate was transferred to a round-bottom flask. This then was attached to a rotary-evaporator vacuum in order to precipitate out the phenolics held in the solution and remove any water. This was achieved by setting the roto-evaporator water bath to 70°C and to 125 rpm. The temperature was not raised above this setting in order to prevent changes in the chemical structures of the degradation products or reconstitution of the lignin structure, (9) When evaporation was fully complete the round-bottom flask was removed from the roto-evaporator and approximately 100 ml of dichloromethane was added to re-dissolve the precipitate, (10) This solution was then transferred to glass vials, which were labelled and weighed, and left to evaporate over 24 hours until only a dry precipitate remained. Often the solution would separate with a layer of carboxylic acids and lipids forming on top of the main body of the solution due to differences in density. These layers were removed using a 250µl adjustable pipette with a 200µl disposable tip and placed in a separate glass vial to evaporate to a dry precipitate ready for Fatty

Acid Methyl Ester (FAME)/ Phospolipid Fatty Acid (PLFA) analysis, (13) This sample was also used for chemical compound analysis using LC-MS (Figure 16).

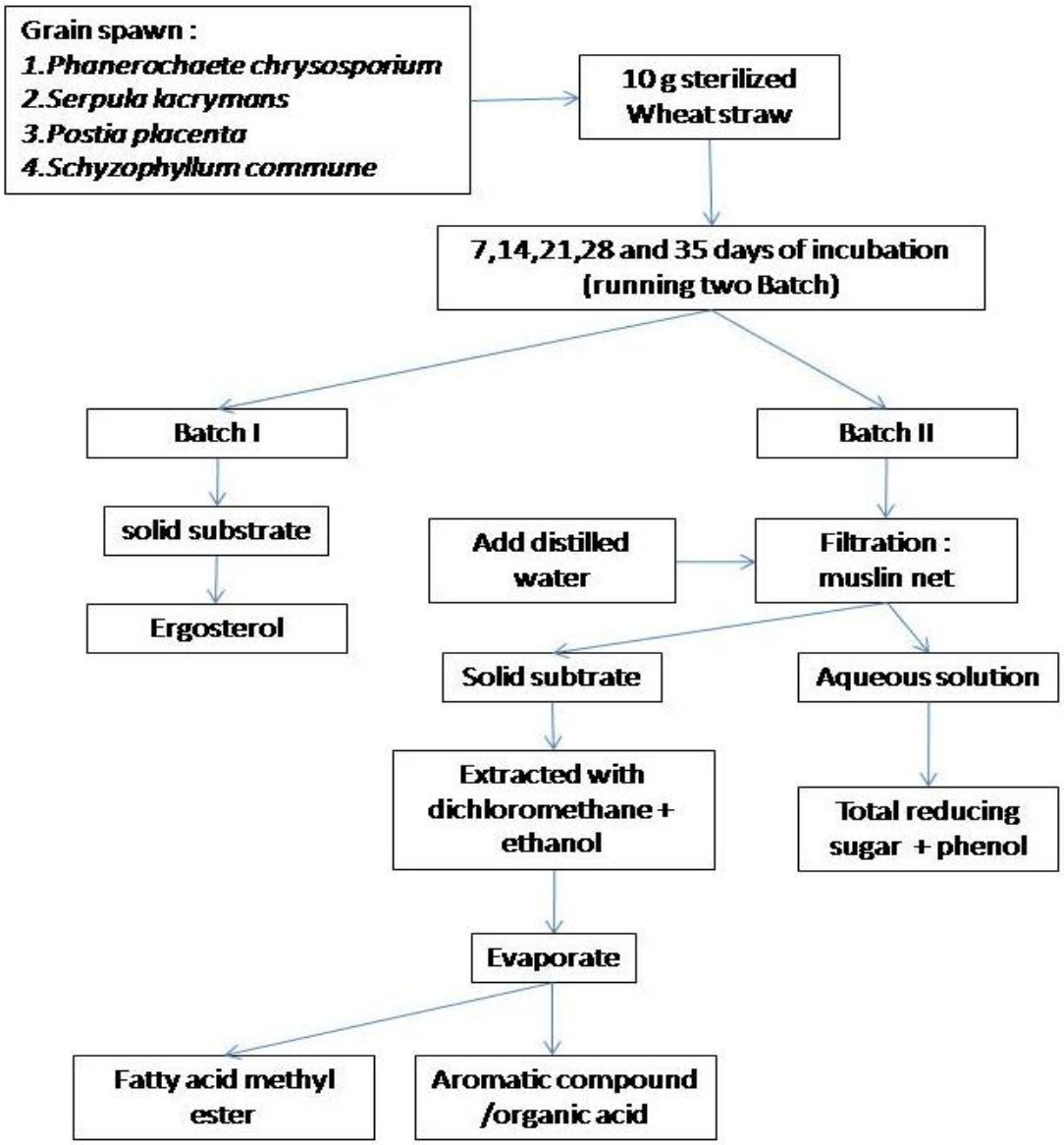

Figure 16. The schematic diagram of the extraction and analytical procedure for straw-based fungal culture

2.2.3. Fungal growth in liquid media and mycelium collection

Mycelium was also grown in liquid culture in order to determine fungal growth rates and for ergosterol analysis. Czapek Dox media was chosen for culturing both white and brown rot fungi in this study. This medium consisted of: (1) 1 g potassium dihydrogen orthophosphate (KH_2PO_4), (2) 0.5 g MgSO4, (3) 10 mg Ferrous sulphate ($FeSO_4$), (40 g l^{-1} sucrose ($C_{12}H_{22}O_{11}$), 2 g l^{-1} sodium nitrate ($NaNO_3$), 1 g l^{-1} KCl (potassium chloride). The medium was sterilized at 121°C; 100kPa (15 Psi) for 15 minutes, before 5 disks from pure agar cultures were added together with1 g of grain spawn. The 4 different fungal species were grown using 5 replicates.

When incubation was complete, the hyphae (mycelium) in liquid media were filtered out using a muslin cloth. The mycelium weight was determined gravimetrically, after freeze-drying for 24 hours. Fungi were selected for molecular assays based on fungal growth performance and product release (water and chemical soluble fraction).

2.2.4. Molecular assay (RNA extraction)

Molecular assays were used to determine genes that regulate degradation lignocellulosic wheat straw biomass.

Principally the RNA from the selected fungus was extracted using Fast RNAPro Soil-Direct Kit (MP-Bio).). The Basic protocol for RNA extraction was as follows: (1) 0.5 to 1.0 g of mycelium was transferred to a purple sample tube which contained Lysing Matrix E; (2) 1 ml of RNAPro^{TM} Soil Lysis Solution were added

into the tube; (3) To resuspend the mixture, the solutions was inverted several times by ensuring that the cap was closed to prevent leakage. The tube was then processed in the Fast Prep Instrument for 40 seconds at a setting of 6.0 ; (4) The tube was then removed and centrifuged at 14.000 x g for 5 minutes at room temperature ; (5) The liquid then was transferred into new microcentrifuge tubes ; (6) Phenol : Chloroform (1:1) was added to the solution and vortexed for 10 seconds ; (7) After incubating for 5 minutes at room temperature to permit nucleoprotein dissociation and increase RNA purity the solution was centrifuged again at 14,000 for 4 minutes at 4^oC ; (8) The aqueous phase was remove to a new centrifuge tube without disturbing the interface; (10) 200µl Inhibitor removal solution was added and the tube was inverted 5 times for complete mixing and then it was centrifuged again at 14,000 x g for 5 minutes at room temperature; (11) The liquid above the pellet was removed to a new microcentrifuge tube; (12) 100 % cold isopropanol (660 µl) was added to the sample, the tube was inverted 5 times for mixing and placed at -20^oC for 30 minutes followed by centrifugation at 14,000 x g for 15 minutes at 4^oC and the supernatant was discard; (13) The RNA pellets were washed with 500 µl of cold 70% ethanol (made with DEPC-H_2O); (14) The ethanol was removed and the pellet was air dried for 5 minutes at room temperature ; (15) The RNA was resuspended in 200 µl of DEPC-H_2O ; (16) RNA MATRIX (600 µl) Binding Solution was added along with 10 µl of RNA MATRIX slurry to the RNA following an incubation at room temperature on a shaker table/rotator with frequent inversion for 5 minutes ; (17) The mixture then was spin in a microcentrifuge at 13,000 rpm for 10 seconds to pellet the RNAMATRIX-bound RNA and the supernatant was discharged; (18) The RNAMATRIX-bound RNA was resuspended in 500 µl of prepared RNAMATRIX

Wash Solution and again spin in a microcentrifuge for 10 seconds and any residual wash solution was removed with a pipette following air dring for 5 minutes ; (19) 50 µl of DEPC-H_2O was added and the RNAMATRIX was resuspended by vortexing then incubated for 5 minutes at room temperature to elute the RNA. The tube bottom was fingered tapped frequently to provide gentle mixing; (20) The mixture again was centrifuged for 10 seconds and the supernatant containing eluted RNA transferred to a new tube; (21) By repeating steps 19 and 20, a final volume of 100 µl RNA was collected.

Chapter 3. Selecting a potential fungal lignocellulosic degraders suitable for solid-state fermentation.

3.1 Introduction

3.1.1 Solid State Fermentation (SSF)

The term solid state fermentation (SSF) is used to refer to culturing microorganisms on moist solid substrates, which can be used as a source of carbon or nitrogen, without a free aqueous phase. These fermentation conditions require less water, thus more closely resemble the natural environment to which the microorganisms are adapted (Pandey et al., 2000). This method is capable of achieving high yields of fermented products (Holker et al., 2004). Due to increase the scale of SSF, several strategies associated with SSF process have been improved, although validation at a large scale is lacking (Mitchell et al., 2000).

Compared to submerged fermentation, SSF has similar yields, however it has the following advantages: (1) no excess water or limited water use, (2) inexpensive sterilization, (3) simple aeration and simple reactor design, (4) reduced operational cost and low energy requirements, (5) inexpensive product recovery and drying, (6) more natural conditions for lignin degrading fungi to grow, (7) lower risk of contamination from bacteria, (8) uniform dispersion of inoculum through the medium, (9) lower levels of pollutants and lower solvent used (Lee, 1997; Toca-Herrera et al., 2007) However, the disadvantages of SSF over submerged fermentation were also reviewed and reported by Toca-Herrera et al. (2007) to be as follows: (1) limited to microorganisms which can grow at low moisture levels, (2) substrate required for pretreatment (chopping, grinding, etc), (3) monitoring

conditions (pH, moisture, oxygen) and biomass yield are difficult, (4) high volume of inoculums is required, (5) risk of contamination by other fungi, (6) lack of aeration and heat transfer, (7) requires a longer period of cultivation.

Figure 17 shows the detail of SSF. Following fungal sporulation fungal hyphae develop into a mycelial mat, while the aerial hypha allow gaseous exchange to occur. The metabolic activities shown mainly occur close to the substrate surface and within the pores and the products, such as enzymes, metabolite and biochemical products are mostly released during fermentation into the solid matrix, therefore these products need to be extracted for further use (Holker and Lenz, 2005).

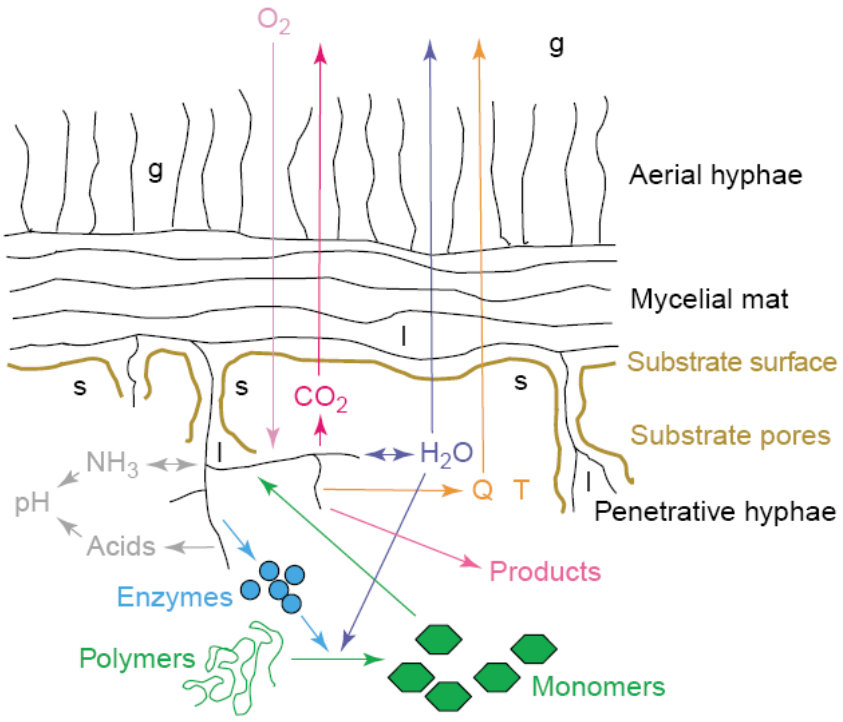

Figure 17. Micro-scale schematic model of SSF
(Holker and Lenz, 2005)

Temperature, pH, oxygen levels, substrate and moisture content are several important aspects that need to be considered in the optimization of SSF (Holker et al.

2004; Lee, 1997). The optimum growth temperature of most basidiomycetes is 28—30˚C (Jennison et al. 1955), with the maximum temperature for some at 35 to 40˚C (Bis'ko et al., 1983). Most white rot fungi are mesophiles, with a temperature optimum between 15 and 35˚C. *P. chrysosporium*, is a moderate thermophile (Lee, 1997), and the specific growth rate of *Coriolus hirsutus* dramatically increases with increasing temperature up to 30˚C (Emelyanova, 2005) and some thermophilic fungi have optimum growth between 45-50˚C (Wojtczak et al., 1987).

The particle size of SSF media is an important factor, and increasing the solid surface area affects the degree of penetration of the substrate by the fungus. Reducing particle size of aspen wood significantly influenced lignin loss and digestibility rate (Reid, 1985). Kerem et al. (1992) observed that reducing particle size of cotton stalks to less than 2mm was very effective in breakdown by a combination of two mixed cultures of the white rot fungi *P. chrysosporium* and *Pleurotas ostreatus*. However, varying particle size in the range of 1 to 8 mm had no effect on wheat straw degradation by *P. chrysosporium* or *Dichomitus squalens* (Zadrazil and Brunnert, 1982).

Moisture content is also important for fungal growth. A moisture film sufficient to cover the substrate but which can still allow air to circulate through the substrate is used for solid substrate fermentation (Lee, 1997). The optimum water content to degrade lignocellulose in straw was 3ml water per gram straw (Zadrazil and Brunnert, 1982), while delignification of aspen wood by *Phlebia tremellosa* was optimal using 2ml water per gram wood (Reid, 1985).

Aeration is also important to biomass production; it has been found in *Coriolus hirsutus* that the effective oxygen supply was 0.9-1.5g O_2 per liter per hour

(Emelyanova, 2005). Increasing O_2 pressure beyond 1 atm (100 kPa) did not increase the rate of lignin degradation by *P. chrysosporium* (Reid and Seifert, 1980), while *Phlebia tremellosa* degraded lignin in aspen wood at a partial pressure of O_2 as low as 7 kPa (Reid, 1985).

Optimum pH for growth varies depending on the microorganism. The optimum pH for basidiomycetes is between 5-6 (Bis'ko, et al., 1983). Most white rot fungi grow best at a pH of between 4 and 5. The optimum pH for growth also varies with substrate composition (Lee, 1997). For example, the optimum radial growth of *Coriolus hirsutus* in agar culture was found to be pH 5-6, Emelyanova, 2005). pH also influences enzyme production, particularly cellulase (Pardo and Forchiassin, 1999). The optimum pH for cellulase production is 5.5 for *Aspergillus niger*, while pH 5.5-6.5 is optimum for β-glucosidase production by *Penicillium robrum*. Enzyme production is dependent on nutrient availability and increases when there is an addition of a nitrogen source, such as ammonium sulfate or nitrate. Similarly, phosphorus availability affects fungal growth and metabolism (Gark and Neelkantan, 1982). Phenolic compounds and sugar levels also influence enzyme production (Kumar et al., 2008).

The degradation of wheat straw SSF is also influenced by nutrient amendment. Lignin degradation by many white rot fungi is maximal under nitrogen supplementation (Lee, 1997). The addition of urea stimulates lignin degradation of wheat straw by *Coprinus sp.* (Yadav, 1987) and greater ligninolytic activity is also influenced by the addition of C, particularly glucose, as shown with *Trametes versicolor* in a straw fermentation system (Zafar et al., 1996). Glucose, ammonium sulphate and molasses were used as nutrient supplements at various stages of *T.*

versicolor SSF. The effects of supplying nitrogen on the production of lignocellulose degrading enzymes (e.g carboxymethyl cellulase, xylanase, laccase, manganese peroxidase) by white rot basidiomycetes (e.g *Pycnoporus coccineus, Cerrena maxima, Funalia trogii, Trametes pubescens, Coriolopsis polyzona, Pleurotus ostreatus*) have been examined by Elisashvili et al. (2008). They compared wheat straw with other substrates (e.g tree leaves, apple peels, banana peels). In general, the addition of nitrogen sources such as KNO_3, $(NH_4)_2SO_4$, and NH_4NO_3 in *P. ostreatus* wheat straw SSF lowers specific enzyme activities (e.g. xylanase, laccase or manganese peroxidase), however, it has a positive impact on protein production (Elisashvili et al. 2008). In contrast, the degradation of wheat straw lignin by *P. chrysosporium* is more effective under nitrogen-starved conditions compared to *Coriolus versicolor* (Zafar et al., 1989 and Fenn and Kirk, 1981). It has been reported that cellulose dropped from 42.3% to 38% after 35 days of incubation. *Coriolus versicolor* degraded cellulose rapidly within the period of 14 and 21 days before levelling off beyond this period and the lignin content declined from 12.4 to 7.2% after 35 days of incubation (Zafar et al., 1989).

3.1.2 Fungal Biomass

Fungal growth is difficult to quantify, as fungi do not grow as single cells, but as hyphae that cannot be quantified using the usual enumeration techniques. Fungi differentiate to produce spores, resulting in large increases in viable counts often with little relationship to biomass (Pitt, 1984). Thus, in order to determine the efficacy of lignocellulose degradation, it is important to know the amount of fungal

mycelium in solid substrate and establish more reliable and convenient methods for measuring fungal growth in solid-state fermentation (SSF). A number of methods have been developed for quantifying fungal growth and their principles and applications comprehensively reviewed (Matcham et al., 1984; Hartog and Notermans, 1988; Williams, 1989; Newell, 1992; Samson et al., 1992; de Ruiter et al., 1993; Pitt and Hocking, 1997). The conventional microscopic method has long been used. However, it is known to be easy to create measurement errors (de Ridder-Duine et al., 2006).

Ergosterol is found as the main sterol in fungal cell membrane, as a minor component in many plants and is also found in most yeasts and algae (Pasanen et al., 1999; Nielsen and Madsen, 2000; Hippelein and Rugamer, 2004; de Ridder-Duine, 2006). It is specifically a major component of mycelia, spores, and vegetative cells (Newell, 1992; Pasanen et al., 1999) and plays a role in several biochemical processes such as membrane fluidity, cation permeability and cell growth (Bossche, 1990; Hippelein 2004). Since there is a good relationship between ergosterol content and hyphal length, ergosterol is recommended for quantifying fungal growth (Schnurer, 1993; Pasanen et al., 1999). However, the amounts of ergosterol are known to vary between different fungal species, period of culture, stages of development, and growth conditions (Gessner and Chaucet, 1993; Newell, 1994; Schnurer, 1993; Pasanen et al., 1999). Ergosterol measurement is recognised as a biomarker for assessing fungal biomass in solid media or soil, since it is difficult to measure mycelial biomass directly when closely associated with the substrate (Niemenmaa et al., 2008). Montgomery et al. (2000) suggested to use a conversion factor to calculate fungal biomass from ergosterol concentration.

The average ergosterol content in several fungal species ranges from 2.6 to 42 µg ml^{-1} of dry mass (Pasanen et al., 1999), while Hippelein and Rugamer (2004) reported that ergosterol concentration in several fungi varies from 0.1 to 130 µg g^{-1} of dry mass. Moreover, Montgomery et al. (2000) obtained an average of 4µg ergosterol/mg of biomass using six species of fungi, in which per 250 µg dry fungal biomass was the equivalent of 1 µg of ergosterol. In liquid cultures the conversion factors for ergosterol to biomass has been shown to vary from 48 to 243 and 185 to 88 for *P. radiata* and *P. chrysosporium* respectively (Niemenmaa et al. 2008). However, this conversion factor cannot be applied to the other type of fungi due to different fungal physiologies and other factors such as media, substrate, and nutrients, along with different fungal growth stages (Klamer and Baath, 2004). Despite the limitation of ergosterol as an indicator of fungal biomass, it has been applied to a wide range of environments such as soil (Gong et al., 2001; Ruzicka et al., 1995: Ruzicka et al., 2000); building material (Hippelein and Rugamer, 2004); indoor environment (Flannigan, 1997); house dust (Saraf et al., 1997) ; grain (Borjesson et al., 1990) ; seeds (Richarson and Logendra, 1997) ; plant litter (Gessner and Newell, 2002) ; plant material (Newell, 1992) agar media, and wood (Niemenmaa et al., 2006). Gong et al. (2001) reported that the ergosterol content of soil samples ranged between 0.34 to 2.5 µg g^{-1}, whilst the amount of ergosterol in fungal agar and wood substrate varied between 149 to 539.5 µg g^{-1} and 15.3 to 42.9 µg g^{-1}, respectively (Niemenmaa et al., 2006). These results show a diverse range in ergosterol content between fungal types and the culture media. However there is little information available for the white rot, and brown rot fungi (basidiomycetes),

therefore studies of ergosterol fungal biomass grown in wheat straw SSF are needed to determine the efficacy of this assay for these species.

Several methods of ergosterol extraction are used: (1) free ergosterol which is soluble in alcohol, (2) total neutral ergosterol from saponification of alcoholic extract, (3) total alkali ergosterol which is extracted and saponified in alkaline alcohol solution (Davis and Lamar, 1992; Hippelein and Rugamer, 2004). Gong et al. (2001) developed a physical disruption technique to simplify extraction by replacing the time-consuming reflux step. In order to maximize ergosterol release from fungal membranes, Ruzicka et al. (1995) proposed using an ultrasonic method in combination with non-alkaline extraction for ergosterol sample from clay loam soil. Following extraction ergosterol abundance was measured using normal phase HPLC. This method has been limited to measuring the ergosterol from soil, and has not previously been used to measure fungal growth during SSF. We used this method to estimate fungal biomass of different types of brown rot and white rot fungi (*Basidiomycetes).* It has been reported that measuring ergosterol is more accurate than other fungal biomass estimation approaches that measure molecules such as chitin or adenosine triphospate (ATP) (Klamer and Baath, 2004). However, another method for measuring fungal biomass such as phospolipid fatty acid (PLFA) has also been used in combination to combine with the ergosterol method. PLFA has been used as another fungal profiling parameter for minimizing the uncertainty of ergosterol assay results and as a complement to measurement of fungal biomass (de Ridder-Duine, 2006; Klamer and Baath, 2004). Total PLFA content has been found to have a positive correlation with bacterial or fungal biomass, at the same time it can be distinguish the fingerprint of microbial communities (Frostegard and Baath,

1996). The PLFA 18:2n6, represents PLFA for fungi (Klamer and Baath, 2004), since it represent 45% of fungal body (Federle, 1986) and is absent in bacteria. This marker is also used for fresh plant biomass (Frostegard and Baath 1996; Snajdr et al., 2011), however the content of this PLFA (18:2n6) in dead plant biomass decreases rapidly (Snajdr et al., 2011).

The PLFA assay has been used successfully to monitor *P. chrysosporium* biomass during its cultivation on rice straw (Yu et al., 2009). A relationship between PLFA (18:2ω6,9) and ergosterol content gave a conversion factor of 1.47 µmol 18:2ω6,9 to 1 mg ergosterol using 12 different fungal species in PDA culture (Klamer and Baath, 2004). In pure culture, Eiland et al. (2001) recorded a value of 2.1 µmol 18:2ω6,9 to 1 mg ergosterol. PLFA (18:2ω6,9) depending on growth and the type of ecosystem (e.g soil and compost). Only a few attempts have been made at determining fungal biomass from direct PLFA measurement (Klamer and Baath, 2004). PLFA does not provide a good taxonomic marker (Lechevalier and Lechevalier (1988) as there is a possibility of obtaining similar fatty acid fingerprints for both Ascomycetes and Basidiomycetes. Multivariate analysis is a powerful tool for distinguishing fatty acid profiles and profiling using this approach for fungi was proposed. Muller et al., (1994) studied the differences in profiles of fatty acid, fatty acids and sterols of fungi using multivariate discriminant analysis.

The objective of the present study was to monitor sequential changes in ergosterol and PLFA 18:2ω6,9 content from selected Basidiomycetes cultured in SSF, in order to estimate fungal biomass. A multivariate statistical analysis was also employed to distinguish the PLFA fingerprint for each fungal species.

3.1.3 Lignocellulose degradation and potential products.

Release of the chemical constituent from wheat straw SSF usually requires a pretreatment process involving steam and acid (eg. H_2SO_4). The impact of pretreatment on wheat straw SSF has been studied by Linde et al. (2008), in which the effect of temperature and duration of pre-treatment significantly impacted the yield of various products such as hydroxymethylfurfural, furfural, acetic acid and glucose (Table 8).

Table 8. Products released after pretreatment of dry straw (Linde et al., 2008)

Temp (^oC)	Time (minute)	Hydroxymethylfurfural (g $100g^{-1}$)	Furfural (g $100g^{-1}$)	Acetic acid (g 100 g^{-1})	Glucose (g 100 g^{-1})
190	2	0.07	0.09	0.04	1.09
190	5	0.09	0.19	0.16	1.43
190	10	0.17	0.47	0.81	1.81
200	2	0.11	0.16	0.11	0.90
200	5	0.18	0.40	0.36	0.92
200	10	0.26	0.70	1.01	2.03
210	2	0.05	0.35	0.39	1.25
210	5	0.11	0.91	0.82	0.95
210	10	0.22	1.18	0.96	0.69

Table 8 revealed that at the lowest temperature (190^oC) for 2 minutes pretreatment, the production of hydroxymethylfurfural (HMF), furfural and acetic acid was 0.07, 0.09 and 0.04 g 100 g^{-1} dry weight straw respectively. At the highest temperature (210^oC) and longest duration of the process produced these components were produced of 0.22, 1.18 and 0.96 g 100 g^{-1} dry weight straw (Linde et al. 2008).

Often several processes are used in conjunction, for example the use of steam combined with the addition of chemicals such as acetic acid and/or ethanol as wheat straw pre-treatment are more effective than steam explosion alone for sugar release.

The treatment of steam explosion only, at 210^{o}C and 10 minutes yielded sugar at 177.3 g kg^{-1} dry basis, whilst steam/acetic acid treatment and steam/ethanol released sugar at the levels of 244.1 g kg^{-1} and 264.3 g kg^{-1} (Zabihi et al., 2010).

The type of substrate affects total sugar production. In *T. viride* SSF, the highest yield of sugars was observed using wheat straw followed by barley straw, wood waste, sawdust, and corn (maize). Moreover, the greatest amount of fungal biomass (5.2 g l^{-1}) was produced using wheat straw (Zayed and Meyer, 1996) (Table 9).

Table 9. The amount of total reducing sugar and its relationship with fungal dry weight and residual substrate following growth of *T. viride* SSF various substrates (Zayed and Meyer, 1996).

Raw material	Total sugar (g l^{-1})	Fungus dry weight (g l^{-1})	Residual substrate (g l^{-1})
Wheat straw	5.7	5.2	10.0
Barley straw	2.8	3.3	14.7
Corn straw	1.8	3.7	17.5
Wood waste	2.4	3.0	16.0
Sawdust	1.8	3.7	19.8

Sugars, ethanol, aromatic and polyaromatic compounds can all be produced from lignocellulose biomass. Two important aromatic compounds; benzaldehyde and vanillin (de Jong et al., 1994), and a novel antibiotic have also been identified as products from the degradation of lignocellulose (Ralp and Catcheside, 2002). Dorado et al. (1999) tested the efficacy of four different white rot fungi (e.g *P.chrysosporium, P eryngii, P.radiata,* and *C.subvermispora*) in SSF for their capacity to degrade wheat straw.

Sun et al. (2005) developed a method for extraction and characterization of lignin and hemicelluloses from wheat straw using chemicals (eg. toluene, HCl, ethanol and dymetyl sulfoxide). These can be extracted as platform chemicals on an

industrial scale for synthesizing further valuable products. The predominant products were vanillin (24.50%) and syringaldehyde (31.50%). Minor quantities of coumaric acid and ferulic acid were also obtained (Table 10).

Table 10. A List of the phenolic acids and aldehydes extracted from the lignin and hemicelluloses fractions isolated from wheat straw by Sun et al., (2005).

	Yield (%)	
Products (Phenolic acid and aldehydes)	Lignin fraction[a]	Hemicelluloses[b]
ρ – hydroxybenzoid acid	1.80	ND
ρ - hydroxybelzaldehyde	3.09	0.17
Vanillic acid	2.81	0.14
Vanillin	24.50	0.82
Syringic acid	4.33	0.07
Syringaldehyde	31.50	0.46
Acetovanillin	5.10	0.25
Acetosyringone	3.12	0.14
ρ – coumaric acid	0.06	ND
Ferulic acid	0.08	ND
Cinnamic acid	0.15	0.07

ND = Not detected

a. Lignin fraction solubilized during treatment with 80% dioxane with 0.05M HCl for 4h at 85ºC
b. Hemicellulose preparation solubilized in 80% dioxane with 0.05M HCl.

Information on the chemical products released during solid state fermentation (SSF) using different microbes is necessary as there are currently only limited studies on the chemicals that could be produced through microbial degradation of lignocelluloses. In this study, the breakdown of wheat straw in SSF was examined using different types of fungus (white rot: *P. chrysosporium, S. commune* and brown rot: *S. lacrymans, P. placenta*).

3.2 Methods

3.2.1 Fungal biomass (Ergosterol assay)

Fungal biomass was assessed through measurement of ergosterol levels in liquid cultures of two white rots (*Phanaerochaete chrysosporium* and *Schizophyllum commune)* and two brown rots (*Serpula lacrymans* and *Postia placenta*). Pure cultures of these fungi were supplied by the Warwick Life sciences collection and stored at 4ºC in a cold room. A single pure culture of each fungus was grown on agar medium and five agar inocula plugs were then transferred into 100 ml liquid media (2% w/v Malt extract) in 1 L tissue culture bottles. Five cultures were made for each fungus and all were cultivated for 35 days. Mycelium was then harvested, freeze-dried and divided into dry weights of (0.2 mg; 1 mg; 5 mg; 7 mg and 10 mg) before measurement of ergosterol. These measurements could then be used to derive a standard curve of ergosterol concentration for each fungus.

The ergosterol content of wheat straw during the SSF (method is described at chapter 2) was measured using a modified method developed by Gong et al. (2001) which involved physical disruption of the mycelium using two different acid washed glass beads (10 mg of 212-300 µm diameter and 10 mg of 710-1180 µm diameter). The different aliquots of mycelium were resuspended in 2ml ethanol and vortexed for 10 seconds in a 20 ml scintillation vial, then were placed into a basket in an orbital shaker for about 1 hour at 25ºC; 350 rpm in darkness. The samples were then allowed to sediment for 15 minutes before a 1.5 ml aliquot was removed into 2ml eppendorf, this was then centrifuged for 10 minutes at 11.000 rpm at 4ºC. The supernatant was filtered (0.2 µm) and the filtrate transferred into 1ml dark vials before being loaded into an auto sampler for HPLC analysis. Ergosterol was

quantified using a C_{18} reverse column with UV detection at 282 nm. Methanol was used as the mobile phase with a flow rate of 1.5 ml min^{-1}. Ergosterol content was calculated as microgram per gram of fungal mycelium. The amount of ergosterol was then compared with the standard (from Sigma-Aldrich) and a conversion factor derived with which to estimate biomass for each fungus.

3.2.2 Identifying fatty acid pattern (PLFA/FAME)

Phospholipid fatty acid (PLFA) or Fatty acid methyl ester analysis (FAME) was carried out on the upper layer of the solvent extraction sample and was performed on the incubation series (0, 7, 14, 21, 28 and 35 days). 0.5mg of powdered extraction was extracted and 10 µL 15:0 TAG (triacylglycerol) internal standard which consist of 25 mg ml^{-1} tripentadecanoin (Sigma p/n T4257) was added to each sample before it was mixed with 500 µL 1 N HCl/MeOH. Subsequently, samples were vortex mixed with and transferred to an oven at 80^{o}C and left to incubate for 10 hours. To release fatty acids, 250 µL 0.9% KCl was added followed by the addition of 800 µL hexane and vortex mixed. The layers were allowed to separate for 10 minutes. Approximately 500 µL of the upper hexane layer was transferred to a fresh vial and stored at 4^{o}C until used for phospholipid fatty acid or fatty acid methyl ester measurement. An automatic sampler unit of the GC machine (Agilent technology 6850 network GC system) transferred and injected the sample into the detector. The amount of fatty acids was assessed by measurement of the summed area of peaks in the chromatogram.

3.2.3 Total reducing sugar and total soluble phenol assay

150 mL hot water (80^{o}C) was used for the extraction of colonized straw; this was added to each jar, which was then placed onto an orbital shaker at 37ºC for 15 minutes at a speed of 100 rpm. The mixture was then filtered through muslin (synthetic) cloth and a particle-free filtrate was obtained after centrifugation at 18000 rpm for 15 minutes. Soluble phenolics and reducing sugar analyses were performed on the aqueous extract samples using 4 replicates for each sampling point. Reducing sugars were determined colourimetrically by the DNS (dinitrosalicylic acid) method using glucose as the standard (Miller, 1959) and the absorbance was read at 540 nm using a spectrophotometer. In order to minimize sugar variation, there were 3 replicates of each sample.

Phenols were measured colourimetrically using the Folin-Ciocalteau method with gallic acid as the standard and the absorbance was read at 760 nm using a spectrophotometer. This colorimetric method is based on chemical reduction of the reagent, a mixture of tungsten and molybdenum oxides which results in a blue colour at measurement at 765nm (Singleton and Rossi, 1965). The intensity of light absorption at that wavelength is proportional to the concentration of phenols.

The concentration of phenols and reducing sugar was expressed per gram of substrate (dry weight).

3.2.4 Analysis of sugar fractionation.

An HPLC (Agilent 1100 series) with refractive index detector (RID) with an Aphera NH_2 polymer HPLC column 25cmx4.6x5µl was used to determine the concentration of the different sugars. The standard monosaccharide kit from Supelco, which contains: arabinose, xylose, fructose, mannose, glucose, galactose and ribose were used to prepare standard curves for each sugar. Calibration curves were prepared using 5 concentrations at 5;10;30;60 to 100 mg/ml. Samples from time courses of white and brown rot fungi grown on wheat straw cultures were subject to aqueous extraction. The samples were dissolved in 1 ml of solvent (Acetonitrile : water) 80:20. Due to the low concentration of sugars in the aqueous extract, samples were concentrated using a vacuum evaporator RC 1022 from 1ml to 100µl of extract. Samples were then separated using HPLC with a mobile phase of ACN:water (80:20) and a flow rate of 1.5ml/min with an injection volume of 30µl. The sugars were detected at 280nm. Comparison of the retention times of the standards with the samples allowed identification of the peaks of the compounds and the respective area could then be used for quantification.

3.2.5 Aromatic/organic compounds in wheat straw SSF extract

To identify aromatic/organic compounds in degraded wheat straw, samples were prepared using dried solvent precipitation (as described in chapter 2). The powdered residue was dissolved in 1ml methanol in a micro-centrifuge tube and mixed with acetonitrile (50:50). After centrifugation the solvent was injected into the LC-MS machine (Thermo Fisher-Serial number LTQ 20SIP) in which samples were

separated by polarity at a flow rate of 1ml min^{-1} using water to solvent gradient 90% water; 10% methanol: acetonitrile (50:50) changing to 10% water: 90% methanol: acetonitrile over 40 minutes. The LC-MS chromatograph uses a reverse phase Hypersil Gold C8 column of 250x4.6mm dimension and maximum particle size of 5µm. In order to provide molecular mass data for each LC peak and to allow potential identification of the compounds in the sample, separated compounds were passed through a mass spectrometer based on their solubility in solvent eluent in the mobile phase, and the samples were flushed with a blank of methanol every run of six samples to avoid contamination. Peaks were identified by Michrom Xcalibur software and the instructions of data analysis using LCMS was presented in Appendix 2.

3.3 Results

3.3.1 Ergosterol and fungal biomass

Fungi were cultured in liquid media in order to collect fungal mycelium and link biomass to ergosterol content. The ergosterol was used as a method of estimating fungal biomass. A standard curve was established by using a relationship between a peak area and ergosterol concentration (mg/g) based on an ergosterol standard solution (Sigma-Aldrich) and all ergosterol values were plotted on 2-dimension graph. Five concentrations of ergosterol were used to produce a linear standard, showed the relationship between the abundance of ergosterol and dry weight of mycelium in liquid culture (Figure 18). Ergosterol content between the fungi tested was significantly different ($P<0.001$, LSD = 6.67). The highest amount of ergosterol/mg of fungal mycelium in liquid media was observed for *P. placenta*,

followed by *P. chrysosporium*, which was similar to *S. lacrymans*, while *S. commune* was the lowest.

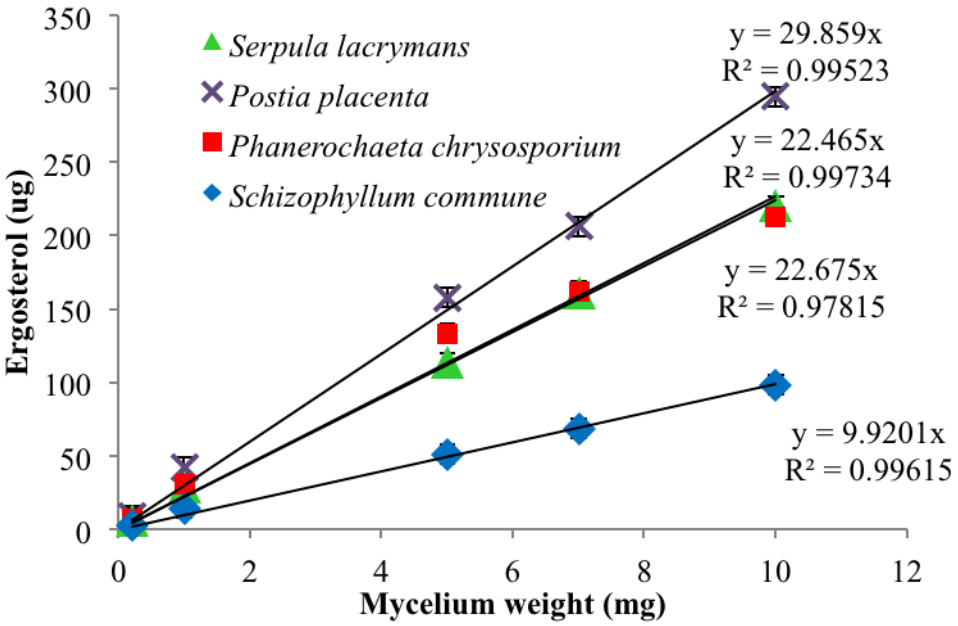

Figure 18. The relationship between ergosterol concentration and the amount of mycelium for the fungi *P. chrysosporium* (PC), *P. placenta* (PP), *S. commune* (SC) *and S. lacrymans* (SL) growing in malt extract liquid medium.
Error bars represent LSD (P<0.05)

It has been reported that ergosterol measurement on liquid media is required to determine if there is any correlation between ergosterol and fungal dry weight before it can be applied to wheat straw SSF (Messner, 1998). In 10 mg of mycelium, *P. placenta* had 294.7µg g^{-1} ergosterol, whereas at the same weight of mycelium *S. commune* contained 98.4µg g^{-1} ergosterol, approximately only 1/3 compared to *P. placenta*, while total ergosterol of *P. chrysosporium* and *S. lacrymans* were similar. Based on the relationship between mycelium weight and total ergosterol, the conversion factor to biomass was derived for four different fungi after they had been incubated for 35 days.

The regressions were all linear with R^2 = 0.995 or even higher. The conversion factors were calculated from the reciprocal of the gradients given in Figure 18. For example, 100 µg ergosterol of *S. lacrymans* is equivalent to 4.45 mg mycelium, higher *P. placenta* which was equivalent to 3.35 mg mycelium. 100 µg ergosterol from *P. chrysosporium* was equivalent to 4.41 mg mycelium which was much lower than 100 µg ergosterol produced by *S. commune* (10.08 mg mycelium).

The constant for each equation was used as conversion factor to determine fungal biomass for each fungus. For comparison, the conversion factors from several fungi reported in the literature varied from 48 to 243 when cultured in liquid medium (Niemenmaa et al., 2008). In the case of *P. chrysosporium* the conversion factor from liquid experiment was 88.

The ergosterol content of *P. chrysosporium* increased during the time course (0, 7, 14, 21, 28 and 35 days) from 24.47-to 98.6 µg g^{-1} wheat straw dry weight, while for *S. lacrymans* it increased significantly from 53.23 to 138.70 µg g^{-1} (Figure 21). In general, a low amount of ergosterol was found at the first time point (7 days). *P. chrysosporium* reached a peak of 98.6 µg g^{-1} after 14 days incubation (Figure 19). A significant difference was found between the fungi and time of incubation ($P < 0.001$), LSD 13.34.

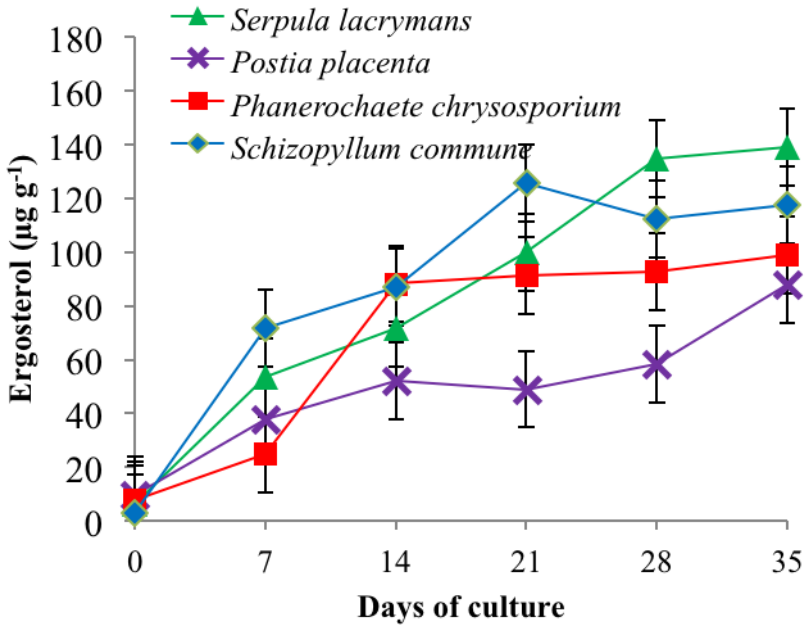

Figure 19. The production of ergosterol during the fungal growth (35 days) by *P. chrysosporium, P. placenta, S. commune and S. lacrymans* growing on wheat straw SSF. Error bars represent LSD (P<0.001)

The amount of ergosterol in wheat straw SSF was higher than ergosterol content previously measured in fungi growing in wood substrate, which was 22.6 µg g^{-1} for *Phlebia radiata* and 23.0 µg g^{-1} for *P. chrysosporium* (Niemenmaa et al. 2006).

By using the conversion factors, the fungal biomasss in wheat straw cultures for each time point was calculated (Table 11). The fungal biomass, in wheat straw after 35 days of incubation with *S. commune* was estimated to be high but this was due to the very different conversion factor obtained (11.98 mg g^{-1}).

Table 11. Predicted fungal biomass content in solid media culture (wheat straw) in mg g^{-1} as calculated from ergosterol measurements.

Fungal Species	**Conversion factor**	**7 days**	**14 days**	**21 days**	**28 days**	**35 days**
Serpula lacrymans	22.46	2.21	3.05	4.34	5.94	6.13
Postia placenta	29.85	0.99	1.48	1.38	1.70	2.74
Phanerochaete chrysosporium	22.67	0.63	3.62	3.77	3.84	4.13
Schizophyllum commune	9.92	7.21	8.78	12.83	11.45	11.98

3.3.2 PLFA/FAME patterns in white and brown rot fungi

A background profile of fatty acids was found in untreated wheat straw, which needed to be subtracted in order to determine the FAME pattern produced by each fungus. Relative abundance (%) of each FAME was measured by comparing the amount of an individual FAME (e.g 18:2n6c) with the total FAME detected. The goal was to distinguish between white and brown rot fungal species based on the FAME structure and to select FAME biomarkers, which could be associated with fungal biomass.

The FAME characteristic of fungus *P. chrysosporium* is presented in Figure 20, 16 types of FAME were detected. Changes in the relative abundance (%) of each FAME were observed from 0 to 35 days after incubation. The most abundant FAMEs of *P. chrysosporium* were found to be 16:0 (20-30%), 18:2n6c (15-30%), 18:1n9c (10%) which reached a peak at 7-14 days after incubation and was significantly different to other FAME ($P< 0.001$). These may contribute 70% of total PLFA. FAME 16:0 indicates *palmitic acid*, 18:2n6c *linoleic acid* and 18:1n9c *oleic*

acid. At the last three time points measured (21, 28 and 35 days), 22:0, 22:2n6, 23:0 and 24:1n9 also appeared.

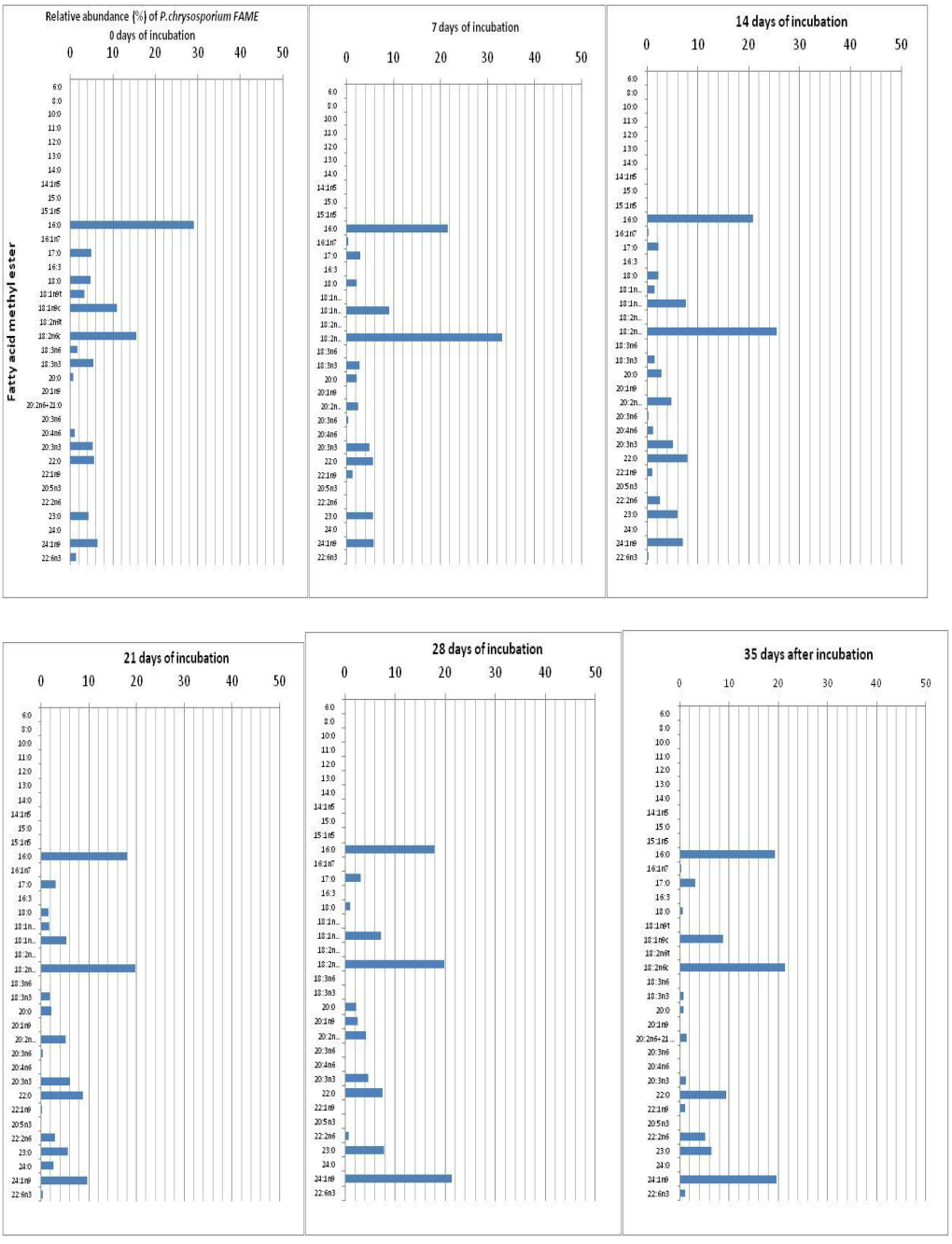

Figure 20. The fatty acid profile showing the relative abundance of each fatty acid methyl ester (%) as a percentage of the total FAME produced by *Phanerochaete chrysosporium* as measured on three separate occasions during the culture period.

A similar pattern of FAME was obtained for *S. lacrymans*, in which 16:0 (20-30%), 18:2n6c (15-50%), and 18:1n9c (10%) were the dominant peaks. These made up 90% of total PLFA. 18:2n6c reached the highest percentage at 28 and 35 days after incubation (50%). 18:1n9t, 22:0, and 24:1n9 (10%) were also dominant peaks in biomass at several time points. Fatty acid 18:1n9t was assigned as *elaidic acid*, 20:0 as *arachidic acid* and 24:1n9 was *nervonic acid* (Figure 21).

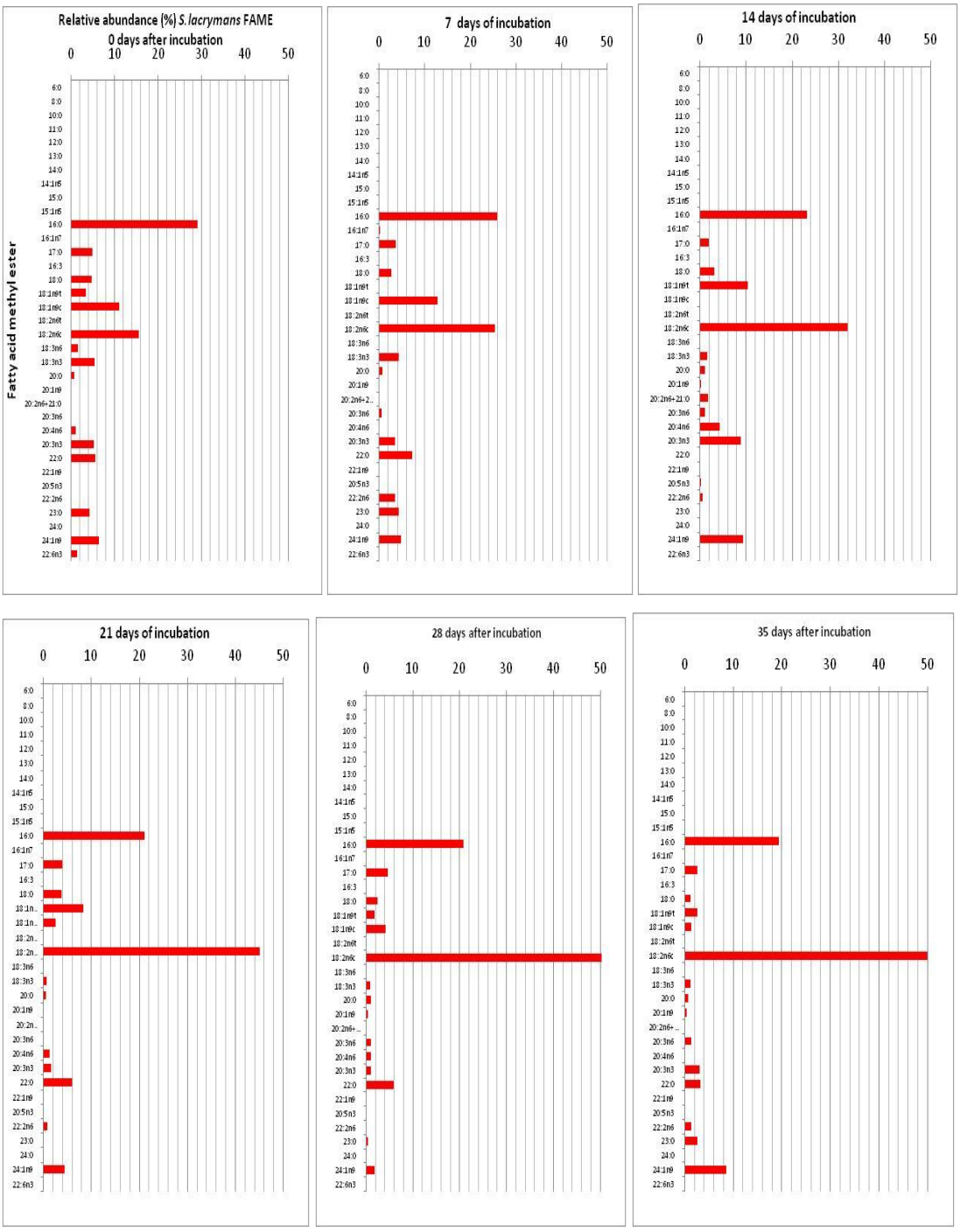

Figure 21. The fatty acid profile showing the relative abundance of each fatty acid methyl ester (%) as a percentage of the total FAME produced by *Serpula lacrymans* as measured on three separate occasions during the culture period.

The FAME pattern of *S. commune* was dominated by 16:0 (*palmitic acid)* ; 18:2n6c (*linoleic acid)* ; 22:2n6 (*docosadienoic acid)* and 18:1n9c *oleic acid* for (Figure 22).

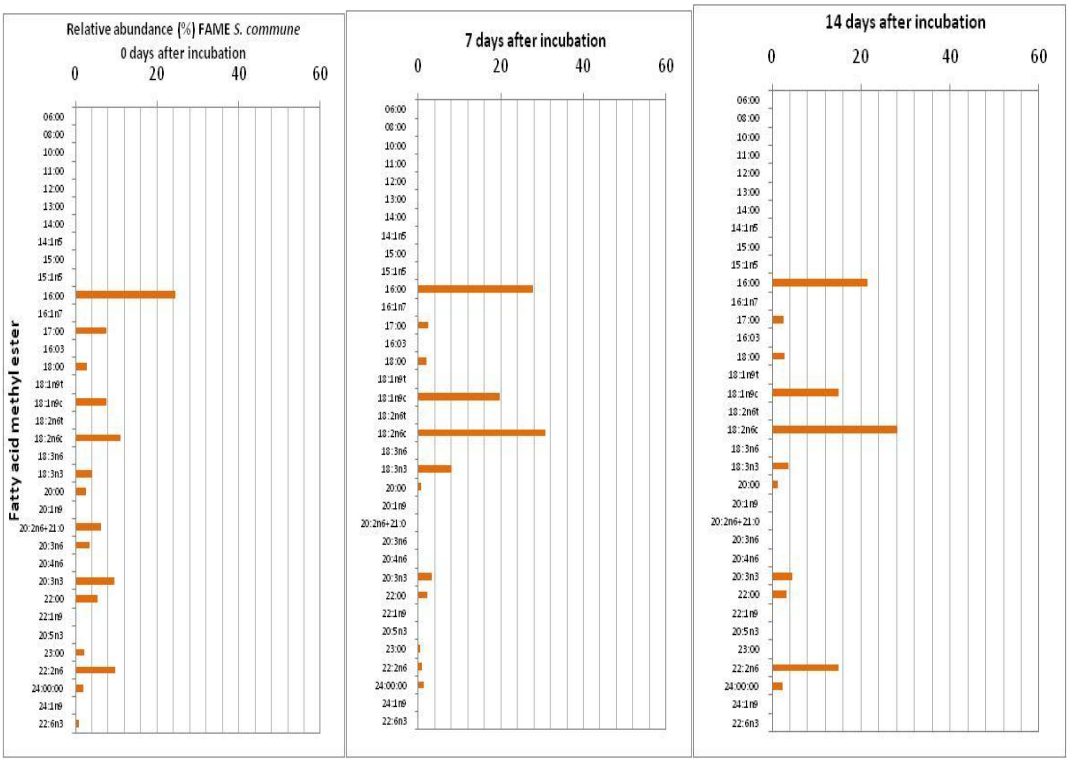

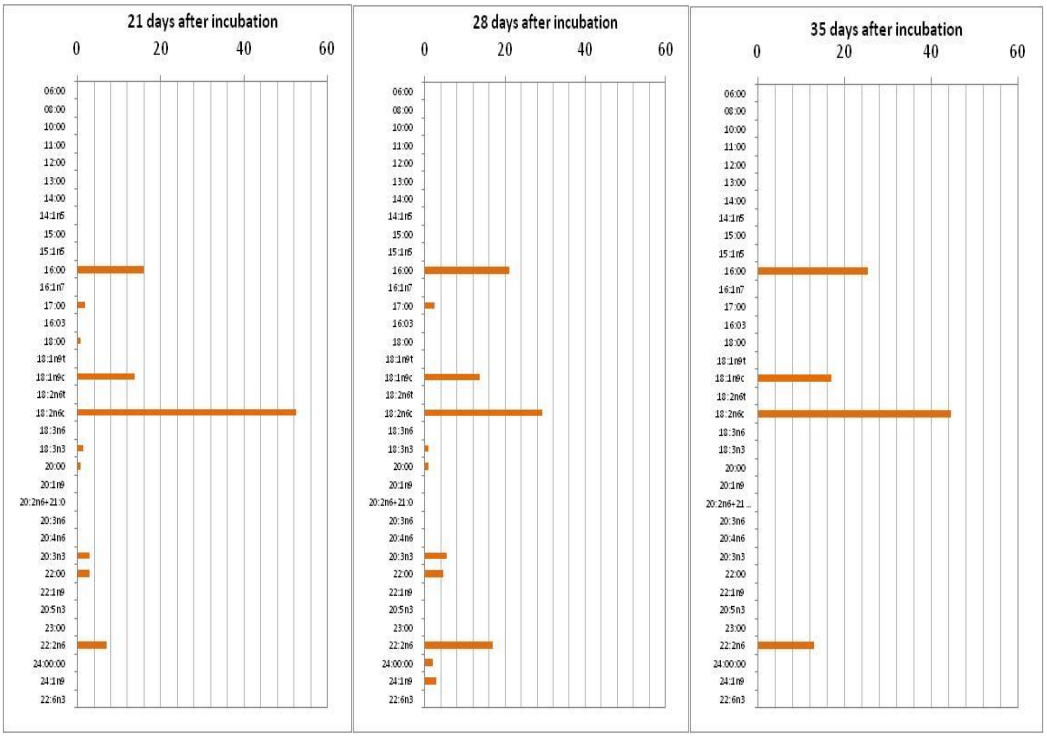

Figure 22. The fatty acid profile showing the relative abundance of each fatty acid methyl ester (%) as a percentage of the total FAME produced by *Schizophyllum commune* as measured on three separate occasions during the culture period.

A different pattern of FAME was found in *P. placenta* which was not only primarily consisted of *palmitic acid*; *linoleic acid* and *oleic acid*, but also 20:3n3 ; 22:1n9 ; 23:00 ; 22:2n6 ; 24:1n9 ; 22:6n3, which made up 60-80 % of total FAME and corresponded to *eicosatrienoic acid, eruric acid, tricosanoic acid, docosadienoic acid, nervonic acid* and *decosahexaenoic acid*, respectively (Figure 23).

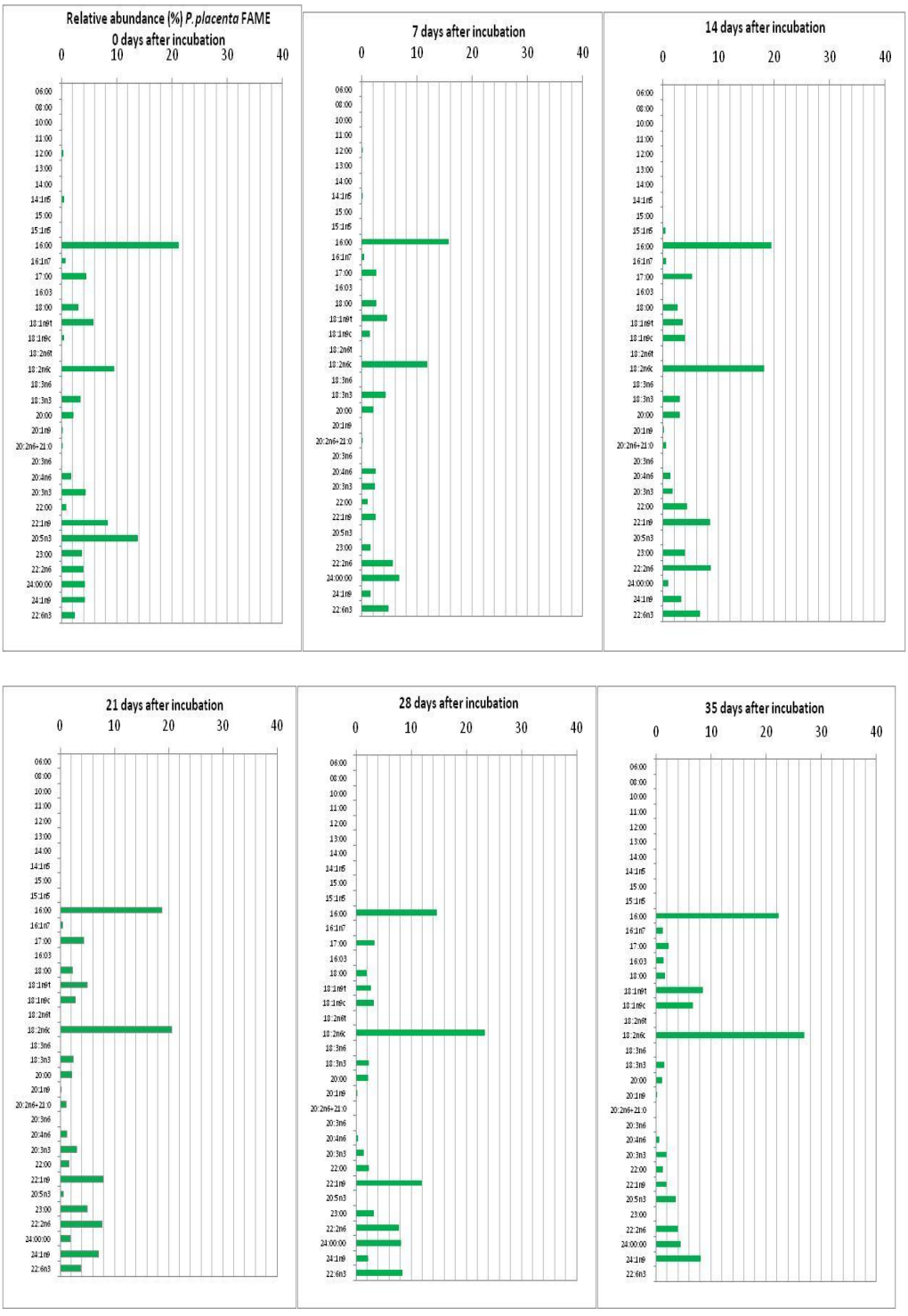

Figure 23. The fatty acid profile showing the relative abundance of each fatty acid methyl ester (%) as a percentage of the total FAME produced by *Postia placenta* as measured on three separate occasions during the culture period.

According to the results above each fungi analyzed has similar types of fatty acid but differed in the relative amount of each. One of the most prevalent PLFA detected in both white and brown rot was 18:2n6c (linoleic acid). The abundance of this fatty acid was 167.46-541.37 μg g^{-1} (*P. chrysosporium*); 186.92-345.78 μg g^{-1} (*S. lacrymans*); 188.49-506.15 μg g^{-1} (*P. placenta*) and 66.35-288.93μg g^{-1} (*S. commune*) (Figure 24). This shows that the white and brown rot fungi have different patterns in the production and use of linoleic acid during fungal growth. The white rot fungi (*P. chrysosporium* and *S. commune*) showed a decrease in the amount of linoleic acid after day 7, while in the brown rots (*S. lacrymans* and *P. placenta*) amount was more correlated with mycelium growth.

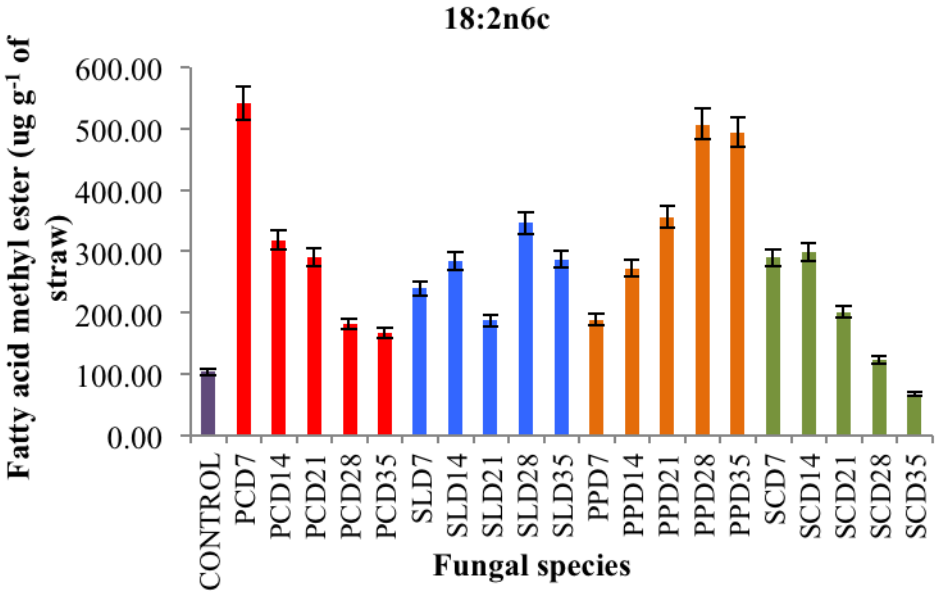

Figure 24. The amount of 18:2n6c (linoleic acid) produced by the white rots (*P. chrysosporium* (PC); *S. commune* (SC)) and brown rots (*S. lacrymans* (SL); *P. placenta* (PP)) during fungal growth (Day (D) 7;14;21;28)). Error bars represent LSD ($P<0.05$)

All of these species had distinct FAME profiles. Due to it is being the biggest proportion of the FAME each fungal species, 18:2n6c (linoleic acid) has become a

biomarker for major fungal species (Klamer and Baath, 2004). Thus, the relationship between this FAME and other parameters (e.g fungal biomass) needs to be established.

To optimize the understanding the effect of incubation and fungal type on the production of fatty acids, multivariate analyses/canonical variance analysis (CVA) was performed (Figure 25). MANOVA was used for determining the significance difference ($P<0.05$) in FAME in each treatment. Canonical Variate Analysis (CVA) was used to examine the effect of treatments on the structure of the microbial community. 95% confidential intervals were used to determine the significance of differences between treatments. The results were plotted in 2 dimensional graphs where the first axis (X) represented 41% of variation and the second axis (Y) accounted for 19%.

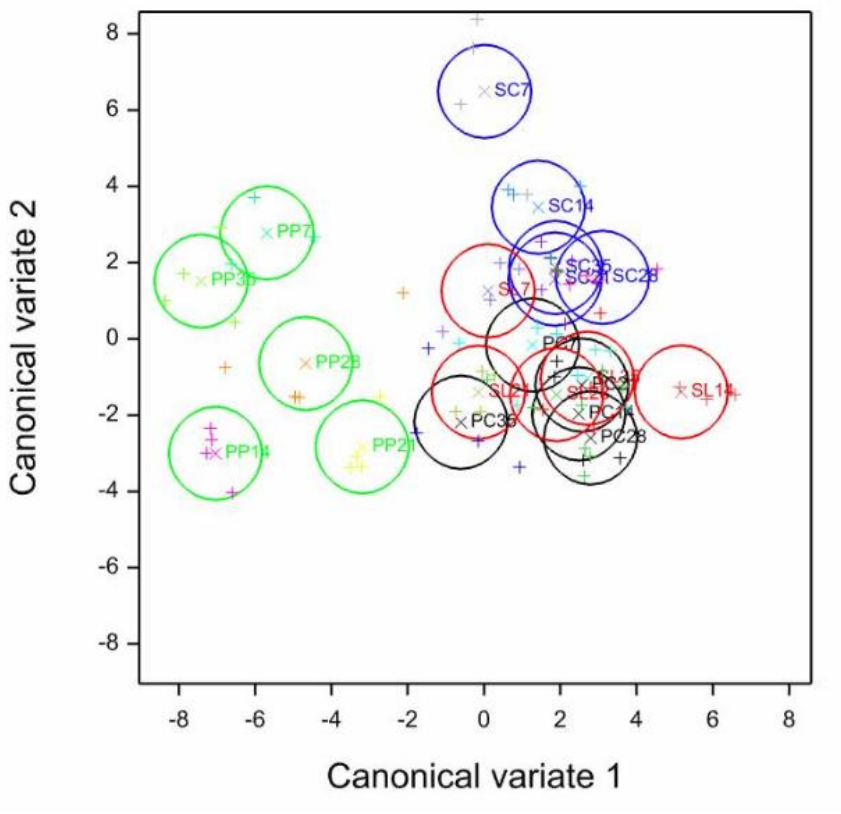

Figure 25. Multicomponent analysis of individual FAME profiles. The samples were plotted against two CVAs (CVA1 and CVA2) functions in each species by different time of cultures. Circles represent confidence plot at P<0.05. (Blue circles: *Schyzoophylum commune*, green: *Postia placenta*, red: *Serpula lacrymans*, black:*Phanerochaete chrysosporium*).

P. placenta fatty acid pattern was completely different compared to the other fungi along the first axis, whilst no separation was found between *P. chrysosporium* and *S. lacrymans* fatty acid. *S. commune* fatty acid was separated from the other fungi along the second axis (Y).

The relationship between ergosterol and fatty acid methyl ester varies between fungal type hence could not be generalized. Each fungus behaves differently and there were no significant correlation between FAME and ergosterol (Figure 26) except for *P.chrysosporium* (r=-0.94, significant p<0.05).

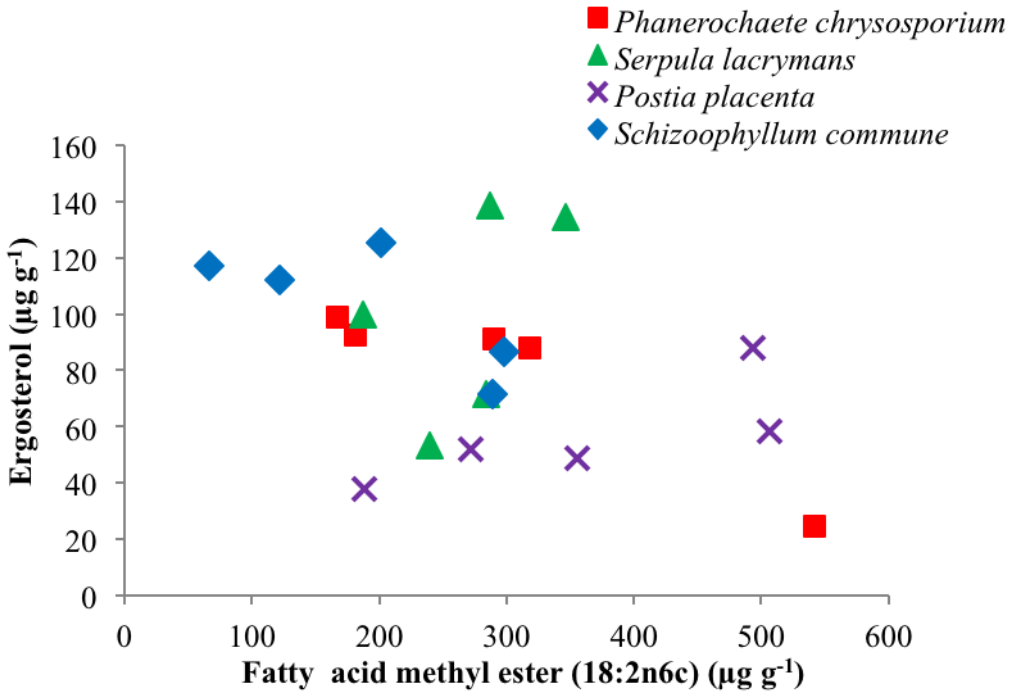

Figure 26. Correlation between ergosterol (µ g^{-1}) and marker PLFA (18:2n6c) content under wheat straw SSF within of incubation as shown by the associated correlation coefficients. Point is an average from 3 replicates.

3.3.3 Lignocellulose degradation

3.3.3.1 Total reducing sugar

The colorimetric assay based on 3,5 dinitrosalisylic acid (DNS) was used for estimating total reducing sugars following lignocellulose degradation in wheat straw SSF. Total reducing sugars released during incubation of the fungus growing on straw were used to identify the effectiveness of the selected fungi to decompose cellulose and hemicellulose in wheat straw. The highest amount of total reducing sugar was found with *P. chrysosporium* after 21 days incubation at 23.1 mg g^{-1} straw followed by *S. lacrymans* (16 mg g^{-1}), while *P. placenta* had the lowest level of total reducing sugar (1.78 – 3.70 mg g^{-1} straw) (Figure 27). The total reducing sugars increased rapidly during the first 3 weeks in *P. chrysosporium* and *S. lacrymans* and

reaching a peak value on day 21 while *S.commune* reached a peak on day 7 (13 mg g^{-1}) and *P. placenta* had no significant affect on the amount of total reducing sugars released.

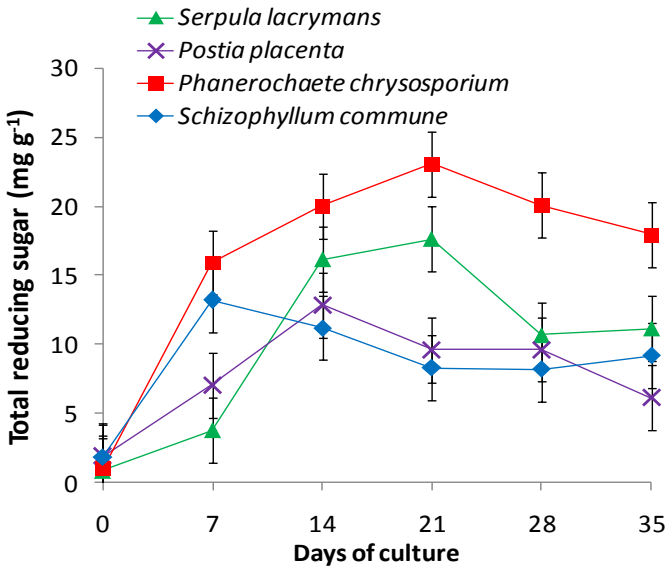

Figure 27. Total reducing sugar (mg g^{-1}) of four different fungal species incubated over 35 days on wheat solid-state fermentation (SSF). Error bars show the least significant difference as calculated in Genstat ($P<0.05$)

The coefficient correlation (r) was calculated using fungal biomass against total reducing sugar between different types of fungus. There were no significant correlations between fungal biomass and total reducing sugar produced except for *S.commune* (r=-0.67 significant $p<0.05$). This correlation might indicate that sugars are consumed during fungal metabolism which is also reflected by the fact that mature *S. commune* white rot fungus released less reducing sugar in total whilst total reducing sugar in *S. lacrymans* and *P. chrysosporium* was optimal at fungal biomass of 4-5 mg dry weight (Figure 28).

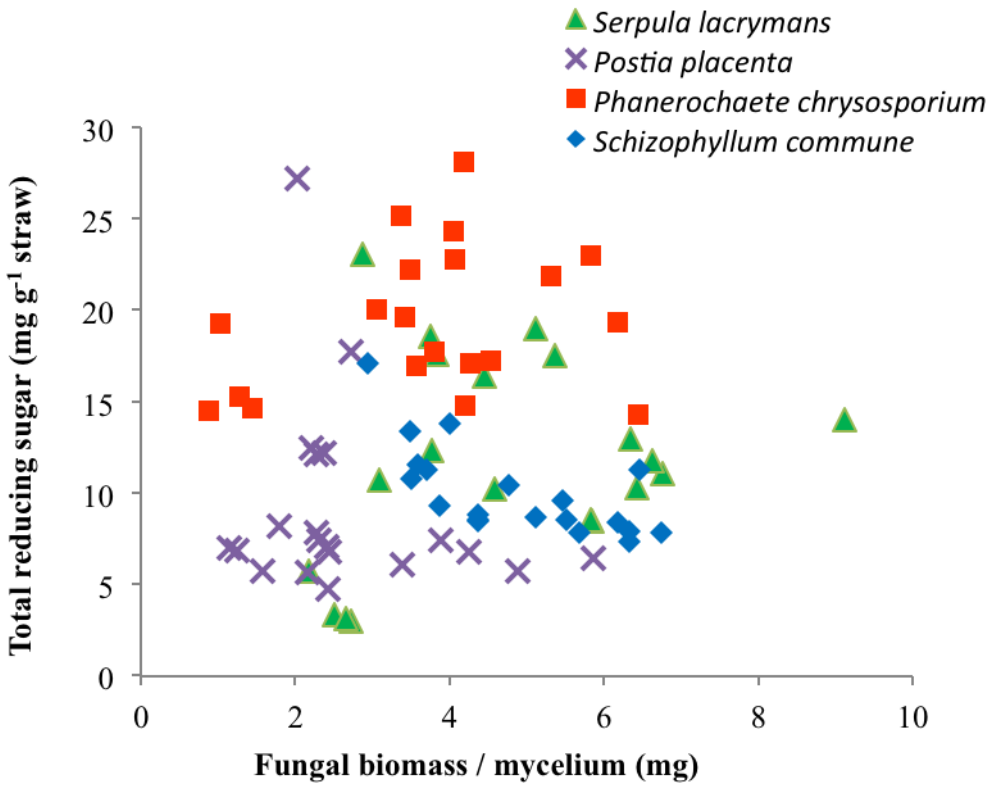

Figure 28. The relationship between fungal biomass and total reducing sugars (All data from each fungus in this experiment were plotted). The possible associations are shown although the relationships are weak.

3.3.3.2 Production of different sugars during growth on wheat straw SSF by fungi.

The degradation of cellulosic and hemicellulosic compounds produced in SSF by different types of fungus was also observed. The amounts of those compounds differed significantly depending on fungal type and time of culture ($P<0.01$). Production of glucose indicates degradation of cellulosic material, while xylose indicates hemicellulosic breakdown. These are the two major sugar fractions released during wheat straw degradation. Due to the low amounts detected, the contribution of mannose, arabinose and fructose are not presented.

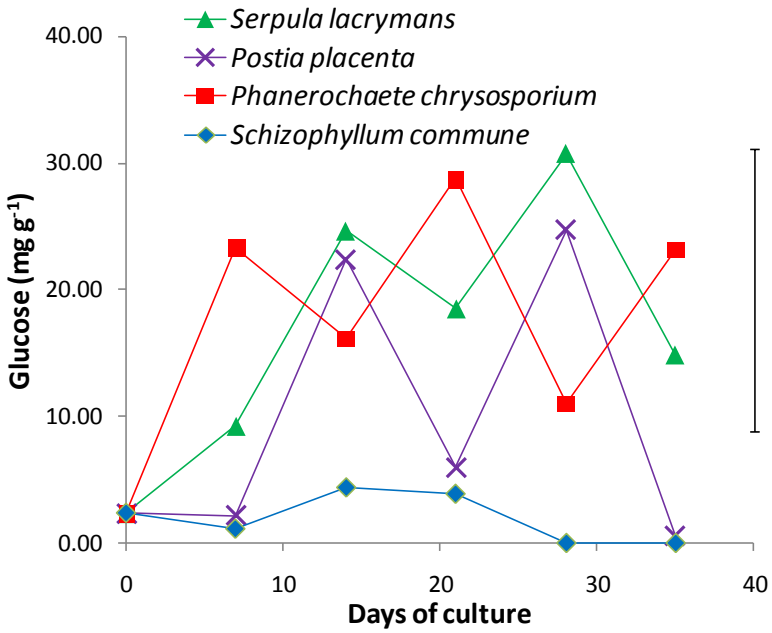

Figure 29. The total glucose (mg g^{-1}) released by four different fungi during 35 days incubations on wheat straw SSF. Vertical lines show LSD (5%) for comparing means at different times.

The highest average amount of glucose released over 35 days was by *P. chrysosporium* (17.4 mg g^{-1}) followed by *S. lacrymans (*16.7 mg g^{-1} or 1.67 %) and *P. placenta*, which yielded 9.7 mg g^{-1} or 0.97 %. While the lowest average glucose released was found using *S. commune* (Figure 29). In contrast *S. commune* has the highest average xylose production (57.84 mg g^{-1} or 5.78 %), which reached a maximum level (14%) after 21 day of culture. Meanwhile *P. chrysosporium* yielded the lowest percentage of xylose (Figure 30).

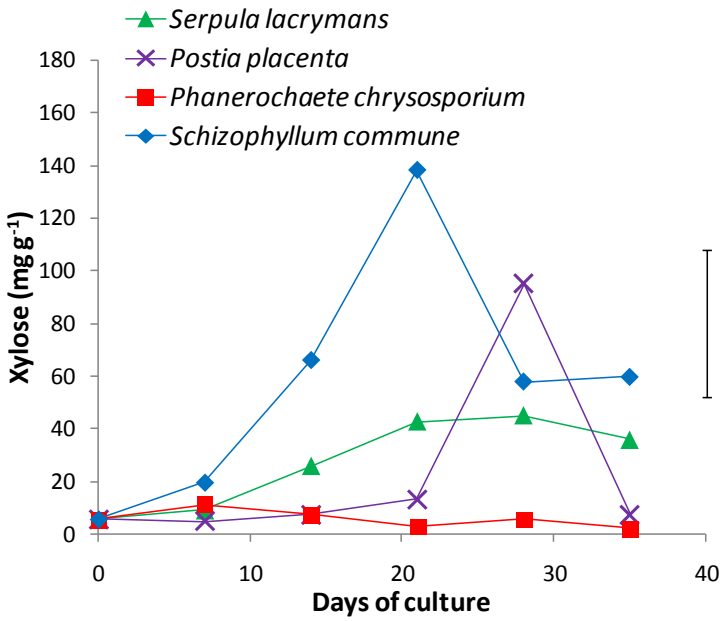

Figure 30. The total xylose (mg g^{-1}) released by four different fungi during 35 days incubations on wheat straw SSF. Vertical lines show LSD (5%) for comparing means at different time.

3.3.3.3 Total Soluble phenols

The highest total phenol concentration 0.64 mg g^{-1} straw dry weight was observed using *S. lacrymans* which peaked 28 day after incubation and subsequently remained constant. Moreover, positive significant correlation ($p<0.05$) between fungal biomass and total soluble phenol has been detected in *S.lacrymans* (r=0.89) and *P.placenta* (r=0.50), whilst no significant correlation were found with *P.chrysosporium* (r=-0.16) and *S.commune* (r=0.29) (Figure 32).

Other fungi showed little phenol release and this did not change with time (Figure 31).

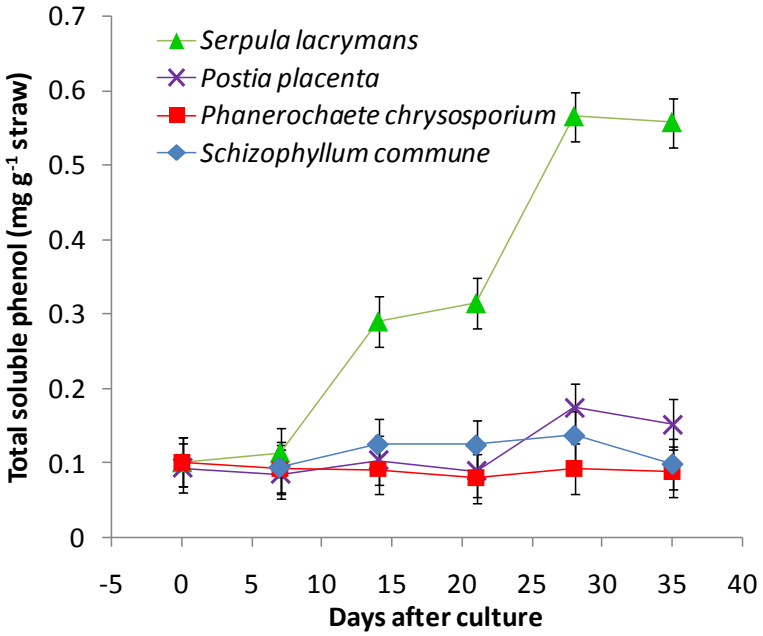

Figure 31. The concentration of total soluble phenols (mg g^{-1}) extracted from wheat straw SSF with four different fungal species, incubated for 35 days. Error bars represent LSD ($P<0.05$)

This implies that only *S. lacrymans* can degrade lignin and hence release phenolic compounds or that other fungi release phenolics but these are instantly catabolized for fungal metabolism (Figure 32).

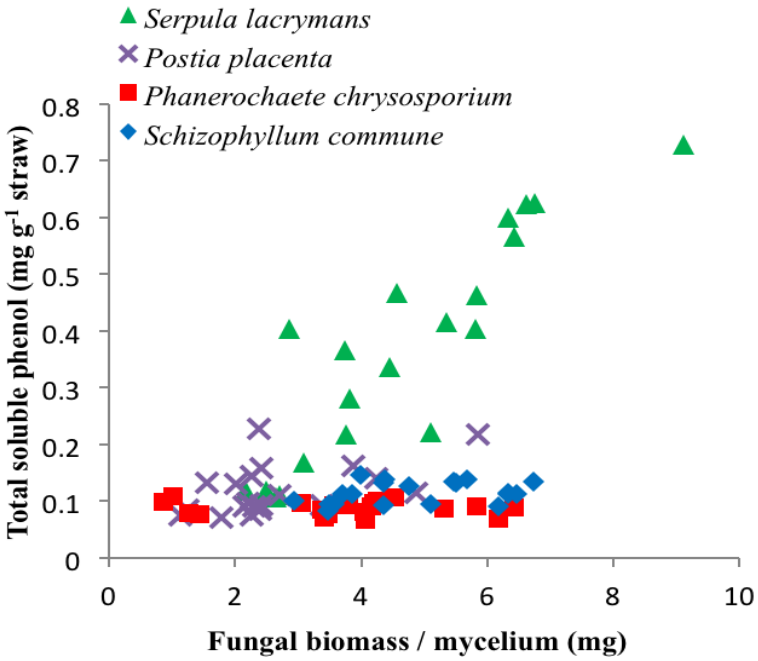

Figure 32. The relationship between fungal mycelium biomass (mg) and total soluble phenols (mg g^{-1} straw) for each of the fungi tested. The line of best fit for each fungus is shown with the predicted formula. (All data from each fungus in this experiment were plotted and linear trend using the highest coefficient of correlation was calculated).

3.3.3.4 Compound identification using LC-MS: analysis of solvent-soluble lignin breakdown products

LC-MS fragments were compared with known standard compounds where available and using information from the literature. The retention time of standard and the compounds peak characteristics and the predicted mass were within the standard limits, the relative abundance was calculated. Several chemical products released (including phenolic and aromatic compounds) by solvent extraction were successfully detected by LC-MS. LC traces suggest reproducible product released of a mixture of compounds. For example the compounds with the following molecular weights 166, 168, 182 and 213 m/z were assigned as homovanillyl alcohol, propylguaiacol, syringaldehyde and carboxy-vanillic acid, respectively.

Products released based on the molecular weight by fungal species are summarized in Table 12, whilst a detailed comparison of the products after 21 days of culture is presented in Appendix 3. There is no difference in the type of product released after 21 days cultures. The identification of products released was focused on low molecular weight chemicals, which ranged from 124 to 358.

Table 12. Estimated number of compounds produced following culture with different fungi based on the molecular weight

Type of fungus	Number of products detected with MW from 124 to 358
Phanerochaete chrysosporium	65
Postia placenta	61
Schizoophlykum commune	27
Serpula lacrymans	75

The greatest number of products released predicted were found using *S. lacrymans* extract (75), followed by *P. chrysosporium* (65), *P. placenta* (61) and then *S. commune* (27) which had the fewest. Many chemicals present in the majority of the fungi were absent in *S. commune* extracts such as: kojic acid, cinnamic acid, vanillin, vannilyl-alchohol, syryngol, protochatehuic acid, eugenol, iso eugenol, coumaric acid and hydrocynamic acid. This suggests that *S. commune* differs in its ability to degrade straw compared to the three other fungi studied. In general, *S. lacrymans* and *P. chrysosporium* produced the greatest amount of chemical compounds released (Appendix 3).

Some of the chemicals produced are known to be valuable. Syringaldehyde, and vanillic acid were identified as the compounds having the most potential (Bozell, 2006) from lignocellulosic material as they can provide a new alternative source of bioenergy and also a basic substance for a number of industrial uses. Several

chemicals derived from lignin were identified such as coumaric acid, sinaphyl dehyde, coniferyl alcohol and sinaphyl alcohol. All of which have been identified as being useful to industry

3.4 Discussions

3.4.1 Fungal Ergosterol and Biomass

The measurement of fungal growth is important and two different approaches were tried. Measurement of total ergosterol content showed variation from 98.4 to 294.7 µg following 28 days culture in liquid media. This was found to equate to 9.84 and 29.47 mg g^{-1} dry weight mycelium. These values are higher than some ergosterol measurements obtained previously e.g. *S. commune* and *P. chrysosporium* grown on Potato Dextrose Agar (PDA) and Carboxymethyl Cellulose Agar (CMC) for 12 and 24 days at 24^{o}C under dark conditions, in which ergosterol measurements ranged between 1-24 mg g^{-1} dry weight mycelium, (Klamer and Baath, 2004). In another liquid culture experiment (ADMS medium), Niemenmaa et al. (2008) observed that mycelium of different types of fungi (*Phlebia radiata*, *P. chrysosporium*, *Physisporinus rivulosus, Ceriporiopsis subvernispora, Gloeophyllum trabeum and P. placenta*) contained ergosterol at the level of 0.4 to 3.9 mg g^{-1} dry weight mycelium, following culture within a 5 week period.

It has been reported that the greatest ergosterol production during culture in liquid medium is found with the brown rot fungus, *Gloeophlyllum trabeum* (3.9 mg g^{1}). These figures are significantly higher than the ergosterol content of other fungi. The brown rot *P. placenta* has the second highest ergosterol content of the brown

rots (1.37 mg g^{-1}), which was similar level to the white rot, *P. chrysosporium* (1.39 mg g^{-1}) (Niemenmaa et al. 2008). These findings are consistent with the ergosterol contents reported in this study. This study shows that the highest ergosterol content in liquid medium was detected in *P. placenta*, followed by *P. chrysosporium*, which was not significantly different to *S. lacrymans*, whilst the lowest was found in *S. commune*.

The ergosterol content of the four basidiomycetes in this study was between 24.47 to 138.7 µg g^{-1} wheat straw dry weight. These values are higher than those reported in previous studies (Niemenmaa et al., 2008; Tothill et al., 1992) but are lower than the ergosterol content in forest boreal soil (243-346 µg g^{-1} organic matter) (Hogberg et al., 2006) or even the ergosterol content in several edible mushrooms. *Agaricus bisporus*, *Pleorotus ostreatus* and *Lentinus edodes* were found to have ergosterol contents ranging between 602 to 679 mg 100 g^{-1} dry weight (Mattila et al., 2002). Measurement of fungal growth on wheat straw (as measured by ergosterol) found that *S. lacrymans* showed the greatest growth, peaking at day 35. Compared to the initial measurements during the first week of fungal growth (7 days), the amount of ergosterol at day 35 was almost double (Figure 19). The pattern of ergosterol production was quite similar between *S. lacrymans* and *S. commune* both showing significant increases from the initial growth (day 0) until 28 days culture and then remain stable thereafter. *P. chrysosporium* however showed fairly high ergosterol values at the beginning of cultivation (from 0 to 14 days incubation).

The conversion factors calculated in this study (Table 11) were lower than conversion factors of several white and brown rot fungus cultured in ADMS media estimated by Niemenmaa et al., (2008), who found that the average conversion factor

of ergosterol to biomass following incubation for 7 to 35 days in *P. radiata, P. chrysosporium, P. rivulosus, C. subvermispora, G. trabeum, P. placenta* were 185, 88, 243, 152, 48 and 63, respectively. This conversion factor resulted in a fungal biomass cultured in wood in *P. radiata* of 77-132 µg and 411 to 430 µg for *P. chrysosporium.* Cultured in solid agar media (2mM-N, 0.1 % glucose) the value reached 500-2072 µg and 4055 to 7305 µg for *P. radiata* and *P. chrysosporium*, respectively.

The amount of fungal biomass gradually increased during the fungal growth. However there was no clear difference in the pattern of production of ergosterol between the fungi tested. The conversion factor differs between different groups and is dependent on the culture conditions, and sampling methods are different. Therefore further investigation using other fungal biomass markers (e.g. the phospholipid fatty acid) is needed to verify the amounts of fungal biomass.

3.4.2 Fungal Phospholipid Fatty Acid profiling

This study examined the relative composition of PLFA in the fungi and the dominant fatty acids in each sample were evaluated and described. The major PLFA for the four Basidiomycetes observed in this research *(P. chrysosporium, S. commune, S. lacrymans and P. placenta)* were similar, which were 16:0, 18:2n6c, 18:1n9c, 22:0, 22:2n6, 23:0 and 24:1n9. The relative composition of the predominant fatty acids in this study was compared to other published works (Table 13). Numerous studies investigating fatty acid profiling of Basidiomycetes in liquid medium have been identified (Stalh and Klugh, (1996); Klamer and Baath, (2004) ;

Muller et al., (1994)). However, data from solid medium and information on sequential production of fatty acids over the duration of fungal culture have until now been limited. This study reveals sequential contribution of each PLFA and their dynamics following culturing in SSF.

Table 13. This table summary our results compared to other publications listing the amounts of the predominant fatty acids produced by a number of Basidiomycetes grown on different substrates expressed as a percentage of the total fatty acids.

Fungus	Fatty acid	(%) of total fatty acid	Substrate	Reference
P. chrysosporium	16:0	18-29	Wheat straw SSF (1-35 days)	This study
	18:2n6c	16-33		
	18:1n9c	5-9		
	24:1n9	6-29		
S. commune	16:0	16-28	Wheat straw SSF (1-35 days)	This study
	18:2n6c	15-54		
	18:1n9c	8-19		
	22:2n6	4-18		
S. lacrymans	16:0	19-29	Wheat straw SSF (1-35 days)	This study
	18:2n6c	16-50		
	18:1n9c	10-13		
	24:1n9	6-9		
P .placenta	16:0	15-21	Wheat straw SSF (10-35 days)	This study
	18:2n6c	9-19		
	18:1n9c	4-8		
	22:2n6	10-18		
P. chysosporium	16:0	18	Malt broth (10 days)	Stahl and Klug, 1996
	18:2n6c	53		
	18:1n9c	21		
P. placenta	16:0	14.24	Malt broth (10 days)	Stahl and Klug, 1996
	18:2n6c	76.54		
	18:1n9c	7.42		
P. chysosporium	16:0	24-33	Potato dextrose agar (12 and 24 days)	Klamer and Baath, 2004
	18:2n6c	57-55		
	18:1n9c	7-12		
S. commune	16:0	27-28	Potato dextrose agar (24 days)	Klamer and Baath, 2004
	18:2n6c	45-49		
	18:1n9c	18-21		

The fatty acid composition can be used to distinguish fungal physiology, (Table 13). In wheat straw SSF, the contribution of fungal fingerprint fatty acid (18:2n6c and 181n9c) were much lower than in liquid medium and in accordance with the previous study (Stalh and Klugh, (1996); Klamer and Baath, (2004). However, there is relatively little previous study of PLFA for Basidiomycetes grown on solid media (in particular wheat straw SSF). A novel finding of this study is that a number of unusual fatty acids are found in Basidiomycetes. These are 20:3n3 ; 22:1n9 ; 23:00 ; 22:2n6 ; 24:1n9 ; 22:6n3, which correspond to *eicosatrienoic acid, eruric acid, tricosanoic acid, docosadienoic acid, nervonic acid* and *decosahexaenoic acid*, respectively.

For more detailed analyses, multivariate analysis (Canonical Variants Analyses) was employed in this study for examining the effect of culture duration (days) on the PLFA pattern on fungal characteristics and behavior. This technique has previously been used to compare 12 different fungal genera (2 Phycomycetes, 4 Ascomycetes and 6 Basidiomycetes) (Muller, 1994). However, none of the Basidiomycetes in that study are similar to the ones studied in this investigation. The CVA analyses showed that *P. placenta* had much greater separation than the other fungi in the X dimension (Score1, CV1), whilst *S. commune* was also distinct based on the X and Y axis (Score2,CV2). No clear separation was found between *S. lacrymans* and *P. chrysosporium*. This suggested they might have similar fatty acid profile and production. The present work has proven that multivariate analyses can be used for distinguishing different characteristics within Basidiomycete fungal classes.

The relationship between PLFA and the amount of fungal biomass differed with only two of the Basidiomycetes showing a positive trend (*S. lacrymans* and *P. placenta*), whilst a negative correlation was found using *S. commune* and *P. chrysosporium* (Figure 24*)*. Previously, the correlation between PLFA 18:2n6c was performed in liquid medium (Eiland et al., (2001) ; Klamer and Baath, 2004) and fewer studies have tested this concept under solid medium. However, some studies of fungi in soil environment were able to successfully obtain a good relationship between PLFA 18:2n6c and fungal biomass (Frostegard and Baath, 1996). Using the PLFA 18:2n6c as an indicator of fungal biomass may not be appropriate, as it may be present in other eukaryotic organisms including plants and animals (Klamer and Baath, 2004). This may mean it is an inappropriate indicator of biomass since it is difficult to separate between PLFA produced by the fungus and from other organisms such as wheat straw. However, there are potential limitations of using ergosterol. For example ergosterol is easily degraded when fungal cells die and for this reason is a really only a measure of living fungal biomass (Niemenmaa et al. 2008). The findings of this experiment do not support previous research by Klamer and Baath, (2004), that reported that there was a linear correlation (R^2 = 0.782), between ergosterol and PLFA 18:2n6c among 11 species of fungi cultured in agar media (e.g, CMC, PDA). In contrast this study used SSF of wheat straw to represent the natural habitat and actual condition of these white and brown rot fungi. Many factors influence fungal growth such as: substrate quality (e.g C, N, P and other nutrients), temperature, water content, sugar or enzymes addition, etc. The results shown in Figure 18 and 24 combined shows that ergosterol appears to be a better indicator of fungal growth than PLFA 18:2n6c.

3.4.3. Total reducing sugars

The amount of reducing sugar and phenolic compounds released can reflect the effectiveness of enzymatic activity of the fungi. This may be influenced by various factor including temperature, moisture, pH and aeration as well as properties of the substrate such as porosity, cellulose fiber crystallinity, lignin and hemicellulose content (Zabihi et al., 2010). For example, an increase in enzymatic activity was found to positively correlate with reducing sugar content of *Phanerocaete sordida*, culture grown on pruning waste of *Nepheris cordifolia* (entire pinnae separated from the rachis) and *Laurus nobilis* (fragmented leaves). The total reducing sugars ranged between 1.5 to 5 mg g^{-1} (0.15 to 0.5 %) dry weights, which fluctuated over 90 days of incubation (Diorio et al., 2009). The use of recombinant enzymes to breakdown cellulose has also been tried. The total amounts of reducing sugars with different concentration of enzymes has been shown to range between 0.1 to 0.8 % (Vaithanomsat et al., (2009).

In this study fungal species and time of culture affected the amounts of total reducing sugars produced. Optimal amounts of total reducing sugars were found after 14 to 28 days after culture. The most effective basidiomycetes were found to be *P. chrysosporium*, followed by *S. lacrymans, S. commune* and *P. placenta*. The total reducing sugars released in *P. chrysosporium* reached a maximum of 23.1 mg g^{-1} in 21 day old cultures. This equated to 0.231 % wheat straw dry weight. This is higher than the total reducing sugars concentration found in previous studies by Diorio et al. (2009) and Vaithanomsat et al., (2009), but lower results reported in Zabihi et al., (2010) and Sun et al., (2005).

It has been observed that the optimum total reducing sugars released from rice straw SSF cultured with *Aspergillus terreus* between the period of 8 – 10 days after incubation, yielded 17 mg g^{-1} (1.7%) total reducing sugar of dry weight (Jahromi et al., 2011). Moreover, the fungal strain of *Trichoderma harzianum* grown in baggase, cellulolignin and cellulose pulp after 48 hours treatments produced total reducing sugar levels of 4.79; 4,14; and 8.95 %, respectively (Thanapimmetha et al., (2011). The total reducing sugar values from Jahromi et al., (2011) and Thanapimmetha et al., (2011) were close to the total reducing sugar level in this study which adopted a low input biorefinery concept (no external chemical input, nutrients or acid pretreatment).

P. chrysosporium produces several lignolytic enzymes such as manganese peroxidase, lignin peroxidase (peroxidases classes) and cellobiose dehydrogenase (CDH). The peroxidases could degrade the lignin fractions by generating the reactive radicals through the oxidizing redox mediators. While the CDH could support the lignin break down by reducing aromatic radicals generated by lignolytic enzymes (Henriksson et al., 2000). In *P. chrysosporium*, CDH was reported to oxidize the reducing end group of cellulose and released cellobiose as the electron donor. Thus, the CDH could generate highly reactive hydroxyl radicals via Fenton reaction (Morpeth, 1985; Henriksson et al., 2000). Similar to *P. chrysosporium*, the brown rot *S. lacrymans* released high amounts of reducing sugars up to 21 days of culture. The mechanism of how *S. lacrymans* degrades lignocellulose has not been reported in detail and forms the basis of this thesis.

Compared to the DNS assay for the measurement of total reducing sugars, high performance liquid chromatography (HPLC) measures the specific sugars and is

more sensitive. The HPLC assay specifically measured the desired products of lignocellulose degradation such as glucose, xylose, mannose and other sugars.

3.4.4 Xylose and glucose production during wheat straw SSF.

Lignocellulose breakdown by fungi represents a transformation of lignocellulose material carried out by various enzymatic activities (Valmaseda et al., 1991). The cellulose and hemicellulose (e.g. glucose and xylose) produced from experiments using a number of different types of fungi in wheat straw SSF and other techniques (e.g. chemical, steam, pressure, etc.) were compared with published information. The type of fungus and technology chosen, had an effect on the composition of the products released during polysaccharide breakdown (Table 14).

In hemicellulose the structures that need to be broken down are more easily accessible by acids than in cellulose. *S. commune* and *P. placenta* preferentially decompose hemicellulose, breaking down the lignocellulose structure, which gives better access to the cellulose.

Table 14. The relative proportions of sugars released during growth on wheat straw SSF from the aqueous extraction/liquid fraction based on the current study and with comparison to others.

Method Fungus/	Glu*	Xyl*	Gal*	Man*	Ara*	Pen*	References
P. chrysosporium (SSF)	75	25	-	-	-	-	This study
S. commune (SSF)	3	97	-	-	-	-	This study
S. lacrymans (SSF)	40	60	-	-	-	-	This study
P. placenta (SSF)	35	65	-	-	-	-	This study
T. viride (SSF)	66.2	33.8	-	-	-	-	Zayed and Meyer, (1996)
T. versicolor (SSF)	18.0	1.7	0.7	1.3	1.1	7.1	Valmaseda et al., (1991)
L. amethystina (SSF)	35.7	4.5	0.4	1.9	2.9	5.1	
P. ostreatus (SSF)	37.1	4.0	0.2	2.1	1.9	6.7	
P. eryngii (SSF)	40.1	7.5	0.9	2.3	4.1	3.7	
P. chrysosporium (SSF)	20.4	11.7	0.6	2.1	3.5	1.5	
T. longibrachiatum (SSF)	28.0	16.0	0.8	3.0	4.3	1.6	
C. virescens (SSF)	27.2	9.5	0.5	3.1	3.6	2.3	
Hydrolisis	35.05	4.96	0.93	10.7	0.83	-	Foyle et al., (2007)
Untreated amonia	38.1	20.2	-	-	2.9	-	Kondo et al., (1992)
Amonia treated	37.7	19.5	-	-	3.2	0.9	

*Glu: glucose; Xyl:xylose; Gal:galactosa; Man:mannose; Ara: arabinose; Pentose: pentose

Our results showed that both *P. chrysosporium* and *S. lacrymans* released greater amounts of glucose compared to *P. placenta* and *S. commune*. The glucose released may not all be available as a product as it is used as a source of energy for fungal growth and regulates fungal metabolism. Interestingly *S. commune* and *P. placenta* released the highest concentration of xylose while *P. chrysosporium* produced the least amount of xylose, followed by *S. lacrymans*. This result suggested that *P. chrysosporium* contains more cellulosic than hemicellulosic enzymes, while on *S. commune* this is reversed. There was no clear pattern to the release of sugars in either the white or brown rots. Therefore, it is not easy to correlate the sugar production by lignocellulosic fungal to fungal biomass.

3.4.5 Total soluble phenols

The release of phenolics by the basidiomycetes can be used as an indicator for the breakdown of lignin. Extracellular enzymes such as LiP, MnP and laccase can enhance the ability of white rot fungi to degrade polymeric phenol in lignocellulosic material. The highest amount of soluble phenol produced (which was extracted using hot water treatments) in this study was observed using *S. lacrymans* cultures after 28 days culture. The level of phenolics reached 0.6 mg g^{-1} wheat straw dry weight. This is less than previously reported. The white rot fungus *P. chrysosporium* grown on waste (straw) mixed with olive mill wastewater composting experiment (Taccari et al., 2009), gave an initial soluble phenolic range of between 1.05 to 5.21 mg g^{-1} substrate, which dropped to 0.72 to 2.1 mg g^{-1} substrate following 8 weeks.

Surprisingly, compared to *S. lacrymans* the other fungi (*P. chrysosporium, S. commune* and *P. placenta*) produced very low amounts of soluble phenols. In this study, there was a strong relationship between total soluble phenols and fungal biomass of *S. lacrymans* culture. This was confirmed during fungal growth where *S. lacrymans* was found to be more active at degrading phenolic compounds than the other fungi studied. This evidence implies that *S. lacrymans* is the most promising lignocellulose degrading microorganism to produce various phenolics and or value added chemicals from SSF. As a brown rot *S. lacrymans* does not utilize lignin in its metabolism. However, it does partially degrade lignin, presumably to gain better access to the cellulose and hemicelluloses compounds. This might be a good target for lignin biorefining as it will degrade the substrate, but not alter the amount of lignin breakdown products obtained.

A strong correlation of soluble phenol and fungal biomass was only detected in *S. lacrymans* culture (r = 0.89) (Figure 32). This may indicate that brown rot fungus *Serpula lacrymans* is more effective at degrading material containing lignin than others white rot fungi in this experiment. A possibility does exist that *S.lacrymans* could release phenolic compounds into the media. This is however extremely unlikely.

3.4.6 Fungal selection

Based on numerous quantitative parameters listed in Table 15, which were identified and described in the previous section, the best candidate for lignocellulosic wheat straw biomass degradation was selected based on their performance.

Table 15. A table simplifying the data collected on the performance of the four Basidiomycetes cultured in wheat straw SSF as measured by the eight assays used .

Parameter	*P. chrysosporium* (white rot)	*S. commune* (white rot)	*S. lacrymans* (brown rot)	*P. placenta* (brown rot)
Ergosterol	Low	High	**High**	Low
Fungal biomass	Low	**High**	High	Low
Reducing sugar	**High**	Low	High	Low
Total soluble phenol	Low	Low	**High**	High
Fatty acid 18:2n6c	Low	High	**High**	Low
Glucose	**High**	Low	High	Low
Xylose	Low	**High**	Low	High
Low molecular weight chemical products released	High	Low	**High**	Low

S. lacrymans performed better than the other fungi studied as it produced high fungal biomass (ergosterol), released more total soluble phenol, produced high quantities of sugar (reducing sugar and glucose, more concentration of fungal fatty

acid fingerprint (18:2n6c), along with a greatest production of low molecular weight chemicals.

Based on the results obtained *S. lacrymans* was selected as the fungus of choice as it appeared to be the most promising lignocellulosic degrader of wheat straw in SSF. Non enzymatic (the Fenton reaction) and enzymatic process have been suggested to be involved in wheat straw lignocellulosic degradation. Understanding which genes regulate this breakdown and the determination of their mechanisms of action is therefore important and forms the basis of the rest of this thesis.

Chapter 4. Evidence for the mechanisms involved in the degradation of wheat straw *by Serpula lacrymans*

4.1 Introduction

4.1.1 *Serpula lacrymans*: characterization and distribution

In temperate regions *Serpula lacrymans* is recognized as the one of the most significant causes of damage to wood used in construction (Kauserud et al., 2007). The damage caused is significant and is widespread, affecting softwood timber in Northern and Central Europe, Australia and Japan (Palfreyman et al., 1995; Schmidt and Moreth-Kebernik, 1991). In the UK, the cost for repairing damage caused by this fungus has been estimated as £150 millions annually (Schmidt, 2000). It was originally described as *Boletus lacrymans* in 1781, being recognized then as a problem in European buildings and sailing ships (Kauserud et al., 2007).

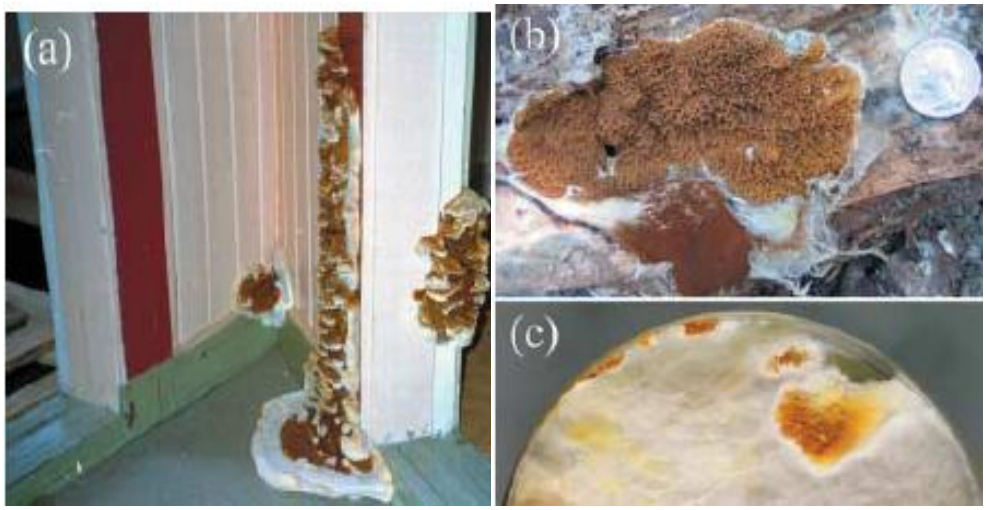

Figure 33. Illustrations showing the aggressive nature of *S. lacrymans* which predominantly occurs in buildings in temperate regions (a), compared to a relative non-aggressive fungus *(Serpula shastensis)* that recently has been detected in mountains regions in California (b), the fruit bodies of isolate of *S. lacrymans* x var *S. shastensis* (c) (Kauserud et al., 2007)

The fungus usually produces large fruiting bodies than its relative *Serpula shastensis* (Figure 33). Unlike *S. lacrymans, S. shastensis* has thinner pancake bodies and grows at higher altitudes (over 300 meters above sea level), such as in the Himalayas, Czech Republic and East Asia (Kauserud et al., 2007). *S. lacrymans* is thought to have originated in India and spread to Europe due to the ability of its spores to adapt to different environmental conditions (Palfreyman et al., 1995).

Recently, various specimens of *S. lacrymans* collected from different countries were compared (77 isolates from Japan vs 67 isolates from Europe) using microsatellites and sequencing of four loci. This study confirmed that the Japanese *S. lacrymans* isolates showed a greater diversity when compared to the European isolates. The average degree of diversity was 0.44 for Japan and 0.31 for Europe, whilst the average number of alleles per locus was 3.86 for Japan and 2.39 for Europe. A similar study was conducted by Kauserud et al., (2007) and was based on DNA sequencing of isolates from California, Mainland Asia, Japan, Europe, North America and Oceania sample (106 isolate and 45 dried specimens). The ratio of the number of micro satellite alleles to range in allele size was 0.64 for Japan followed by Mainland Asia (0.59) and Europe, Oceania and North America groups (0.36).

These findings support the assumption that *S. lacrymans* originated in Mainland Asia (Engh et al., 2010), and subsequent in became distributed all over the world. This was a result of word wide shipping activities initially using wooden ship vessels. The exact position of its origin is difficult to determine, since there is a lack of *S. lacrymans* isolates from Mainland Asia (Kauserud et al., 2007).

4.1.2. The pathways of biodegradation and modification of lignocellulosic material

Biomass degradation by the white and brown rot fungi is carried out by a complex mixture of cellulases, hemicellulase and ligninase. In order to degrade lignins complex structure, basidiomycetes secrete ligninases, these include various enzymes such as phenol oxidase (laccase), and heme peroxidases (LiP: Lignin peroxidase or MnP: Manganese peroxidase). In general laccase use molecular oxygen as an electron acceptor while the peroxidase enzymes use hydrogen peroxide. White rot fungi use peroxidase to degrade lignin, whilst brown rot modify and oxidize lignin using hydroxyl radicals released following demethylation of aryl methoxyl groups and ring hydroxylatyon (Varela and Tien, 2003), which gives rise to a brown color (Martinez et al., 2005). In the past, studies on lignocellulosic degradation focused on enzymatic reaction, and have revealed that in brown rot decay wood cell degradation is initiated at a distance from the fungal hyphae (Hyde and Wood, 1997). It is thought that non-enzymatic reactions or low molecular weight chelators which mediate the Fenton reaction may contribute to the early stages of lignocellulose biodegradation in brown rot and specific white rot fungi (Arantes et al., 2009; Shimonokawa et al., 2004). Two other reducing agents, which have been suggested to be involved in lignocellulose breakdown by brown rot fungi, are oxalate and hydroquinone (Varela and Tien, 2003). These iron-binding compounds are thought to have the ability to reduce Fe^{3+} to Fe^{2+} (Goodell et al., 1997).

In many white and brown rot fungi free hydroxyl radicals (·OH) are released through the redox cycling of hydrogen peroxide (H_2O_2) (Koenigs, 1972) (Figure 2). In combination with Fe^{3+} the hydroxyl radicals can catalyse the Fenton reaction

(Aguiar and Ferraz, 2006). The hydroxyl radical attacks non-specifically both the polysaccharide and lignin component, allowing the lignocellulosic enzymes to target the cell wall.

Previous studies from Xu and Goodell (2001) ; Qian et al., (2002) and Suzuki et al., (2006) showed that the Fenton reaction in *Gloeophyllum trabeum* and *Postia placenta* was controlled by the presence of iron and H_2O_2, and that organic chelators mediated the generation of hydroxyl and superoxide radicals and the degradation of cellulose and hemicelluloses. At present, in the case of brown rot fungi it is hypothesized that the most important co-factor involved in the Fenton's reaction is iron. Iron is oxidized from Fe^{2+} in the presence of hydrogen peroxide to generate oxygen radicals following the reaction: $Fe^{2+} + H^{+} + H_2O_2 \Leftrightarrow Fe^{3+}\ H_2O + OH\bullet$. The hydroxyl radicals (OH•) released disrupt bonds within the lignin structure leading to degradation. Hyde and Wood, (1997) proposed that CDH genes regulate the Fenton's reagent for oxidative degradation of cellulose.

4.1.3. Low molecular weight iron binding compounds: chelating mechanism and production

Knowledge of the low molecular weight iron binding compounds and their mechanism of action in the basidiomycetes is limited but they have been successfully extracted from several species (Table 16). Low molecular iron binding compounds and phenolic lignin breakdown products play a crucial role in the Fenton reaction. Various non-enzymatic low molecular weight iron-reducing compounds have been reported in previous studies, which targeted macromolecular cell wall to attack. The

functional role of these compounds in the degradative system varies from laccase mediator to Fe reducing compound as shown in Table 16.

Table 16. Various compounds released by fungi, which are involved in the break down of lignocellulose and their mechanism of action.

Type of compounds	Functional degradative system	Reference
3-Hydroxy-anthranilic acid	Laccase mediator	Arantes et al., (2009)
Veratryl alcohol	AVA/LiP mediator	Arantes et al., (2009)
2Cl-1,4DMB (2-cloro-1,4-dimethoxy benzene	2Cl-1.4DMB/LiP mediator/oxalate Mn^{3+}	Arantes et al., (2009)
Linoleic acid	Fatty acid peroxidation	Arantes et al., (2009)
Carboxylic acid	Oxalate direct attack	Arantes et al., (2009)
2,5-dimethoxyhydroquinone (2,5-DMHQ)	Fe reduction agent	Kerem at al., (1999); Jensen et al., (2001)
2,5-dimethoxy-1,4-benzoquinone (2,5-DMBQ)	Fe reduction agent	Kerem at al., (1999); Shimonokawa et al., (2004); Jensen et al., (2001)
4,5-dimethoxy-1,2-benzoquinoene (4,5-DMBQ)	Fe reduction agent	Kerem et al., (1999); Shimokawa et al., (2004)
4,5-dimethoxy-1,2-benzenediol (DMC)	Fe reduction agent	Paszczynski et al., (1999)
2,5-dimethoxyl-1,4-benzenediol (DMH)	Fe reduction agent	Paszczynski et al., (1999)
2,3 dihydroxynenzoic acid (DHBA)	Fe reduction agent	Goodell et al., (1997)
3,4-dihydrophenylacetic acid (DOPAC)	Fe reduction agent	Arantes and Milagres (2006)

Basiodiomycetes can produce more than one iron reducing agent, for example, *Gloeophyllum trabeum* not only released 2,5-DMHQ (2,5-dimethoxyhydroquinone) but also other quinones such as 4,5-dimethoxy-1,2-benzoquinone (4,5-DMBQ) and 4,5-dimethoxycatechol (DMC) (Jensen et al., 2001)

and it has been referred to as the *Gt chelator* (Goodell et al., 1997; Shimokawa et al., 2004). In general, these compounds have an aromatic C ring with different arrangement of aryl or alkyl bonds (Figure 34).

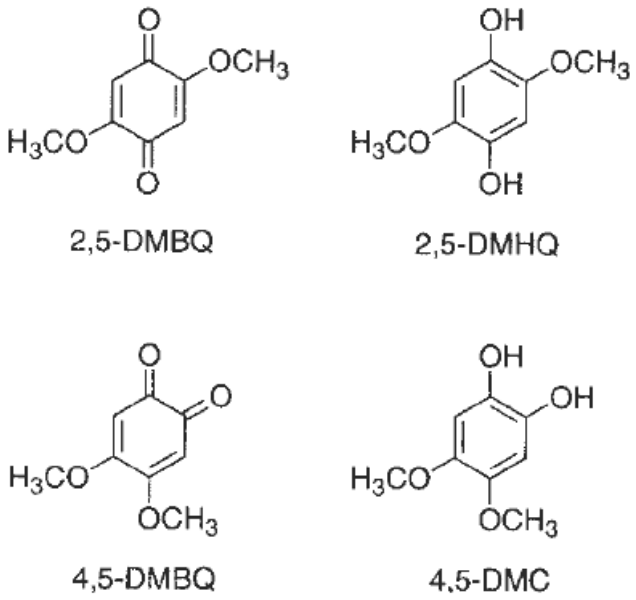

Figure 34. The chemical structure of low molecular quinone compounds from *Gloeophyllum trabeum* (Jensen et al., 2001)

The quinones produced by brown rot fungi have a strong affinity for Fe^{3+} and could mediate the redox cycling of iron under the low pH conditions associated with fungal cultures. The reduction of Fe^{3+} to Fe^{2+}, is considered important for initiation of the Fenton reaction. In brown rot fungi, Fe^{2+} will react with H_2O_2 to produce active oxygen species, which is involved in the breakdown of lignocellulose (Paszczynski et al., 1999).

According to Jensen et al. (2001), when extracellular quinone or hydroquinone was involved, iron reduction in the brown rot *G. trabeum* can be explained by the following reactions:

(1) $Fe^{2+} + H_2O_2 + H+ \rightarrow Fe^{3+} + H_2O + \cdot OH$

(2) $H_2Q + Fe^{3+} \leftrightarrow HQ\cdot + H^+ + Fe^{2+}$

(3) $HQ\cdot + O_2 \leftrightarrow Q + \cdot OOH$

(4) $HQ\cdot + Fe^{3+} \leftrightarrow Q + H^+ + Fe^{2+}$

(5) $Q + 2^{e-} + 2H^+ \rightarrow H_2Q$

From the reaction, the extracellular quinone or hydroquinones reduce Fe^{3+}, followed by the production of quinone or hydroquinone radicals (HQ·) which then act with O_2 to produce the perhydroxy radical (·OOH). Remaining quinone or hydroquinone radicals (HQ·) may also react to reduce the available Fe^{3+}, and finally the quinone undergoes cyclic oxidation-reduction reaction. Numerous studies have tried to quantify quinone or hydroquinone production in both in white and brown rot fungi. The total production of 2,5 dimethoxyhydroquinone and 4,5-dimethoxycatechol in *Gloeophyllum striatum* reached 43 µM (7.4 mg l^{-1}) (Kramer et al.,2004), while 2,5 dimethoxyhydroquinone and 4,5-dimethoxycatechol levels in *G. trabeum, ranged* between 51µM to 17µM (Jensen et al., 2002).

2,3 dihydroxybenzoic acid (2,3-DHBA) has been found in *Gloeophyllum trabeum.* It has been shown that this acts as a phenolate chelator compound with the capacity to reduce the iron complex (Arantes et al., 2009). The mechanism of iron reduction by 2,3-DHBA has been described by Xu and Jordan, (1988), and involves two steps. First, Fe^{3+} is bound to DHBA, which is followed by the creation of a DHBA-Fe^{3+} complex, which is subsequently oxidized. The second step involves the simultaneous reduction of Fe^{3+} by an intermediate quinone form.

Cultures of brown rot fungi often contain significant amounts of oxalic acid, while the white rot fungi have little or no oxalic acid produce during the growth (Kaneko et al., 2005). Oxalic acid is an organic acid commonly occurring in plants, animals and fungi, which play different roles in different organisms. The role of oxalate as a chelating agent in basidiomycetes is unclear (Varela and Tien, 2003). A difference in oxalic acid production between white and brown rot fungi and its potential role in modifying the acidity of the environment has been previously shown (Goodell et al., 2002). In wood decay by white rots the oxalic acid may play multiple roles such as an inhibitor of lignin peroxidase, electron donor for production of NADH, a source of radicals to reduce dioxygen or ferric iron to yield the ferrous iron, and as a chelating agent for lignin degradation. While in the brown rot fungi, oxalic acid may serve as a proton source for enzymatic and non enzymatic hydrolysis of carbohydrates and as a metal chelator (Shimada et al., 1997). Furthermore, Varela and Tien (2003) proposed that the role of oxalic acid was to assist in hydroxyl radical formation (Figure 35) but that higher concentrations had the opposite role.

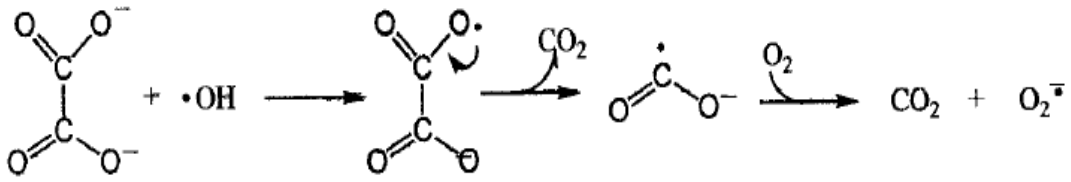

Figure 35. A schematic showing how a superoxide can be generated through the degradation of oxalic acid (Varela and Tien, 2003).

The oxalic acid binds with the hydroxyl radical (·OH) to form an oxalic acid radical, which can release CO_2. The C=O bond radical then reacts with O_2 to produce superoxide (Figure 35).

Although similar chelating mechanisms are observed in other types of white or other brown rot fungi, different fungal types may produce different amounts and types of quinone or hydroquinone as Fe reducing agents. In this current work the quinones produced by *S. lacrymans* culture were examined, in conjunction with the quantity of oxalic acid production during culture. This study showed that *S.lacrymans* was similar to the brown rot *G. trabeum* in its production of hydroquinones. This suggests that they both are capable of degrading wheat straw biomass using non-enzymatic conditions or in combination with fungal extracts. These may consist of various enzymes, oxalic acid and quinones or hydroquinone.

4.1.4. Quantifying lignocellulosic degradation

Quantification of the biodegradation of lignocellulosic material is important if we are to understand how fungi achieve the breakdown of cellulose, hemicellulose or lignin. Brown rots can rapidly breakdown the cellulose and hemicellulose complex, whilst lignin remains un-changed (Agosin et al., 1989). In contrast white rot fungi simultaneously degrade all of those components. Various methods have been employed and tested to quantify the evidence of degradation, such as: weight/mass loss (Hammel et al., 2002; Ray et al., 2010); klason lignin (wet chemicals) and NMR (Nuclear Magnetic Resonance) spectroscopy (Yelle et al., 2008); and IR (infrared) spectroscopy (Valmaseda et al., 1991: Buta et al., 1989: Sun et al., 2005).

Several basidiomycetes have been reported to degrade wood significantly following 12 weeks of culture (Hammel et al., 2002). This study compared the weight loss of wood (%) caused by different type of fungus. These included white rots (e.g. *Ceriporiopsis subvermispora*, *P. chrysosporium*), brown rots (e.g

Coniophora puteana, *G. trabeum*, *P. placenta*) and soft rots (e.g. *Daldinia concentrica*, *Xylaria polymorpha*). The greatest wood loss was found using *P. chrysosporium* (51.9%), followed by *G. trabeum* (48.9%) *Ceriporiopsis subvermispora* (45.3%), *Daldinia concentrica* (30.3%), *P. placenta* (24.2%), *Xylaria polymorpha* (13.2%) and *C. puteana* (10.3%).

A more advanced technique uses klason lignin (wet chemicals) analysis in combination with NMR methods. Yelle et al., (2008) reported that the amount of klason acid soluble lignin decreased by 28% from its initial value following decay by *G. trabeum.*. NMR spectra showed the methoxyls and polysaccharide anomeric components declined by 29% in a spruce wood sample inoculated with *G. trabeum* following 16 weeks culture. However, sample preparation for the NMR technique is time consuming, laborious and needs an expert to operate the machine and to interpret results.

Alternatively, a simple and quick technique using IR spectroscopy can be used to detect changes in the functional groups present in organic materials. This is useful for identifying lignin structure (Hergert, 1971), since the use of FT-IR (Fourier Transform-Infra Red) spectroscopy provides an accuracy measurement of assignments frequencies, higher signals and reduced noise ratios (Buta et al., 1989). Minimal sample preparation is required compared to conventional gravimetric techniques (Pandey et al., 2003). This technique was used to monitor the region assigned to aromatic compounds (Faix, 1986), and to measure lignin degradation by fungi (Buta et al., 1989).

The FT-IR technique uses infra red light, which is absorbed or transmitted in each wavelength by the sample. Each wavelength represents a specific functional

group that may exist. The correlation between the assignments of absorption bands of IR spectroscopy with key wavelengths is presented in Table 17 (Buta et al., 1989 and Sun et al., 2005).

The results from FTIR spectra of wheat straw degraded by the white rot fungus *Stropharia rugosoannulata* showed clear changes in the absorbance between the most degraded and least degraded wheat straw. The most degraded sample had the smallest absorbance and the least degraded the opposite. Changes were observed in wavelength/band at 1717 cm^{-1} which is assigned to carbonyl stretching, 1660-1680 cm for conjugated ketone and 1425-1430 cm^{-1}, 1505-1515 cm^{-1}, 1595-1605 cm^{-1} for aromatic skeleton (Buta et al., 1989).

Table 17. Assignment of IR absorbance wavelengths with functional groups (Buta et al., 1989 and Sun et al., 2005)

Wavelength (band) (cm^{-1})	Assignment for functional group	References
3430	Hydroxyl group in aliphatic and phenolic structure	Sun et al., (2005)
2933	C-H stretching in the aromatic methoxyl group	Sun et al., (2005)
1720	C=O aliphatic carboxyl stretch	Buta et al., (1989)
1710-1715	C=O saturated open chain ketone stretch	Buta et al., (1989)
1660-1680	C=O conjugated ketone stretch	Buta et al., (1989)
1595-1605	Aromatic skeletal vibration	Buta et al., (1989); Sun et al., (2005)
1505-1515	Aromatic skeletal vibration	Buta et al., (1989); Sun et al., (2005)
1425-1430	Aromatic skeletal vibration	Buta et al., (1989); Sun et al., (2005)
1454	Asimetric C-H deformation	Sun et al., (2005)
1355	Symmetric C-H bending	Sun et al., (2005)
1322	Syringyl ring breathing	Sun et al., (2005)
1262	Guaiacyl ring breathing with C-O stretching	Sun et al., (2005)
1123	Aromatic C-H in plane deformation	Sun et al., (2005)
1076	C-O deformation of secondary alchohol and aliphatic ether	Sun et al., (2005)
1030	Aromatic C-H in plane deformation plus C-O in primary alchohol, guaiacyl type	Sun et al., (2005)
919	C-H out of plane in aromatic ring	Sun et al., (2005)

The FTIR technique was employed in the current study to examine the impact of brown rot *S. lacrymans* fungal inoculation on wheat straw SSF in conjunction with the measurement of extracellular metabolites over a period of 35 days of culture.

4.2. Methods

4.2.1 Sample preparation

Serpula lacrymans was cultured in wheat straw solid-state fermentation (SSF) over a time courses (0, 7, 14, 21, 28, 35, 42 and 49 days) at 20ºC. These were prepared for analysis as described in chapter two.

4.2.2 pH fungal culture

S. lacrymans fungal culture extract was collected and pH was determined using a pH meter (AR50-Accument Research, USA) (described in detail in Chapter 2). 10 ml of fungal extract was added into a 250 ml plastic tube and shaker for 15 minutes. The pH was measured immediately, without filtering by submerging the pH electrode into culture extract. For calibration, pH standard solutions at 4 and 7 were used. Each measurement was repeated three times to determine variation.

4.2.3 Quantification of oxalic acid production

Oxalic acid level was detected using HPLC, at a wavelength of 210 nm and an organic acid column (Synergi 4U.Hydro.RT80A) with an eluent of 0.005 N H_2SO_4 at 0.5 ml min^{-1} (Clausen et al., 2008). 60 µl of fungal extract was injected. A standard oxalic acid curve was prepared using concentrations as follows: 1.67, 3.13, 6.25, 12.5 and 25 mM, in order to derive the oxalic acid concentration from the absorbance

reading. The retention time for oxalic acid was at 10 minutes. The concentration of oxalic acid in fungal extracts was determined by measuring the total area under the peak and it was converted into mM units (Hunt et al., 2004). The results were plotted against other parameters (e.g. pH and quinone production).

4.2.4 Quinone production

In order to measure 2,5 DMBQ and 4,5 DMBQ, a modified method from Shimokawa et al., (2004) was used. Using 60 µl filtered supernatant (fungal extract), was applied to a C-18 HPLC column (Lichrospher 100; RP-18; 5µm). The column was eluted isocratically with water-acetonitrile-formic acid (80:20:0.1) as a carrier and it was run at 1.5 ml min^{-1} at the ambient temperature. The absorbance was monitored at 280 nm and the quantitative results were obtained by calculating the product concentration using a standard curve and presented in mg units. The retention time for 2,5-DMBQ was detected at 3.8 minutes. The quinone 4,5 DMBQ was also measured in the wheat straw SSF aqueous extract.

4.2.5 Iron reductase assay in *S. lacrymans* fungal extract (Ferrozine assay)

The measurement of any potential non-enzymatic reactions was carried out using a modified method to that developed by Arantes et al., (2009) and Kerem et al., (1999). The reduction of Fe^{3+} was determined using Ferrozine reagent [3-(2-pyridyl)-5,6-bis-(4-phenylsulfonic acid)-1,2,triazine] (Sigma) and the experiment was conducted in 96-well micro titer plates. To test for iron reducing capabilities, fresh $FeCl_3$ was prepared and mixed in acetic acid buffer pH 4.6 solution with 2 mM

Ferrozine, before the aliquot (e.g. Gt chelator, DHBA) was added to initiate the reaction (Goodell et al., 2006). In this experiment, 2,3-DBHA was used as a positive control for convertion of Fe^{3+} into Fe^{2+} during the reaction. 10 µl Ferrozine reagent was added to the reaction before spectrophotochemical measurement to detect the presence of Fe^{2+}. The absorbance was recorded at 550 nm using a TECAN spectrophotometer, following incubation for 10 minutes. Each treatment was done in triplicate. A stock solution of 0.1mM $FeCl_3$ was prepared and used to perform a standard curve.

Using different amounts of fungal extract (25; 50; 75; and 100 µl), the experiment was conducted without the addition of $Fe3^{+}$, with the presence/absence of 2,3-DHBA (50µl).

A parallel experiments were performed to observe the effect of different rates of Fe^{3+} application on iron reduction using the optimal amount of fungal extract selected from the previous experiment described above with the following treatments :

- 25 µl fungal extract + 10 µl Ferrozine + no 2,3-DHBA + 10 µl Fe^{3+}
- 25 µl fungal extract + 10 µl Ferrozine + no 2,3-DHBA + 30 µl Fe^{3+}
- 25 µl fungal extract + 10 µl Ferrozine + no 2,3-DHBA + 50 µl Fe^{3+}
- 25 µl fungal extract + 10 µl Ferrozine + 50 µl 2,3-DHBA + 10 µl Fe^{3+}
- 25 µl fungal extract + 10 µl Ferrozine + 50 µl 2,3-DHBA + 30 µl Fe^{3+}
- 25 µl fungal extract + 10 µl Ferrozine + 50 µl 2,3-DHBA + 50 µl Fe^{3+}

4.2.6 Chemical composition of degraded wheat straw using FTIR

Possible modifications of the structural composition of the straw was determined using FTIR (Fourier Transform Infra Red Spectrophotometer) using a Perkin Elmer 100-in the Chemistry Department, University of Warwick,UK), following a combination of the methods from Dorado et al., (1999) and Sun et al., (2005) using a wavelength range of 650 to 4000 cm^{-1}. The spectral background was determined using no sample, which was subsequently subtracted from experimental samples. Wheat straw from the different time points of incubation was finely ground and 1 g of sample was placed onto a diamond plate for analysis.

The following wavelength ranges were selected to provide index peaks as they reflected chemical changes in the lignocellulosic matrix of wheat straw as suggested by Dorado et al., (1999). These ranges were: 1510 cm^{-1} and 1610 cm^{-1} (aromatic bond), 1740 cm^{-1} (non-conjugated carbonyl group), 1660 cm^{-1} (conjugated carbonyl groups), 1460 cm^{-1} (alkyl bending vibration), 1330 cm^{-1} (syringyl ring breathing), 1270 cm^{-1} (guaiacyl unit), 1040 cm^{-1} (pyranose ring vibration of carbohydrate). Changes in lignin can be detected within the 1040/1510 cm^{-1} bands, while an increasing aliphatic/aromatic ratio can be observed at 1460/1510 cm^{-1}. Moreover, oxidative alteration of aromatic lignin moieties can be seen using a ratio of bands at 1740/1510 cm^{-1} or 1660/1510 cm^{-1} (Dorado et al., 1999).

4.3 Results

4.3.1 The relationship between pH, oxalic acid and quinone production in *S. lacrymans* wheat straw SSF

In the wheat straw *S. lacrymans* SSF, the oxalic acid production of *S. lacrymans* over 49 days of culture was monitored at regular time intervals. No production of oxalic acid was detected before 21 days; subsequently it increased progressively up to day 35 when it levelled off around 10mM (Figure 36). Meanwhile, the pH of cultures gradually decreased from an initial pH of 5.7 to 4.4 after 49 days of culture (Figure 36). The relationship between the quantity of oxalic acid and pH showed a negative correlation (data not shown).

The quinone (2.5-DMBQ) was detected using HPLC and the temporal production of 2.5-DMBQ in *S. lacrymans* culture is presented in Figure 36. 4.5 DMBQ was also measured although the standard behaved correctly none of this compound was detected in the experimental samples. In contrast 2.5-DMBQ levels significantly increased during culture and reached a maximum level of 28.69mM (0.48 mg g^{-1} straw) after 28 days of culture before falling again to a level of 12.22mM (0.20 mg g^{-1} straw) at 49 days (Figure 36).

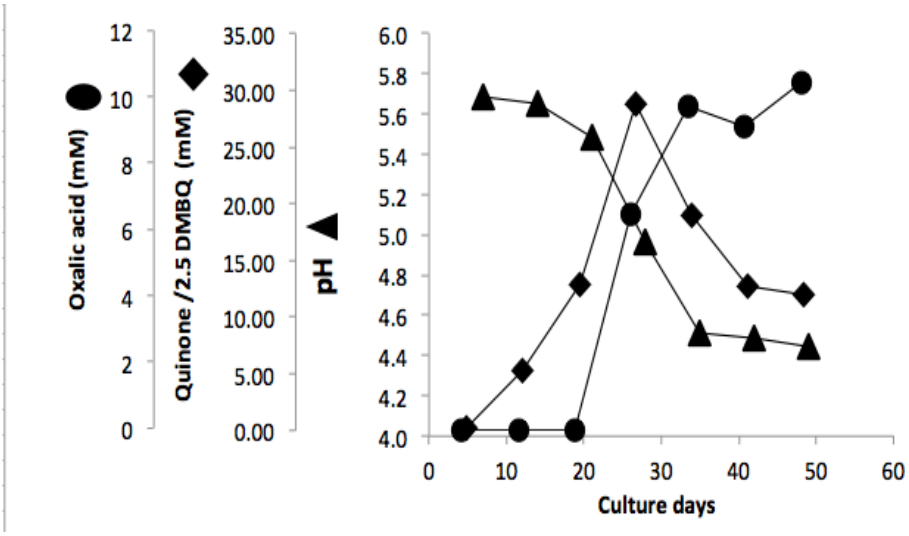

Figure 36. The relationship between pH, oxalic acid and quinone release by *Serpula lacrymans* cultures during a time courses of wheat straw SSF.

4.3.2. Detection of Iron reducing compounds using Ferrozine assay

4.3.2.1.The effect of incubation time on the production of Fe reduction

The highest concentration of oxalic acid and 2,5- DMBQ released by *S. lacrymans* was at on 28-35 day (Figure 36). This is correlated with an increase in iron reduction (Fe^{2+}). The strongest Ferrozine response was detected in the 28 day old culture, however there was no significant iron reduction in the first three weeks after inoculation. There was no definitive effect of addition of DHBA on the production of Fe^{2+} (Figure 37).

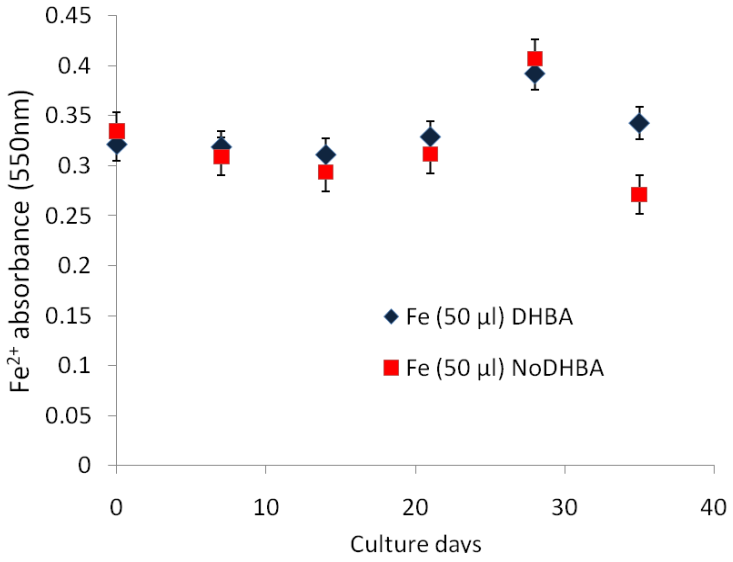

Figure 37. Results from the Ferrozine assay of extracts from wheat straw inoculated by *S. lacrymans* after different times of incubation. Absorbance values at 550nm represent the amount of iron reduced as Fe^{2+}. Error bars represent LSD (P<0.05)

4.3.2.2 The effect of fungal extract, 2,3-DHBA and time of reaction on Fe reduction

In order to examine how the addition of Fe^{3+} affects the non enzymatic Fenton reaction, Fe^{2+} absorbance was measured using the Ferrozine assay. The results are presented in Figure 38. The absorbance was similar between with and without the addition of 2,3-DHBA. The amount of extract added had a significant effect (P<0.05). The highest absorbance was found with the highest application of fungal extracts (100 µl). These might be due to the effect of the excess of Fe^{3+} reacting with oxalic acid present in the extract. This lowers the pH to allow more Fe^{3+} to be reduced to Fe^{2+}. But, the role of 2,3-DHBA in reduction of Fe^{3+} and increase the absorbance was not significant.

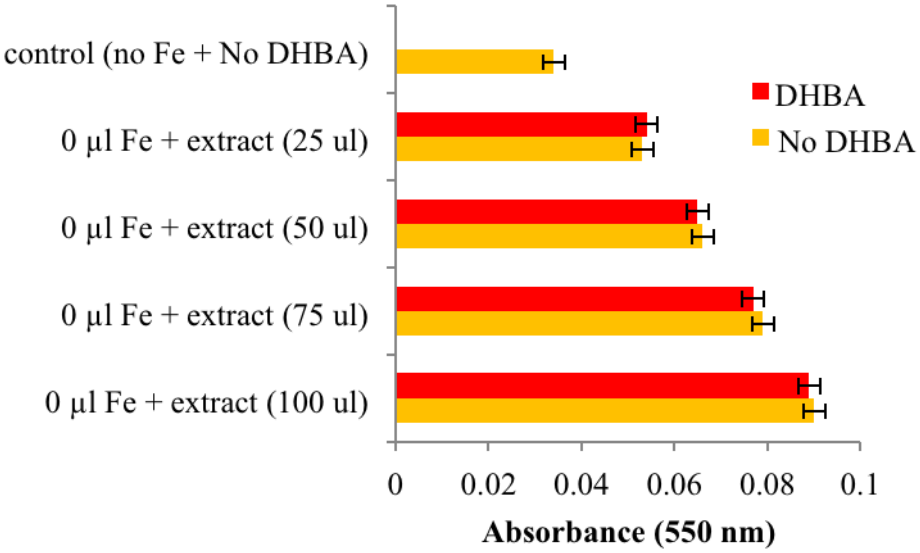

Figure 38. The effect of different amounts of fungal extract on the reduction of iron in the absence of Fe^{3+}. Absorbance values at 550nm are representative of the amount of iron reduced (Fe^{2+}). Error bars show the least significance difference/LSD ($P<0.05$)

4.3.2.3 The effect of the addition of Fe^{3+} and 2,3-DHBA on iron reduction

Different concentration of Fe^{3+} solution was added to the same amount of fungal extract (25 µl). The reduction of Fe^{3+} ($P<0.05$) significantly increased with the application of increasing amounts of Fe^{3+} solution (Figure 39). The greatest Fe^{2+} absorbance was detected using 50 µl Fe^{3+} in the presence of 2,3-DHBA. This was 20% higher compared to a non 2,3-DHBA treatment using the same concentration of Fe^{3+} (Figure 39). Regardless of the presence of 2,3-DHBA, the increasing amount of Fe^{3+} from 10 to 50µl had a significant effect.

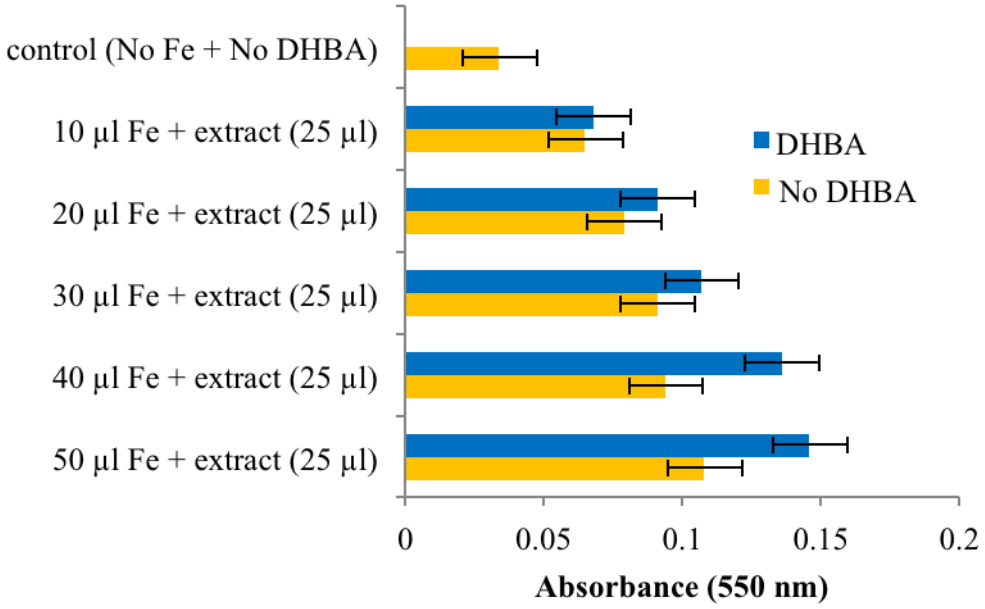

Figure 39. The effect of differing amount of Fe^{3+} (µL) added with the same amount of fungal extract (25 µl). Absorbance values at 550nm are representative of the amount of iron reduced (Fe^{2+}). Error bars represent LSD ($P<0.05$)

4.3.3 Loss of wheat straw substrate following *S. lacrymans* colonization

Based on gravimetric assay, the weight of the wheat straw was determined. After incubation for 35 days (Figure 40) this decreased significantly by 10-20%.

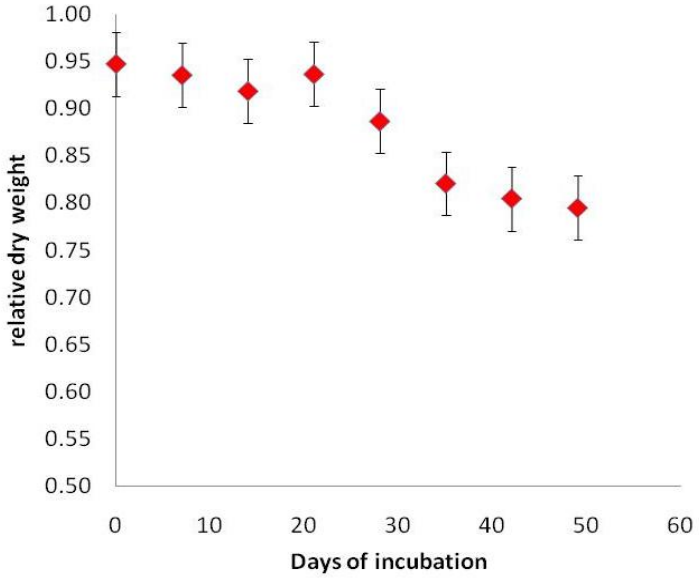

Figure 40. The changes of relative dry weight of wheat straw SSF inoculated by *S. lacrymans.* Error bars represent LSD (P<0.05)

4.3.4 FTIR carbon chemistry signatures

Sample characterization using FTIR spectroscopy identified obvious changes in the composition. The FTIR spectra illustrating possible lignocellulose breakdown is shown in Figure 41. The peak at 3430 cm^{-1} corresponds to hydroxyl groups, whilst the bands at 2930 and 2840 cm^{-1} are attributed to increase of C-H stretching of the aromatic methoxyl groups and methylene groups.

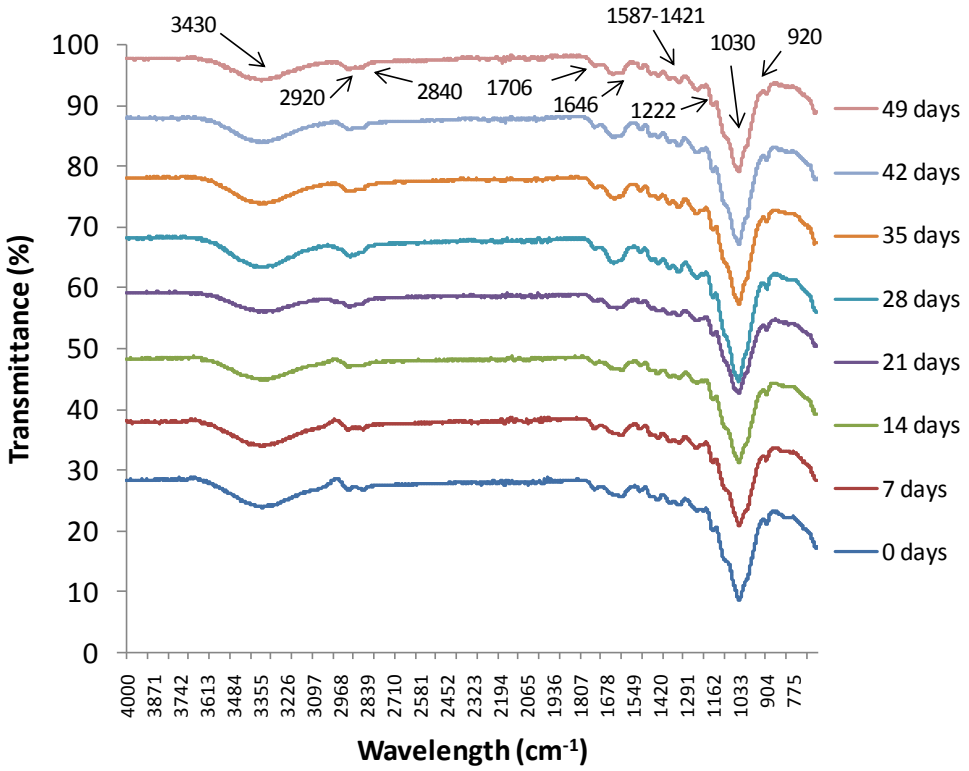

Figure 41. FTIR spectra of representative profiles showing how *S,lacrymans* degrades wheat straw during SSF as indicated by the spectra produced from samples collected on different days of culture. The wavelength measurements allow specific functional groups to be determined. Some peaks are related to compounds produced from lignocellulose degradation. An arrow shows the position of such compounds.

The peak at 1706 and 1646 cm^{-1} represented the conjugated carbonyl stretches and the aromatic skeletal gave a peak at 1587-1421 cm^{-1}. Moreover, the aromatic ring with C-O and C=O stretching are at 1222 cm, aromatic C-H plane, C-O primary alcohol, guaiacyl type or polysaccharide is at 1030 cm^{-1}, whilst 920 cm^{-1} is for C-H out of place aromatic ring. The peak size of some key elements (eg. conjugated carbonyl stretches, aromatic ring and carbohydrate), increased under the treatments with *S. lacrymans* over the period of 0-42 days culture (Figure 41), indicating the oxidation of aromatic lignin compounds and lignin breakdown. A detailed statistical analysis of the changes in selected bonds presented in Table 18.

Table 18. Analysis of FITR results showing change in selected key wavelengths indicating changes following growth of *Serpula lacrymans*. Letters (a and b) represent a change following 28 days in culture at which point a significant difference can be observed for each functional group ($P<0.05$).

Wavelength (cm^{-1})	Functional groups	Days of incubation	Transmittance	LSD
1030	Pyranose ring vibration of carbohydrate or C-O primary alchohol	0	79.38 a	6.15
		7	82.90 a	
		14	83.36 a	
		21	83.12 a	
		28	75.75 b	
		35	77.07 b	
		42	77.40 b	
1510	Aromatic skeletal vibration	0	96.55 a	1.15
		7	96.85 a	
		14	97.50 a	
		21	97.59 a	
		28	96.01 b	
		35	95.87 b	
		42	96.00 b	
1660	Conjugated carbonyl group or C=O conjugated keton stretch	0	96.23 a	1.47
		7	96.63 a	
		14	97.16 a	
		21	97.10 a	
		28	94.76 b	
		35	94.89 b	
		42	95.08 b	
1740	Non conjugated carbonyl group or C=O aliphatic carboxyl stretch	0	97.05 a	1.11
		7	97.23 a	
		14	97.86 a	
		21	98.16 a	
		28	96.77 b	
		35	96.57 b	
		42	96.63 b	

There was a significant reduction in the pyranose ring vibration of carbohydrate or C-O primary alcohol (1030-1040 cm^{-1}) over the period of incubation (Table 18). A similar trend was also observed in other bands (1500-1510, 1600-1660 and 1700-1740 cm^{-1}), which correspond to aromatic skeletal vibration, conjugated carbonyl group or C=O conjugated ketone stretch and non-conjugated carbonyl group, respectively. These changes in IR transmittance were associated with an

increase in absorbance of selected chemical fingerprint showing the presence of novel compounds.

4.4 Discussion

In this study a significant increases of oxalic acid was observed at 21 to 35 days after culture of *S. lacrymans*. At the same time the amount of total reducing sugar was observed to decrease (this information has been presented in Chapter 3). For comparison, the production of oxalic acid in the brown rot *Fomitopsis palustris*,, reached an optimum oxalic acid after 14 days cultured in PDA agar at 33^{o}C, supported by 2% (w/v) glucose (Munir et al., 2001). A similar fungus *F. palustris*, was reported to have optimum production of oxalic acid at 14 days (3.5 g l^{-1}), which dropped the pH to 2.2 from the initial level (pH = 5) (Yoon et al., 2007). The production of oxalic acid by *P. placenta* grown on three substrates (1% crystalline cellulose (Avicel), 1% amorphous cellulose (Waste) and 0.5% glucose became obvious after 3 weeks (0.1^{-1} g l^{-1}) growth culture, this was accompanied by a decrease in the pH to 2.8-3.2 (Ristchkoff et al., 1995). This fall in pH was even greater (pH 1.7) using wood culture medium (Green et al., 1994).

The production and accumulation of extracellular oxalic acid by brown rot fungi is responsible for the rapid drop in pH (Green et al., 1991). This is substantiated by the results of a study by Espejo and Agosin, (1991), which showed that oxalic acid production by *Wolfiporia cocos* and *P. placenta* reached 2.00 and 0.95 mg l^{-1} after 4 days cultivation, respectively, whilst the pH dropped to around 3.0. Oxalic acid not only reduces the pH but can also act as a strong chelator of Fe^{3+}

(Fe oxalate complex), (Gamauf et al., 2007). In this study, pH of *S. lacrymans* culture declined from 5.7 to 4.4 after 49 days.

Oxalic acid production has been described in previous publications (Shimada et al., 1993; Munir et al., 2001). Brown rot fungi have been reported to employ two enzymes for oxalic acid production, these are: glyoxyl oxidase (dehydrogenase) and oxaloacetate hydrolase (Ritschkoff et al., 1995). It has been suggested that sugars are oxidized to CO_2 by the fungus, however the sugars might also be converted to oxalate through a unique metabolic linkage between the TCA (trycarboxylic acid) and glyoxylate cycle (Munir et al., 2001). The belief is that the glyoxylate cycle is used only when microorganisms are grown in the absence of sugars (Kornberg, 1966; Cioni et al., 1980 and Munir et al., 2001). Oxalic acid as an extracellular metabolite thought to be involved in cellulosic breakdown due to its ability to increase pore size allowing penetration of fungal enzymes into the cellular structure (Dutton et al., 1993; Ritschkoff et al., 1995). However the biochemical role of oxalic acid in the brown rot fungi is not clear (Ritschkoff et al., 1995).

pH has also been reported to be an important factor in controlling cellulose degradation by *G. trabeum* (termed *Gt chelator*) via mediation of the Fenton system (Xu and Goodell, 2001). Lu (1994) noted that *Gt chelator* activity was more pronounced at a pH of 2 than 4. However the most suitable pH for cellulose degradation was 4 (Xu and Godell, 2001). This is similar to the final pH (pH = 4.4) found after 49 days of culture with *S. lacrymans*.

It has been proposed that several low molecular weight phenolic compounds (e.g. 2,5-dimethoxyhydroquinone/2,5DMBQ and 4,5 dimethoxycatechol/4,5DMC), might also function within the Fenton reaction by reducing Fe^{3+} to Fe^{2+} (Kerem et al.,

1999; Hammel et al., 2002; and Shimokawa et al., 2004). Two hydroquinones produced by *G. trabeum* (2,5-DMBQ and 4,5 DMBQ) are able to reduce this Fe^{3+} oxalate complex. But, 2,5-DMBQ was more effective than 4,5-DMBQ in the stimulation of extracellular Fenton chemistry (Jensen et al., 2001). 4,5-DMBQ has not been found within our SSF of wheat straw with *S. lacrymans*. In this study the optimum production of quinone (2,5-DMBQ) was found after 28 days before declining. Shimokawa et al., (2004) reported that the production of 2,5 DMBQ by *S. lacrymans* liquid culture reached a peak level of 90 µM within 2 weeks. The reduction in amounts of (2,5 DMBQ) detected after 28 days of culture suggests that *S. lacrymans* might reduce 2,5 DMBQ to 2,5 dimethoxy hydroquinone (2,5 DMHQ) as previously suggested (Shimokawa et al., 2004). 2,5 DMBQ has also been discovered in *P. placenta* cultured aspen wood wafer culture (Wei et al., 2010).

Quinone (2,5-DMBQ) was detected 20 years ago in *Gloephyllum sepiarium* but its biodegradative function was not known (Kerem et al., 1999). The production of Fe^{2+} and H_2O_2 for non-enzymatic reaction in *G. trabeum* culture is due to the participation of quinone (DMBQ) following the mechanism which has been described by Kerem et al., (1999) : 1). *G. trabeum* mycelia reductase reduces DMBQ to DMHQ, 2). DMHQ reduces Fe^{3+} to release Fe^{2+} non-ezymatically and yields DMHQ semiquinone radical, 3.) The re-oxidation of semiquinone radical by O_2 into DMBQ generates H_2O_2. However, the production of DMHQ in *P. placenta* is not stable (Wei et al., 2010). The results obtained within this study supports the idea that a similar pathway occurs in *S. lacrymans*.

2,3-DHBA is highly effective at reducing Fe^{3+} to Fe^{2+} and in the current experiment was expected to mimic DMBQ. The ability of 2,3-DHBA to reduce Fe^{3+}

contained in culture extract or derived from additional $FeCl_3$ was confirmed in this study. The low molecular weight chelator and phenolic compounds isolated from *G. trabeum* wood decay fungi known as *(Gt chelator)* (Goodell et al., (1997), included compounds such as derivatives of hydroxyphenylacetic acid, hydroxybenzoic acid, dihydroxyphenlpentane-1,4 diol, and hydroxybenzene. These compounds are altered to form semiquinone and quinone following oxidation. Many of these compounds were shown to have a similar function to 2,3-DHBA (Goodell et al., 1997). Some of these compounds were detected in the *S. lacrymans* culture extract and are listed in the previous chapter (Chapter 3).

In this study the interaction between fungal extract, 2,3-DHBA and Fe^{3+} were tested. Without the addition of Fe^{3+} no significant difference in the production of Fe^{2+} with or without the addition of 2,3-DHBA was found. This suggested that the presence of sufficient iron is essential. Goodell et al. (1997) reported that the application of different rates of pure Gt chelator (1.1 µM to 5.6µM) with 30 µM Fe^{3+} and 2.5 mM Ferrozine in pH 4.5 acetate buffer increased the rate of reduction of iron in solution. Reducing the pH of the solution from 8 to 2 in the presence of *Gt chelator* at 100 µM rapidly increased the absorbance of available reducing iron. Moreover, the *Gt chelator* effect is substantially reduced when the reaction was carried out in the presence of oxalate. Oxalate is a weak chelator for iron (Goodell et al., 1997). Xu and Goodell (2001) noted that when the Fe^{3+} to *Gt* chelator ratio was less than a critical value (14:1 for 3 hour reaction and 100:1 for 24 and 48 hour reaction), increasing amounts of *Gt* chelator did not substantially increase cellulose degradation. Larger amount of *Gt* chelator (ratio <111:1) actually suppressed cellulose degradation. Similar evidence was also reported by Xu and Goodell (2001),

who examined the effect of oxalic acid on wood cellulose degradation. Fe^{3+} acts as an important key in this cellulose degradation, since it has a strong affinity for *Gt* chelator (Xu and Goodell, 2001). To release oxalate-Fe chelation or by other low molecular weight compound, there should be an excess of Fe in the solution.

Since the fungal extract not only contained quinone, but also oxalic acid, the proportional quantity of these compounds in the Fenton reaction needs to be examined to ensure the effectiveness of the reaction simultaneously. Increasing the *Gt* chelator to iron ratio is thought to increase the Fe reduction (Xu and Goodell, 2001).

The weight loss of wheat straw following growth of *S. lacrymans* was found to be 10-20% following 35 days of incubation. Compared to other research, this value was found to be similar to that found for wheat straw SSF with other fungi (*P. chrysosporium, P. eryngii, P. radiata* and *C. subvermispora*), in which a weight loss of about 10% has been reported following 30 days of incubation. *P. chrysosporium* after 60 days incubation can reduce straw weight by up to 45%, while over the same period *P. eryngii, P. radiata* and *C. subvermispor*a only achieved a 20-30% drop in mass (Dorado et al., 1999).

In this study, the degradation of cellulosic component might well be due to the combined contribution of oxalic acid, quinone and other low molecular weight compounds. The role of oxalic acid is revealed; it can reduce pH of *S. lacrymans* wheat straw SSF culture and modify wheat straw biochemical composition.

The effect of *S. lacrymans* SSF on the structure of the straw was measured by the IR technique. The results showed that there was a reduction in the polysaccharide functional group and an increase in aromatic bonds. Similar trends have been shown

following culture of *C. subvermispora* and *P. radiata* on wheat straw SSF (Dorado et al., 1999). The IR technique may only observe small changes in the chemical transformation of wheat straw, in general the changes can not detect an extensive process of lignin degradation but it can monitor the oxidative reaction of aliphatic or aromatic structure in wheat straw SSF. The IR results can provide complementary information to those obtained from relative weight loss, low molecular weight and phenolic compound (Chapter 3), pH and quinone production, and total reducing sugar (Chapter 3).

Chapter 5. The identification and expression of iron reductase genes in *Serpula lacrymans*.

5.1 Introduction

The brown rot fungus *Serpula lacrymans* causes one of the most destructive types of decay in wooden structures, dry rot. In general brown rot fungi lack class II peroxidases, which are used by white rot fungi to depolymerise lignin. In the white rots the CDH family of genes are known to play a vital role in lignocellulosic breakdown. Two CDH genes have been identifed in *S. lacrymans* but neither are expressed when the fungus grows on a wood subtrate (Eastwood et al., 2011; Watkinson and Eastwood, 2012). The genome sequence of compatible homocaryons of *S. lacrymans* S7 (S7.3 and 7.9) were sequenced during my project. A bioinformatic search of the genome sequence identified two putatives genes with some similarity to CDH, containing similar iron reductase domains. One of these genes also contained a cellulose binding module-1 (CBM1). It was postulated that these genes might play a role in the breakdown of lignocellulose. These genes were named iron reductase genes IR-1 and IR-2. This chapter aims to characterize these iron reductases and their expression during fungal growth on wheat straw SSF.

Genes related to decomposition of lignocellulose biomass are potentially upregulated during cultivation of *S. lacrymans*. However, the relative transcription of the genes or the expressed protein may vary widely depending on the growth medium and the cultivation condition (Allen and Roche, 1989). For instance *S. lacrymans* gene expression differs significantly when grown on

wood, soil or minimal medium. The endoglucanases glycoside hydrolases (GH74) for example exhibit a 100 fold greater expression when grown on wood samples compared to a glucose medium (Eastwood et al, 2011). Due to the different gene expression patterns identified during growth on different media, we were interested to compare the expression patterns of key genes when the fungi are grown on wheat straw as differences in growth had been shown (chapter three).

5.1.1 Cellobiose dehydrogenase (CDH): Occurence, Functionality and Structure

Cellobiose dehydrogenases (CDH; E.C. 1.1.99.18; cellobiose (acceptor) 1-oxidoreductase) are extracellular hemoflavoenzyme produced by various lignocellulose-degrading fungi (Bey, 2011). As monomeric enzyme, CDH contains two prosthetic groups a flavin and cytochrome b type heme group (Bey, 2011) in two separate domains (Yoshida et al., 2005). The heme binding domain in N terminal position contains a cytochrome b-type heme which contains unusual Met/His ligation of the heme co-factor (Hallberg et al., 2000). Using the electron acceptors of CDH such as dioxygen, quinones, phenoxyradicals and others, the FAD-binding domain in the C terminal catalyses two electron oxidation of cellobiose and more generally cellodextrin, mannodextrins and lactose to coresponding lactones. It was reported that in CDH enzymes, the cellulose binding site is located on the flavin domain but not in the catalytic domain, because the enzyme bound to cellulose can still oxidize cellobiose

(Renganathan et al., 1989). Some results indicated that the oxidation of electron donor (cellobiose) was carried by the FAD group, then it was converted to $FADH_2$. However, the presence of the heme domain could stimulate the reduction of one-electron acceptor such as ferricyanide, phenoxy radical and cytochrome c (Henriksson et al., 1991). The heme domain, has also been suggested to play a role in the oxidoreductase activity to breakdown cellobiose (Cox et al., 1992). The CDH enzymes can reduce a wide range of substance such as cytochrome-c, dichlorophenol-indophenol (DCPIP), benzoquinone, Fe^{3+}, MnO_2, Mn^{3+} complexes and even oxygen. These enzymes have also been reported to contribute to lignin degradation and reduce quinones, phenoxy and cation radicals. The reduction of MnO_2 by the enzymes can reduce Mn^{3+} complexes directly and provide Mn^{2+} (Fang, et al., 1998).

The sequence corresponding to the heme domain is located in the N terminus following a short signal peptide indicating extracellular secretion of the protein (Raices et al., 1995). The heme domain consists of 190 residues, which has one disulfide bonds and mostly contains high of aromatic amino acids (Cox et al., 1992).

CDH enzymes have been described as produced by various wood degrading fungi such as: *Phanerochaete chrysosporium* EC 1.1.99.18 (Henriksson et al., 1997, Samejima et al., 1997); *Grifola frondosa* AB083245 (Harreither et al., 2009); *Trametes versicolor* AF029668 (Dumonceaux, 1998); *Schizophyllum commune* AS 5.391 (Fang et al., 1998); *Pycnoporus cinnabrinus* AF081574 (Moukha et al., 1997) *Coniophora puteana* AB161046 (Schimdhalter et al., 1993, Kajisa et al., 2004); and *Ceriporiopsis subvermispora* EU660051

(Harreither et al., 2011, Blanchette et al., 1997). CDHs have been shown to bind cellulose in different ways depending on the species (Harreither et al., 2011). In terms of oxidoreductase genes, the CDH gene have not been identified in the brown rot *P. placenta* (Table 16).

The depolymerization of non-phenolic lignin model compounds by the CDH system has been reported by Henriksson et al., (2000b). CDH released hydroxyl radicals by reducing Fe^{3+} to Fe^{2+} and O_2 to H_2O_2 (Kremer and Wood, 1992a; 1992b) following the reaction presented in Figure 42.

$$\text{Cellobiose} + 2\,Fe^{3+} \xrightarrow{\text{CDH}} \text{cellobionolactone} + 2\,Fe^{2+}$$

$$\text{Cellobiose} + O_2 \xrightarrow{\text{CDH}} \text{cellobionolactone} + H_2O_2$$

$$Fe^{2+} + H_2O_2 \xrightarrow{\text{Spontaneous}} Fe^{3+} + OH^- + OH\cdot$$

Figure 42. A schematic showing the mechanisms by which CDH enzymes can produce hydroxyl radicals (Henriksson et al., 2000b).

Moreover, it has been reported that CDH enzymes are able to depolymerize cellulose, xylan and lignin. The depolymerization of lignin can be achieved through the cleavage of the chain between Carbon-α and Carbon-β, oxidizing secondary alcohol on Carbon-α to carbonyl groups or performing aromatic ring cleavage (Figure 43) (Henriksson et al., 2000b).

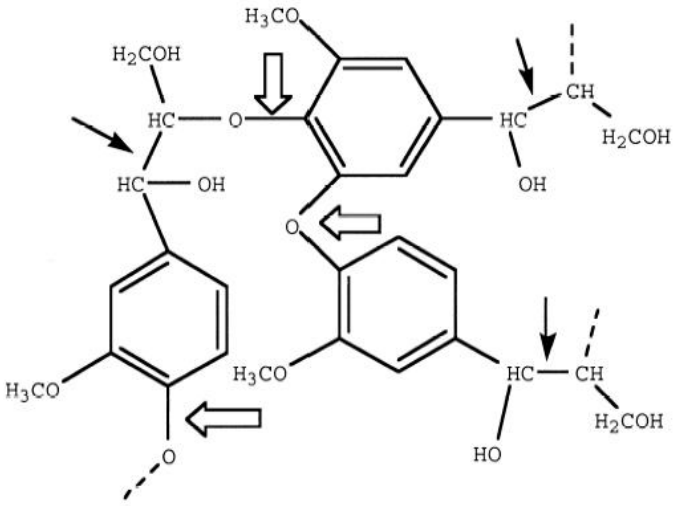

Figure 43. The sites of lignin depolymerization
The larger arrows (⇒) show the cleavage sites for the demethoxylation used by the CDH system, while this arrow (→) shows the oxidative cleavage normally used by LiP or laccases (Henrikssson et al., 2000b)

5.1.2 Cellulose binding module type-1 (CBM1)

Another key group of genes involved in lignocellulosic degradation are the carbohydrate-active enzymes (CAZy) many of them contain a carbohydrate binding module (CBMs), which is defined as a noncatalytic polysaccharide-recognizing module. CBMs are classified into 42 families based on similarity of amino acids sequence and the three dimensional structure in CAZy database. Among the CBMs families, CBM1 has been recoqnized related to the catalytic function of carbohydrate binding modules (CBMs) which play an important role in the initial stages of degradation of cyrstalline cellulose (Yoshida et al., 2005). The removal of the CBM cause significant decrease in both binding and catalytic activity againts cellulose (Linder, 1997), suggesting that the CBM1 is directly related to the catalyctic function of these enzymes (Henriksson et al., 1991;

Henriksson et al., 1997). The structures of CBMs from different families are similar, and their carbohydrate binding capacity can be attributed at least in part, to several aromatic amino acids that constitute the hydrophobic surface (Shoseyov et al., 2006). Even though there is similarity between all CBMs, their specific properties are not always identical, even among members from the same family (Linder and Teeri, 1997). The CBMs consist from about 30 to 200 amino acids and exist as single, double or triple domains in one protein which may be located in both N or C terminals and is occasionally centrally positioned within the polypeptide chain (Shoseyov et al., 2006). The CBMs have been decribed in polysaccharide degrading enzymes such as hemicellulases, endomannanase and acetylxylanesterase in *Trichoderma reseei*, esterase (*Penicillium funicusolum*), isomaltodextranase (*Arthrobacter globiformis*), arabinofuranosidases (*Aspergillus kawachii*), pectate lyase (*Pseudomonas cellulose*) and β-glucosidase (*Phanerochaete chrysosporium*) (Shoseyov et al., 2006).

The proportions of crystalline and amorphous cellulose varies in the cell wall of plants (Reinikainen et al., 1992). The functional domain of cellulases and xylanase can usually be of two types: single or multidomain, the majority consists of multiple domain which are joined by the characteristic linker sequences enriched in proline and hydroxyaminoacids (threonine and serine) (Tomme et al., 1995).

Comparative studies of many different cellulases have been applied to determine the common features enabling enzymes to hydrolyze cellulose (Linder et al., 1997), however not all cellulases are effective in binding crystalline cellulose. The overall binding efficiency of the enzymes is enhanced by the

presence of cellulose binding domain (CBD) (Tomme et al., 1998). Cellulose binding modules, CBM1s, are found in cellulases and xylanases which are involved in the degradation of plant biomass (Boraston et al., 2001).

The distribution of CAZy and oxidoreductase genes in Basidiomycetes thought to play a role in lignocellulose degradation is shown in (Table 19). Compared to the white rot fungi, the brown rot fungi mostly lack the GH7 gene family (endogluconase) for the decomposition of cellulose. *P. placenta* is mising both the GH6 and GH7 genes (Table 19). Thus it is important to understand the mechanism by which *S. lacrymans* decompose cellulose.

Table 19. Comparison of the lignocellulolytic carbohydrate active (CAZy) and oxidoreductase genes from four Basidiomycetes (Eastwood. et al., 2011)

	Brown rot		**White rot**	
	S. lacrymans	***P. placenta***	***P. chrysosporium***	***S. commune***
Gene family				
CAZY enzymes:				
Glycosyl Hydrolase (GH)	154	248	182	236
GH3	10	9	11	12
GH5	20 (3)	36(0)	19(4)	16(0)
GH6	1	0	1	1
GH7	0	0	9	2
GH10	1	4	6	5
GH11	0	0	1	1
GH12	1	4	2	1
GH28	7	11	4	3
GH43	2	1	4	19
GH51	1	3	2	2
GH61	5	4	15	22
GH74	1	0	4	1
GT	61	102	66	75
PL	5	8	4	16
CE	12	25	17	30
CE1	1	0	5	9
CE16	4	9	1	4
CBM	23	28	48	30
CBM1	**8**	**0**	**31**	**5**
EXP	8	19	11	19
Oxidoreductase enzyme:				
POX	0	?	16	0
MCO	6	8	5	5
CDH	2	0	1	1
AAOX	6	8	3	1
GlyOX	3	5	7	2
PryOX	0	0	1	1
GluOX	0	0	1	4
QR	2	2	4	4
AOX	1	2	1	1
OXO	3	10	7	5
IGP	3	8	3	7

It is expected that genes involved in lignocellulosic breakdown will differ in their expression patterns compared to those genes involved in prymary metabolism

pathways. Increased enzymatic activity is often preceded by increased gene expression or the modifcation of gene regulators.

5.1.3 The iron reductase genes expression during fungal growth

Gene expression analysis plays an important role in further understanding the signalling and metabolic pathways which underlie developmental and cellular processes in fungi (Hu et al., 2009). In many fields of biological research, microarray analysis, high throughput sequencing technologies and real-time PCR (RT-PCR) are commonly used for measuring transcription abundance and for understanding patterns of gene expression. While RT-PCR provides the simultaneous measurement of gene expression in many different samples for a limited number of genes. However, the micrroarrays allow the measurement of enormous number of genes in parallel analysis in differentially labeled RNA populations (Schena et al., 1995 and Vandesompele et al., 2002) and *Serpula lacrymans* data is not provided in microarrays system.

The use of the RT-PCR to amplify the cDNA reverse transcribed from mRNA has become a routine tool in molecular biology to study low abundance gene expression (Pfaffl, 2001). In general, validation of gene expression following RT-PCR assay can be carried out in two ways: relative quantification and absolute quantification. Relative quantification determines the changes in steady-state transcription of a gene and is often adequate. The absolute quantification,

determines the precise copy number per cell, however, information on the total RNA concentration or unit mass of tissues is a prerequisite (Bustin, 2000).

Relative quantification is based on normalising the expression of gene target to the expression level of a stable reference gene, which is known as internal standard or housekeeping gene. A relative quantification is more appropriate for determining gene expression quantity. For measuring relative quantification of a target gene in real time RT-PCR (Pfaffl, 2001) a new mathematical model has been developed in which they were compared to a reference gene. The normalization of gene expression is a prerequisite for acurate RT-PCR expression profiling (Vandesompele et al., 2002). Errors in RT-PCR quantification transcript of mRNA can easily be compounded by variation in the amount of starting material between samples, especially when the samples have been obtained from different individuals (Thellin et al., 1999).

The choice of the internal standard is very important when normalising the level of expression. The common reference genes could be the one of the following parameters: (1) endogenous control, e.g. a constant expressed reference genes or another GOI (gene of interest), (2) an exogenous control, e.g. an universal and/or/artificial control RNA or DNA, (3) a reference gene index, e.g. consiting of multiple averaged endogenous controls or (4) a target index genes, e.g. consisting an averaged GOIs analysed in the study (Pfaffl, 2002).

Studies show that transcript levels of housekeeping genes used for the standardisation of mRNA expression can vary with experimental conditions (Nicot et.al., 2005). In order to avoid bias during the quantification of gene expression using RT-PCR, the condition of the experiment should not influence the expression of

internal control gene (Schimittgen and Zakrajsek, 2000). Among different tissues, the transcript level of housekeeping gene ideally should be the same in all cells at every developmental stage (Castanera et al., 2012) and remain unaffected by the experimental treatment (Bustin, 2000). Therefore, the use of more than one housekeeping genes as internal standards in an experiment is advantages (Nicot et al., 2005). In our studies three housekeeping genes were used for normalisation (actin, β-tubulin and 60S rRNA).

In this chapter the expression of iron reductase genes during the fungal growth in wheat straw SSF is presented and related to the breakdown of lignocellulose as determined by the products released, including phenolic compounds and total reducing sugars as decribed in Chapter 3.

5.2 Methods

5.2.1 Strains, culture condition and plasmid (general methods)

5.2.2 mRNA isolation

To profile the iron reductases (IR1-IR2) gene expression in SSF cultures, the mycelium of *Serpula lacrymans* was incubated for about 41 days culture in wheat straw solid state fermentation (SSF). At each time point (every three days), 100mg of mycelium was collected, mixed with dry ice and crushed using a coffee grinder. The samples then were incubated overnight at -80ºC to allow evaporation of the dry ice (CO_2). The RNA then was extracted from 100mg of mycelium powder of *S. lacrymans* using a fast RNA Pro-Soil Direct Kit (MP Biomedicals). The purified RNA was quantified using spectrophotometer NanoDrop^{TM} ND-1000 and evaluated using the RNA 6000 Nano assay Kit (Agilent

2100 Bioanalyser). First strand cDNA was synthesised using the ThermoScript™ RT-PCR system from INVITROGEN following the manufacture guidelines.

5.2.3 cDNA synthesis and Polymerase Chain Reaction (PCR)

The genome sequence of *Serpula lacyrmans* has been recently released and initial search for putative iron reductases gene (IR1 and IR2) was done within the JGI *Serpula lacrymans* S7.3 V2.0 database at http://genome.jgi-psf.org/SerlaS7_3_2/SerlaS7_3_2.home.html. Primers specific to both these genes were designed in order to amplify any mRNA products. The IR1 and IR2 genes were amplified using primers, designed from the sequence from the *Serpula lacrymans* genome (Table 20). All primers were ordered form INVITROGEN. 5µg RNA and 2µM Oligo dT18 (Invitrogen) were denatured at 65˚C for 5min and cooled on ice for 2 minutes. The 5x cDNA synthesis mix, (0.1M DTT (Invitrogen), 1xSuperScript Buffer (Invitrogen), 10mM dNTPs (Invitrogen), x1 RNaseOUT (Invitrogen), x1 SuperScript RT (Invitrogen) and DEPC- H_2O) were added and the following cycles was completed: 1 cycle of 96ºC (5min); 30cycles of 95ºC (20sec), 59ºC(20sec), 73ºC(40sec) and 1 cycle of 73ºC(10min). The cDNA was then stored at -20ºC.

5.2.4 PCR amplification and cloning of iron reductase from the brown rot fungus *Serpula lacrymans*

cDNA encoding iron reductases (IR1 and IR2) were cloned using a binary vector/plasmid and following a protocol from TA cloning kit INVITROGEN Cat no K2020-20. All PCR products were ligated into pCR.2.1. The ligation was performed

overnight at 4ºC as follow: 2µl PCR product, 1µl 10x ligation buffer, 2µl pCR 2.1 vector and 1µl t4 DNA ligase.

The constructs then were transformed into *E. coli* (DH5α cells) and the transformants were cultured overnight at 37ºC in LB agar plate containing 50µg/ml kanamycin (KAN) selective media. Plasmid DNA from positive colonies was isolated using the alkaline lysis miniprep method (QIAGEN Plasmid Mini Purification protocol). The presence of a fragment of the correct size was confirmed by PCR using gene specific primers or plasmid specific M13 Forward and M13 Reverse primers and the yield of DNA were determined by both UV spectrophotometer (Nano-drop) and quantitative analysis on a 1.2% agarose gel.

5.2.5 cDNA sequencing analysis

Sequencing reactions were performed using the ABI BigDye terminator V.1.1/3.1 seq Kit. Each reaction contained a vector specific primer (3.2pmol), 2µl ready reaction mix (Big dye V3.1), 1µl big dye sequencing buffer and 1µl of plasmid cDNA (100ng) samples. Each reaction was made up to 10µl with pure distilled water. PCR cycles (25) were as followed: 96°C for 10 sec, 50°C for 5 sec and 60°C for 4 min. The product were then analysed using a ABI3130xl sequencer at the School of Life Sciences-Wellesbourne campus. Searches were performed using BLAST algorithms against various databases in the GenBank (http://www.ncbi.nlm.nih.gov/BLAST) and also from the *S. lacrymans* genome databases.

5.2.6 Real Time-PCR analysis

Transcript level of selected genes were determined from mycellium growing on wheat straw solid state fermentation media using RT-PCR. Gene specific primers were designed using Primer select from DNASTAR- Lasergene and the following criteria: melting temperature approximately 60°C and the product size in the range of 100-150bp. To avoid false positive results which are caused by contaminating genomic DNA, the primers were designed over the boundary of two separate exons using the sequence information of IR1 and IR2 obtained in section 5.2.5. The primer design is shown in Table 20. The exon-intron arrangment for the genes following cDNA and genomic DNA allignment can be seen in Appendix 1.

Table 20. The primers used for cDNA synthesis

Primers cDNA			
Name	**Accesion Number**	**Primer Sequence 5'-3'**	**Primer sequence 5'-3'**
Iron reductase (IR1)	452187	AGCAGGATGTTTAGCCACCT	GTAGCATCACAGCCACT
Iron reductase (IR2)	417465	ACATGTTCCAGAAGCTCTTGGT	TGCACGACCATCGTTCACA

Table 21. The QRT-PCR primer design

QRT-PCR primers				
Name	**Primer Sequence 5'-3' Forward**	**Primer sequence 5'-3' Reverse**	**Length (bp)**	**Tm (°C)**
Iron reductase (IR10	GGCCTTGTCTTACCCCCTTTGTC	CCATAGTACCCCCAACGCT GAG	118	56.7
Iron reductase (IR2)	GCCTCACATTCCCTCCCGTATC	ATGGCCAGAGAACGAACA GTAAGC	147	56.7

Table 22. The primers designed for amplification of housekeeping genes

Housekeeping gene				
Name	**Primer Sequence 5'-3' Forward**	**Primer sequence 5'-3' Reverse**	**Lengh t (bp)**	**Tm (°C)**
Actin	AGAAGCCAAGATAGATCCA CCAAT	TGACCTCGCTGTCGCCA TC	137	55.9
β-Tubulin	CGTTCCCCGTGCTGTCTTGG TC	CTCACGTCCTTTTGCCC AGTTGTT	142	57
60S	GGTGCCGCTGCCCTTGAACG	TCCTGCCAGGCTTGAG ACGC	118	56

PCR amplification was performed in 20µl total reaction volume, using 1µl of cDNA solution as template, 10µl of Lightcycler 480 SYBR Green master (Roche Diagnostic Ltd) and 0.5µM of each primers. The RT-PCR was performed using the Lightcycler 480 system multiwell plate (Roche Applied Science).

The following amplification programme consisted of one cycle of 60°C for 1 min an initial cycle (95°C for 1 min), followed by 45 cycles of denaturation at 95°C for 30 sec, 60-62°C for 1 min (temperature specific for each primer pairs). The melting curve was obtained by performing 45 cycles at 95°C for 1 min, 40°C for 1 min, and 60°C for 30 sec and followed by 72°C for 5 min. The validity of primers for non specific products in the reaction was validated by analyzing the melting curves and the standard curve were generated for each gene using cDNA with 5 times dilution. The control treatment included sterilised diethylpyrocarbonate (DEPC)-treated water instead of cDNA, to detect any contaminant or primer-based artefact.

All reactions were done in triplicate in 384-well microtiter plates and a no-template control was run for each primer pair. Verification of the products was confirmed on a 1.25% agarose gel.

5.2.7 The quantification of gene expression

cDNA of IR1 and IR2 *S. lacrymans* genes was used to create a relative standard curve for determining the differences of target quantity between a test sample. Quantification of gene expression was determined relative to a standard curve for each target gene. In this study the relative quantities of RT-PCR IR-1 and IR-2 were determined every 3 days over a 41 days period.

The concentration and crosing point (Cp) of each gene was calculated by reference to the respective standard curve using the Lightcycler software. While the efficiency of RT-PCR amplification (E) and dynamic range of the standard curve can be determined by generating relative standard curve, which required a dilution series of the reference genes (cDNA). The E value for specific Lightcycler PCR is determined based on the slope of the standard curve and calculated using the equation $E= 10^{-1/slope}$. Theoretically the optimal efficiency is achieved when the slope of the standard curve is approximately -3.3, giving an E of ~2.0. In this experiment, the efficiency of qPCR amplification and standard curve equation was generated automatically by the Lightcycler PCR (Roche RT-PCR machine).

The relative gene expression was expressed as a ratio of target gene (IR1 and IR2) concentration compared to a housekeeping gene (Actin, β-Tubulin and 60S), and a value reported which represents the mean gene expression. The normalization of test sample and calibrator sample can be achieved by correcting it with the endogenous control results, following the formula as described below (Applied Biosystem, 2004):

$$\textbf{Normalized target (test sample)} = \frac{\textbf{Target}}{\textbf{Endogenous control}}$$

5.3. RESULTS.

5.3.1 Cloning and sequencing

A BLAST search of the *Serpula lacrymans* genome database with a CDH (G15298) gene from the Basidiomycetes identified two CDH genes and two genes which had similarities but were different genes. These genes were labelled as iron reductases (IR), IR1 (protein ID: 452187) and IR2 (protein ID: 417465). These genes were cloned from total RNA of *S. lacrymans*. The cDNA of IR1 contains an open reading frame (ORF) 774bp, which encode 258 amino acids, while IR2 has 642 bp (214 amino acids) (Figure 44).

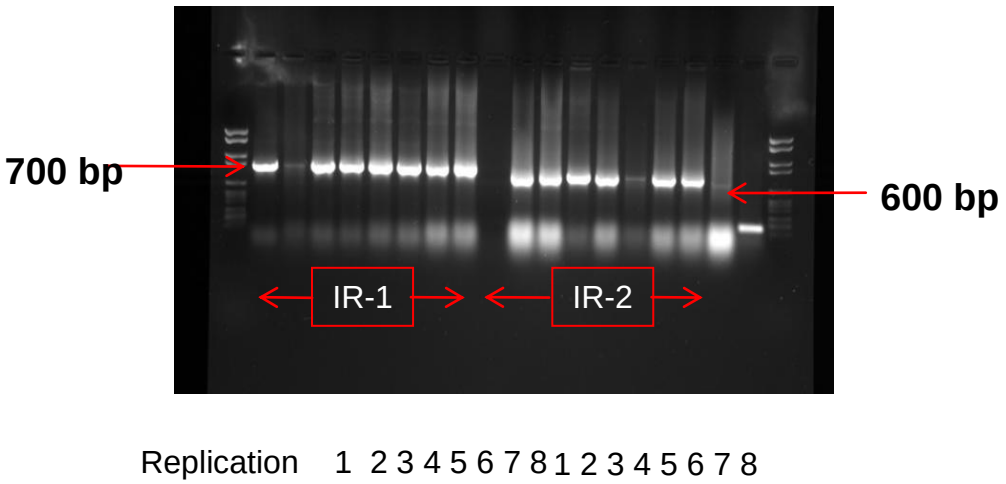

Figure 44. PCR analysis of cloned cDNA of IR1 and IR2 genes. The cDNA of these genes have been successfully isolated, cloned and transferred into specific vector before amplified and sized using 1.2% agarose gel electrophoresis. The IR1 genes has 700bp; IR2: 600bp.

The first 20 amino acids of both genes were predicted to be signal sequences using SignalIP 4.1 Server. Thus the mature protein of IR1 and IR2 approximately 238 and 194 amino acids respectively and are likely to be secreted proteins. Both genes showed 100% identity with the *S. lacrymans* genome sequence.

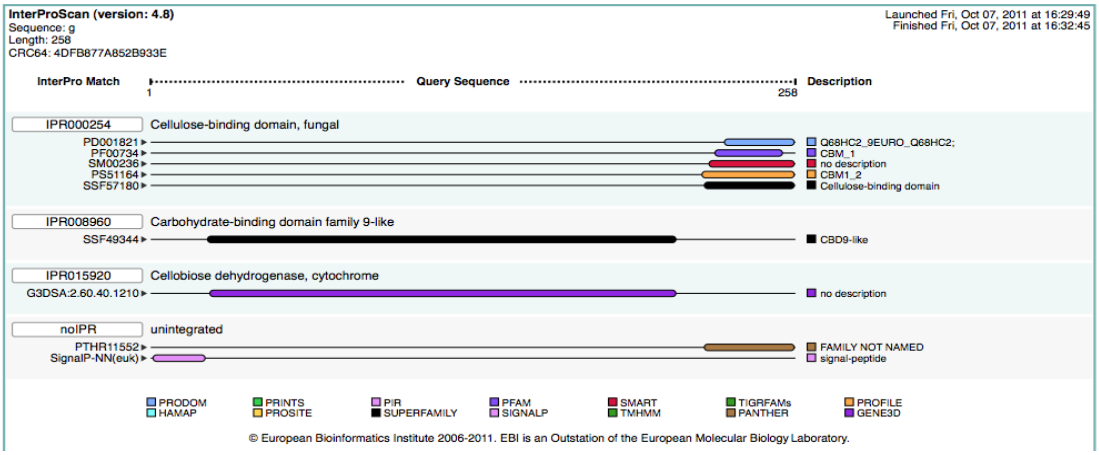

(a)

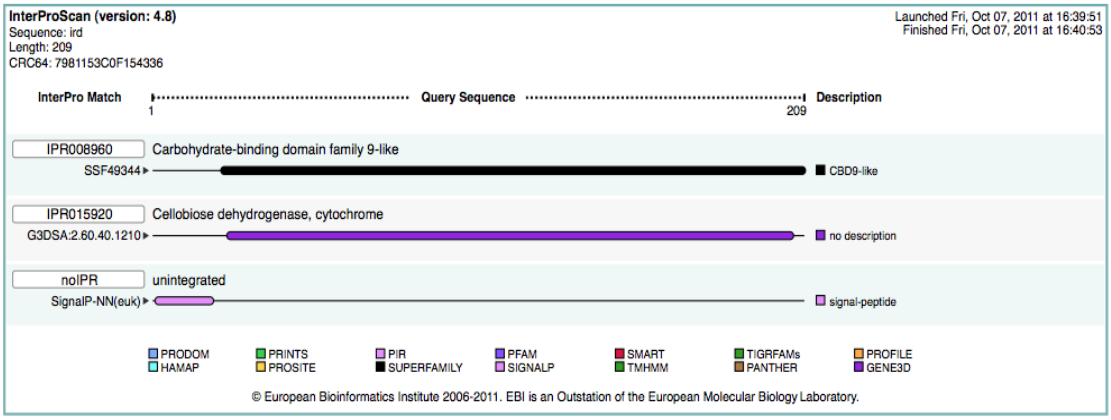

(b)

Figure 45. A diagrammatic representation of the domain structure of IR1 (a) and IR2 (b), analysed using InterProscan version: 4.8

The IR1 and IR2 genes do not belong to the cellobiose dehydrogenase (CDH) family as they are lacking the mono-oxygenase machinery of the CDHs, but they are putative iron reductases as they contain the cytochrome domain. IR1 also contained a C-terminal cellulose binding modules (CBM1), indicating potential direct targeting of crystalline cellulose. IR2 only contained the cellobiose dehydrogenase cytochrome (Figure 45).

BLASTN alignment with the NCBI databases found no significant alignments with previously described sequences however comparison of the iron

reductases sequence protein by BLASTP search showed that IR1 shares high identity (74.2%) with the amino acid sequence of carbohydrate binding module (CBM1) of different fungi e.g. *Coniophora puteana* (accession number EIW84939), 65.9% identity with that from carbohydrate binding cytochrome (CBcyt b562) from *Stereum hirsutum* (accession number EIM89944.1), 61.4% identity with cellulose binding cytochrome b562 from *Phanerochaete chrysosporium* (accession number BAD95668), and 59.8% identity with IR2 (protein ID: 417465). While the sequence peptide of *S. lacrymans* IR2 itself has 57.5% identity with that from CBM1 *Coniophora puteana* (accession number EIW84939), 54.8% identity with carbohydrate binding cytochrome b562 from *Stereum hirsutum* (accession number EIM89944.1) and it has only 46.9% identity with that from CBcyt b562 *Phanerochaete chrysosporium* (accession number BAD95668).

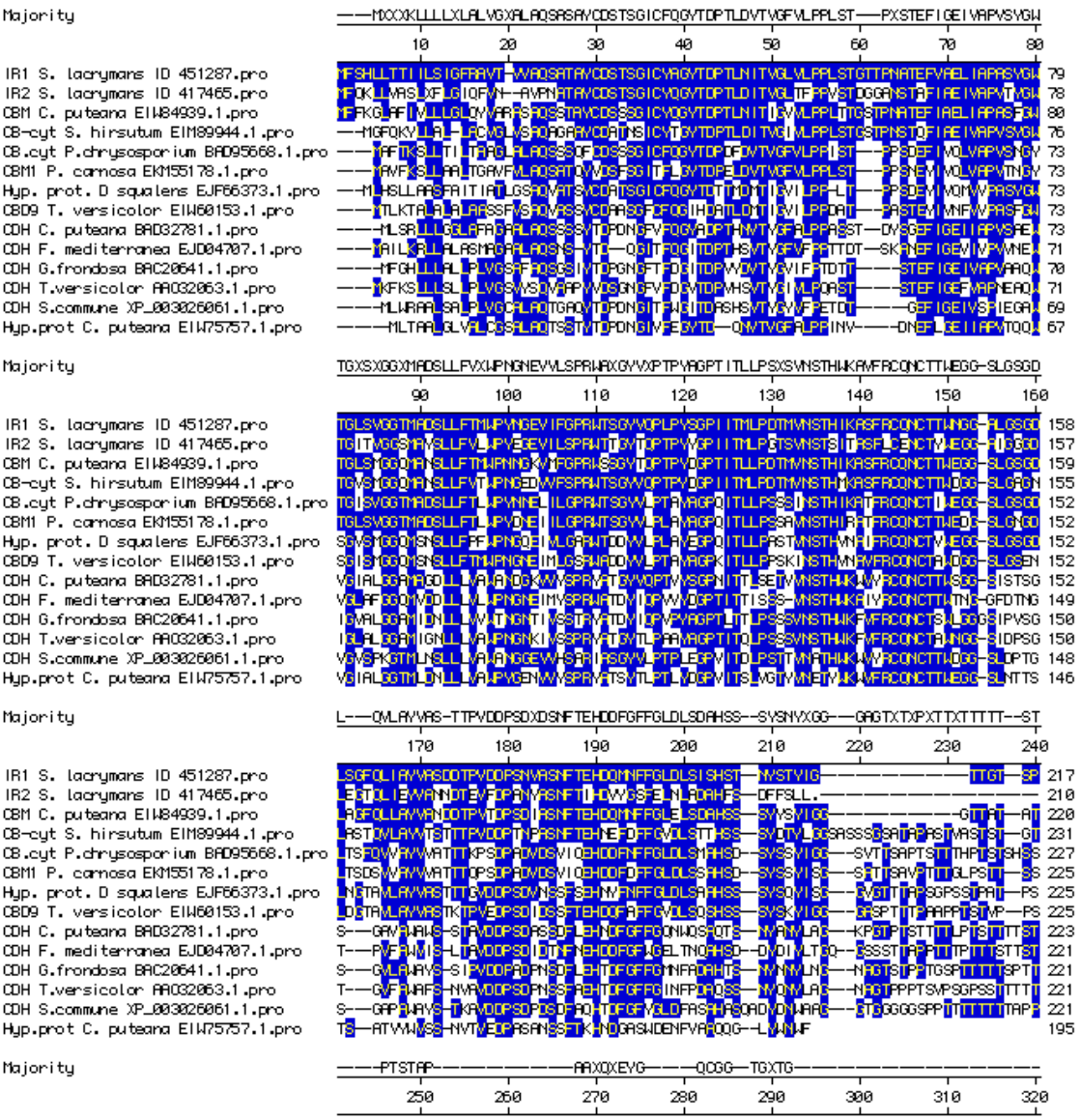
Majority
IR1 S. lacrymans ID 451287.pro
IR2 S. lacrymans ID 417465.pro
CBM C. puteana EIW84939.1.pro
CB-cyt S. hirsutum EIM89944.1.pro
CB.cyt P.chrysosporium BAD95668.1.pro
CBM1 P. carnosa EKM55178.1.pro
Hyp. prot. D squalens EJF66373.1.pro
CBD9 T. versicolor EIW60153.1.pro
CDH C. puteana BAD32781.1.pro
CDH F. mediterranea EJD04707.1.pro
CDH G.frondosa BAC20641.1.pro
CDH T.versicolor AAO32063.1.pro
CDH S.commune XP_003026061.1.pro
Hyp.prot C. puteana EIW75757.1.pro
Majority
Majority
Majority

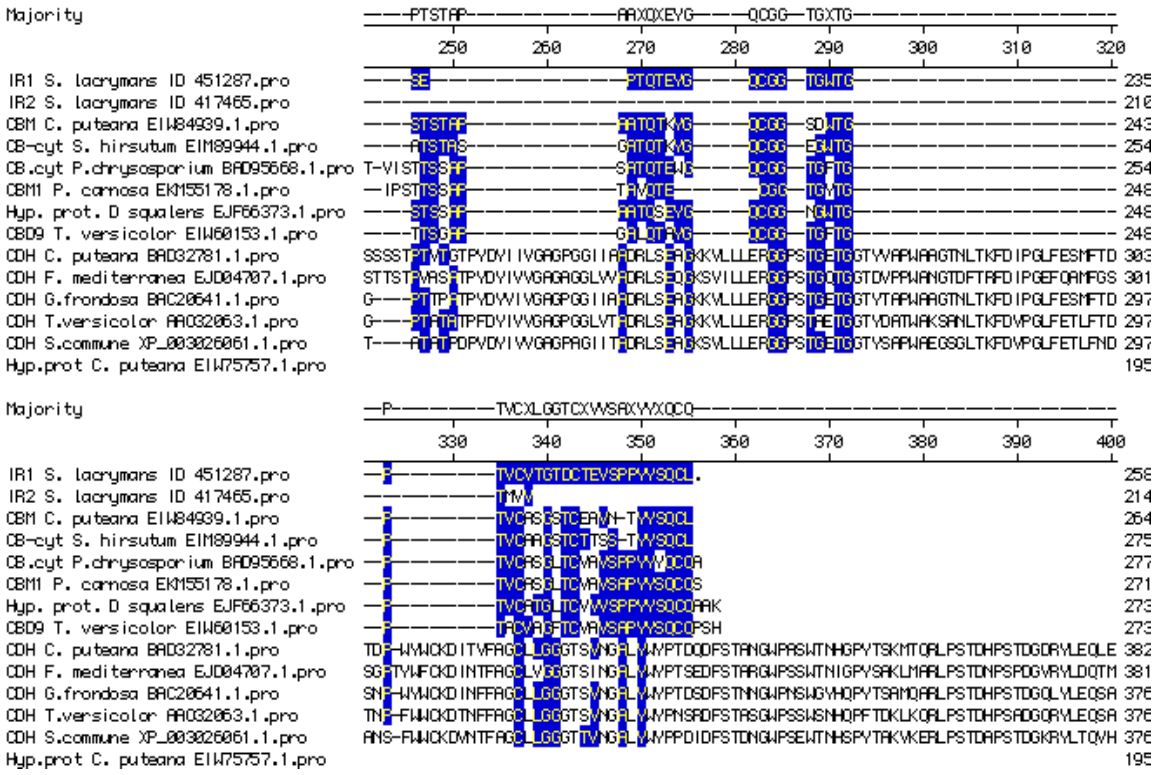

Figure 46. A multiple alignment of the predicted amino acid sequences of the iron reductases from *Serpula lacrymans* and other lignocellulosic enzymes from other Basidiomycetes (6 species of each from CBM family and CDH genes). Dark blue blocks show identical amino acids.

Alignment of 6 CDH and 6 cellulose binding domain genes of basidiomycete fungi was compared to the *S. lacrymans* iron reductases genes (IR1 and IR2) which revealed that the genes contained the heme domain which is present in CDH. The heme domain is defined by the presence of a methionine (M90) and by the presence of conserved histidine residues (H1140; only for IR1); H193; H205). The heme domain consists of approximately 190 residues, and has one disulphide bond formed from a pair of cysteines (Cys145:148) and mostly contains aromatic amino acids. The last 20 residues of the heme domain are followed by a region which is rich in threonine and serine residues. An

alignment of the CDH of IR-1 and IR-2 of *S. lacrymans* compared to other fungal genes, is presented in Figure 46. Using MrBayes version 3.2 software (Fredrik et al. 2010), a phylogenetic tree was constructed based on the sequence alignment of 14 fungal genes encoding cellobiose dehydrogenase and cellulose or cabohydrate binding module and the iron reductases (IR1 and IR2) from *Serpula lacrymans.* Results indicated that IR1 and IR2 had the greatest similarity to the cellulose binding module/cyctrochrom gene from others fungi (e.g. *Coniophora puteana, Phanerochaete chrysosporium, Stereum hirsutum, Dichomitus squalens* or *Trametes versicolor)* (Figure 48) rather than to the sequences of CDH from other fungal species (e.g *Grifila frondosa, Trametes versicolor, Schizophyllum commune, Coniophora puteana, Fomitiporia mediterranea*).

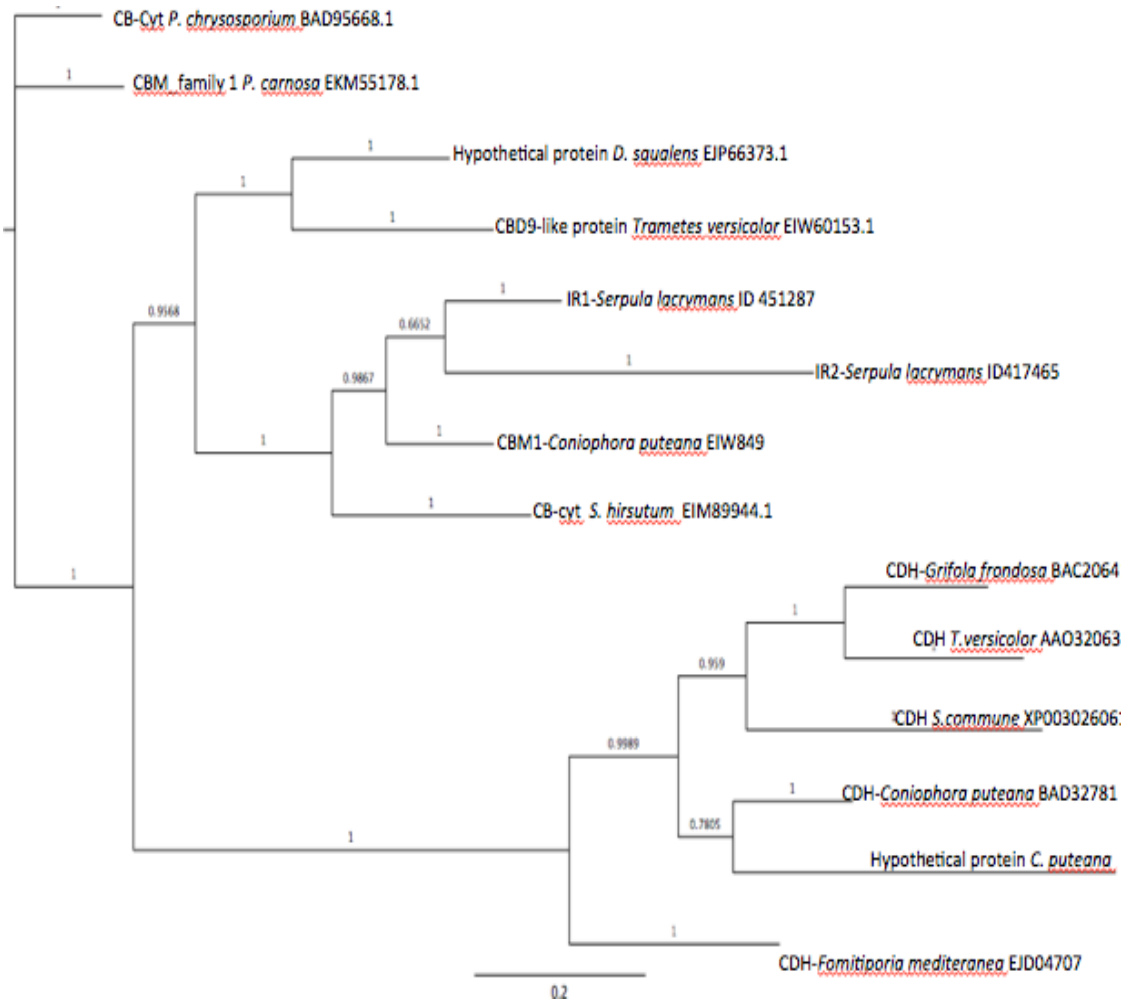

Figure 47. A phylogenetic tree showing the evolutionary relationships of genes containing a carbohydrate binding module (CBM) and cellobiose dehydrogenase (CDH) from *Serpula lacrymans* and related fungi (others Basidiomycetes). The scale bar represents 0.2 substitutes per nucleotide side.

5.3.2 Gene expression stability analysis

The efficacy of each gene-specific primer combination was determined using melting curve analysis using SYBR Green I dye. The specificity of cDNA can be identified based on its peak fluorescence at a specific temperature. The melting curve should ideally show a single amplified product for all genes and no primer dimers. The iron reductase genes (IR1 and IR2) and the housekeeping genes show a single

peak at the expected temperature, no non-specific amplification was found. Figure 48 shows the example one of the melting curve from the gene expressed.

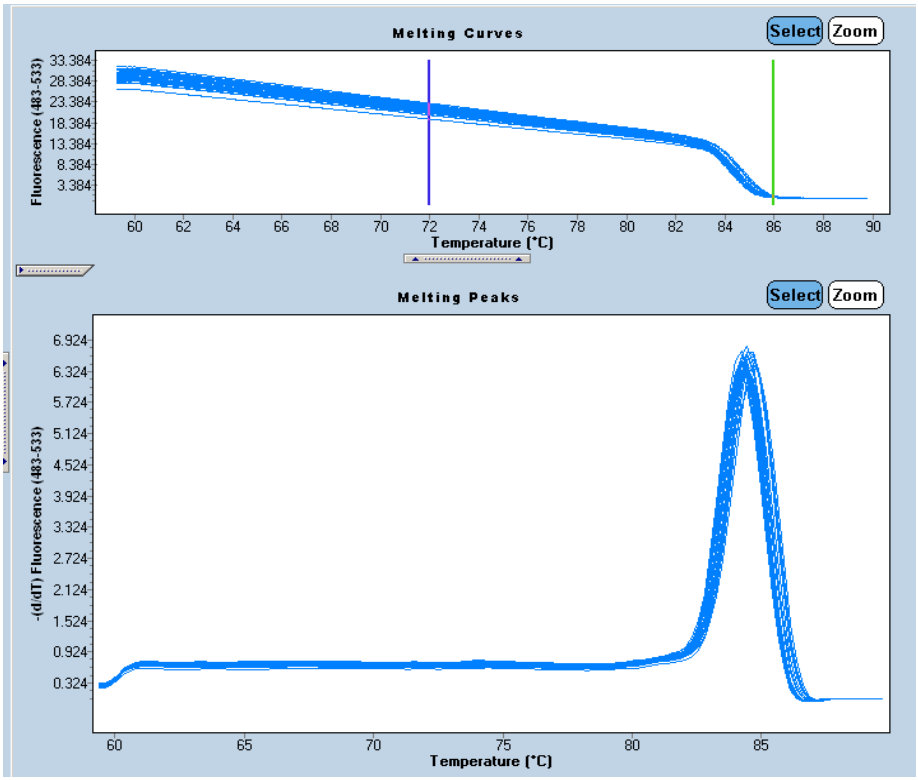

Figure 48. Amplification of iron reductase gene (IR1) was determined by a single peak of melting curve analysis.

To evaluate the stability of housekeeping genes, the mRNA transcription level were measured every 3 days and the Lightcycler results were verified using agarose gel electrophoresis 1.2%. All the amplification products have a single band of the expected molecular weight (Figure 49).

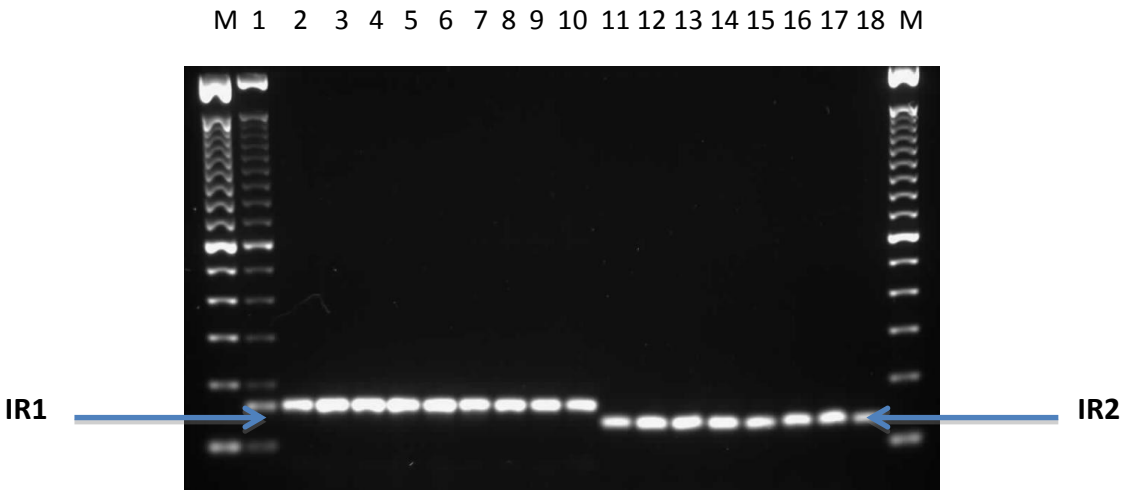

Figure 49. The specifity of the Lightcycler PCR was confirmed by a single amplified product of the expected molecular weight using agarose gel electrophoresis of Lightcycler PCR products. M:marker, 1-10: IR1 (different day cultures from 3-41 days), 11-18: IR2 (different day cultures from 3-41 days)

The housekeeping genes were assayed to determine their stability over the period of fungal growth. Analysis was based on the Cp value on each different housekeeping genes. Only small variation was detected in the Cp values during the period observation of housekeeping genes, which shows a slightly increment of Cp value after 35 days of culture (Figure 50).

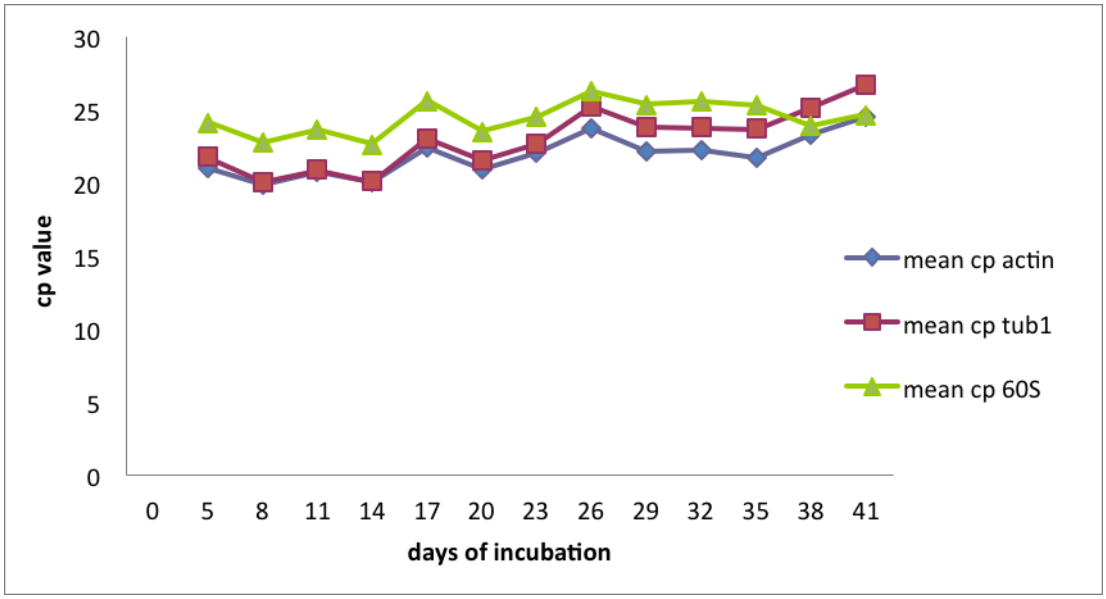

Figure 50. Variation and validation of three different housekeeping genes (Actin, β-tubulin, 60S) in wheat straw SSF using mean Cp as a measure of level of expression for the different time points sampled over the period of fungal culture (41 days)

For further analysis, the median, minimum and maximum Cp were calculated using SigmaPlot Software version 12 (University of Warwick-UK). Using the box whisker plot allows us to visualize the least variable genes among the samples (Figure 51). The median of Cp value for actin, tubulin and 60S reference genes were at 21.85, 22.92 and 24.38, respectively. The most stable genes, 60S and actin have the narrowest Cp range, but the smallest deviation from the median was found in 60S reference genes. The Cp values of the candidate reference genes, in all samples were within 19.78 to 26.70, and showing a wide range of variation between them. The highest Cp variation was observed in tubulin, which also had the greatest range between the minimum and maximum Cp value from the median.

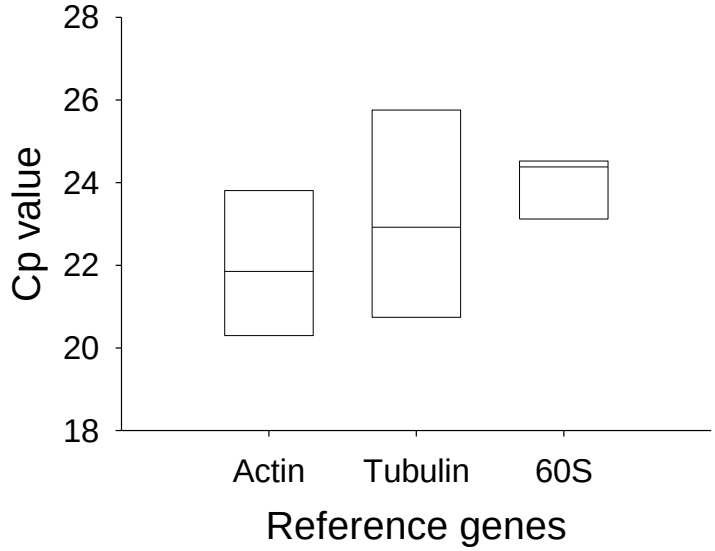

Figure 51. A Box whisker plot showing the cycle threshold (Cp) variations of three reference genes (actin, β-tubulin, 60S).

In order to determine the efficiency of transcription of iron reductase genes while it's grown on wheat straw SSF, the RNA samples were collected over the period of optimal fungal growth on wheat straw and the transcript levels of the Iron reductases genes (IR1-IR2) of *S. lacrymans* were quantified using RT-PCR. Transcript level profiles are presented in Figure 53 (a,b,c).

Table 23. Characteristics of target and reference standard curve used for relative quantification of gene expression showing the efficiency of calibrated method.

Reference genes[a]	Slope of the standard curve[b]	E[c]	Error[d]
ACTIN	-4.43	1.68	0.11
β-TUBULIN	-3.51	1.90	0.09
60S	-2.93	2.19	0.13

[a] Endogenous reference genes, [b] Standard curve were generated by plotting quantification cycles value (cp) againts the logaritmic values of the relative cDNA copy numbers in the reference samples, [c] PCR amplification efficiency calculated from the slope of standard curve [d] Error

The efficacy shows that the housekeeping gene 60S (2.19) was the best followed by tubulin (1.9) and actin (1,68). However the lowest error was found using tubulin (0.09).

(a)

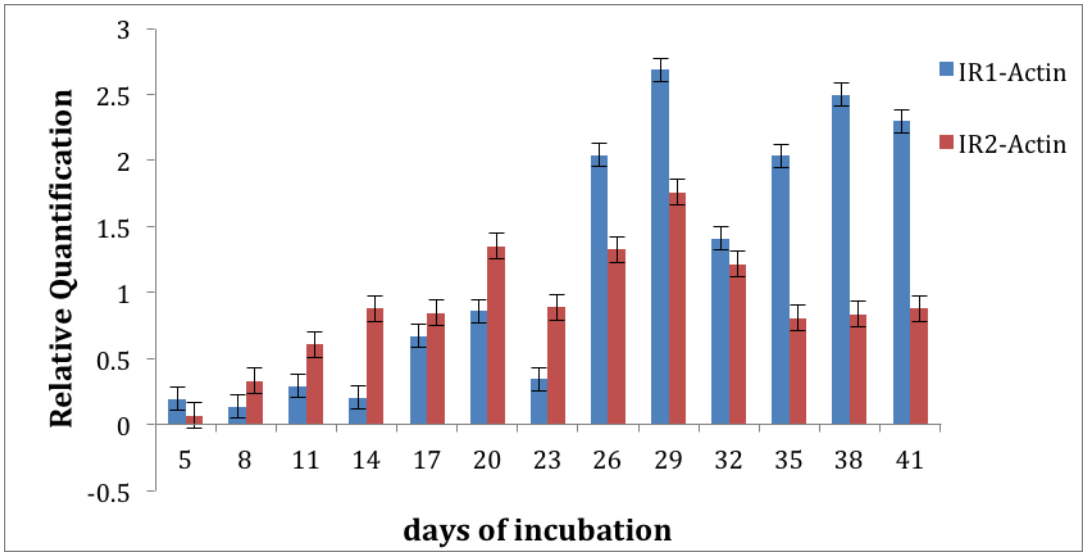

(b)

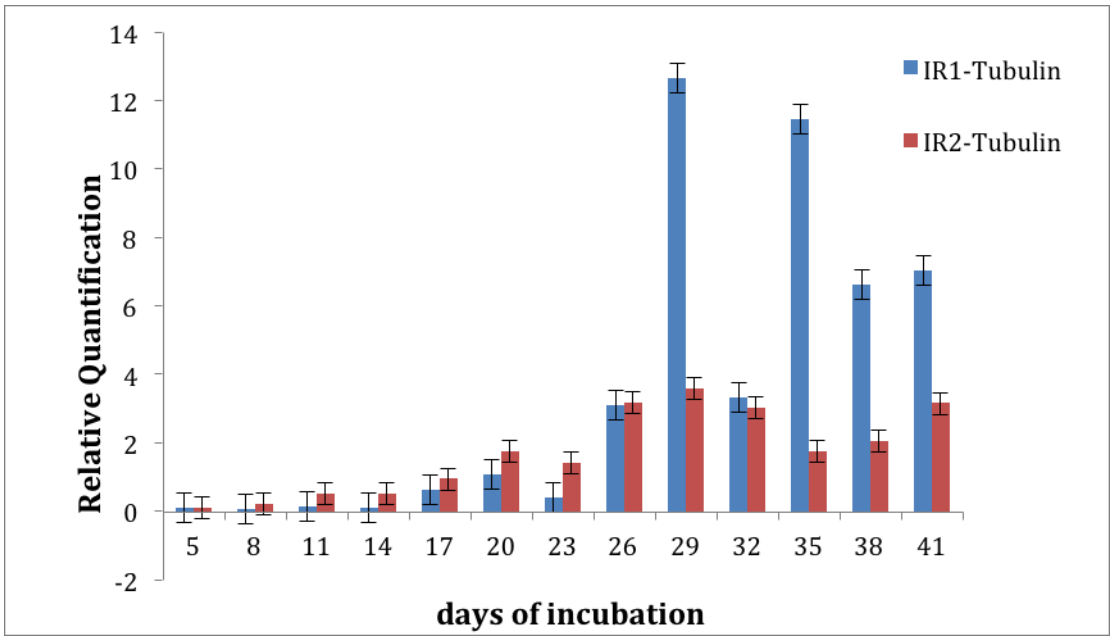

(c)

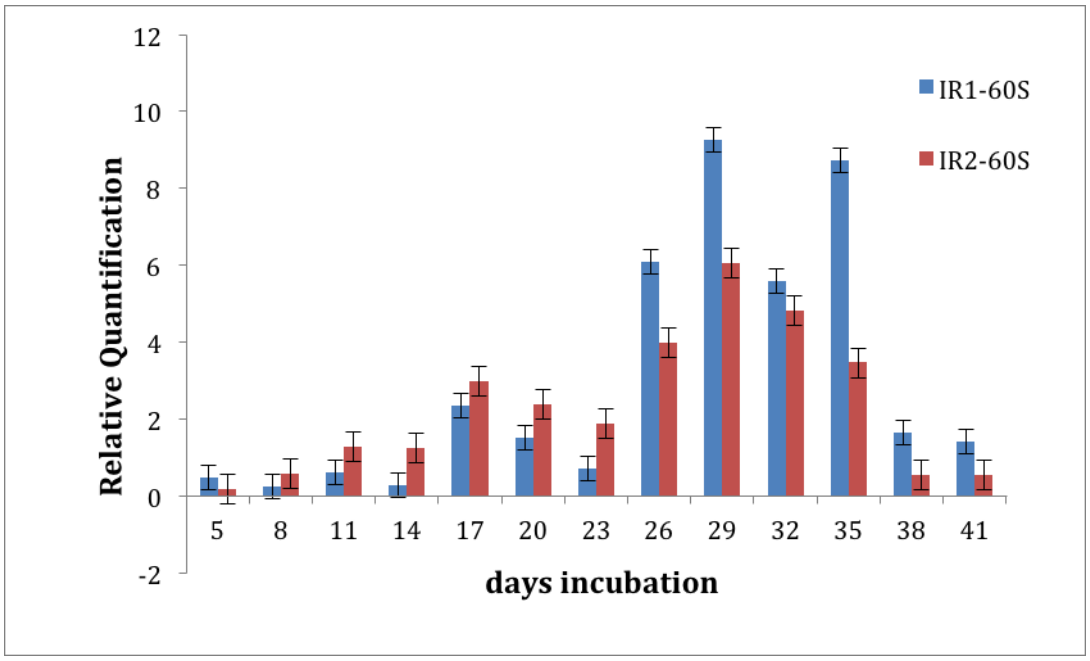

Figure 52. Relative quantification of Iron reductases (IR1-IR2) of *Serpula lacrymans* expression normalised to a) actin; b) tubulin c) 60S housekeeping genes during fungal growth (41 days) on wheat straw SSF. Error bars represent the LSD (P<0.05)

Using actin as housekeeping gene for the normalisation, the IR gene expression increased steadily up to 29 days incubation (Figure 52a). There was a significant diference (P<0.05) in the level of gene expression with time (0-41 days). After 29 days, the transcript abundance levelled off or slightly decreased from 32 to 41 days after culture. In general gene expression of IR2 was subtantially higher than IR1 up to 23 days. Similar pattern were detected when the IR-1 and IR-2 iron reductase genes were normalised using tubulin and 60S genes housekeeping (Figure 52b and Figure 52c).

5.4 Discussion

5.4.1 The identification of genes encoding iron reductase from *Serpula lacrymans*

In this study, two genes of *S. lacrymans* IR-1 and IR-2 were identified with predicted open reading frames (ORF) of 774 bp and 642 bp open respectively which encode polypeptides of 258 and 214 amino acid. Both genes have recently been shown to be significantly up-regulated when *S. lacrymans* grows on wood (Eastwood et al., 2011). The genes (IR1 and IR2) have a carbohydrate binding familiy 9-like (CDH cytochrome) domain and predicted signal peptides of about 20 amino acids. The presence of a signal sequence suggests that the proteins are secreted.

The IR1 gene contains an additional cellulose binding module (CBM1). CBM1 are often found in fungal carbohydrate-acting enzymes, and they are thought to contribute to binding crystalline cellulose. Removal of the CBM domain cause a significant decrease in both binding and catalytic activity again cellulose (Linder, 1997), suggesting that the CBM1 is important for the catalytic function of these enzymes (Henriksson et al., 1991;1997), a CBM1 domain in IR1 suggests this protein may be involved in interaction with the hosts celullose following secretion.

For comparison the amino acids sequences of IR1 and IR2 from *S. lacrymans* were aligned with several fungal enzymes that contains the CDH and CBM1 domain. The alignments showed that both IR1 and IR 2 contain the key amino acids important for heme ligands. These are methionine and histidine (Met 89 and His 139, 191) which are highly conserved in either to the CDH enzymes

or CBM family. Cysteine residues are also present forming a disulfide bond (Cys30 and Cys37). It has been reported that cellulose binding domains normally only contain one aromatic residue, such as tyrosine (Tomme et al., 1998). The recombinant protein IR1 contains three aromatic residues (W296, Y336;337) which might contribute to binding cellulose and an additional of cysteine residues capable of forming disulfide bonds (Cys291; Cys302; Cys308; Cys340).

Comparison of the genes sequences of both the IR1 and IR2 indicated that they belong to the CBM. The protein sequences of both the IR1 and IR2 *S. lacrymans* indicate that they have the greatest degree of similarity to CBM. The phylogenetic analysis also indicated that both recombinant proteins IR1 and IR2 have more homology with the enzymes belong to the CBM family than CDH groups. A CBM family CB.Cyt-*b*562 from *P. chrysosporium* has been reported previously by Yoshida et al., (2005) which has similarities of 61.4% to IR1 and 47.8% to from IR2 *S. lacrymans.* The IR1 and IR2 *S. lacrymans* have a lower molecular mass, but IR1 has a similar length of amino acid to CBCyt-*b*562 from *P. chrysosporium* BAD95668.1 (258 amino acid). Comparison of the genes sequences indicated that the genes showed very low level of sequence similarity between the iron reductase genes and the related genes of fungal origin. The iron reductase genes were align to *Phanerochaete carnosa* with a 70% identity at the protein level but only 30% to sequence.

Based on the multiple alignment analysis of the predicted amino acid sequences of the iron reductases with other fungal enzymes, showed that IR1 had similarity to the CBM genes family, including CBcyt-b562 from *P chrysosporium*,

which was thought to have a unique structure. Both IR1 and IR2 lack the cellobiose-oxidizing flavin domain of CDH but carry a C terminal CBM1 domain which suggested that this domain may be related to the catalytic function of the IR1 enzymes.

5.4.2 Quantification of iron reductase genes and the relationship to lignocellulosic breakdown.

Transcription of the iron reductase genes (IR1 and IR2) was normalised and quantiifed by extrapolation to standard curves generated by plotting the logarithm of fluoresence versus cycle number for a serial dilution of cDNA template. The efficacy of the gene specific primers was estimated using melting curves analysis for both target and references genes. The melting curves showed a single amplified product which indicates that primer dimers were not present. This was confirmed by the presence of a single amplified product at the expected molecular weight using agarose gel electrophoresis (Figure 50). The stability of reference/housekeeping genes is important for estimating the relative quantification of gene expression and their expression should remain stable during the period of treatment (Bustin, 2000). The use of incorrect normalisation could lead to erroneous interpretation of data quantification (Zhou et al., 2012).

The stability of three different housekeeping genes was compared (Figure 51). The Cp value indicates the detection sensitivity and corresponds to the internal variability of the RT-PCR method along with their biological variation (Stolf-Moreira et al., 2011). Actin is often used as reference as it is often the most stable housekeeping gene (Bezier et al. 2002; Langer et al., 2002; Thomas et al., 2003). In

this study, however actin showed greater variation in Cp value compare to that found with 60S (Figure 50). This was supported by the used of further statistical analysis (box whiskers). Even though the Cp value of the three different housekeeping genes varied during fungal growth, they showed a similar pattern and effect when used to quantifiy iron reductase genes expression. The Cp value of the housekeeping genes was within the range of Cp value from four reference genes (i.e. Lectin, GAPDH, 18S rRNA and Actin) which was used to validate RT-PCR value in drought strees soybean experiment, ranged between 16.63 to 35.85, with the stable genes was Actin followed by 18S as the second (Stolf-Moreira et al., 2011).

During the 41 days of cultivation, the level of iron reductases was dominated by IR2 in the early stage of fungal cultivation (until 23 days culture), while IR1 gene expressed increased significantly after 26 days (Figure 52a). The results show transcriptional and metabolic activity was highest around 29-35 days fungal culture. The pattern of IR genes expression showed corelation with metabolite released by *S. lacrymans*. The increased level of expression of the iron reductase genes was also correlated with an increase in phenols released which peaked around 30 days incubation (Figure 53). However, total reducing sugars which were most abundant around 15-20 days incubation and decreased afterward which doesn't corelate with the expression of these genes. This may due to the use of sugars as a metabolic energy source during fungal growth.

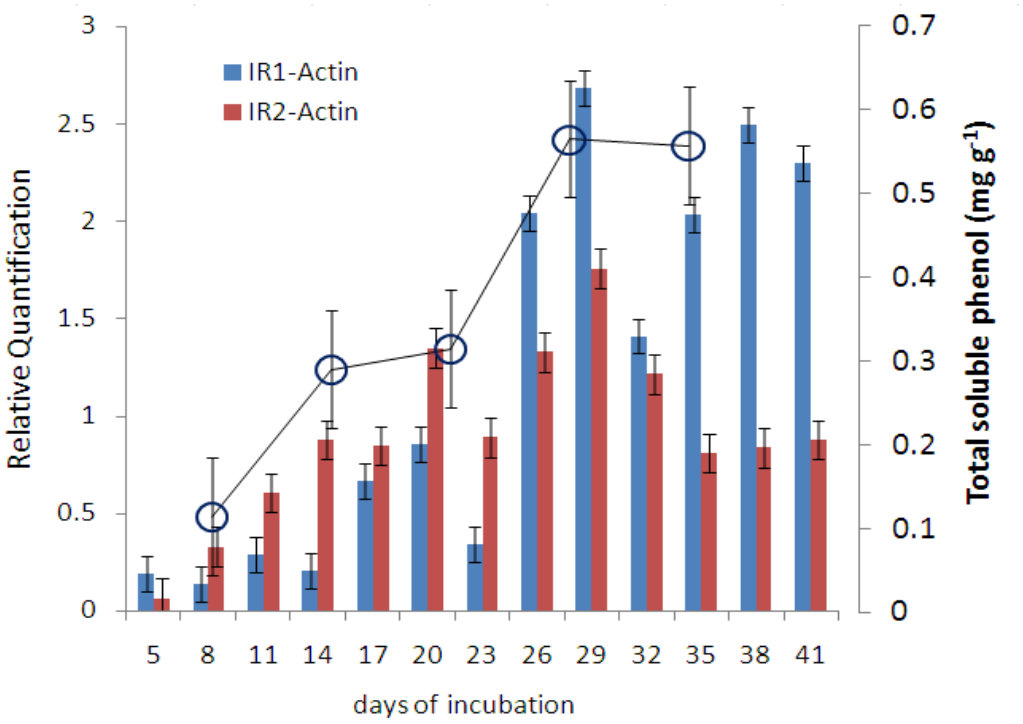

Figure 53. The relationship between the level of gene expression with production of total soluble phenols during the fungal growth (41 days). Error bars represent LSD ($P<0.05$)

During the fungal growth, the amount of oxalic acid increased rapidly after 20 days of culture and peaked at day 32 then remained stable thereafter. The pH decreased from 5.6 to 4.4 over the same period resulting in a pH which is optimal for growth of brown rot fungi. The drop in pH could enhance the solubilisation of ferric iron to ferrous iron and the generates the hydroxyl radical. This then can breakdown the lignin structure releasing phenol as seen in Figure 53.

Chapter 6. The expression and functional characterisation of recombinant protein from iron reductase encoding genes of brown rot fungus *Serpula lacrymans*

6.1 Introduction

Protein encoded by the iron reductase genes identified (IR1 and IR2) in chapter five were postulated to play a role in lignocellulose decomposition since both genes, IR1 and IR2 contained the heme domain of CDH enzymes. It was hypothesised that they had similar function to the CDH genes. The IR1 gene also contains the CBM1 domain and was hypothesised to be involved in degradation of crystalline cellulose through the steric effect of localising IR activity close to the cellulose chain. In order to determine the functionality of the iron reductase genes (IR1 and IR2), they were cloned using the Gateway system and expressed

6.1.1 Iron reductase

In wood decay, iron plays a key role being involved in the active site of enzymes such as the class peroxidase and CDH. The iron binding compounds produced by wood-decaying basidiomycetes are responsible for cyclic redox system that produce active oxygen species which are hypothesised to be involved in the breakdown of lignocellulose (Goodell et al., 1997). The brown rot fungus *S. lacrymans* produces phenolate derivative compounds that are low molecular weight (LMW) Fe^{3+} reductant (Arantes et al., 2011) e.g. hydroquinones. In nature, iron is commonly present as ferric iron oxide which must be sequestered and reduced to ferrous iron to participate in the Fenton reaction (Qian et al.,

2002). This reaction is now known to occur via the reduction of ferric iron with electron donors. The production of hydrogen peroxide is metabolically generated by oxidase enzymes such as glyoxal oxidase. The oxidation of the resultant ferrous iron produces hydroxyl radicals (Goodell et al., 1997) which attack the cell wall. As an essential component of heme groups and iron clusters, iron is also important for electron transport in the respiratory chain and for various enzymatic reactions (Riemer et al., 2004).

In the Fenton reaction as described in the introduction, an electron acceptor such as ferric iron is needed in order to react with derivatives of catecholate through a two-step mechanism with intermediate formation of a semiquinone radical (Mentasti et al., 1977). The radical then has to be stabilized through its resonance structures and can react with molecular oxygen to form a peroxide radical as an active oxygen radical species (Goodell et al., 1997). The phenolate chelator 2,3-dihydroxybenzoic acid (DHBA) is capable of reducing ferric iron and the initial complex promotes the generation of hydroxyl radicals via a Fenton based reaction (Arantes et al., 2009). The iron binding and reducing ability of the model compound 2,3-DHBA was studied as a function of the chelator : iron ratio. It has been observed that the increasing concentration of 2,3-DHBA (0.25-15mM), in the same concentration of iron (5mM) at pH 4.0 acetate buffer could also promote the increasing of iron binding ability by this chelator in the beginning of measurement and levelled off of after 40 minutes observation. However, after reaching an the optimum concentration, the adition of 2,3-DHBA which dependence on a pH could become an inhibitor (Qian et al., 2002).

Among the compounds used for colorimetric assay, Ferrozine is acknowledged as an effective chelator of ferrous iron and has been used for the determination of ferrous iron in biological samples. Ferrozine forms a complex with ferrous iron, and not ferric iron that strongly absorbs light at 550nm (Fish, 1988). The ferrozine (monosodium salt hydrate of 3-(2-pyridil)-5,6-diphenyl-1,2,4-triazine-p-p'-disulfonic acid) reagent proposed by Stookey (1970), reacts with divalent iron (Fe^{2+}) to form a stable magenta complex species (Violler et al., 2000). The Ferrozine assay should be monitored for a minimum of 5 minutes, since the Fe^{2+} reacts with Ferrozine and can reach equilibrium between Fe^{2+} and Fe^{3+} over long periods of time (Qian et al., 2002). Goodell et al. (2006) monitored the absorbance of the reduction Fe^{3+} wood extract colonized by several brown and white fungi, after 5 and 30 minutes of incubation with this assay.

6.1.2 Evidence for lignin degradation using a nitrated lignin assay

The evidence of the role of Fe^{2+} and reduction agent such as quinone (DMBQ or DHBA) via the Fenton reaction which is known to be involved on the breakdown of lignocellulose by *S. lacrymans* is described in Chapter 4. Loss of moisture of wheat straw following incubation has been shown and changes in the lignocellulosic structure identified using FTIR technique (Chapter 4). The production of oxalic acid was measured using HPLC and a concomitant decrease in pH observed (Chapter 4). However, the chemical composition of lignin in wheat straw remained complex even after this initial breakdown and is difficult to monitor. A simplified assay was needed

to determine the functional role of iron reductase (IR1 and IR2) of *S. lacrymans* in lignin degradation. At present, the most commonly used assay for lignin breakdown requires the use of ^{14}C labelled lignin (Ahmad et al., 2010; Kawai et al., 1995), which is a radioactive compound, and the method is hazardous, time consuming and laborious.

Recently, a novel assay for lignin degradation has been developed by Ahmad et al., (2010), which uses a 96 well microtitre plate spectrometric approach in which a chemically nitrated lignin is used as the substrate to measure lignin degradation. The release of nitrated phenol causes an increase in UV/VIS absorbance at 430nm. These nitrated lignin structure are a closer match to the natural substrate compared to low molecular lignin compounds (Ahmad et al., 2010). In this study the ability of the recombinant protein iron reductases (IR1 and IR2) were tested using this assay.

6.1.3 The break down of cellulose by *S. lacrymans*

Every source of biomass will have different cellulosic characteristics which can alter the ability of microorganisms to degrade the cellulose. Assays to determine cellulase activity can be classified according to the approach (Sharrock, 1988). Zhang et al. (2006) classified all the cellulase activity into three different groups (1) assays which measured the final product released by cellulases after hydrolysis (2) assays which monitored the amount of reduction product in substrate (3) assays in which the change of the properties of the substrate was measured. In order to measure the cellulase activity, measurement of reducing sugars is normally used (Dashtban et al. 2010).

The carbohydrate binding module (CBM) of cellulolytic enzymes plays a role in cellulose decomposition by binding to the non-hydrolytic crystalline substrate ensuring the enzyme is close to its substrate. Although the function of the CBMs during enzymatic hydrolysis of cellulose has not been fully elucidated, in general it is thought that the proteins containing CBM are involved in the breakdown of cellulose and hence increase the release of sugars (Arantes and Jack., 2010) and promote the disruption of crystalline cellulose by weakening and splitting the hydrogen bonds which causes a change in the cellulose chains (Gao et al., 2001).

In order to verify functionality, several assays were used including iron reductase activity, the ability of recombinant protein to catalyse break-down of lignin, the CDH assay (the ability of the recombinant proteins to reduce electron acceptors) and the release of total reducing sugars assay.

6.2 Methods

6.2.1 Strains, culture condition and plasmid (general method)

The brown rot basidiomycete *Serpula lacrymans* S7 was obtained from the culture collection of Warwick HRI (School of Life Sciences) and grown in the dark on malt extract agar (MEA) plate at 20ºC for 3-4 weeks. The MEA medium containing malt extract 20g/l and agar 12g/l. The detail of this method has been described in chapter 2.

6.2.2 Gateway cloning strategy

The Invitrogen Gateway Cloning system (www.invitrogen.com) was used in this study which utilises site-specific recombination *att*B x *att*P→*att*L x *att*R of α phage, which is schematically presented below:

*att*B1-gene-*att*B2 x *att*P1-*ccd*B-*att*P2 ↔ *att*L1-gene-*att*L2 x *att*R1-*ccd*B-*att*R2
(Expression clone) (pDONR) (Entry clone) (Destination vector)

The major steps of the Gateway cloning system are the BP and LR reactions. The *att*B x *att*P reaction is mediated by Gateway BP clonase II enzyme mix, while the *att*L x *att*R reaction is mediated by Gateway LR clonase II enzyme mix. The BP reactions utilize the recombination between attB of the DNA segment of interest and attP of the donor to create entry clones. The LR reaction is used to introduce the DNA segment from the entry clone into a destination vector by recombination between the attL of entry clone and the attR of destination vector. During recombination, the foreign DNA in the Gateway clone replaces the lethal gene ccdB between attR1 and attR2. The lethal gene *ccd*B is a selection marker in the recombination cassette (*att*R-Cmr-ccdB-*att*R2) used to ensure high efficiency isolation of recombinant DNA.

6.2.3 Primer design

The design of Gateway primers, *att*B1 and *att*B2 primers are dependent on the type of protein desired, e.g. as a native or fusion protein and also in what organism (host) the proteins will be expressed. In *E. coli,* the ribosome binding sequence Shine-Dalgarno needs to be present. The proper design of *att*B–attached primer is a crucial point for the BP and LR reaction of the Gateway clone and functional expression of the gene. The iron reductases genes, IR1 and IR2 fragment minus the signal peptide plus stop codon was amplified from plasmid containing the IR1 and IR2 genes with the primers. In this experiment the detail of primers designed is presented in Table 24.

Table 24. Primer sequence for IR1 and IR2 genes as used for cloning into the Gateway system.

Name	Primer Sequence 5'-3'
AttB1-IR1plusSP-F	AAAAAGCAGGCTTCatgGCTACAGCTTACTGCGATTC
AttB2-IR1minSTP-R	AGAAAGCTGGGTTCACAGGCACTGGCTATAATAC
AttB1-IR2minSP-F	AAAAAGCAGGCTTCatgGCTACTGCATACTGCGACTC
AttB2-IR2plusSTP-R	AGAAAGCTGGGTTCACAAGAGACTGAAAAAGTC
AttB1-adapter-F	GGGGACAAGTTTGTACAAAAAAGCAGGCT
AttB2-adapter-R	GGGGACCACTTTGTACAAGAAAGCTGGGT

Table 25. M13 Primers used for sequencing

Name	Primer Sequence 5'-3'	Primer sequence 5'-3'
M13	GTAAAACGACGGCCAG	CAGGAAACAGCTATGAC

6.2.4 PCR

In order to amplify the target sequence of both genes (IR1 and IR2), the first and second steps of the gateway system (50µl) were carried out as follows. 2µl (10mM) primers, 2µl plasmid cDNA (100ng), 25µl taq DNA polymerase were mixed with 21µl pure water. The PCR reaction was performed using 1 cycle of 94ºC (3 min), followed by 5 cycles of denaturation (30sec at 94ºC), annealing (30sec at 55ºC) and extension (1.5min at 72ºC) and then 25 cycles: 94ºC for 30sec, 65ºC for 30sec and 72ºC for 1.5min, and a final extension at 72ºC for 7 min. 5µl of product was electrophoresed on a 1.2%(w/v) agarose gel, followed by gel purification (Qiaquick gel extraction protocol). The first PCR

product was then used for the second plasmid step using the same kit and conditions as the first PCR, but the primers were adapter primers (Table 24). The purified amplicon from the second PCR reactions was used for the Gateway BP reaction.

6.2.5 Recombination attB primers with pDONR/Zeo vector to create entry clone

To introduce the DNA fragment into the entry clone (pDONR/Zeo, Invitrogen), *in vitro* BP clonase recombination reactions were carried out according to the manufacturer's instructions (Invitrogen). The product of the recombination reactions (BP reactions) were used to transform competent DH5α *E. coli* using heat shock. Positive transformants were cultured overnight at 37˚C in 5ml LB containing antibiotic selection 30 µg ml^{-1} Zeocin. The plasmid was extracted using the Qiagen plasmid mini-prep kit.

6.2.6 Performing the LR Recombination Reaction

The entry clone from the BP reaction and destination vector pDEST15 was mixed with the LR clonase II enzyme mix. pDEST15 is N-terminal fusion vectors which contain an ATG initiation codon upstream of GST tag. The product of recombination of LR reaction were transformed into the DH5α *E. coli* strain. Positive transformants were cultured overnight at 37˚C in 5ml LB containing antibiotic selection 30µg/ml Zeocin. The plasmid was then purified using the Qiagen plasmid mini-prep kit.

6.2.7 Verification of Gateway Product

Using the ABI BigDye terminator V.1.1/3.1 seq Kit, the BP and LR products and appropriate primers were verified by sequencing. Each sequencing reaction contains 3.2pmol primers, 2µl ready raction mix (Big dye V3.1), 1µl big dye sequencing buffer and 1µl of BP product. Each reaction was made up to 10µl with pure distilled water, and the sequencing condition were as followed : 1 cycles 96ºC for 2min; 35cycles: 96°C for 10 sec, 50°C for 10sec and 60°C for 3 min. These were sequenced using an ABI3130XL.

6.2.8 Expressing the recombinant protein

The transformant colonies were inoculated into 10ml of LB medium containing the selective antibiotics 50µg/ml carbenicellin and 34µg/ml chloramphenicol in 50ml falcon tube, and grown overnight at 37ºC with shaking 220rpm. 2.5ml of overnight culture was inoculated into 50ml of prewarmed LB media (with antibiotics) on the shaking incubator (220 rpm for approximately 1.5 hours), until the OD_{600} is 0.5—0.7. The transformants were induced using 0.4mM of isopropyl-β-D-thiogalactopiranoside (IPTG) and the culture incubated at 30ºC for an additional 5-6 hours. 1ml induced and non induced samples were collected in different time points; 0, 3, 5, 12 and 20 hours. The optical density (OD) significantly increased after 5 hours induction. Cells were harvested by centrifugation at 5000rpm (20min) for the SDS-PAGE analysis and resuspended in an appropriate volume at lysis buffer prior to sonication and purification over the Gluthathione Sepharose.

The cell pellet was resuspended in 1 ml of lysis buffer containing 50mM Tris-HCl pH 8; 1mM EDTA pH 8,0; 1mM tris2 carboxyethyl-phosphine (TCEP) ; 1mM phenyl methylsulfonyl- fluoride (PMSF) ; 200mM NaCl, and deionized water (dH_2O) and the cell pellet was frozen under liquid nitrogen and thawed in cold water. The cells were then sonicated for 6 x 10sec with 10 sec pauses at 200-300W and the lysate was centrifuged at 5000 x g at 4ºC for 20min. This supernatant was refered to as the 'crude extract' and was used subsequently in various assays.

6.2.9 SDS PAGE and Western blotting analysis

The soluble and insoluble fractions were tested for the presence of recombinant protein using SDS-PAGE with a 12% SDS-PAGE gel. 15µl samples were added with 5µl 2x SDS-PAGE sample buffer and heated at 95ºC for 5min. Prior to the samples being separated by 12% SDS-PAGE gel for approximately 1 hour, samples were centrifuged at 13,000 x rpm for 1 min. The gel was stained with Coomasie instant blue from Expedeon. All the procedures were done according the manufacturer's recommendations. Molecular weights were determined according to mobilities of molecular weight protein standard (Biolab color plus prestained 7-175kDa).

Western blotting was carried out using standard protocols (Sambrook and Russell, 2001). The protein was transfered to nitrocellulose membrane for 1.5 hour and treated for 2-3 hours at room temperature using 5% skimmed milk as the blocking agent. The membrane was then incubated overnight at 4ºC with

primary antibody (monoclonal anti GST antibody (SIGMA G-1160) at a dilution of 1:2000. The membrane was washed using three washes of PBST (Phosphate Buffer Saline with Tween 20) for 5-10min each, then incubated with secondary antibody (SIGMA-A4416 anti GST antibody-peroxidase conjugate produced in mouse diluted in 1:10,000) for 2 hours at room temperature. The blot was washed three to five times for 15 minutes using buffer PBST, then incubated with the ECL (Enhance chemiluminesence) Western blotting detection reagents (according to manufacture instructions from Amersham) for 5 minutes at room temperature analysis using a hyperprocessor machine.

6.2.10 Purification of recombinant iron reductases

500ml LB medium was prepared for the purification of recombinant protein (IR1 and IR2) as described above. All the protein purification was undertaken at 4°C. The supernatant was centrifuged at 5000 x g for 20 minutes, 4°C using a SORVALL RC 5B and resuspended on lysis buffer contains 50mM Tris-HCl pH 8; 1mM EDTA pH 8,0; 1mM tris2 carboxyethyl-phosphine (TCEP) ; 1mM phenyl methylsulfonyl- fluoride (PMSF) ; 200mM NaCl, and deionized water (dH_2O). The cells were lysed using combination of freeze thaw and sonication method and then centrifuged at 13,000 xg for 10 minutes, 4°C and the supernatant was collected for the purification. The soluble fraction of recombinant protein (IR1 and IR2) was purified using the Glutathione Sepharose 4B. The crude cell extract was passed through a column pre-equilibrated with binding buffer PBS pH 7.5 (140mM NaCl, 2.7mM KCl, 10mM Na_2HPO_4, and

1.8mM KH_2PO_4). The columns were prepared according to the manual (Glutathione Separose 4B, 52-2303-00 AK). After extensive washing using binding buffer, the GST fusion proteins were eluted with elution buffer (50mM Tris-HCl, 20mM reduced glutathione, pH 8.0). The fractions collected and were ran on the SDS-PAGE gradient gel 4-12%.

6.2.11 Protein analysis

Concentration of the recombinant protein was determined using the Bradford RC-DC protein assay (from BIO-RAD) using 1mg ml^{-1} BSA as the standard and absorption measured at 750nm.

6.2.12 Functionality of Iron reductase genes

6.2.12.1 Iron reductase assay

A modified method developed by Arantes et al., (2009) and Kerem et al., (1999), to determine the reduction of iron using Ferrozine reagent [3-(2-pyridyl)-5,6-bis-(4-phenylsulfonic acid)-1,2,triazine] (Sigma) was used. The experiment was conducted in 96-well micro titre plates. 50µl of crude extract/supernatant from soluble fusion protein of IR1 and IR2 cultures were combined with 0.1 mM $FeCl_3$, 1M acetate buffer pH4.6, in the presence and absent of 50µM 2,3 dihydroxybenzoic-acid (DHBA). 10µM Ferrozine reagent was then added to the reaction. The absorbance was measured at 550nm using a spectrophotometer TECAN-Genious plate reader for 30 minutes kinetically and every 30 minutes up to 3 hours.

6.2.12.2 The ability of recombinant protein to modify/degrade lignin (nitrated lignin assay)

6.2.12.2.1. Preparation of nitrated organosolv lignin solution

A stock solution of nitrated organosolv lignin was prepared from the mixture of 25mg organosolv lignin with 5ml of acetic acid glacial (80mM of organosolv lignin in acteic acid glacial) and filtered to remove the insoluble material. The solution was then added with 750µl of concentrated nitric acid (HNO_3) and stirred on ice for 1 hour. The reaction was neutralized with 1M NaOH pH 7.0 and then was added with 10ml of H_2O. The nitrated lignin stock solution was stored on 4-5ºC and diluted 25-fold in deionized H_2O.

6.2.12.2.2 Nitrated lignin assay

Diluted nitrated organosolv lignin (110 µl) was added to each well of a 96 well plate, followed by 40µl 0.1mM $FeCl_3$, 10µl of 50uM 2,3dihydroxybenzoic-acid (2,3-DHBA), 30µl recombinant protein of IR1 or IR2 and 10µl 4mM H_2O_2. The assay was monitored at 430nm every minutes for 20 minutes and carried out in quadruplicate. The whole plate was repeated as above but with 2,3-DHBA and/or H_2O_2 being replaced by deionized H_20. The bacteria lignin degrading enzyme (dypB) and an *E. coli* GFP construct was used as positive and negative controls respectively.

6.2.12.3 Cellobiose dehydrogenase assay

The CDH assay was slightly modified from Baminger et al., (1999) and Nakagame, (2006). Recombinant enzyme activity was determined at room temperature using 0.1.M 2,6-dichlorophenol-indophenol (DCPIP; Sigma-Aldrich) as an electron acceptor in two different buffers 50mM sodium acetate buffer (pH 5) and 50mM tris-HCL (pH 7.5) with cellobiose as the substrate. The reaction mixture (in a total volume 200µl) containing: 100µl of recombinant protein of IR1 or IR2; 40µl of 0.6mM cellobiose; 10µl of Fe^{3+} (Ferric chloride); 10µl 2,3 dihydroxyl-benzoic acid 3,3 DHBA) ; 10µl 4mM H_2O_2 and 10µl 0.5mM DCPIP. The decreased of absorption of DCPIP was monitored using kinetic spectrophotometry at 540nm every minutes for 30 minutes. Using a spectrophotometer TECAN GENious plate reader and the whole assay was repeated without cellobiose, 2,3-DHBA and recombinant proteins. All readings were taken in quadruplicate.

6.2.12.4. Total reducing sugars assay by the recombinant proteins

The CBM assay was modified from Hall et al., (2010) and Yoon et al., (2005). The ability of recombinant iron reductase to bind micro-crystalline cellulose was tested using Avicel-PH 101 (Sigma Aldrich) while the degradation of lignocellulose was detected using wheat straw powder as the substrate. Hydrolysis of Avicel and wheat straw powder (30mg/ml) in a crude extract solution containing the iron reductase enzymes from *Serpula lacrymans* was measured for 24 hours at room temperature and 50°C, pH 7.5. An aliquot of the

crude extract (250μl) was taken and centrifuged for 1 min at 13.000 rpm. The purified cellulose (Avicel) and cellulose in wheat straw was estimated by quantifying the total reducing sugars using DNS (Dinitrosalicylic Acid) method and using glucose as the standard. The absorbance was measured at 540nm using a spectrophotometer TECAN GENious plate reader with four replicate and buffer include with the same substrate (Avicel and wheat straw powder) was used as negative controls. The absorbance refer to the amount of total reducing sugars released.

6.3. Results

6.3.1 The expression the recombinant protein in *E. coli* (BL21)

IR1 and IR2 minus the signal peptide were expressed in *E. coli* BL21 as GST fusion proteins. The predicted molecular weight for GST-IR1 and GST-IR2 are 55kDa and 49kDa respectively. After solubilization using lysis buffer, the soluble and insoluble fractions were analysed on 12% SDS-PAGE gels. Western blot analysis, did not identify anything in the insoluble fraction. The crude extract of soluble intracellular culture after 5 hours induction showed highest production of the recombinant proteins of the expected size (Figure 54). The total amount of proteins of IR1 was 4.84 mg ml^{-1} while IR2 was 4.98mg ml^{-1}.

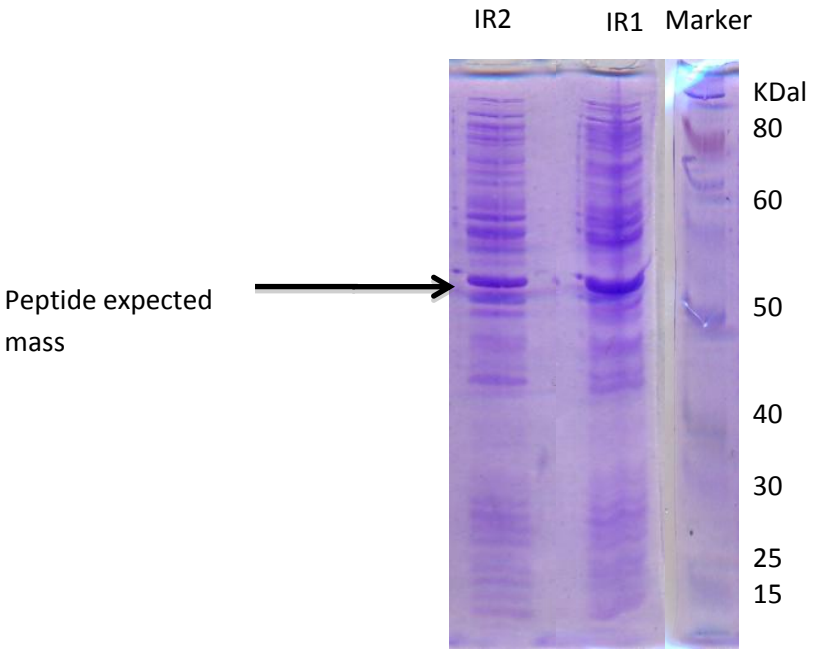

Figure 54. SDS-PAGE of the soluble fraction from crude lysate showing expression of recombinant forms of IR1 and IR2 prepared from extract of *E. coli* BL21 after 5 hours induction at 30°C with 0.4mM IPTG. Lane 1 (molecular weight marker protein); lane 2 (IR1); lane 3: IR2

6.3.2 Purification of iron reductases (IR1 and IR2) expressed in *E. coli*

Supernatant was collected by the centrifugation of *E. coli* lysate at 13,000rpm for 15 min at 4°C. This was column purified using GST-Sepharose 4B beads (GE Healthcare, UK) according to the manufacturer's instructions. The presence of recombinant protein IR1 was confirmed by a band at 55kDa by SDS-PAGE (gel gradient 4-12%) (Figure 55). The protein concentration of IR1 and IR2 after purification are 0.066 mg ml^{-1} and 0.043 mg ml^{-1} respectively.

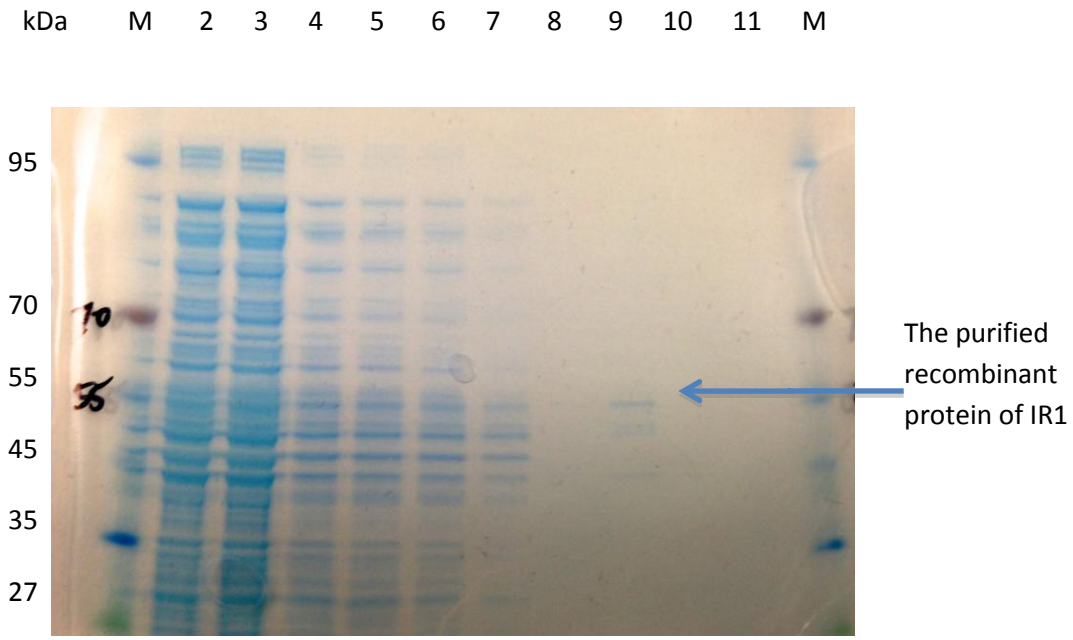

Figure 55. An SDS-PAGE showing purification of recombinant fusion protein GST-IR1 using GST-Sepharose 4B. Lane 1 and 12: molecular weight markers (kDa); lane 2 and 3: the flow through fraction; lane 4-8: washing fractions; 9-11: Elute fractions

Western blotting was used to confirm the presence of recombinant IR1 with a band also visible at 55kDa using an anti GST antibody (Figure 56).

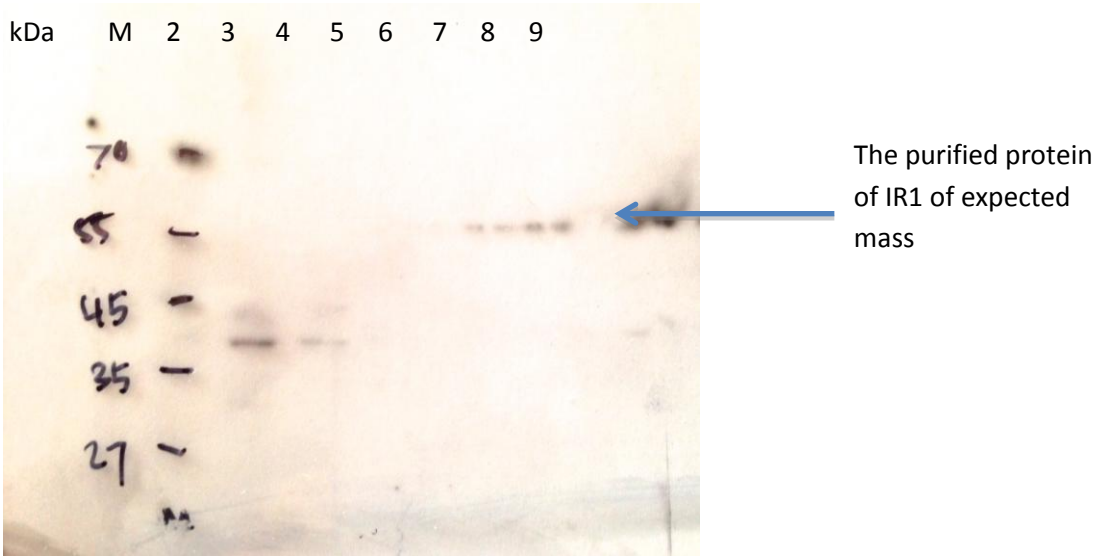

Figure 56. Western Blotting analysis of IR1 from *Serpula lacrymans* purified using the GST-monoclonal (primary antibody) and anti-GST polyclonal (secondary antibody). The arrow indicates the band coresponding to recombinant IR1. (Lane (M): molecular weight markers (kDa); lane 2: the flow through fraction; lane 3: wash fractions; lane 4: empty; lane5-7: Elute fractions; lane 8: empty; lane 9: Concentrated elute fractions)

In the case of IR2, elution from GST-Sepharose column gave fractions containing the expected band at 49kDa, but also a number of other protein bands (Figure 57). Western blotting confirmed that the 49kDa band reacted with an anti GST antibody (Figure 58).

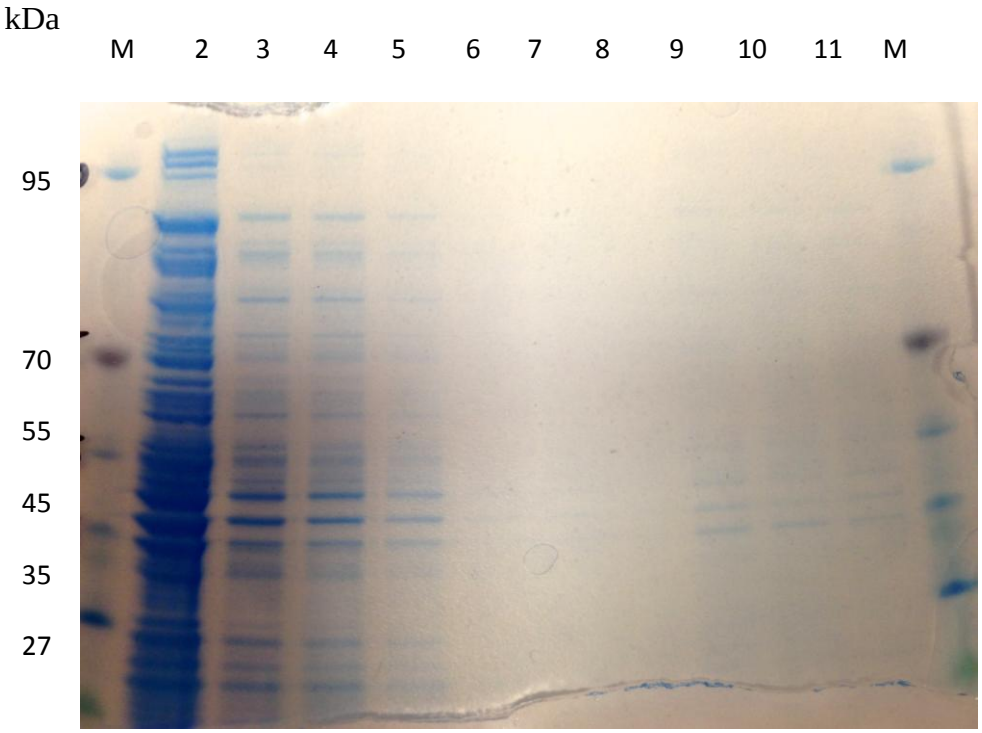

Figure 57. SDS-PAGE showing purification of recombinant GST-IR2 by GST-Sepharose 4B. (Lane 1 and 12: molecular weight markers (kDa); lane 2: the flow through fraction; lane 3-8: washed fractions; 9-11: Elute fractions).

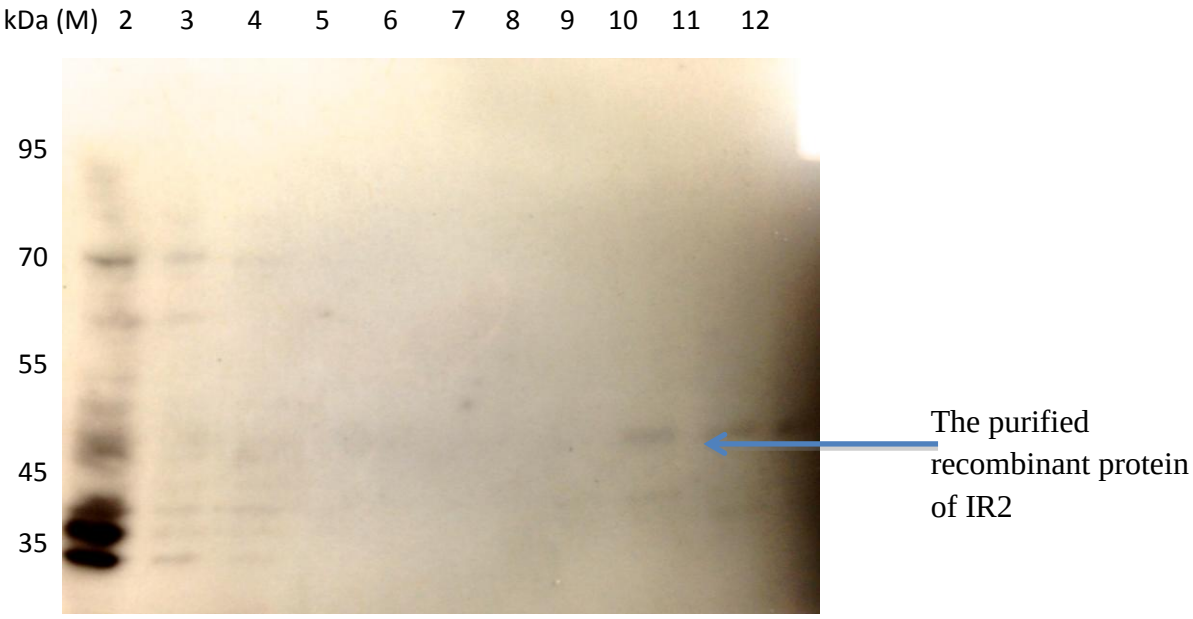

Figure 58. Western Blotting analysis of IR2 from *S. lacrymans* purified using the GST-antibody monoclonal (primary antibody) and anti-GST polyclonal. The arrow indicated the recombinant protein of IR2. (Lane 1 (M): molecular weight markers (kDa); lane 2: the flow through fraction; lane 3-9: washed fractions; lane 10-12: Elute fractions).

6.3.3 Determination of the function of iron reductase (IR1 and IR2)

6.3.3.1 Iron reductase capacity

The IR1 and IR2 proteins where predicted to have iron reducing function. To test this, a Ferrozine spot assay was used to detect production of Fe^{2+} by reduction of Fe^{3+}, using the crude extract of both recombinant proteins which was monitored for 30 minutes. To investigate the iron binding and reducing ability of the model compound, 2,3-DHBA was used as the positive control.

It was observed that in the presence of 2,3-DHBA, all treatments showed a significant increase in absorbance indicating production of the ferrous iron

(Fe^{2+}) complex (Figure 60), which is indicated by the change of colour. After 30 minutes observation, the highest absorbance was identified in the extract of IR1 recombinant protein after induction for 5 hours (0.175). The absorbance increased by approximately 25%, compared to the baseline while data obtained for IR2 was not significantly different from the negative controls (Figure 59). While in the absence of 2,3-DHBA, the recombinant protein of IR1 also showed a significant increase in the absorbance, detected using both IR1-5H and IR2-5H with IR1-5H showing activity although this was not significant. No significant difference in the absorbance was found with the negative controls.

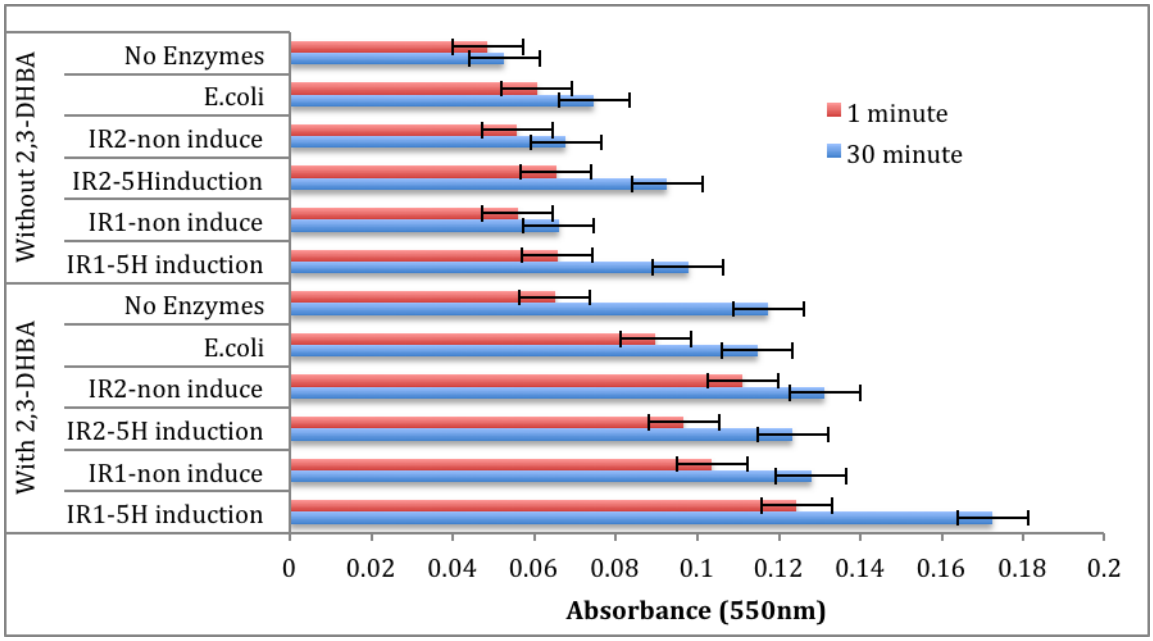

Figure 59. The changes in absorbance (550 nm) following addition of recombinant protein IR1 and IR2 at 1 and 30 minutes observation in the presence and absence of 2,3-DHBA. The error bar represent the least significant difference (LSD 5%).

6.3.3.2 The ability of iron reductases to degrade nitrated lignin and the effect of addition of 2,3-DHBA, ferric cholride and H_2O_2.

In this study the ability of recombinant proteins IR1 and IR2 to decompose the nitrated lignin was tested. The effect of Fe^{3+}($FeCl_3$) and 2,3-dihydroxybenzoic-acid (2,3-DHBA) with and without hydrogen peroxide (H_2O_2) on their activity was also measured. This was modified from a previous method (Ahmad et al., 2010) through the addition of Fe^{3+} as a substrate, as it plays an important role in the Fenton reaction which has been predicted to be involved in lignocellulose decomposition by *S. lacrymans*.

In the presence of ferric chloride (Fe^{3+}) and hydrogen peroxide (H_2O_2), the results showed an increased release of phenolic compounds over time (Figure 60). This indicates that the nitrated lignin was being affected and phenolic compounds released. Release of these phenolic compounds increased continuously during the incubation period.

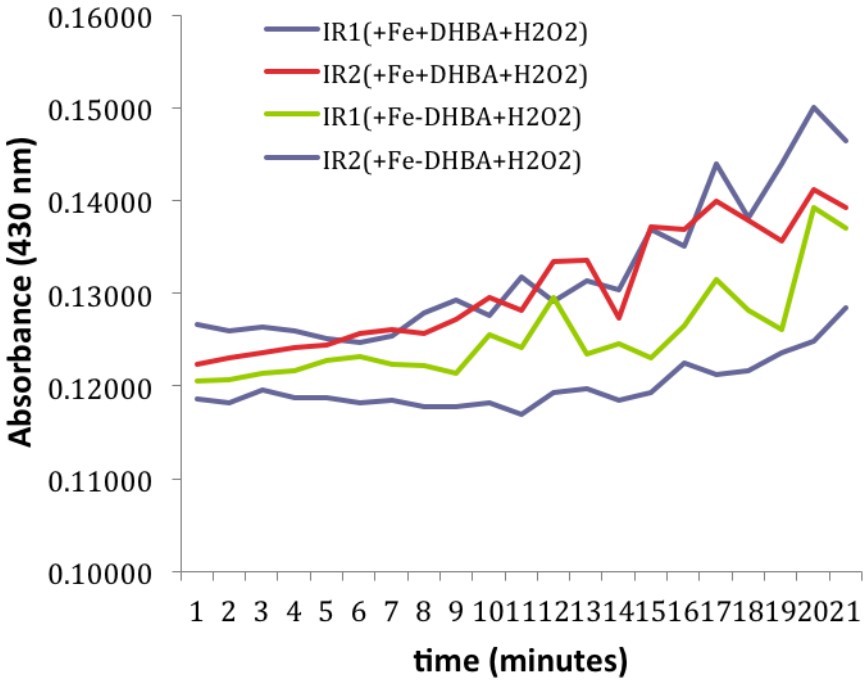

Figure 60. Release of phenolic compounds by recombinant iron reductases (IR1 and IR2) from *S. lacrymans* as measured by changes in the absorbance (430nm) using the nitrated lignin assay in the presence of H_2O_2 (with and without 2,3-DHBA).

The addition of 2,3 DHBA as a reducing agent did not significantly affect the absorbance. The greatest difference was found using recombinant IR1 with 2,3-DHBA (0.1501), followed by IR2 (0.1412), while without the addition of 2,3-DHBA the absorbance of IR1 and IR2 were 0.1393 and 0.1249 respectively (Figure 60).

The addition of hydrogen peroxide (H_2O_2) which also plays an important role in the Fenton reaction, was found to accelerate the activity of recombinant protein IR1 and IR2. Again IR1 showed greater activity than IR2 in the presence or absence of 2,3-DHBA, which indicates IR1 under these conditions has a greater enzymic activity to degrade nitrated lignin than IR2.

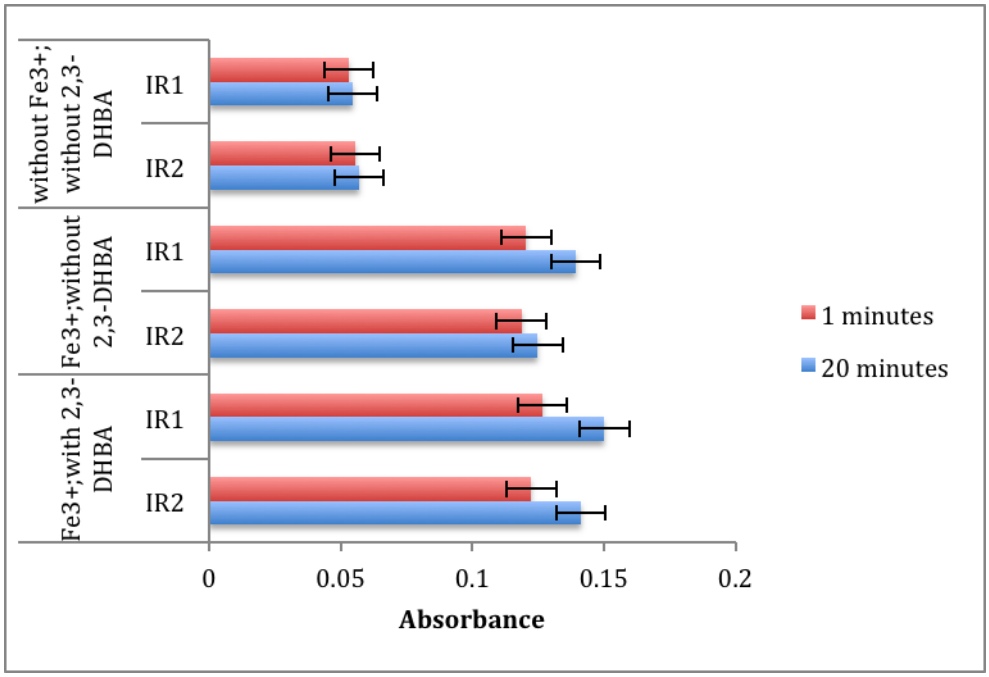

Figure 61. The release of phenolics by the recombinant protein (IR1 and IR2) in the presence of hydrogen peroxide (H_2O_2), is shown by a change in absorbance (430 nm). This was measured at 1 and 20 minutes observation in the presence and absence of 2,3-DHBA. The error bar represent the least significant difference (LSD 5%).

In the absence of iron and 2,3-DHBA after 20 minutes measurement, recombinant IR1 and IR2 had not significantly increased compared to initial measurements (1 minutes). However in the presence of Fe^{3+}, even without the addition of 2,3-DHBA, there was a significant increase ($P<0.05$) after 20 minutes when recombinant protein IR1 was used. IR2 on the other hand, only showed a significant difference in the presence of Fe^{3+} and 2,3-DHBA. Without the presence of 2,3-DHBA, there was no significant difference after 20 minutes incubation (Figure 61).

In the absence of hydrogen-peroxide (H_2O_2) and with the same concentration of Fe^{3+}, with or without 2,3-DHBA, recombinant proteins IR1 and IR2 showed no significant change in the absorbance (Figure 62). The absorbance of IR1 was similar

to IR2 throughout the experiment. The range of absorbance of IR1 and IR2 genes in the present of 2,3-DHBA were between 0.1258 to 0.1301. This was greater than the absorbance of IR1 and IR2 genes in the absence of 2.3-DHBA, which ranged between 0.1156 to 0.1225 (Figure 62).

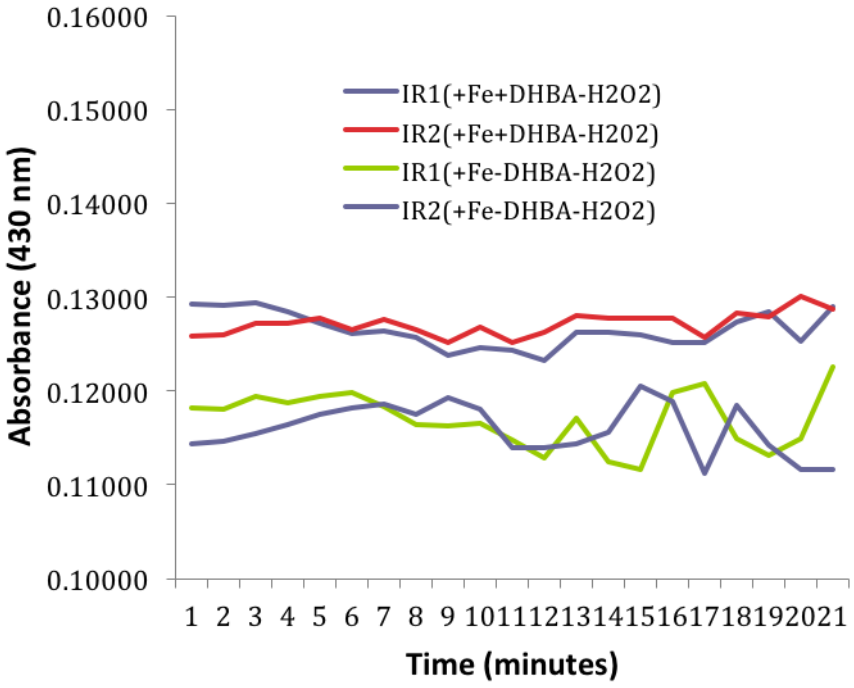

Figure 62. Absorbance readings (430nm) indicating release of phenolic compounds by the recombinant iron reductases (IR1 and IR2) as measured using the nitrated lignin assay in the absence of H_2O_2 (with and without 2,3-DHBA).

In the absence of hydrogen peroxide (H_2O_2), there was no significant difference using recombinant proteins of IR1 and IR2 compared to the control even after 20 minutes. 2,3-DHBA had no effect with or without Fe^{3+} (Figure 63).

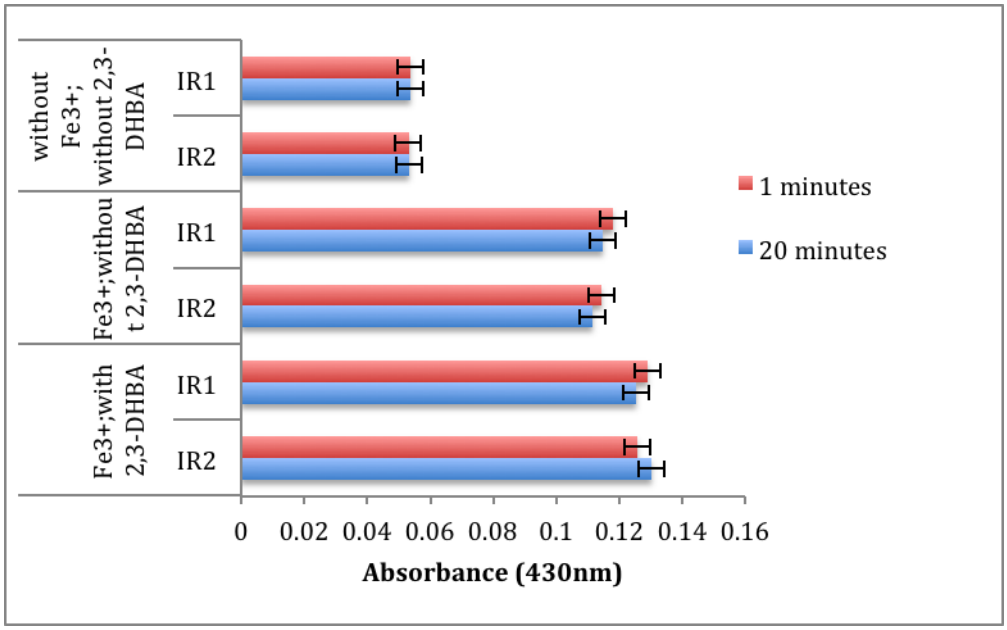

Figure 63. Phenolic production as measured by the changes in absorbance (430 nm) with recombinant protein (IR1 and IR2) at 1 and 20 minutes with and without 2,3-DHBA in the absence of hydrogen peroxide (H_2O_2). The error bar represents the least significant difference (LSD 5%).

E. coli-GFP construct was used as a negative control treatment, for comparing the effectiveness of this organism on nitrated lignin degradation relative to the activity of IR1 and IR2. In the presence of hydrogen-peroxide (H_2O_2), 2,3-DHBA and under similar concentration of Fe^{3+}, the absorbance of *E. coli*-GFP were similar to the treatment without H_2O_2 (data not shown). The absorbance of phenolic compound released by negative controls *E. coli*-GFP was almost constant during 20 min, which means this sample has no ability to degrade nitrated lignin. The absorbance of *E. coli*-GFP under no presence of Fe^{3+} was in similar pattern, where the absorbance was remain steady. The range of absorbance of *E. coli* was 2 times lower than the treatment with the presence of Fe^{3+}. The absorbance was within the value of 0.054 to 0.065.

6.3.3.3 The ability of iron reductases as an electron acceptor as measured by the effect of 2,3-DHBA in the presence of H_2O_2

The DCPIP-based assay was used for the detection of CDH activity (Baminger U. et al., 1999). Sequence alignment results (Chapter 5, Figure 47) showed that the recombinant protein of IR1 and IR2 partially contain the heme domain of CDH genes which are reported to play a role in the decomposition of lignocellulose. Therefore, this assay which measures the absorbance from the reduction of the electron acceptor DCPIP over a 30 minute incubation was conducted to assess whether the recombinant proteins of IR1 and IR2 have the potential ability to degrade lignocellulose. To complement the nitrated lignin assay, the DCPIP-based assay for the detection of CDH activity was employed as this is a quick approached for detecting low activity of CDH (Baminger et al., 1999).

The activity of recombinant proteins IR1 and IR2 was indicated by the reduction of DCPIP absorbance over the 10 minutes observation which increased significantly ($P<0.05$) with the addition of Fe^{3+}, 2,3-DHBA and hydrogen-peroxide (H_2O_2). To characterize the effect of pH on the recombinant protein iron reductases, several buffers were used for instance the potassium phospate buffer at pH 5 and 7.5.

In the presence of 2,3-DHBA and H_2O_2, the greatest reduction of DCPIP could be seen after 10 minutes observation before leveling off. The greatest reduction of DCPIP was found using IR1 at pH 7.5 followed by IR1 (pH 5), IR2 (pH 7.5) and IR2 (pH 5). The negative controls (either *E. coli*-GFP or buffer alone) gave an initial increase in the absorbance in the beginning of the reaction and then levelled off after 2 minutes. This phenomenon was hypothesized to be due to a lack of iron reductase enzyme raising the absorbance of DCPIP (Figure 64).

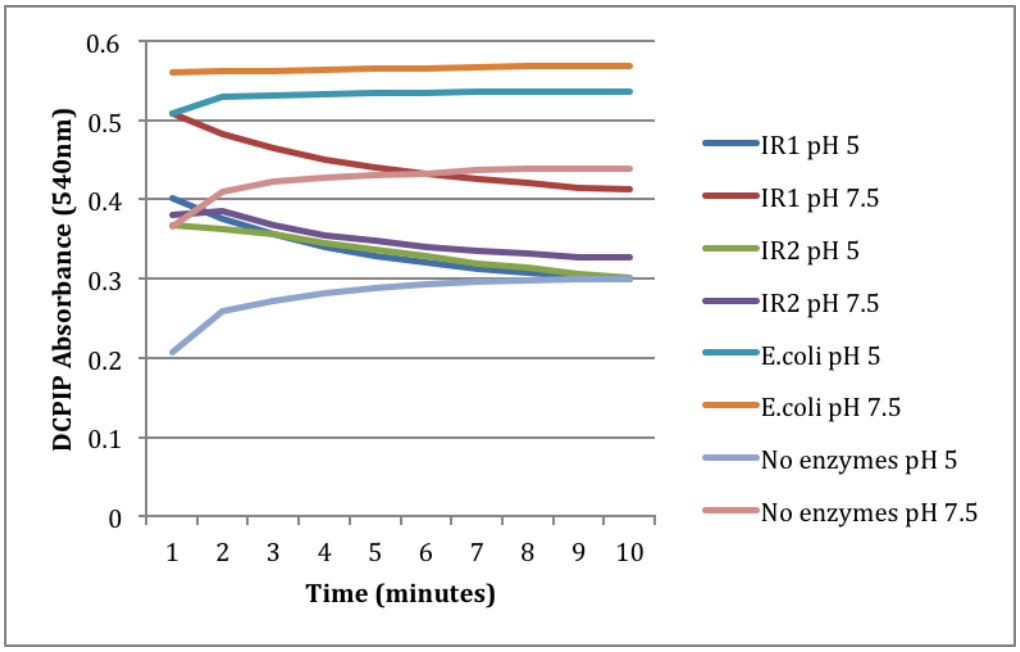

Figure 64. Changes in DCPIP absorbance (540 nm) over 10 minutes observation in the presence of Fe^{3+}, 2,3-DHBA and H_2O_2 at different pH (5 and 7.5).

To examine the significance of the reduction in DCPIP absorbance due the different treatment, at least 10 minutes observation is required by which time all DCPIP is assumed to be completely degraded and no remaining DCPIP left in the solution. After 10 minutes, a significant reduction ($P<0.05$) in the asbsorbance of DCPIP was apparent in the presence of IR1 and IR2 supplemented with Fe^{3+}, 2,3-DHBA and hydrogen peroxide (H_2O_2) (Figure 65). Meanwhile, there was no reduction in DCPIP absorbance observed with the negative controls (buffer alone and *E. coli*-GFP) treatment.

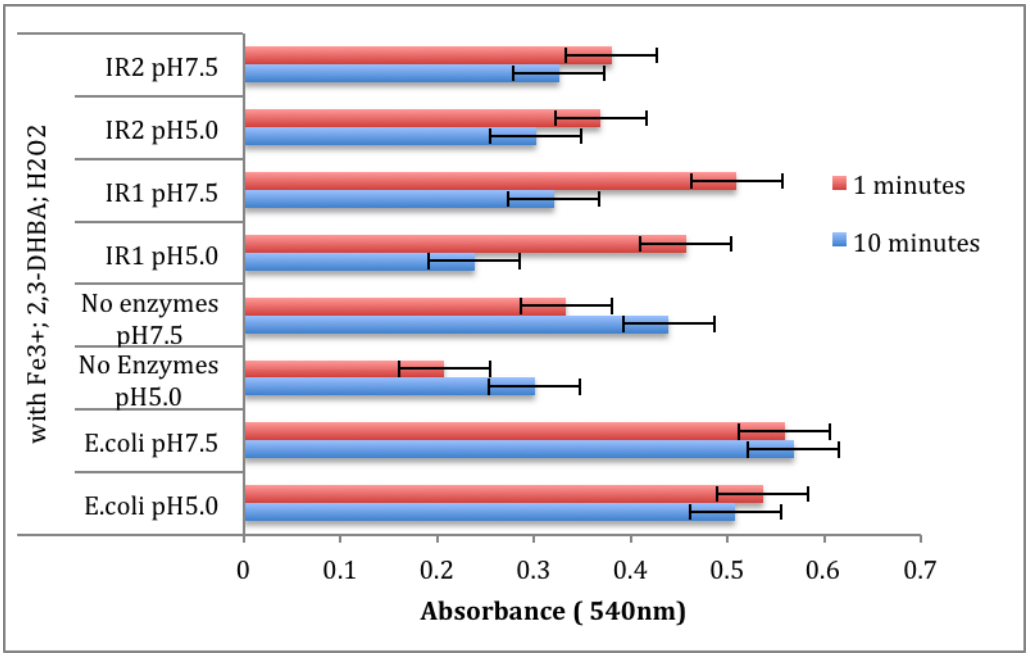

Figure 65. The changes in DCPIP absorbance (540 nm) after 1 and 10 minutes incubation period for both IR1 and IR2 in the presence of Fe^{3+}, 2,3-DHBA and hydrogen peroxide (H_2O_2) at different pH (5 and 7.5). The error bar represent the least significant different (LSD 5%).

An increase in absorbance was shown in the negative controls (No Enzyme and *E. coli*-GFP) in the presence of Fe^{3+}, 2,3-DHBA and hydrogen peroxide, whilst the treatment with the presence of iron reductases (IR1 and IR2) have negative trends (Figure 65). These results indicate that both IR1 and IR2 can actively reduce the electron acceptor (DCPIP).

Without addition of 2,3-DHBA, the trends on the DCPIP absorbance was found similar to the treatment with the presence of 2,3-DHBA in which the reduction of DCPIP occured (Figure 66). While there was an an increase on the absorbance on the negative controls (No Enzymes and *E. coli*-GFP). This provides evidence that iron reductases IR1 and IR2 can replace the role of 2,3-DHBA as reducing agent, and these enzymes are expected to have iron reductase activity.

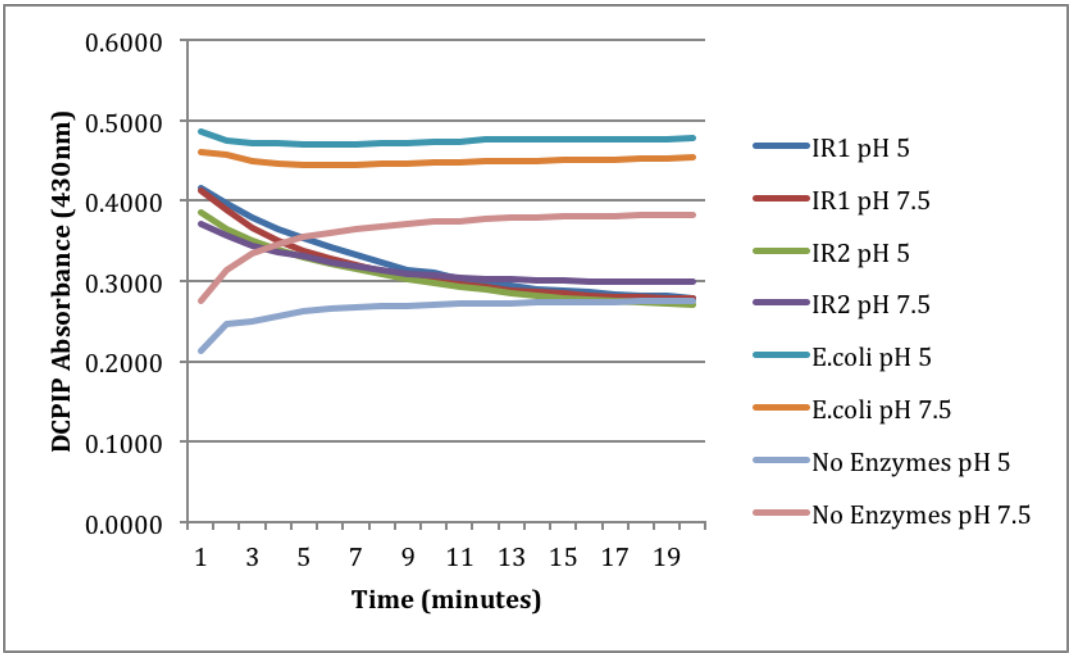

Figure 66. Changes in DCPIP absorbance (540 nm) over 10 minutes observation in the presence of Fe and H_2O_2 but absence of 2,3-DHBA at different pH (5 and 7.5) over 20 minutes.

The changes in DCPIP absorbance after 10 minutes (Figure 68) showed that there was a significant difference in DCPIP absorbance when IR1 and IR2 where compared to the negative control ($P<0.05$)(Figure 67). The reduction of DCPIP absorbance using IR1 treatment was greater than that observed with IR2.

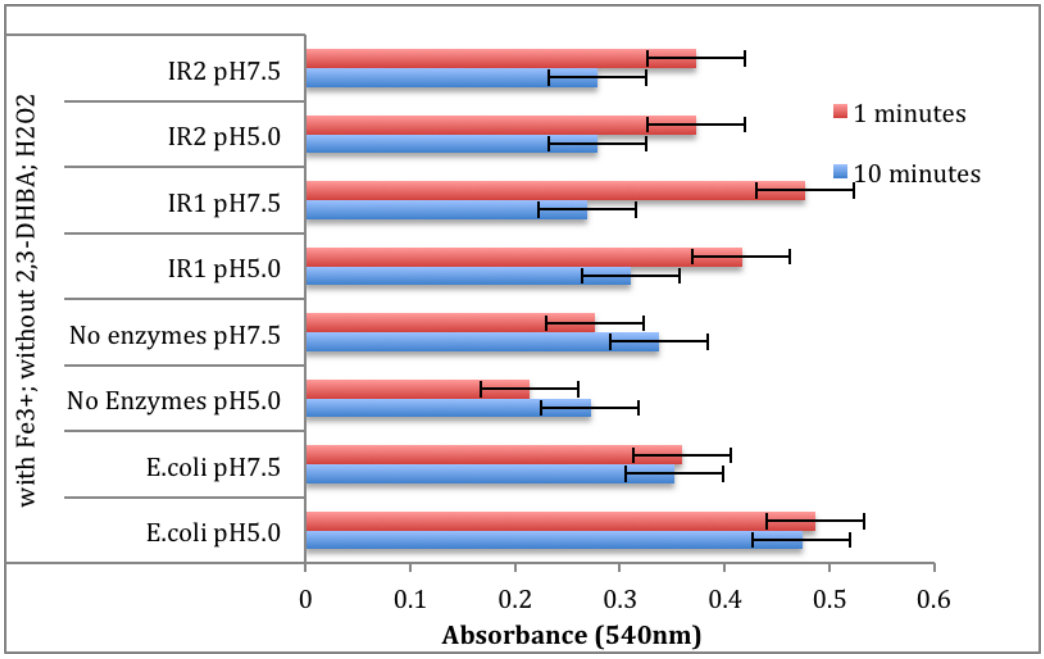

Figure 67. The changes in DCPIP absorbance (540 nm) for 10 minutes observation under the presence of Fe^{3+}, 2,3-DHBA and peroxide H_2O_2 at different level of pH (5 and 7.5). The error bar represent the least significant different (LSD 5%).

6.3.3.4 The ability of iron reductases to degrade cellulose

As described before that the recombinant iron reductase IR1 of *S. lacrymans* contains a cellulose binding module 1 (CBM1) while IR2 does not. The results illustrate that both IR1 and IR2 enzymes have the ability to degrade cellulose when either purified cellulose (Avicel) or cellulose in lignocellulose (wheat straw powder) is used.

There were a significant difference in the absorbance between the negative control and either recombinant protein IR1 or IR2 . Using Avicel as substrate of recombinant protein, no significant difference between IR1 and IR2 was detected after 1 hour incubation at room temperature (Figure 68). However,

after 24 hours incubation significant differences were seen, with powdered wheat straw giving higher readings when compare to the Avicel (Figure 68).

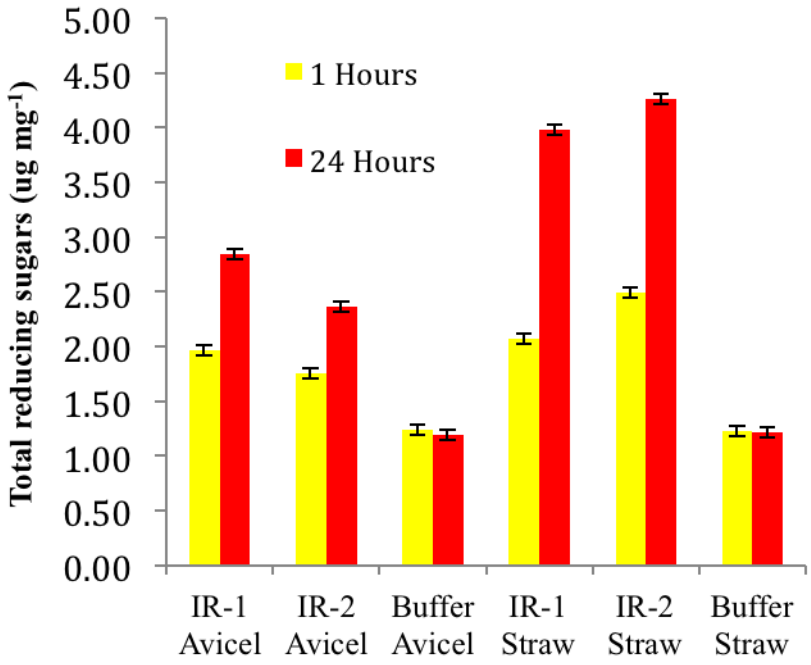

Figure 68. Comparison of the enzymatic activity of recombinant protein IR1; IR2 and Buffer (negative control) at room temperature (22°C) on avicel and wheat straw powder during 24 hours incubations. The error bar represent the least significant different (LSD 5%)

There were similar trends between IR1 and IR2 while they were incubated at 50°C, where the production of sugars was greater than that found at room temperature (Figure 69).

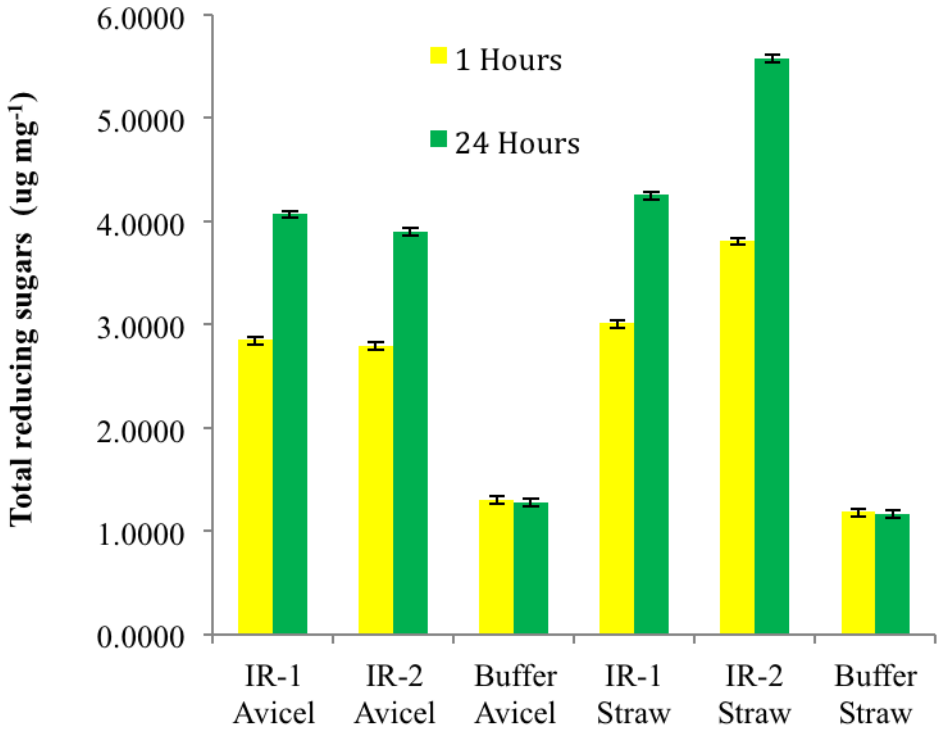

Figure 69. The comparison of the enzymatic activity of recombinant protein IR1; IR2 and Buffer (negative control) at 50°C on avicel and wheat straw powder during 24 hours incubations. The error bar represent the least significant different (LSD 5%)

The average sugar concentration released by recombinant IR1 and IR2 at room temperature and at 50^{o}C following incubation for 1 and 24 hour using Avicel and wheat straw as a substrate were range between 1.75 to 5.58 µg mg^{-1} samples.

6.4. Discussions

Since we have shown that IR1 contains a heme domain which is also present in CDH enzymes (Chapter 5, Figure 47), the functions of the recombinant IR proteins might be similar. An ability to reduce the iron (III) to iron (II) would confirm this. It has also been speculated that the heme domain of CDH may have the

peroxidase or superoxide dismutase activity (Ayers et al., 1978; Henriksson et al., 1991).

6.4.1 The ability of recombinant protein iron reductases (IR1 and IR2) to reduce iron and degrade nitrated lignin

Several mechanism might explain how the brown rot reduce Fe^{3+} to Fe^{2+} in order to participate in the degradation of lignocellulose. Oxalic acid, quinone and others low molecular phenolic compounds have all been implicated. The release of all these compounds by *S. lacrymans* grown on wheat straw SSF was shown (Chapter 3 and 4). However, in this chapter 2,3-DHBA was added as positive control which is already known to have the ability to reduce iron. Results indicated that the recombinant forms of both IR1 and IR2 have the ability to reduce iron. This confirms that the iron reduction ability of recombinant protein is likely due to the presence of the heme domain in both IR1 and IR2 (detail discussion in chapter 5).

In order to determine the role of the recombinant iron reductases in the breakdown of lignin, the nitrated lignin assay was used. The assay was first tested on IR-1 and IR-2 with and without the addition of 2,3-DBHA in the presence and absence of iron (Fe^{3+}) and hydrogen peroxide (H_2O_2). Without the presence of iron, there was no significant increase in the production of nitrated lignin breakdown compounds. This sugessted that iron is important for both enzymatic and non enzymatic reactions. In the absence of 2,3-DHBA, the results showed that the production of phenolics significantly increased after 20 minutes incubation with IR1 (Figure 61), while IR2 showed a difference this was not

significant. In the presence of 2,3-DHBA, both IR1 and IR2 showed the ability to degrade nitrated lignin (Figure 63). The presence of 2,3-DHBA is obviously support the recombinant protein to reduce iron. Then the Fe^{2+} obtained will react with the H_2O_2 provided in this assay to generates hydroxyl radicals and the release of phenolic compounds from nitrated lignin occurred.

These results confirm findings obtained with *P. putida* crude extract where, the greatest absorbance using the UV-visible assay of nitrated wheat straw was achieved after 20 minutes reaction in the presence of hydrogen peroxide (2 mM) (Ahmad et al., 2010). The results obtained using wheat straw SSF, showed the highest activity in *P. chrysosporium,* followed by *Lepista nuda*, *S. commune* and *S. lacrymans.* This activity was higher than mycorizal fungi such as *Paxillus involutus*, *Lactarius controversus*, and *Cenococcum geophilum* (Ahmad et al., 2010).

In the absence of hydrogen peroxide (H_2O_2), no significant changes in the absorbance was found, even with the addition of 2,3-DHBA, this suggests that hydrogen peroxide plays an important role in lignocellulosic degradation. This study, shows that the iron reductases IR1 and IR2 are able to degrade nitrated lignin. This acts as a model for more complex lignocellulosic structure. However, the activity is dependant on the presence of H_2O_2. This suggests that the Fenton reaction is responsible for the lignin degradation. This is supported by other research that implies the generation of hydroxyl radicals and/or superoxide radicals are required to break down the lignocellulose and that the presence of iron, H_2O_2 and chelators agent also play a role (Xu and Goodell 2001; Qian et al., 2002 and Suzuki et al. 2006).

6.4.2 The ability of recombinant protein iron reductases to reduce the electron acceptor (DCPIP)

CDH enzymes are known to be able to reduce Fe^{3+} to Fe^{2+} in the presence of H_2O_2 and remain active at high concentration of H_2O_2. Subsequently the Fe^{2+} reacting with H_2O_2 generates the hydroxyl radical which is able to depolymerise both cellulose and lignin (Fang et al., 1998). CDH enzymes oxidase the reducing ends of cellobiose and a wide range of substances including cytochrom c, dichlorophenolindophenol (DCPIP), benzoquinone and Fe^{3+}. However in the presence of cellobiose and Fe^{3+}, incubation of CDH resulted in its activation and the degree of the inactivation was dependent mainly on the amount of CDH and cellobiose present (Fang et al., 1998). In this study, we have shown the ability of the iron reductases (IR1 and IR2) to reduce the electron acceptor (DCPIP) and how optimizing parameters such as pH can influence the efficacy of these enzyme that may play a role in lignocellulosic degradation.

When the 2,3-DHBA was present, the highest reduction was found using IR1 at pH 7.5 whilst for IR2 the greater reduction was observed at pH 5, thus the effect of pH on the degradation DCPIP appears to be gene dependent. A similar pattern was found on the absent of 2,3-DHBA, the decreasing absorbance of DCPIP as electron acceptor might be caused by the taking over of IR1 and IR2 genes on the reaction. Similar to the nitrated lignin assay, on this assays the ability of recombinant protein to reduce the electron aceptor (DCPIP) showed the activity. Therefore this indicted that the genes are active and the activity may be due to the presence of heme domain on the N terminal domain of recombinant

protein which have been indicated have the functionality to reduce Fe(III) to Fe(II).

The enzyme activity is controlled by various factors which can influence their quality and quantity including pH of the culture and time of culture. CDH from *Cladosporium* for example, its shown the optimum enzyme activity achieved at 14 days and when pH was at 4.5, cultured at 28^{o}C (1300 unit/mg protein). This was higher compared to enzyme activity at pH 3.5 (650 unit/mg protein) or 6.5 (300 unit/mg protein) at the same period and temperature of culture. Lower CDH enzyme activity was observed in lower temperature (25^{o}C) or even higher than 28^{o}C (32^{o}C and 35^{o}C) (Ghahfarokhi et al., 2004). In other experiment the heme group of the *P. chrysosporium* CDH was less active by pH above 5.9 (Samejima et al., 1992), when the study was carried out at pH 6 there was a slow reduction of CDH heme activity of *Sporotricum pulverulentum* (Jones and Wilson, 1988).

In addition an optimum CDH activity was obtained from culture rich cellulose activity, but it can also produce under lack of nitrogen culture (Henriksson et al., 2000a; Costa-Ferreira et al., 1994). The catalytic and binding domain of different cellulases may have different binding preferred binding sites on the cellulose surface and the dominating mode of binding may depend on the enzyme concentration (Stahlberg et al., 1991; Srisodsuk et al., 1993).

6.4.3 The total reducing sugars released by iron reductases (IR1 and IR2)

The average sugar concentration released by recombinant IR1 and IR2 at room temperature and at 50^{o}C following incubation for 1 and 24 hour using Avicel and straw as a substrate ranged between 1.75 to 5.58 μg mg^{-1}.

Our results using both recombinant IR1 and IR2 showed they were able to liberate sugars from different kind of substrate such as Avicel and wheat straw. Both recombinants showed greater sugar release when they were cultured on straw compared to Avicel which is a form of microcrystaline cellulose. This might be due their nature having been adapted to work best in the presence of various lignocellulosic components. Recombinant IR2 showed a marginally greater ability to degrade straw compared to IR1 despite the lack of CBM module, while recombinant IR1 performed slightly better in the breakdown of Avicel compared to IR2 at room temperature. It has been reported that enzymes which showed relatively higher activity on Avicel than on carboxymetyl cellulose (CMC) are identified as exoglucanases which has the ability to cleave the β-1,4-glycosidic bonds from chain ends of releasing cellobiose and some glucose molecule (Dashtban et al., 2010).

As previous assay results suggested that the presence of iron, H_2O_2 and reducing or chelating agents such as DHBA and oxalic acids are important in the break down of lignocellulose via the Fenton reactions we have shown that even without the addition of those chemicals, both IR1 and IR2 are capable of degrading cellulose. But how this is achieved this requires further work.

Chapter 7. General Conclusion and Future Work

7.1 General conclusion

Study of the mechanism of lignin degradation and enzymes produced in basidiomycetes has predominantly focused on the white rot rather than brown rot fungi (Vares et al., 1995). The mechanisms employed by individual fungi are not all the same. Unlike the white rot fungi, the brown rots in general do not produce enzymes such as the laccases, lignin peroxidases and manganese peroxidases, which would allow direct decay of lignin and its aromatic structure. It has been assumed that the brown rot fungi all use the same mechanism for lignocellulose decay, based on a Fenton-type catalytic system that produces hydroxyl radicals, which attack the lignocellulose.

We have shown that *S. lacrymans* has the ability to break down lignocellulose using both enzymatic and non-enzymatic processes. Of the fungi tested it is the most promising lignocellulosic degrader of wheat straw and out-performed the other fungi tested (i.e. *Phanerochaete chrysosporium*, *Schizoophyllum commune* and *Postia placenta*). Evidence obtained in this study showed that *S. lacrymans* is well suited to wheat straw solid-state fermentation, requiring minimal external inputs (without adding any nutrients). Fatty acid measurement of 18:2n6c in the brown rots was shown to correlate with fungal growth although the rate of production differed between fungi. In conjunction with ergosterol measurements *S. lacrymans* was shown to grow very well on straw. The production of total soluble phenolics and the release of low molecular compound aromatic compounds (molecular weight <400 kDa) were also highest when *S. lacrymans* was used compared to the other fungi

(data from Chapter 3). Early changes in the wheat straw during SSF were also obvious when methods were used which recorded the weight loss of wheat straw. This was attributed to the release of organic and aromatic compounds and use of sugars during fungal growth.

Using FTIR, changes in the intensity of signal attributable to selected functional groups during culture was detected such as: the peak at 3430 cm^{-1} which corresponds to the hydroxyl groups, 2930 and 2840 cm^{-1} and which has been assigned to C-H stretching of the aromatic methoxyl groups and methylene groups (data from Chapter 4). The breakdown of lignocellulose compounds using solid samples appeared to be slower than that found with liquid samples although the products released were similar.

In this study, *S. lacrymans* was shown to produce oxalic acid (OA) and quinone (2,5 DMBQ). The OA production reached a maximum of 10mM after 35 days, which caused a pH decrease of more than 1 unit from pH 5.7 to 4.4 (data from Chapter 4). This high level of oxalic acid is known to hydrolyse lignocellulose making the cell wall more accessible to the complex enzymes and to enhance the reduction of ferric ion to ferrous ion (Shimada et al., 1996). Production of 2,5-dimethoxyhydroquinone (DMHQ) as a reducing agent is known to drive the Fenton reaction in brown rot fungi. In this study the measurement of DMHQ was not possible however it is known to be produced from the conversion of 2,5 DMBQ.

The amount of available Fe^{2+} is also important. The amount of Fe^{2+} produced by the Fenton reaction increases if a combination of oxalic acid and DMHQ interacts with the available Fe^{3+}. The resulting Fe^{2+} will, in the presence of H_2O_2 (also produced by fungal enzymes), generate hydroxyl radicals, which subsequently cause

the break down of lignocellulose. H_2O_2 production might also be triggered by the oxidation of oxalic acid. This could produce an anion radical, which reduces O_2 to the superoxide anion and this superoxide then could reduce Fe^{3+} to Fe^{2+} and forms the H_2O_2 in a disproportional reaction (Kaneko et al., 2005).

The results obtained suggested break down of lignocellulose by *S. lacrymans*, is dependent on an optimum ratio of chelating/reducing agent and that the availability of Fe^{3+} is important. High level of DHBA (chelating/reducing agents) was also shown to be capable of inhibiting the formation of OH°.

Two previously uncharacterised genes with Iron reductase capabilities from *S. lacrymans* were identified. The biological function of IR1 and IR2 of *S. lacrymans* was previously unknown, but bioinformatics analysis suggested a role for these in the degradation of lignocellulolytic material. It was thought that IR1 and IR2 might be involved in the reduction of Fe^{3+} to Fe^{2+} performing a function in the Fenton reaction and to interact with H_2O_2 to breakdown the lignocellulose structure. Analysis of these showed that presence of a heme domain and a cytochrome domain similar to that of CDH however they lacked any monooxygenase domain. Phylogenic analysis confirmed that these iron reductase genes belong to the cellulose binding module/cytochrome gene family of proteins (have more similarity to CBMs family)

Analysis showed a significant difference in IR1 and IR2 genes expression over the period of culture. IR2 reaching a maximum at 23 days, after which IR1 appeared to be expressed more strongly. The time at which these genes are highly expressed correlated with the release of soluble and aromatic phenolic compounds, which occurs approximately 3 weeks of incubation.

In order to determine the exact function of these enzymes, these genes were cloned and expressed as recombinant proteins in *E. coli.* The production of purified protein was confirmed using both SDS-PAGE and Western blotting (data from chapter 6). The Ferrozine assay was employed to test the iron-reduction capabilities of the recombinant proteins. Both IR1 and IR2 genes encoded proteins that could reduce Fe^{3+} to Fe^{2+}(data from chapter 6).

In order to determine if the genes also functioned as lignin modifiers the nitrated lignin assay was used. Results suggested that the addition of Fe^{3+} to the reaction mix is important. The presence of H_2O_2 was shown to be important as it is a crucial agent for the formation of hydroxyl radicals and it reacted with the recombinant proteins to degrade/modify nitrated lignin.

Due to the similarity of the heme domain IR1 and IR2 to that of CDH, (chapter 5), the DCPIP (dichlorophenol-indophenol) based assay were used to complement the nitrated lignin and Ferrozine assay. Both IR1 and IR2 indicated the ability to reduce the electron acceptor (data chapter 6).

Interestingly using both synthetic and natural sources of cellulose or lignocellulose (avicel and wheat straw powder), the IR genes were also shown to have the capabilities to break down cellulose (data chapter 6). This suggested that the recombinant genes might be a significant addition to those currently used within biomass based biorefineries.

This works has tremendous implications for understanding the mechanism by which the brown rot fungus *S. lacrymans* breaks down lignocellulose. The results showed that both fungal extract and the IR1 and IR2 enzymes have the ability to breakdown or decompose lignocellulose. Research on lignocellulose decomposition

has suggested that the use of enzymes based technologies for biomass conversions are efficient, low cost and environment friendly. However, further work on protein secretion and the efficacy of these iron reductases to break down lignocellulose is needed, before they can be used on a large scale within biorefineries.

7.2. Future work

The development of a biorefinery process using either fungal biomass or their enzymes to break down the lignocellulosic biomass offers potential advantages such as low energy input, higher yields and reduction in pollutants. However, when natural fungal approaches are used they need much longer for the process to complete which means a high risk of contamination. Enzymes capable of breaking down lignocellulose are highly sought after as they are more efficient but can be costly to produce depending on the expression system. The potential of the iron reductases from *S. lacrymans* for use within the biorefinery process is obvious. They do however need to be developed further, for example the optimal proportion of enzymes and biomass substrate needs to be determined in order to produce the maximum yield of value added chemicals. Further experiments are required to increase the enzyme activity and stability.

Other biomass sources besides straw are available such as waste plant biomass, woody biomass, bagasse and grasses. It would be interesting to determine the efficacy of these enzymes against such biomass and if further optimisation is required to boost the yield of products released from such sources. It is also important to optimize the feedstock yield and composition of each biomass. Control

of the physical and/or chemical modification of biomass during storage or transportation is another challenge to feedstock processing.

The concept of biorefining using the iron reductases of *S. lacrymans*, could be implemented for processing other agricultural waste such as paddy straw from Indonesia. Paddy straw, has similar characteristic to wheat straw, Indonesia is one of the biggest countries in South East Asia, which produces a massive amount of rice waste biomass during the paddy-harvesting season. The production of paddy straw biomass in Indonesia was recorded at the level of 40.8×10^6 T. This placed it as the third largest paddy straw producer among Asian countries, after China (138.1×10^6 T) and India (104.4×10^6 T).

Paddy straw contains high levels of elements such as: N (40-50%), P (30-35%), K (80-85%) and S (40-50%), which remain in the plant biomass. Paddy straw is usually taken out from the field for use as animal feedstock, burnt in the field, or left on the soil surface as a mulch. This means there is a great deal of opportunity to use paddy straw biomass or the husks from around the grain as a media, which the iron reductases could convert, in order to produce numerous value added chemicals

Other agroindustry wastes are available as liquids e.g. molasses from sugar cane which contains high concentration of sugars that may be useful for the production of ethanol. Other waste have different composition in which case the use of the iron reductase enzymes could be used to preprocess the liquids which contain a high fibre content prior to use of normal cellulases. However, optimization within the laboratory would have to be done first before it's applied to the larger scale. We can conclude that the IR genes from *S. lacrymans* demonstrate how fungal enzymes have a great deal of potential in a future biobased economy.

References

Agosin, E., Jarpa, S., Rojas, E. and Espejo, E. (1989). Solid state fermentation of pine sawdust by selected brown rot fungi. *Enzyme and Microbial Technology*, **11**, 511-517.

Aguiar, A., de Souza-Cruz, P.B. and Ferraz, A. (2006). Oxalic acid, $Fe3^{+}$ reduction activity and oxidative enzymes detected in culture extracts recovered from *Pinus taeda* wood chips biotreated by *Ceriporiopsis subvermispora*. *Enzyme and Microbial Technology*, **38**, 873-878.

Aguiar, A. and Ferraz, A. (2007). $Fe3^{+}$ and $Cu2^{+}$ reduction by phenol derivatives associated with Azure B degradation in Fenton-like reactions. *Chemosphere*, **66**, 947-954.

Ahmad, M., Taylor, C.R., Pink, D., Burton, K., Eastwood, D., Bending, G.D. and Bugg, T. D.H. (2010). Development of novel assays for lignin degradation: comparative analysis of bacterial and fungal lignin degraders. *Molecular Biosystems*, **6**, 815-821.

Alinia, R., Zabihi, S., Esmaeilzadeh, F. and Kalajahi, J.F. (2010). Pretreatment of wheat straw by supercritical CO_2 and its enzymatic hydrolysis for sugar production. *Biosystems Engineering*, **107**, 61-66.

Allen, A.L. and Roche, C.D. (1989). Effects of strain and fermentation conditions on production of cellulase by *Trichoderma reesei*. *Biotechnology and Bioengineering*, **33**, 650-656.

Applied Biosystem (2004). Relative quantification: Applied Biosystem 7300/7500 Real Time PCR System.

Arantes, V. and Milagres, A.M.F. (2006a). Degradation of cellulosic and hemicellulosic substrates using a chelator-mediated Fenton reaction. *Journal of Chemical Technology and Biotechnology*, **81**, 413-419.

Arantes, V. and Milagres, A.M.F. (2006b). Evaluation of different carbon sources for production of iron-reducing compounds by *Wolfiporia cocos* and *Perenniporia medulla-panis*. *Process Biochemistry*, **41**, 887-891.

Arantes, V., Milagres, A.M.F., Filley, T.R. and Goodell, B. (2011). Lignocellulosic polysaccharides and lignin degradation by wood decay fungi: the relevance of nonenzymatic Fenton-based reactions. *Journal of Industrial Microbiology and Biotechnology*, **38**, 541-555.

Arantes, V., Qian, Y., Milagres, A.M.F., Jellison, J. and Goodell, B. (2009). Effect of pH and oxalic acid on the reduction of $Fe3^{+}$ by a biomimetic chelator and on $Fe3^{+}$ desorption/adsorption onto wood: Implications for brown-rot decay. *International Biodeterioration and Biodegradation*, **63**, 478-483.

Arantes, V. and Saddler, J.N. (2010). Access to cellulose limits the efficiency of enzymatic hydrolysis: the role of amorphogenesis. *Biotechnology for Biofuels*, **3**

Arora, D.S. (1995). Biodelignification of wheat straw by different fungal associations. *Biodegradation*, **6**, 57-60.

Arora, D.S., Garg, K.K. and Sindhwani, A. (1995). Semisolid fermentation of paddy straw and eucalyptus wood sawdust by different fungi. *Geobios (Jodhpur)*, **22**, 13-17.

Atwell, W.A. (2001). An overview of wheat development, cultivation, and production. *Cereal Foods World*, **46**, 59-62.

Ayers, A.R., Ayers, S.B. and Eriksson, K.E. (1978). Cellobiose oxidase, purification, and partial characterization of a hemoprotein from *Sporotrichum pulverulentum*. *European Journal of Biochemistry*, **90**, 171-181.

Baldrian, P. and Valaskova, V. (2008). Degradation of cellulose by basidiomycetous fungi. *FEMS Microbiology Reviews*, **32**, 501-521.

Ballesteros, I., Negro, M. J., Oliva, J. M., Cabanas, A., Manzanares, P. and Ballesteros, M. (2006). Ethanol production from steam-explosion pretreated wheat straw. *Applied biochemistry and biotechnology*, **129-132**, 496-508.

Baminger, U., Nidetzky, B., Kulbe, K.D. and Haltrich, D. (1999). A simple assay for measuring cellobiose dehydrogenase activity in the presence of laccase. *Journal of Microbiological Methods*, **35**, 253-259.

Bey, M., Berrin, J.G., Poidevin, L. and Sigoillot, J.C. (2011). Heterologous expression of *Pycnoporus cinnabarinus* cellobiose dehydrogenase in *Pichia pastoris* and involvement in saccharification processes. *Microbial Cell Factories*, **10**.

Bezier, A., Lambert, B. and Baillieul, F. (2002). Cloning of a grapevine Botrytis-responsive gene that has homology to the tobacco hypersensitivity-related hsr203J. *Journal of Experimental Botany*, **53**, 2279-2280.

Bezier, A., Lambert, B. and Baillieul, F. (2002). Study of defense-related gene expression in grapevine leaves and berries infected with *Botrytis cinerea*. *European Journal of Plant Pathology*, **108**, 111-120.

Bis'ko, N., Buchalo, A.S. and Vasser, S.P. (1983). Higher edible basidiomycetes in surface and submerged culture (Kiev: Naukova Dumka).

Blanchette, R.A., Burnes, T.A., Eerdmans, M.M. and Akhtar, M. (1992). Evaluating isolates of *Phanerochaete chrysosporium* and *Ceriporiopsis subvermispora* for use in biological pulping processes. *Holzforschung*, **46**, 109-115.

Blanchette, R. A., Krueger, E.W., Haight, J.E., Akhtar, M. and Akin, D.E. (1997). Cell wall alterations in loblolly pine wood decayed by the white-rot fungus, *Ceriporiopsis subvermispora*. *Journal of Biotechnology*, **53**, 203-213.

Boraston, A.B., McLean, B. W., Guarna, M. M., Amandaron-Akow, E. and Kilburn, D.G. (2001). A family 2a carbohydrate-binding module suitable as an affinity tag for proteins produced in *Pichia pastoris*. *Protein Expression and Purification*, **21**, 417-423.

Boraston, A.B., Warren, R. A. J. and Kilburn, D.G. (2001). Glycosylation by *Pichia pastoris* decreases the affinity of a family 2a carbohydrate-binding module from *Cellulomonas fimi*: a functional and mutational analysis. *Biochemical Journal*, **358**, 423-430.

Borjesson, T., Stollman, U. and Schnurer, J. (1990). Volatile metabolites and other indicators of *Penicillum aurantiogriseum* growth on different substrates. *Applied and Environmental Microbiology*, **56**, 3705-3710.

Bozell, J.J. (2006). Feedstocks for the future using technology development as a guide to product identification. *Feedstocks for the Future: Renewables for the Production of Chemicals and Materials*, **921**, 1-12.

Bruce, A., King, B. and Highley, T.L. (1991). Decay resistance of wood removed from poles biologically treated with *Trichoderma*. *Holzforschung*, **45**, 307-311.

Buranov, A.U. and Mazza, G. (2008). Lignin in straw of herbaceous crops. *Industrial Crops and Products*, **28**, 237-259.

Bustin, S.A. (2000). Absolute quantification of mRNA using real-time reverse transcription polymerase chain reaction assays. *Journal of Molecular Endocrinology*, **25**, 169-193.

Buta, J. G., Zadrazil, F. and Galletti, G.C. (1989). FT-IR determination of lignin degradation in wheat straw by white rot fungus *Stropharia rugosoannulata* with different oxygen concentration *Journal of Agricultural and Food Chemistry*, **37**, 1382-1384.

Cai, D.Y. and Tien, M. (1993). Lignin degrading peroxidases of *Phanerochaete chrysosporium*. *Journal of Biotechnology*, **30**, 79-90.

Canevascini, G., Borer, P. and Dreyer, J.L. (1991). Cellobiose dehydrogenases of *Sporotrichum (Chysosporium) thermophile European Journal of Biochemistry*, **198**, 43-52.

Carvalheiro, F., Duarte, L.C. and Girio, F.M. (2008). Hemicellulose biorefineries: a review on biomass pretreatments. *Journal of Scientific and Industrial Research*, **67**, 849-864.

Castanera, R., Perez, G., Omarini, A., Alfaro, M., Pisabarro, A. G., Faraco, V., Amore, A. and Ramirez, L. (2012). Transcriptional and enzymatic profiling of *Pleurotus ostreatus*

Laccase genes in submerged and solid-state fermentation cultures. *Applied and Environmental Microbiology*, **78**, 4037-4045.

Cho, K.M., Hong, S.Y., Math, R.K., Lee, J.H., Kambiranda, D.M., Kim, J.M., Islam, S.M. A., Yun, M.G., Cho, J.J., Lim, W.J. and Yun, H.D. (2009). Biotransformation of phenolics (isoflavones, flavanols and phenolic acids) during the fermentation of cheonggukjang by *Bacillus pumilus* HY1. *Food Chemistry*, **114**, 413-419.

Cho, Y., Sun, J., Wu, X. and Liu, R.H. (2002). Antioxidant and antiproliferative activity of common vegetables. *Journal of Agricultural and Food Chemistry*, **50**, 6910-6916.

Cioni, M., Pinzauti, G. and Vanni, P. (1981). Comparative biochemistry of the glyoxylate cycle. *Comparative Biochemistry and Physiology B-Biochemistry and Molecular Biology*, **70**, 1-26.

Clark, J.H. (2007). Green chemistry for the second generation biorefinery - sustainable chemical manufacturing based on biomass. *Journal of Chemical Technology and Biotechnology*, **82**, 603-609.

Clausen, C.A., Kenealy, W. and Lebow, P.K. (2008). Oxalate analysis methodology for decayed wood. *International Biodeterioration and Biodegradation*, **62**, 372-375.

Cohen, R., Jensen, K. A., Houtman, C. J. and Hammel, K.E. (2002). Significant levels of extracellular reactive oxygen species produced by brown rot basidiomycetes on cellulose. *FEBS Letters*, **531**, 483-488.

Contreras, D., Freer, J. and Rodriguez, J. (2006). Veratryl alcohol degradation by a catechol-driven Fenton reaction as lignin oxidation by brown-rot fungi model. *International Biodeterioration and Biodegradation*, **57**, 63-68.

Copeland, J. and Turley, D. (2008) National and regional supply/demand balance for agricultural straw in Great Britain. Sand Hutton-York-UK:

Costaferreira, M., Ander, P. and Duarte, J. (1994). On the relationship between cellobiose dehydrogenase and cellobiose quinone oxidoreductase under condition where C-14 DHP is mineralized by whole culture of *Phanerochaete chrysosporium*. *Enzyme and Microbial Technology*, **16**, 771-776.

Cox, M. C., Rogers, M. S., Cheesman, M., Jones, G. D., Thomson, A. J., Wilson, M. T. and Moore, G. R. (1992). Spectroscopic identification of the heme ligands of cellobiose oxidase. *FEBS Letters*, **307**, 233-236.

Cullen, D. and Kersten, P. J. (1996). Enzymology and molecular biology of lignin degradation. *The Mycota, III. A comprehensive treatise on fungi as experimental systems for basic and applied research: Biochemistry and molecular biology*, 295-312.

Dashtban, M., Schraft, H. and Qin, W. (2009). Fungal Bioconversion of Lignocellulosic

Residues; Opportunities & Perspectives. *International Journal of Biological Sciences*, **5**, 578-595.

David, G.B. and Roy, L.W. (2008). *Cellulose*. **In**: AccesScience-McGraw-Hill.

Davis, M.W. and Lamar, R.T. (1992). Evaluation of methods to extract ergosterol for quantitation of soil fungal biomass. *Soil Biology and Biochemistry*, **24**, 189-198.

de Ridder-Duine, A.S., Smant, W., van der Wal, A., van Veen, J.A. and de Boer, W. (2006). Evaluation of a simple, non-alkaline extraction protocol to quantify soil ergosterol. *Pedobiologia*, **50**, 293-300.

de Ruiter, G.A., Noterman, S.H.W. and Romboust, F.M. (1993). New methods in food mycology. *Trends Food Science Technology*, **4**, 91-97.

Dejong, E., Cazemier, A. E., Field, J. A. and Debont, J.A.M. (1994). Physiological role of chlorinated aryl alchohols biosynthesized de novo by the white rot fungus *Bjerkandera sp* strain BOS55. *Applied and Environmental Microbiology*, **60**, 271-277.

Dejong, E., Field, J.A. and Debont, J.A.M. (1994). Aryl alchohol in the physiology of ligninolytic fungi. *FEMS Microbiology Reviews*, **13**, 153-188.

Dekker, R.F.H. (1988). Cellobiose dehydrogenase produced by *Monilia sp*. *Methods in Enzymology*, **160**, 454-463.

Den Haan, R., McBride, J.E., La Grange, D.C., Lynd, L.R. and Van Zyl, W.H. (2007). Functional expression of cellobiohydrolases in *Saccharomyces cerevisiae* towards one-step conversion of cellulose to ethanol. *Enzyme and Microbial Technology*, **40**, 1291-1299.

Diorio, L., Galati, B., Amela Garcia, M. and Papinutti, L. (2009). Degradation of pruning wastes by *Phanerochaete sordida* growing in SSF: Ultrastructural, chemical, and enzymatic studies. *International Biodeterioration and Biodegradation*, **63**, 19-23.

Dorado, J., Almendros, G., Camarero, S., Martinez, A.T., Vares, T. and Hatakka, A. (1999). Transformation of wheat straw in the course of solid-state fermentation by four ligninolytic basidiomycetes. *Enzyme and Microbial Technology*, **25**, 605-612.

Dumonceaux, T.J., Bartholomew, K.A., Charles, T.C., Moukha, S.M. and Archibald, F.S. (1998). Cloning and sequencing of a gene encoding cellobiose dehydrogenase from *Trametes versicolor*. *Gene*, **210**, 211-219.

Dutton, M.V., Evans, C.S., Atkey, P.T. and Wood, D.A. (1993). Oxalate production by Basidiomycetes, including the white rot species *Coriolus versicolor* and *Phanerochaete chrysosporium*. *Applied Microbiology and Biotechnology*, **39**, 5-10.

Eastwood, D. C., Floudas, D., Binder, M., Majcherczyk, A., Schneider, P., Aerts, A., Asiegbu, F. O., Baker, S. E., Barry, K., Bendiksby, M., Blumentritt, M., Coutinho,

P.M., Cullen, D., de Vries, R.P., Gathman, A., Goodell, B., Henrissat, B., Ihrmark, K., Kauserud, H., Kohler, A., LaButti, K., Lapidus, A., Lavin, J. L., Lee, Y.H., Lindquist, E., Lilly, W., Lucas, S., Morin, E., Murat, C., Oguiza, J.A., Park, J., Pisabarro, A.G., Riley, R., Rosling, A., Salamov, A., Schmidt, O., Schmutz, J., Skrede, I., Stenlid, J., Wiebenga, A., Xie, X., Kuees, U., Hibbett, D.S., Hoffmeister, D., Hogberg, N., Martin, F., Grigoriev, I.V. and Watkinson, S. C. (2011). The plant cell wall-decomposing machinery underlies the functional diversity of forest fungi. *Science*, **333**, 762-765.

Eiland, F., Klamer, M., Lind, A. M., Leth, M. and Baath, E. (2001). Influence of initial C/N ratio on chemical and microbial composition during long term composting of straw. *Microbial Ecology*, **41**, 272-280.

Elisashvili, V., Kachlishvili, E. and Penninckx, M. (2008). Effect of growth substrate, method of fermentation, and nitrogen source on lignocellulose-degrading enzymes production by white-rot basidiomycetes. *Journal of Industrial Microbiology and Biotechnology*, **35**, 1531-1538.

Emelyanova, E.V. (2005). Effects of cultivation conditions on the growth of the basidiomycete *Coriolus hirsutus* in a medium with pentose wood hydrolyzate. *Process Biochemistry*, **40**, 1119-1124.

Engh, I. B., Carlsen, T., Saetre, G.P., Hogberg, N., Doi, S. and Kauserud, H. (2010). Two invasive populations of the dry rot fungus *Serpula lacrymans* show divergent population genetic structures. *Molecular Ecology*, **19**, 706-715.

Enoki, A., Hirano, T. and Tanaka, H. (1992). Extracellular substance from the brown rot *Gloeophyllum trabeum* that produces and reduces hydrogen peroxide. *Material Und Organismen*, **27**, 247-261.

Eriksson K.E.L., Blanchette, R.A. and Ander, P. (1990). Springer series in wood science microbial and enzymatic degradation of wood and wood components. *Eriksson, K.-E. L., R. a. Blanchette and P. Ander. Springer Series in Wood Science: Microbial and Enzymatic Degradation of Wood and Wood Components. Ix+407p. Springer-Verlag New York, Inc.: Secaucus, New Jersey, USA; Berlin, Germany. Illus*, IX+407P-IX+407P.

Eriksson, K.E. and Kirk, T.K. (1985). Biopulping, biobleaching, and treatment of kraft bleaching effluents with white-rot fungi. In *Comphrehensive biotechnology*, pp. 271-294. Edited by M. Mooo Young. New York: Pergamon Press.

Espejo, E. and Agosin, E. (1991). Production and degradation of oxalic acid by brown rot fungi. *Applied and Environmental Microbiology*, **57**, 1980-1986.

Fahr, K., Wetzstein, H. G., Grey, R. and Schlosser, D. (1999). Degradation of 2,4-dichlorophenol and pentachlorophenol by two brown rot fungi. *FEMS Microbiology Letters*, **175**, 127-132.

Faix, O. (1986). Investigation of lignin polymer models (DHPS) by FTIR spectroscopy. *Holzforschung*, **40**, 273-280.

Fang, J., Liu, W. and Gao, P.J. (1998). Cellobiose dehydrogenase from *Schizophyllum commune*: Purification and study of some catalytic, inactivation, and cellulose-binding properties. *Archives of Biochemistry and Biophysics*, **353**, 37-46.

Federle, T.W. (1986). Microbial distribution in soil - New technique. In *Perspective in microbial ecology*, pp. 493-498. Edited by F. Megusar and M. Gantar. Slovenia: Slovenia Society for Microbiology.

Fenn, P. and Kirk, T.K. (1981). Relationship of nitrogen to the onset and suppression of ligninolytic activity and secondary metabolism in *Phanerochaete chrysosporium*. *Archives of Microbiology*, **130**, 59-65.

Filley, T.R., Cody, G.D., Goodell, B., Jellison, J., Noser, C. and Ostrofsky, A. (2002). Lignin demethylation and polysaccharide decomposition in spruce sapwood degraded by brown rot fungi. *Organic Geochemistry*, **33**, 111-124.

Fish, W.W. (1988). Rapid colorimetric micromethod for quantitation of complexed iron in biological samples. *Methods in Enzymology*, **158**, 357-364.

Flannigan, B. (1997). Air sampling for fungi in indoor environments. *Journal of Aerosol Science*, **28**, 381-392.

Foyle, T., Jennings, L. and Mulcahy, P. (2007). Compositional analysis of lignocellulosic materials: Evaluation of methods used for sugar analysis of waste paper and straw. *Bioresource Technology*, **98**, 3026-3036.

Frade, J. P., Warnock, D.W. and Arthington-Skaggs, B.A. (2004). Rapid quantification of drug resistance gene expression in *Candida albicans* by reverse transcriptase LightCycler PCR and fluorescent probe hybridization. *Journal of Clinical Microbiology*, **42**, 2085-2093.

Fredrik, R., Huelsenbeck, J. and Teslenko, M. (2011) Draft MrBayes version 3.2 manual: tutorial and model summaries.

Frostegard, A. and Baath, E. (1996). The use of phospholipid fatty acid analysis to estimate bacterial and fungal biomass in soil. *Biology and Fertility of Soils*, **22**, 59-65.

Gamauf, C., Metz, B. and Seiboth, B. (2007). Degradation of plant cell wall polymers by fungi. *Mycota*, 325-340.

Gamper, H.A., Young, J.P.W., Jones, D.L. and Hodge, A. (2008). Real-time PCR and microscopy: Are the two methods measuring the same unit of arbuscular mycorrhizal fungal abundance? *Fungal Genetics and Biology*, **45**, 581-596.

Gao, Y., Chen, T. and Breuil, C. (1993). Ergosterol - A measure of fungal growth in wood

for staining and pitch control fungi. *Biotechnology Techniques*, **7**, 621-626.

Garg, S.K. and Neelakantan, S. (1982). Production of SCP and cellulase by *Aspergilus terreus* from baggase substrate. *Biotechnology and Bioengineering*, **24**, 2407-2417.

Gessner, M.O., Bauchrowitz, M.A. and Escautier, M. (1991). Extraction and quantification of ergosterol as a measure of fungal biomass in leaf litter. *Microbial Ecology*, **22**, 285-291.

Gessner, M.O. and Chauvet, E. (1993). Ergosterol to biomass conversion factors for aquatic hyphomycetes. *Applied and Environmental Microbiology*, **59**, 502-507.

Gessner, M.O. and Newell, S.Y. (2002). Biomass, growth rate, and production of filamentous fungi in plant litter. In *Manual of Environmental Microbiology-2nd Edition*, pp. 390-408. Edited by C. J. Hurst, R. L. Crawford, G. Knudsen, M. McInerney and L. Stetzenbach. Washington DC-USA: ASM Press.

Gessner, M.O. and Schmitt, A.L. (1996). Use of solid-phase extraction to determine ergosterol concentrations in plant tissue colonized by fungi. *Applied and Environmental Microbiology*, **62**, 415-419.

Gomez-Toribio, V., Garcia-Martin, A. B., Martinez, M. J., Martinez, A. T. and Guillen, F. (2009). Enhancing the production of hydroxyl radicals by *Pleurotus eryngii* via quinone redox cycling for pollutant removal. *Applied and Environmental Microbiology*, **75**, 3954-3962.

Gong, P., Guan, X. and Witter, E. (2001). A rapid method to extract ergosterol from soil by physical disruption. *Applied Soil Ecology*, **17**, 285-289.

Goodell, B. (2003). Brown-rot fungal degradation of wood: Our evolving view. *Wood Deterioration and Preservation: Advances in Our Changing World*, **845**, 97-118.

Goodell, B., Daniel, G., Jellison, J. and Qian, Y. (2006). Iron-reducing capacity of low-molecular-weight compounds produced in wood by fungi. *Holzforschung*, **60**, 630-636.

Goodell, B., Jellison, J., Liu, J., Daniel, G., Paszczynski, A., Fekete, F., Krishnamurthy, S., Jun, L. and Xu, G. (1997). Low molecular weight chelators and phenolic compounds isolated from wood decay fungi and their role in the fungal biodegradation of wood. *Journal of Biotechnology*, **53**, 133-162.

Goodell, B., Nicholas, D.D. and Schult, T.P. (2003). Introduction to wood deterioration and preservation. In *Wood Deterioration and Preservation: Advances in Our Changing World*, pp. 2-7. Edited by B. Goodell, D. D. Nicholas and T. P. Schultz.

Goodell, B., Qian, Y.H., Jellison, J., Richard, M. and Qi, W.H. (2002). Lignocellulose oxidation by low molecular weight metal-binding compounds isolated from wood degrading fungi: A comparison of brown rot and white rot systems and the potential application of

chelator-mediated Fenton reactions. *Biotechnology in the Pulp and Paper Industry: 8th Icbppi*, **21**, 37-47.

Green, F., Larsen, M.J., Winandy, J.E. and Highley, T.L. (1991). Role of oxalic acid in incipient bronw rot decay. *Material Und Organismen*, **26**, 191-213.

Grinhut, T., Salame, T.M., Chen, Y. and Hadar, Y. (2011). Involvement of ligninolytic enzymes and Fenton-like reaction in humic acid degradation by *Trametes sp*. *Applied Microbiology and Biotechnology*, **91**, 1131-1140.

Guenin, S., Mauriat, M., Pelloux, J., Van Wuytswinkel, O., Bellini, C. and Gutierrez, L. (2009). Normalization of qRT-PCR data: the necessity of adopting a systematic, experimental conditions-specific, validation of references. *Journal of Experimental Botany*, **60**, 487-493.

Hall, M., Bansal, P., Lee, J.H., Realff, M.J. and Bommarius, A.S. (2010). Cellulose crystallinity - a key predictor of the enzymatic hydrolysis rate. *FEBS Journal*, **277**, 1571-1582.

Hallberg, B. M., Bergfors, T., Backbro, K., Pettersson, G., Henriksson, G. and Divne, C. (2000). A new scaffold for binding haem in the cytochrome domain of the extracellular flavocytochrome cellobiose dehydrogenase. *Structure with Folding & Design*, **8**, 79-88.

Hammel, K. E. (1997). Fungal degradation of lignin. *Driven by nature: Plant litter quality and decomposition*, 33-45.

Hammel, K. E. (1995). Mechanisms for polycyclic aromatic hydrocarbon degradation by ligninolytic fungi. *Environmental Health Perspectives*, **103**, 41-43.

Hammel, K. E., Kapich, A.N., Jensen, K.A. and Ryan, Z.C. (2002). Reactive oxygen species as agents of wood decay by fungi. *Enzyme and Microbial Technology*, **30**, 445-453.

Harreither, W., Sygmund, C., Augustin, M., Narciso, M., Rabinovich, M. L., Gorton, L., Haltrich, D. and Ludwig, R. (2011). Catalytic properties and classification of cellobiose dehydrogenases from Ascomycetes. *Applied and Environmental Microbiology*, **77**, 1804-1815.

Harreither, W., Sygmund, C., Duenhofen, E., Vicuna, R., Haltrich, D. and Ludwig, R. (2009). Cellobiose Dehydrogenase from the Ligninolytic Basidiomycete Ceriporiopsis subvermispora. *Applied and Environmental Microbiology*, **75**, 2750-2757.

Hartog, B.J. and Notermans, S. (1988). The detection and qualification of fungi in food. In *Introduction to food borne fungi - 4th edition*, pp. 220-230. Edited by R. A. Samson and E. S. van Reenen-Hoestra. Baarn-Netherland: Centraalbureau voor Schimmelcultures.

Hatakka, A. (2001). Biopolymer, Biology, Chemistry, Biotechnology Application. In *Lignin, Humic Substance and Coal*, pp. 129-180. Edited by M. Hofrichter and A.

Steinbuchel. Weinheim: Wiley-VCH.

Hatakka, A. (1994). Lignin modifying enzymes from selected white rot fungi - Production and role in liginin degradation. *FEMS Microbiology Reviews*, **13**, 125-135.

Henriksson, G., Ander, P., Pettersson, B. and Pettersson, G. (1995). Cellobiose dehydrogenase (cellobiose oxidase) from *Phanerochaete chrysosporium* as a wood degrading enzyme - Studies on cellulose, xylan and synthetic lignin. *Applied Microbiology and Biotechnology*, **42**, 790-796.

Henriksson, G., Hilden, L., Ljungquist, P. and Pettersson, B. (2000). Cellobiose dehydrogenase as a ligninase. *Abstracts of Papers of the American Chemical Society*, **219**, U282-U283.

Henriksson, G., Johansson, G. and Pettersson, G. (1993). Is cellobiose oxidase from *Phanerochaete chrysosporium* a one electron reductase. *Biochimica Et Biophysica Acta*, **1144**, 184-190.

Henriksson, G., Pettersson, G., Johansson, G., Ruiz, A. and Uzcategui, E. (1991). Cellobiose oxidase from *Phanerochaete chrysosporium* can be cleaved by papain into 2 domains. *European Journal of Biochemistry*, **196**, 101-106.

Henriksson, G., Polk, V. and Eriksson, K. E. L. (1997). Assay for cellobiose dehydrogenase in the presence of laccase. *Biotechnology Techniques*, **11**, 743-745.

Henriksson, G., Zhang, L.M., Li, J. B., Ljungquist, P., Reitberger, T., Pettersson, G. and Johansson, G. (2000). Is cellobiose dehydrogenase from *Phanerochaete chrysosporium* a lignin degrading enzyme? *Biochimica Et Biophysica Acta-Protein Structure and Molecular Enzymology*, **1480**, 83-91.

Hietala, A. M., Eikenes, M., Kvaalen, H., Solheim, H. and Fossdal, C.G. (2003). Multiplex real-time PCR for monitoring *Heterobasidion annosum* colonization in Norway spruce clones that differ in disease resistance. *Applied and Environmental Microbiology*, **69**, 4413-4420.

Highley, T.L. and Dashek, W.V. (1998). Biotechnology in the study of brown- and white-rot decay. *Forest Products Biotechnology*, 15-36.

Hilden, K., Hakala, T.K., Maijala, P., Lundell, T.K. and Hatakka, A. (2007). Novel thermotolerant laccases produced by the white-rot fungus *Physisporinus rivulosus*. *Applied Microbiology and Biotechnology*, **77**, 301-309.

Hippelein, M. and Rugamer, M. (2004). Ergosterol as an indicator of mould growth on building materials. *International Journal of Hygiene and Environmental Health*, **207**, 379-385.

Hofrichter, M., Vares, T., Kalsi, M., Galkin, S., Scheibner, K., Fritsche, W. and

Hatakka, A. (1999). Production of manganese peroxidase and organic acids and mineralization of C-14-labelled lignin (C-14-DHP) during solid-state fermentation of wheat straw with the white rot fungus Nematoloma frowardii. *Applied and Environmental Microbiology*, **65**, 1864-1870.

Hogberg, M.N. (2006). Discrepancies between ergosterol and the phospholipid fatty acid 18 : 2 omega 6,9 as biomarkers for fungi in boreal forest soils. *Soil Biology & Biochemistry*, **38**, 3431-3435.

Holker, U., Hofer, M. and Lenz, J. (2004). Biotechnological advantages of laboratory-scale solid-state fermentation with fungi. *Applied Microbiology and Biotechnology*, **64**, 175-186.

Holker, U. and Lenz, J. (2005). Solid-state fermentation - are there any biotechnological advantages? *Current Opinion in Microbiology*, **8**, 301-306.

Hong, Y., Dashtban, M., Chen, S., Song, R. and Qin, W. (2012). Enzyme production and lignin degradation by four basidiomycetous fungi in submerged fermentation of peat containing medium. *International Journal of Biology*, **4**, 172-180.

Horisawa, S., Sakuma, Y. and Doi, S. (2009). Qualitative and quantitative PCR methods using species-specific primer for detection and identification of wood rot fungi. *Journal of Wood Science*, **55**, 133-138.

Horne, R. E., Mortimer, N.D., Hetherington, R. and Grant, J.F. (1996). A comparative assessment of the energy and carbon balance of utilizing straw. *Energy*, **21**, 77-86.

Hu, R., Fan, C., Li, H., Zhang, Q. and Fu, Y.F. (2009). Evaluation of putative reference genes for gene expression normalization in soybean by quantitative real-time RT-PCR. *BMC Molecular Biology*, **10**.

Hunt, C., Kenealy, W., Horn, E. and Houtman, C. (2004). A biopulping mechanism: Creation of acid groups on fiber. *Holzforschung*, **58**, 434-439.

Hyde, S.M. and Wood, P.M. (1997). A mechanism for production of hydroxyl radicals by the brown-rot fungus *Coniophora puteana*: Fe(III) reduction by cellobiose dehydrogenase and Fe(II) oxidation at a distance from the hyphae. *Microbiology*, **143**, 259-266.

Igarashi, K., Samejima, M., Saburi, Y., Habu, N. and Eriksson, K. E. L. (1997). Localization of cellobiose dehydrogenase in cellulose-grown cultures of *Phanerochaete chrysosporium*. *Fungal Genetics and Biology*, **21**, 214-222.

Jahromi, M.F., Liang, J.B., Rosfarizan, M., Goh, Y.M., Shokryazdan, P. and Ho, Y.W. (2011). Efficiency of rice straw lignocelluloses degradability by *Aspergillus terreus* ATCC 74135 in solid state fermentation. *African Journal of Biotechnology*, **10**, 4428-4434.

Jeffries, T.W., Grigoriev, I. V., Grimwood, J., Laplaza, J. M., Aerts, A., Salamov, A.,

Schmutz, J., Lindquist, E., Dehal, P., Shapiro, H., Jin, Y.S., Passoth, V. and Richardson, P. M. (2007). Genome sequence of the lignocellulose-bioconverting and xylose-fermenting yeast *Pichia stipitis*. *Nature Biotechnology*, **25**, 319-326.

Jennison, M., Newcomb, M. and Henderson, R. (1955). Physiology of wood rotting basidiomycetes. *Mycology*, **47**, 275-304.

Jensen, K.A., Houtman, C.J., Ryan, Z.C. and Hammel, K.E. (2001). Pathways for extracellular Fenton chemistry in the brown rot basidiomycete *Gloeophyllum trabeum*. *Applied and Environmental Microbiology*, **67**, 2705-2711.

Jensen, K.A., Ryan, Z.C., Wymelenberg, A.V., Cullen, D. and Hammel, K.E. (2002). An NADH : quinone oxidoreductase active during biodegradation by the brown-rot basidiomycete *Gloeophyllum trabeum*. *Applied and Environmental Microbiology*, **68**, 2699-2703.

Jones, G.D. and Wilson, M.T. (1988). Rapid kinetic studies of the reduction of cellobiose oxidase from the white rot fungus *Sporotricum pulverulentum* by cellobiose. *Biochemical Journal*, **256**, 713-718.

Joo, S. S., Ryu, I. W., Park, J.K., Yoo, Y. M., Lee, D.H., Hwang, K. W., Choi, H.T., Lim, C.J., Lee, D. I. and Kim, K. (2008). Molecular cloning and expression of a laccase from Ganoderma lucidum, and its antioxidative properties. *Molecules and Cells*, **25**, 112-118.

Jorgensen, H., Vibe-Pedersen, J., Larsen, J. and Felby, C. (2007). Liquefaction of lignocellulose at high-solids concentrations. *Biotechnology and Bioengineering*, **96**, 862-870.

Kajisa, T., Igarashi, K. and Samejima, M. (2009). The genes encoding glycoside hydrolase family 6 and 7 cellulases from the brown-rot fungus *Coniophora puteana*. *Journal of Wood Science*, **55**, 376-380.

Kajisa, T., Yoshida, M., Igarashi, K., Katayama, A., Nishino, T. and Samejima, M. (2004). Characterization and molecular cloning of cellobiose dehydrogenase from the brown-rot fungus *Coniophora puteana*. *Journal of Bioscience and Bioengineering*, **98**, 57-63.

Kamm, B. and Kamm, M. (2004). Principles of biorefineries. *Applied Microbiology and Biotechnology*, **64**, 137-145.

Kaneko, S., Yoshitake, K., Itakura, S., Tanaka, H. and Enoki, A. (2005). Relationship between production of hydroxyl radicals and degradation of wood, crystalline cellulose, and a lignin-related compound or accumulation of oxalic acid in cultures of brown-rot fungi. *Journal of Wood Science*, **51**, 262-269.

Kanokratana, P., Chantasingh, D., Champreda, V., Tanapongpipat, S., Pootanakit, K.

and Eurwilaichitr, L. (2008). Identification and expression of cellobiohydrolase (CBHI) gene from an endophytic fungus, *Fusicoccum sp* (BCC4124) in *Pichia pastoris*. *Protein Expression and Purification*, **58**, 148-153.

Kaparaju, P., Serrano, M., Thomsen, A.B., Kongjan, P. and Angelidaki, I. (2009). Bioethanol, biohydrogen and biogas production from wheat straw in a biorefinery concept. *Bioresource Technology*, **100**, 2562-2568.

Kauserud, H., Svegarden, I. B., Saetre, G.-P., Knudsen, H., Stensrud, O., Schmidt, O., Doi, S., Sugiyama, T. and Hogberg, N. (2007). Asian origin and rapid global spread of the destructive dry rot fungus *Serpula lacrymans*. *Molecular Ecology*, **16**, 3350-3360.

Kawai, S., Jensen, K.A., Bao, W. and Hammel, K.E. (1995). New ploymeric model substrate for the study of microbial ligninolysis. *Applied and Environmental Microbiology*, **61**, 3407-3414.

Kerem, Z., Friesem, D. and Hadar, Y. (1992). Lignocellulose degradation during soild state fermentation *Pleorotus ostreatus* versus *Phanerochaete chrysosporium*. *Applied and Environmental Microbiology*, **58**, 1121-1127.

Kerem, Z., Jensen, K.A. and Hammel, K.E. (1999). Biodegradative mechanism of the brown rot basidiomycete *Gloeophyllum trabeum*: evidence for an extracellular hydroquinone-driven fenton reaction. *FEBS Letters*, **446**, 49-54.

Kim, S. and Dale, B.E. (2004). Global potential bioethanol production from wasted crops and crop residues. *Biomass and Bioenergy*, **26**, 361-375.

Klamer, M. and Baath, E. (2004). Estimation of conversion factors for fungal biomass determination in compost using ergosterol and PLFA 18 : 2 omega 6,9. *Soil Biology & Biochemistry*, **36**, 57-65.

Kleinert, M. and Barth, T. (2008). Phenols from lignin. *Chemical Engineering & Technology*, **31**, 736-745.

Klinke, H.B., Ahring, B.K., Schmidt, A.S. and Thomsen, A.B. (2002). Characterization of degradation products from alkaline wet oxidation of wheat straw. *Bioresource Technology*, **82**, 15-26.

Koenigs, J.W. (1972). Production of extracellular hydrogen peroxide and peroxidase by wood rotting fungi. *Phytopathology*, **62**, 100.

Kondo, T., Ohshita, T. and Kyuma, T. (1992). Comparison of characteristic of soluble lignins from untreated and ammonia treated wheat straw. *Animal Feed Science and Technology*, **39**, 253-263.

Kornberg, H.L. (1966). The role and control of the glyoxylate cycle in *Escherichia coli*. *The Biochemical journal*, **99**, 1-11.

Kramer, C., Kreisel, G., Fahr, K., Kassbohrer, J. and Schlosser, D. (2004). Degradation of 2-fluorophenol by the brown-rot fungus *Gloeophyllum striatum* : evidence for the involvement of extracellular Fenton chemistry. *Applied Microbiology and Biotechnology*, **64**, 387-395.

Kremer, S.M. and Wood, P.M. (1992). Continuous monitoring of cellulase action on microcrystalline celulose. *Applied Microbiology and Biotechnology*, **37**, 750-755.

Kremer, S.M. and Wood, P.M. (1992). Production of Fenton reagent by cellobiose oxidase from cellulolytic cultures of *Phanerochaete chrysosporium*. *European Journal of Biochemistry*, **208**, 807-814.

Kristensen, J. B., Felby, C. and Jorgensen, H. (2009). Yield-determining factors in high-solids enzymatic hydrolysis of lignocellulose. *Biotechnology for Biofuels*, **2**.

Kuhad, R.C., Singh, A. and Eriksson, K.E.L. (1997). Microorganisms and enzymes involved in the degradation of plant fiber cell walls. *Advances in Biochemical Engineering Biotechnology; Biotechnology in the pulp and paper industry*, **57**, 45-125.

Kumar, R., Singh, S. and Singh, O.V. (2008). Bioconversion of lignocellulosic biomass: biochemical and molecular perspectives. *Journal of Industrial Microbiology & Biotechnology*, **35**, 377-391.

Langer, K., Ache, P., Geiger, D., Stinzing, A., Arend, M., Wind, C., Regan, S., Fromm, J. and Hedrich, R. (2002). Poplar potassium transporters capable of controlling K(+) homeostasis and K(+)-dependent xylogenesis. *Plant Journal*, **32**, 997-1009.

Laureano-Perez, L., Teymouri, F., Alizadeh, H. and Dale, B.E. (2005). Understanding factors that limit enzymatic hydrolysis of biomass. *Applied Biochemistry and Biotechnology*, **121**, 1081-1099.

Lechevalier, H. and Lechevalier, M.P. (1988). Chemotaxonomic use of lipids - An overview. *Ratledge, C. and S. G. Wilkinson (Ed.). Microbial Lipids, Vol. 1. Xviii+963p. Academic Press: London, England, Uk; San Diego, California, USA. Illus*, 869-902.

Lee, I. H., Hung, Y.H. and Chou, C.C. (2008). Solid-state fermentation with fungi to enhance the antioxidative activity, total phenolic and anthocyanin contents of black bean. *International Journal of Food Microbiology*, **121**, 150-156.

Lee, J. (1997). Biological conversion of lignocellulosic biomass to ethanol. *Journal of Biotechnology*, **56**, 1-24.

Lee, K.H., Wi, S.G., Singh, A.P. and Kim, Y.S. (2004). Micromorphological characteristics of decayed wood and laccase produced by the brown-rot fungus *Coniophora puteana*. *Journal of Wood Science*, **50**, 281-284.

Lehner, D., Zipper, P., Henriksson, G. and Pettersson, G. (1996). Small-angle X-ray scattering studies on cellobiose dehydrogenase from *Phanerochaete chrysosporium*. *Biochimica Et Biophysica Acta-Protein Structure and Molecular Enzymology*, **1293**, 161-169.

Lenoven-Munoz, E., Bon, D.H. and Daugulis, A.J. (1983) Studies on fractionation of lignocelulosic of Oat straw by Basidiomycetes-Technical Report. Canada:

Lin, Y. and Tanaka, S. (2006). Ethanol fermentation from biomass resources: current state and prospects. *Applied Microbiology and Biotechnology*, **69**, 627-642.

Linde, M., Jakobsson, E.L., Galbe, M. and Zacchi, G. (2008). Steam inretreatment of dilute H_2SO_4-impregnated wheat straw and SSF with low yeast and enzyme loadings for bioethanol production. *Biomass and Bioenergy*, **32**, 326-332.

Linder, M. and Teeri, T.T. (1997). The roles and function of cellulose-binding domains. *Journal of Biotechnology*, **57**, 15-28.

Liu, Y.S., Zeng, Y., Luo, Y., Xu, Q., Himmel, M. E., Smith, S. J. and Ding, S.Y. (2009). Does the cellulose-binding module move on the cellulose surface? *Cellulose*, **16**, 587-597.

Livak, K.J. (1997). *Relative quantification of genes expression: ABI Prism 7700 Sequence Detection System*. 2, Applied Biosystem Bulletin.

Livak, K.J. and Schmittgen, T.D. (2001). Analysis of relative genes expression data using real-time quantitative PCR and the 2(T)(-Delta Delta C) method. *Methods*, **25**, 402-408.

Lu, J. (1994). *The role of high affinity iron chelators isolated from wood decay fungus Gleophyllum trabeum in one electron oxidation reactions and in hydroxyl radical production*. Master Thesis, University of Maine.

Malherbe, S. and Cloete, T.E. (2002). Lignocellulose biodegradation: Fundamentals and applications. *Re/Views in Environmental Science and Bio/Technology*, **1**, 105-114.

Malosso, E., English, L., Hopkins, D.W. and O'Donnell, A.G. (2004). Use of C-13-labelled plant materials and ergosterol, PLFA and NLFA analyses to investigate organic matter decomposition in Antarctic soil. *Soil Biology and Biochemistry*, **36**, 165-175.

Martinez, A.T., Ruiz-Duenas, F.J., Martinez, M.J., del Rio, J.C. and Gutierrez, A. (2009). Enzymatic delignification of plant cell wall: from nature to mill. *Current Opinion in Biotechnology*, **20**, 348-357.

Martinez, A.T., Speranza, M., Ruiz-Duenas, F.J., Ferreira, P., Camarero, S., Guillen, F., Martinez, M.J., Gutierrez, A. and del Rio, J.C. (2005). Biodegradation of lignocellulosics: microbial chemical, and enzymatic aspects of the fungal attack of lignin. *International Microbiology*, **8**, 195-204.

Martinez, D., Challacombe, J., Morgenstern, I., Hibbett, D., Schmoll, M., Kubicek, C. P., Ferreira, P., Ruiz-Duenas, F. J., Martinez, A. T., Kersten, P., Hammel, K. E., Wymelenberg, A. V., Gaskell, J., Lindquist, E., Sabat, G., BonDurant, S. S., Larrondo, L. F., Canessa, P., Vicuna, R., Yadav, J., Doddapaneni, H., Subramanian, V., Pisabarro, A. G., Lavin, J. L., Oguiza, J. A., Master, E., Henrissat, B., Coutinho, P. M., Harris, P., Magnuson, J. K., Baker, S. E., Bruno, K., Kenealy, W., Hoegger, P. J., Kuees, U., Ramaiya, P., Lucash, S., Salamov, A., Shapiro, H., Tu, H., Chee, C. L., Misra, M., Xie, G., Teter, S., Yaver, D., James, T., Mokrejs, M., Pospisek, M., Grigoriev, I. V., Brettin, T., Rokhsar, D., Berka, R. and Cullen, D. (2009). Genome, transcriptome, and secretome analysis of wood decay fungus *Postia placenta* supports unique mechanisms of lignocellulose conversion. *Proceedings of the National Academy of Sciences of the United States of America*, **106**, 1954-1959.

Matcham, S.E., Jordan, B.R. and Wood, D.A. (1984). Methods for assessment of fungal growth on solid substrate. In *Microbiological methods for environmental biotechnology*, pp. 5-18. Edited by J. M. Grainger and J. M. Lynch. London: Academic Press.

Mattila, P., Lampi, A. M., Ronkainen, R., Toivo, J. and Piironen, V. (2002). Sterol and vitamin D-2 contents in some wild and cultivated mushrooms. *Food Chemistry*, **76**, 293-298.

Mentasti, E., Pelizzetti, E. and Baiocchi, C. (1977). Electron transfer reactions of benzene-1,2-diols with hexachloroiradiate (IV) in acidic perchlorate media. *Journal of the Chemical Society-Dalton Transactions*, 132-135.

Messner, K., Koller, K., Wall, M.B., Akhtar, M. and Schott, G.M. (1998). Fungal treatment of wood chip for chemical pulping. In *Environmentally friendly technologies for the pulp and paper industry* pp. 385-419. Edited by R. A. Young and M. Akhtar. New York: John Wiley and Sons.

Micales, J.A. and Highley, T.L. (1989). Physiological characteristics of a non degradative isolate of *Postia (Poria) placenta*. *Mycologia*, **81**, 205-215.

Michniewicz, A., Ullrich, R., Ledakowicz, S. and Hofrichter, M. (2006). The white-rot fungus *Cerrena unicolor* strain 137 produces two laccase isoforms with different physico-chemical and catalytic properties. *Applied Microbiology and Biotechnology*, **69**, 682-688.

Miller, G.L. (1959). Use of dinitrosalicylic acid reagent for determination of reducing sugars. *Analytical Chemistry*, **31**, 426-428.

Mitchell, D.A., Krieger, N., Stuart, D.M. and Pandey, A. (2000). New developments in soil state fermentation: II. Rational approaches to the design, operation and scale up of bioreactors. *Process Biochemistry*, **35**, 1211-1225.

Montgomery, H. J., Monreal, C. M., Young, J. C. and Seifert, K. A. (2000). Determination of soil fungal biomass from soil ergosterol analyses. *Soil Biology and Biochemistry*, **32**, 1207-1217.

Moredo, N., Lorenzo, M., Dominguez, A., Moldes, D., Cameselle, C. and Sanroman, A. (2003). Enhanced ligninolytic enzyme production and degrading capability of *Phanerochaete chrysosporium* and *Trametes versicolor*. *World Journal of Microbiology and Biotechnology*, **19**, 665-669.

Morpeth, F.F (1985). Some properties of cellobiose oxidase from the white rot fungus *Sporotrichum pulverulentum.* Biochemistry Journal. 228. 557-564.

Mottonen, M., Jarvinen, E., Hokkanen, T. J., Kuuluvainen, T. and Ohtonen, R. (1999). Spatial distribution of soil ergosterol in the organic layer of a mature Scots pine *(Pinus sylvestris L.)* forest. *Soil Biology and Biochemistry*, **31**, 503-516.

Moukha, S.M., Dumonceaux, T.J., Record, E. and Archibald, F.S. (1999). Cloning and analysis of *Pycnoporus cinnabarinus* cellobiose dehydrogenase. *Gene*, **234**, 23-33.

Muller, M. M., Kantola, R. and Kitunen, V. (1994). Combining sterol and fatty acid profiles for the characterization of fungi. *Mycological Research*, **98**, 593-603.

Munir, E., Yoon, J.J., Tokimatsu, T., Hattori, T. and Shimada, M. (2001). New role for glyoxylate cycle enzymes in wood-rotting basidiomycetes in relation to biosynthesis of oxalic acid. *Journal of Wood Science*, **47**, 368-373.

Nakagame, S., Furujyo, A. and Sugiura, J. (2006). Purification and characterization of cellobiose dehydrogenase from white-rot basidiomycete *Trametes hirsata*. *Bioscience Biotechnology and Biochemistry*, **70**, 1629-1635.

Newell, S.Y. (1992). Estimating fungal biomass and productivity in decomposing litter. *Carroll, G. C. and D. T. Wicklow (Ed.). Mycology Series, Vol. 9. the Fungal Community: Its Organization and Role in the Ecosystem, Second Edition. Xxv+976p. Marcel Dekker, Inc.: New York, New York, USA; Basel, Switzerland. Illus*, 521-561.

Newell, S.Y. (1994). Total and free ergosterol in mycelia of salt marsh ascomycetes with access to whole leaves of aquaeous extract of leaves. *Applied and Environmental Microbiology*, **60**, 3479-3482.

Nicot, N., Hausman, J. F., Hoffmann, L. and Evers, D. (2005). Housekeeping gene selection for real-time RT-PCR normalization in potato during biotic and abiotic stress. *Journal of Experimental Botany*, **56**, 2907-2914.

Nielsen, K.F. and Madsen, J.O. (2000). Determination of ergosterol on mouldy building materials using isotope dilution and gas chromatography-tandem mass spectrometry. *Journal of Chromatography A*, **898**, 227-234.

Niemenmaa, O., Galkin, S. and Hatakka, A. (2008). Ergosterol contents of some wood-rotting basidiomycete fungi grown in liquid and solid culture conditions. *International Biodeterioration and Biodegradation*, **62**, 125-134.

Niemenmaa, O., Uusi-Rauva, A. and Hatakka, A. (2008). Demethoxylation of O(14)(CH_3) -labelled lignin model compounds by the brown-rot fungi *Gloeophyllum trabeum* and *Poria (Postia) placenta*. *Biodegradation*, **19**, 555-565.

Niemenmaa, O., Uusi-Rauva, A. and Hatakka, A. (2006). Wood stimulates the demethoxylation of (OCH_3)-C14 -labeled lignin model compounds by the white-rot fungi *Phanerochaete chrysosporium* and *Phlebia radiata*. *Archives of Microbiology*, **185**, 307-315.

Oboh, G., Ademosun, A.O. and Lajide, L. (2012). Improvement of the nutritive value and antioxidant properties of citrus peels through *Saccharomyces cerevisiae* solid substrate fermentation for utilization in livestock feed. *Livestock for Rural Development*, **24**, 1-10.

Olofsson, K., Rudolf, A. and Liden, G. (2008). Designing simultaneous saccharification and fermentation for improved xylose conversion by a recombinant strain of *Saccharomyces cerevisiae*. *Journal of Biotechnology*, **134**, 112-120.

Padgett, D.E. and Posey, M.H. (1993). An evaluation of the efficiencies of several ergosterol extraction techniques. *Mycological Research*, **97**, 1476-1480.

Palfreyman, J.W., White, N.A., Buultjens, T.E.J. and Glancy, H. (1995). The impact of current research on the treatment of infestations by the dry rot fungus *Serpula lacrymans*. *International Biodeterioration and Biodegradation*, **35**, 369-395.

Panagiotou, G. and Olsson, L. (2007). Effect of compounds released during pretreatment of wheat straw on microbial growth and enzymatic hydrolysis rates. *Biotechnology and Bioengineering*, **96**, 250-258.

Pandey, A. (2003). Solid-state fermentation. *Biochemical Engineering Journal*, **13**, 81-84.

Pandey, A., Soccol, C.R. and Mitchell, D. (2000). New developments in solid state fermentation: I-bioprocesses and products. *Process Biochemistry*, **35**, 1153-1169.

Pardo, A. G. and Forchiassin, F. (1999). Influence of temperature and pH on cellulase activity and stability in *Nectria catalinensis*. *Revista Argentina de Microbiologia*, **31**, 31-35.

Pasanen, A. L., Yli-Pietila, K., Pasanen, P., Kalliokoski, P. and Tarhanen, J. (1999). Ergosterol content in various fungal species and biocontaminated building materials. *Applied and Environmental Microbiology*, **65**, 138-142.

Paszczynski, A., Crawford, R., Funk, D. and Goodell, B. (1999). De novo synthesis of 4,5-dimethoxycatechol and 2,5-dimethoxyhydroquinone by the brown rot fungus *Gloeophyllum trabeum*. *Applied and Environmental Microbiology*, **65**, 674-679.

Peirson, S.N., Butler, J.N. and Foster, R.G. (2003). Experimental validation of novel and conventional approaches to quantitative real-time PCR data analysis. *Nucleic Acids Research*, **31**.

Perie, F.H. and Gold, M.H. (1991). Manganese regulation of manganese peroxidase expression and lignin degradation by the white rot fungus *Dichomitus squalens*. *Applied and Environmental Microbiology*, **57**, 2240-2245.

Pfaffl, M.W. (2001). A new mathematical model for relative quantification in real-time RT-PCR. *Nucleic Acids Research*, **29**.

Pfaffl, M.W. (2010). Relative quantification. In *Real Time PCR*. Edited by T. Dorak: International University Line.

Pitt, J.I. (1984). The significance of potential toxigenic fungi in foods. *Food Technology Australia*, **36**, 218-219.

Pitt, J.I. and Hocking, A.D. (1997). Fungi and food spoilage-2nd edition (London: Blackie Academic and Profesional).

Qian, Y.H., Goodell, B. and Felix, C.C. (2002). The effect of low molecular weight chelators on iron chelation and free radical generation as studied by ESR measurement. *Chemosphere*, **48**, 21-28.

Rabinovich, M.L., Melnick, M.S. and Bolobova, A.V. (2002). Microbial cellulases (Review). *Prikladnaya Biokhimiya i Mikrobiologiya*, **38**, 355-373.

Raices, M., Paifer, E., Cremata, J., Montesino, R., Stahlberg, J., Divne, C., Szabo, I. J., Henriksson, G., Johansson, G. and Pettersson, G. (1995). Cloning and characterization of CDNA encoding a cellobiose dehydrogenase from the white rot fungus *Phanerochaete chrysosporium*. *FEBS Letters*, **369**, 233-238.

Ralph, J.P. and Catcheside, D.E.A. (2002). Biodegradation by white-rot fungi. *The Mycota: A comprehensive treatise on fungi as experimental systems for basic and applied research. Industrial applications*, 303-326.

Ray, M. J., Leak, D.J., Spanu, P. D. and Murphy, R.J. (2010). Brown rot fungal early stage decay mechanism as a biological pretreatment for softwood biomass in biofuel production. *Biomass and Bioenergy*, **34**, 1257-1262.

Reid, I.D. (1985). Biological delignification of aspen wood by solid state fermentation with the white rot fungus *Merulius tremellosus*. *Applied and Environmental Microbiology*, **50**, 133-139.

Reid, I.D. and Seifert, K.A. (1980). Lignin degradation by *Phanerochaete chrysosporium* in hyperbaric oxygen. *Canadian Journal of Microbiology*, **26**, 1168-1171.

Reinikainen, T., Ruohonen, L., Nevanen, T., Laaksonen, L., Kraulis, P., Jones, T.A., Knowles, J.K.C. and Teeri, T.T. (1992). Investigation of the fungtion of mutated cellulose

binding domains of *Trichoderma reesei* cellobiohydrolase-1. *Proteins-Structure Function and Genetics*, **14**, 475-482.

Reinikainen, T., Teleman, O. and Teeri, T.T. (1995). Effect of pH and high ionic strength on the adsorption and activity of native and mutated cellobiohydrolase-1 from *Trichoderma reesei*. *Proteins-Structure Function and Genetics*, **22**, 392-403.

Renganathan, V. (1989). Possible involment of toluene 2,3 dioxidase in deflourination of 3-flouro-substituted benzenes by toluene degrading *Pseudomonas sp* strain T-12. *Applied and Environmental Microbiology*, **55**, 330-334.

Renganathan, V. and Johnston, J.B. (1989). Catechols of novel substrates produced using the toluene ring oxidation pathway of *Pseudomonas sp* strain T-12. *Applied Microbiology and Biotechnology*, **31**, 419-424.

Richardson, M.D. and Logendra, S. (1997). Ergosterol as an indicator of endophyte biomass in grass seeds. *Journal of Agricultural and Food Chemistry*, **45**, 3903-3907.

Riemer, J., Hoepken, H. H., Czerwinska, H., Robinson, S. R. and Dringen, R. (2004). Colorimetric ferrozine-based assay for the quantitation of iron in cultured cells. *Analytical Biochemistry*, **331**, 370-375.

Ritschkoff, A.C., Buchert, J. and Viikari, L. (1994). Purification and characterization of a thermophilic xylanase from the brown rot fungus *Gloeophyllum trabeum*. *Journal of Biotechnology*, **32**, 67-74.

Ritschkoff, A.C., Ratto, M., Buchert, J. and Viikari, L. (1995). Effect of carbon source on the production of oxalic acid and hydrogen peroxide by brown rot fungus *Poria placenta*. *Journal of Biotechnology*, **40**, 179-186.

Rodriguez, J., Parra, C., Contreras, D., Freer, J. and Baeza, J. (2001). Dihydroxybenzenes: driven Fenton reactions. *Water Science and Technology*, **44**, 251-256.

Ruzicka, S., Edgerton, D., Norman, M. and Hill, T. (2000). The utility of ergosterol as a bioindicator of fungi in temperate soils. *Soil Biology and Biochemistry*, **32**, 989-1005.

Ruzicka, S., Norman, M.D.P. and Harris, J.A. (1995). Rapid ultrasonication method to determine ergosterol concentration in soil. *Soil Biology and Biochemistry*, **27**, 1215-1217.

Sadana, J.C. and Patil, R.V. (1985). The purification and properties of cellobiose dehydrogenase from *Sclerotium rolfsii* and it's role in cellulolysis. *Journal of General Microbiology*, **131**, 1917-1923.

Sambrook, J.F. and Russell, D.W. (2001). Molecular cloning: A laboratory manual, Volume I,II,III: Cold Spring Harbor Laboratory Press).

Samejima, M., Ohkubo, T., Igarashi, K., Isogai, A., Kuga, S., Sugiyama, J. and Eriksson, K. E. L. (1997). The behaviour of *Phanerochaete chrysosporium* cellobiose dehydrogenase on adsorption to crystalline and amorphous celluloses. *Biotechnology and Applied Biochemistry*, **25**, 135-141.

Samson, R. A., Hocking, A. D., Pitt, J. I. and King, A. D. (1992). Modern methods in food mycology (Amsterdam: Elsevier Bioscience).

Sanchez, C. (2009). Lignocellulosic residues: Biodegradation and bioconversion by fungi. *Biotechnology Advances*, **27**, 185-194.

Saraf, A., Larsson, L., Burge, H. and Milton, D. (1997). Quantification of ergosterol and 3-hydroxy fatty acids in settled house dust by gas chromatography mass spectrometry: Comparison with fungal culture and determination of endotoxin by a *Limulus amebocyte* lysate assay. *Applied and Environmental Microbiology*, **63**, 2554-2559.

Schena, M., Shalon, D., Davis, R.W. and Brown, P.O. (1995). Quantitative monitoring of gene expression pattern with a complementary DNA microarray. *Science*, **270**, 467-470.

Schmidhalter, D.R. and Canevascini, G. (1993). Isolation and characterization of cellobiose dehydrogenase from the brown rot fungus *Coniophora puteana* (Schum ex Fr) Karst. *Archives of Biochemistry and Biophysics*, **300**, 559-563.

Schmidt, O. (2000). Molecular methods for the characterization and identification of the dry rot fungus *Serpula lacrymans*. *Holzforschung*, **54**, 221-228.

Schmidt, O. and Morethkebernik, U. (1991). A simple method for producing basidiomes of *Serpula lacrymans* in culture. *Mycological Research*, **95**, 375-376.

Schmittgen, T.D. and Zakrajsek, B.A. (2000). Effect of experimental treatment on housekeeping gene expression: validation by real-time, quantitative RT-PCR. *Journal of Biochemical and Biophysical Methods*, **46**, 69-81.

Schnurer, J. (1993). Comparison of methods for estimating the biomass of 3 food borne fungi with different growth pattern. *Applied and Environmental Microbiology*, **59**, 552-555.

Schou, C., Christensen, M.H. and Schulein, M. (1998). Characterization of a cellobiose dehydrogenase from *Humicola insolens*. *Biochemical Journal*, **330**, 565-571.

Schultz, T.P., Templeton, M.C., Biermann, C.J. and McGinnis, G.D. (1984). Steam explosion of mixed hardwood chips, rice hulls, corn stalks and sugar cane baggase. *Journal of Agricultural and Food Chemistry*, **32**, 1166-1172.

Sharrock, K. R. (1988). Cellulase assay methods - A review. *Journal of Biochemical and Biophysical Methods*, **17**, 81-105.

Shimada, M., Akamtsu, Y., Tokimatsu, T., Mii, K. and Hattori, T. (1997). Possible

biochemical roles of oxalic acid as a low molecular weight compound involved in brown-rot and white-rot wood decays. *Journal of Biotechnology*, **53**, 103-113.

Shimada, M., Ma, D. B., Akamatsu, Y. and Hattori, T. (1994). A proposed role of oxalic acid in wood decay system of wood rotting basidiomycetes. *FEMS Microbiology Reviews*, **13**, 285-296.

Shimokawa, T., Nakamura, M., Hayashi, N. and Ishihara, M. (2004). Production of 2,5-dimethoxyhydroquinone by the brown-rot fungus *Serpula lacrymans* to drive extracellular Fenton reaction. *Holzforschung*, **58**, 305-310.

Shoseyov, O., Shani, Z. and Levy, I. (2006). Carbohydrate binding modules: Biochemical properties and novel applications. *Microbiology and Molecular Biology Reviews*, **70**, 283-+.

Singh, D. and Chen, S. (2008). The white-rot fungus *Phanerochaete chrysosporium*: conditions for the production of lignin-degrading enzymes. *Applied Microbiology and Biotechnology*, **81**, 399-417.

Singleton, V.L. and Rossi, J.A.J. (1965). Colorimetry of total phenolics with phosphomolybdic-phosphotungtic acid reagents. *American Journal Enology Viticulture*, 144-158.

Snajdr, J., Cajthaml, T., Valaskova, V., Merhautova, V., Petrankova, M., Spetz, P., Leppanen, K. and Baldrian, P. (2011). Transformation of *Quercus petraea* litter: successive changes in litter chemistry are reflected in differential enzyme activity and changes in the microbial community composition. *FEMS Microbiology Ecology*, **75**, 291-303.

Soong, R., Ruschoff, J. and Tabiti, K. (2000). *Detection of colorectal micrometastatsis by quantitative RT-PCR of cytokeratin 20 mRNA*. **In**: Roche Diagnostic Internal Publication.

Srisodsuk, M., Reinikainen, T., Penttila, M. and Teeri, T.T. (1993). Role of interdomain linker petide of *Trichoderma reesei* cellobiohydrolase-1 an it's interaction with crystalline cellulose. *Journal of Biological Chemistry*, **268**, 20756-20761.

Stahl, P.D. and Klug, M.J. (1996). Characterization and differentiation of filamentous fungi based on fatty acid composition. *Applied and Environmental Microbiology*, **62**, 4136-4146.

Stahlberg, J., Johansson, G. and Pettersson, G. (1991). A new model for enzymatic hydrolysis of cellulose based on the 2 domain structure of cellobiohydrolase-1. *Bio-Technology*, **9**, 286-290.

Stolf-Moreira, R., Lemos, E. G. M., Carareto-Alves, L., Marcondes, J., Pereira, S.S., Rolla, A.A.P., Pereira, R.M., Neumaier, N., Binneck, E., Abdelnoor, R.V., de Oliveira, M.C.N., Marcelino, F.C., Farias, J.R.B. and Nepomuceno, A.L. (2011). Transcriptional Profiles of Roots of Different Soybean Genotypes Subjected to Drought Stress. *Plant*

Molecular Biology Reporter, **29**, 19-34.

Stookey, L.L. (1970). Ferrozine - A new spectrophotometric reagent for iron. *Analytical Chemistry*, **42**, 779-&.

Sun, R., Lawther, J.M. and Banks, W.B. (1997). A tentative chemical structure of wheat straw lignin. *Industrial Crops and Products*, **6**, 1-8.

Sun, R.C. and Tomkinson, J. (2002). Comparative study of organic solvent-soluble and water-soluble lipophilic extractives from wheat straw 2: spectroscopic and thermal analysis. *Journal of Wood Science*, **48**, 222-226.

Sun, X.F., Sun, R.C., Fowler, P. and Baird, M.S. (2005). Extraction and characterization of original lignin and hemicelluloses from wheat straw. *Journal of Agricultural and Food Chemistry*, **53**, 860-870.

Sun, Y. and Cheng, J.J. (2005). Dilute acid pretreatment of rye straw and bermudagrass for ethanol production. *Bioresource Technology*, **96**, 1599-1606.

Suzuki, M. R., Hunt, C.G., Houtman, C.J., Dalebroux, Z.D. and Hammel, K.E. (2006). Fungal hydroquinones contribute to brown rot of wood. *Environmental Microbiology*, **8**, 2214-2223.

Szabo, I.J., Johansson, G. and Pettersson, G. (1996). Optimized cellulase production by *Phanerochaete chrysosporium*: Control of catabolite repression by fed-batch cultivation. *Journal of Biotechnology*, **48**, 221-230.

Tabka, M.G., Herpoel-Gimbert, I., Monod, F., Asther, M. and Sigoillot, J.C. (2006). Enzymatic saccharification of wheat straw for bioethanol production by a combined cellulase xylanase and feruloyl esterase treatment. *Enzyme and Microbial Technology*, **39**, 897-902.

Taccari, M., Stringini, M., Comitini, F and Ciani M (2009). Effect of Phanerochaete chrysosporium inoculation during maturation of composted agricultural waste mixed with olive mill waste water. Waste Management. 29. 1615-1621.

Talebnia, F., Karakashev, D. and Angelidaki, I. (2010). Production of bioethanol from wheat straw: An overview on pretreatment, hydrolysis and fermentation. *Bioresource Technology*, **101**, 4744-4753.

Tanaka, H., Hirano, T. and Enoki, A. (1993). Extracellular sustance from the white rot basidiomycete *Irpex lacteus* for production and reduction of H_2O_2 during wood degradation. *Mokuzai Gakkaishi*, **39**, 493-499.

Tanaka, H., Itakura, S. and Enoki, A. (1999). Hydroxyl radical generation by an extracellular low-molecular-weight substance and phenol oxidase activity during wood

degradation by the white-rot basidiomycete *Trametes versicolor*. *Journal of Biotechnology*, **75**, 57-70.

Tellenbach, C., Gruenig, C.R. and Sieber, T.N. (2010). Suitability of quantitative real-time PCR to estimate the biomass of fungal root endophytes. *Applied and Environmental Microbiology*, **76**, 5764-5772.

Tellmann, G. (2006). *The E-Method: A high acurate technique for gene expression analysis*. **In**: 3, i-ii. Natural Methods.

Terashima, K., Matsumoto, T., Hasebe, K. and Fukumasa-Nakai, Y. (2002). Genetic diversity and strain-typing in cultivated strains of *Lentinula edodes* (the shii-take mushroom) in Japan by AFLP analysis. *Mycological Research*, **106**, 34-39.

Thanapimmetha, A., Vuttibunchon, K., Titapiwatanakun, B. and Srinophakun, P. (2012). Optimization of solid state fermentation for reducing sugar production from agricultural residues of sweet sorghum by *Trichoderma harzianum*. *Chiang Mai Journal of Science*, **39**, 270-280.

Thellin, O., Zorzi, W., Lakaye, B., De Borman, B., Coumans, B., Hennen, G., Grisar, T., Igout, A. and Heinen, E. (1999). Housekeeping genes as internal standards: use and limits. *Journal of Biotechnology*, **75**, 291-295.

Thomas, C., Meyer, D., Wolff, M., Himber, C., Alioua, M. and Steinmetz, A. (2003). Molecular characterization and spatial expression of the sunflower ABP1 gene. *Plant Molecular Biology*, **52**, 1025-1036.

Tomme, P., Boraston, A., McLean, B., Kormos, J., Creagh, A. L., Sturch, K., Gilkes, N.R., Haynes, C.A., Warren, R.A.J. and Kilburn, D.G. (1998). Characterization and affinity applications of cellulose-binding domains. *Journal of Chromatography B*, **715**, 283-296.

Tomme, P., Warren, R.A.J., Miller, R. C., Jr., Kilburn, D.G. and Gilkes, N.R. (1995). Cellulose-binding domains: Classification and properties. *ACS Symposium Series; Enzymatic degradation of insoluble carbohydrates*, **618**, 142-163.

Tothill, I.E., Harris, D. and Magan, N. (1992). The relationship between fungal growth and ergosterol content of wheat grain. *Mycological Research*, **96**, 965-970.

Uihlein, A. and Schebek, L. (2009). Environmental impacts of a lignocellulose feedstock biorefinery system: An assessment. *Biomass and Bioenergy*, **33**, 793-802.

Vaithanomsat, P., Cuichulcherm, S. and Apiwatanipat, W. (2009). Bioethanol production from enzymatically saccharified sunflower stalk using steam explosion as pretreatment. *Word Academy of Science, Engineering and Technology* **49**, 140-143.

Vallim, M.A., Janse, B.J.H., Gaskell, J., Pizzirani-Kleiner, A.A. and Cullen, D. (1998).

Phanerochaete chrysosporium cellobiohydrolase and cellobiose dehydrogenase transcripts in wood. *Applied and Environmental Microbiology*, **64**, 1924-1928.

Valmaseda, M., Almendros, G. and Martinez, A.T. (1991). Chemical transformation of wheat straw constituents after soild state fermentation with selected lignocellulose degrading fungi. *Biomass and Bioenergy*, **1**, 261-266.

Vanden Wymelenberg, A., Gaskell, J., Mozuch, M., Kersten, P., Sabat, G., Martinez, D. and Cullen, D. (2009). Transcriptome and secretome analyses of *Phanerochaete chrysosporium* reveal complex patterns of gene expression. *Applied and Environmental Microbiology*, **75**, 4058-4068.

Vandenbossche, H., Marichal, P., Willemsens, G., Bellens, D., Gorrens, J., Roels, I., Coene, M.C., Lejeune, L. and Janssen, P.A.J. (1990). Saperconazole-Aslective inhibitor of the cytochrome P-450 dependent ergosterol sythesis in *Candida albicans*, *Arpergillus fumigatus* and *Thichophyton mentagrophytes*. *Mycoses*, **33**, 335-352.

Vandesompele, J., De Preter, K., Pattyn, F., Poppe, B., Van Roy, N., De Paepe, A. and Speleman, F. (2002). Accurate normalization of real-time quantitative RT-PCR data by geometric averaging of multiple internal control genes. *Genome biology*, **3**,

Varela, E. and Tien, M. (2003). Effect of pH and oxalate on hydroquinone-derived hydroxyl radical formation during brown rot wood degradation. *Applied and Environmental Microbiology*, **69**, 6025-6031.

Vares, T., Kalsi, M. and Hatakka, A. (1995). Lignin peroxidases, manganese peroxidases, and other ligninolytic enzymes produced by *Phlebia radiata* during solid state fermentation of wheat straw. *Applied and Environmental Microbiology*, **61**, 3515-3520.

Viollier, E., Inglett, P.W., Hunter, K., Roychoudhury, A.N. and Van Cappellen, P. (2000). The ferrozine method revisited: Fe(II)/Fe(III) determination in natural waters. *Applied Geochemistry*, **15**, 785-790.

Wallander, H. and Nylund, J.E. (1991). Effect of excess nitrogen on carbohydarte concentration and mycorrhizal development of *Pinus sylvestris L* seedling. *New Phytologist*, **119**, 405-411.

Wang, W., Huang, F., Lu, X. M. and Gao, P.J. (2006). Lignin degradation by a novel peptide, Gt factor, from brown rot fungus *Gloeophylium trabeum*. *Biotechnology Journal*, **1**, 447-453.

Ward, O.P. and Singh, A. (2002). Bioethanol technology: Developments and perspectives. *Advances in Applied Microbiology, Vol 51*, **51**, 53-80.

Wariishi, H., Valli, K., Renganathan, V. and Gold, M.H. (1989). Thiol mediated oxidation of nonphenolic lignin model compounds by manganese peroxidase of *Phanerochaete chrysosporium*. *Journal of Biological Chemistry*, **264**, 14185-14191.

Watkinson, S.C. and Eastwood, D.C. (2012). *Serpula lacrymans*, Wood and Buildings. In *Advances in Applied Microbiology, Vol 78*, pp. 121-149. Edited by A. I. Laskin, S. Sariaslani and G. M. Gadd.

Wei, D., Houtman, C.J., Kapich, A. N., Hunt, C.G., Cullen, D. and Hammel, K.E. (2010). Laccase and its role in production of extracellular reactive oxygen species during wood decay by the brown rot basidiomycete *Postia placenta*. *Applied and Environmental Microbiology*, **76**, 2091-2097.

Williams, D.H., Stone, M.J., Hauck, P.R. and Rahman, S.K. (1989). Why are secondary metabolites (natural products) biosynthesised? *Journal of Natural Product*, **52**, 1189-1208.

Winton, L.M., Manter, D.K., Stone, J.K. and Hansen, E.A. (2003). Comparison of biochemical, molecular, and visual methods to quantify *Phaeocryptopus gaeumannii* in Douglas-Fir foliage. *Phytopathology*, **93**, 121-126.

Wojtczak, G., Breuil, C., Yamada, J. and Saddler, J.N. (1987). A comparison of the thermostability of cellulases from various thermophilic fungi. *Applied Microbiology and Biotechnology*, **27**, 82-87.

Wong, D.W.S. (2009). Structure and action mechanism of ligninolytic enzymes. *Applied Biochemistry and Biotechnology*, **157**, 174-209.

Wyman, C.E., Dale, B.E., Elander, R.T., Holtzapple, M., Ladisch, M.R. and Lee, Y.Y. (2005). Coordinated development of leading biomass pretreatment technologies. *Bioresource Technology*, **96**, 1959-1966.

Xia, Z.X. and Mathews, F.S. (1990). Molecular structure of flavocytochrome B2 AT 2.4 resolution. *Journal of Molecular Biology*, **212**, 837-863.

Xiao, B., Sun, X. F. and Sun, R.C. (2001). Chemical, structural, and thermal characterizations of alkali-soluble lignins and hemicelluloses, and cellulose from maize stems, rye straw, and rice straw. *Polymer Degradation and Stability*, **74**, 307-319.

Xiao, Z. Z., Gao, P.J., Qu, Y.B. and Wang, T.H. (2001). Cellulose-binding domain of endoglucanase III from *Trichoderma reesei* disrupting the structure of cellulose. *Biotechnology Letters*, **23**, 711-715.

Xu, G. and Goodell, B. (2001). Mechanisms of wood degradation by brown-rot fungi: chelator-mediated cellulose degradation and binding of iron by cellulose. *Journal of Biotechnology*, **87**, 43-57.

Xu, J.H. and Jordan, R.B. (1988). Kinetics and mechanism of the oxidation of 2,3 dihydroxybenzoic acid by iron (III). *Inorganic Chemistry*, **27**, 4563-4566.

Yadav, J.S. (1987). Influence of nutritional supplementation on solid substrate fermentation

of wheat straw with an alkaliphilic white rot fungus *(Coprinus sp)*. *Applied Microbiology and Biotechnology*, **26**, 474-478.

Yang, Q., Qin, X. and Zhang, L. (2011). Properties of cellulose films prepared from NaOH/urea/zincate aqueous solution at low temperature. *Cellulose*, **18**, 681-688.

Yelle, D.J., Ralph, J., Lu, F. and Hammel, K.E. (2008). Evidence for cleavage of lignin by a brown rot basidiomycete. *Environmental Microbiology*, **10**, 1844-1849.

Yoon, J.J., Cha, C.J., Kim, Y.S., Son, D.W. and Kim, Y.K. (2007). The brown-rot basidiomycete *Fomitopsis palustris* has the endo-glucanases capable of degrading microcrystalline cellulose. *Journal of Microbiology and Biotechnology*, **17**, 800-805.

Yoon, J.J., Hattori, T. and Shimada, M. (2002). A metabolic role of the glyoxylate and tricarboxylic acid cycles for development of the copper-tolerant brown-rot fungus *Fomitopsis palustris*. *FEMS Microbiology Letters*, **217**, 9-14.

Yoon, J.J. and Kim, Y.K. (2005). Degradation of crystalline cellulose by the brown-rot basidiomycete Fomitopsis palustris. *Journal of Microbiology*, **43**, 487-492.

Yoshida, M., Igarashi, K., Wada, M., Kaneko, S., Suzuki, N., Matsumura, H., Nakamura, N., Ohno, H. and Samejima, M. (2005). Characterization of carbohydrate-binding cytochrome b(562) from the white-rot fungus *Phanerochaete chrysosporium*. *Applied and Environmental Microbiology*, **71**, 4548-4555.

Yu, M., Zeng, G., Chen, Y., Yu, H., Huang, D. and Tang, L. (2009). Influence of *Phanerochaete chrysosporium* on microbial communities and lignocellulose degradation during solid-state fermentation of rice straw. *Process Biochemistry*, **44**, 17-22.

Zabihi, S., Alinia, R., Esmaeilzadeh, F. and Kalajahi, J.F. (2010). Pretreatment of wheat straw using steam, steam/acetic acid and steam/ethanol and its enzymatic hydrolysis for sugar production. *Biosystems Engineering*, **105**, 288-297.

Zadrazil, F. and Brunnert, H. (1982). Solid state fermentation of lignocellulose containing plant residues with *Sporotrichum pulverulentum*-Nov and *Dichomitus squalens* (Karst)-Reid. *European Journal of Applied Microbiology and Biotechnology*, **16**, 45-51.

Zafar, S. I., Abdullah, N., Iqbal, M. and Sheeraz, Q. (1996). Influence of nutrient amendment on the biodegradation of wheat straw during solid state fermentation with *Trametes versicolor*. *International Biodeterioration and Biodegradation*, **38**, 83-87.

Zafar, S.I., Sheeraz, Q., and Abdullah, N. (1989). Degradation of lignocellulosic component on wheat straw *Coriolus versicolor* solid state fermentation under nitrogen starved condition. Biological Waste. 27. 67-70.

Zayed, G. and Meyer, O. (1996). The single-batch bioconversion of wheat straw to ethanol employing the fungus *Trichoderma viride* and the yeast *Pachysolen tannophylus*. *Applied*

Microbiology and Biotechnology, **45**, 551-555.

Zelles, L. (1997). Phospholipid fatty acid profiles in selected members of soil microbial communities. *Chemosphere*, **35**, 275-294.

Zhang, Y.H.P., Himmel, M.E. and Mielenz, J. R. (2006). Outlook for cellulase improvement: Screening and selection strategies. *Biotechnology Advances*, **24**, 452-481.

Zhou, Y.-H., Zhang, Y.J., Luo, Z.B., Fan, Y.H., Tang, G.R., Liu, L.J. and Pei, Y. (2012). Selection of optimal reference genes for expression analysis in the entomopathogenic fungus *Beauveria bassiana* during development, under changing nutrient conditions, and after exposure to abiotic stresses. *Applied Microbiology and Biotechnology*, **93**, 679-685.

Appendix 2. Instruction for data analysis from LCMS.

Open raw data file

In top window (UV trace), position cursor at the correct time peak (e.g. 18.30 minutes below)

If you need to be more exact you can use the left and right arrows on the menu bar to adjust it

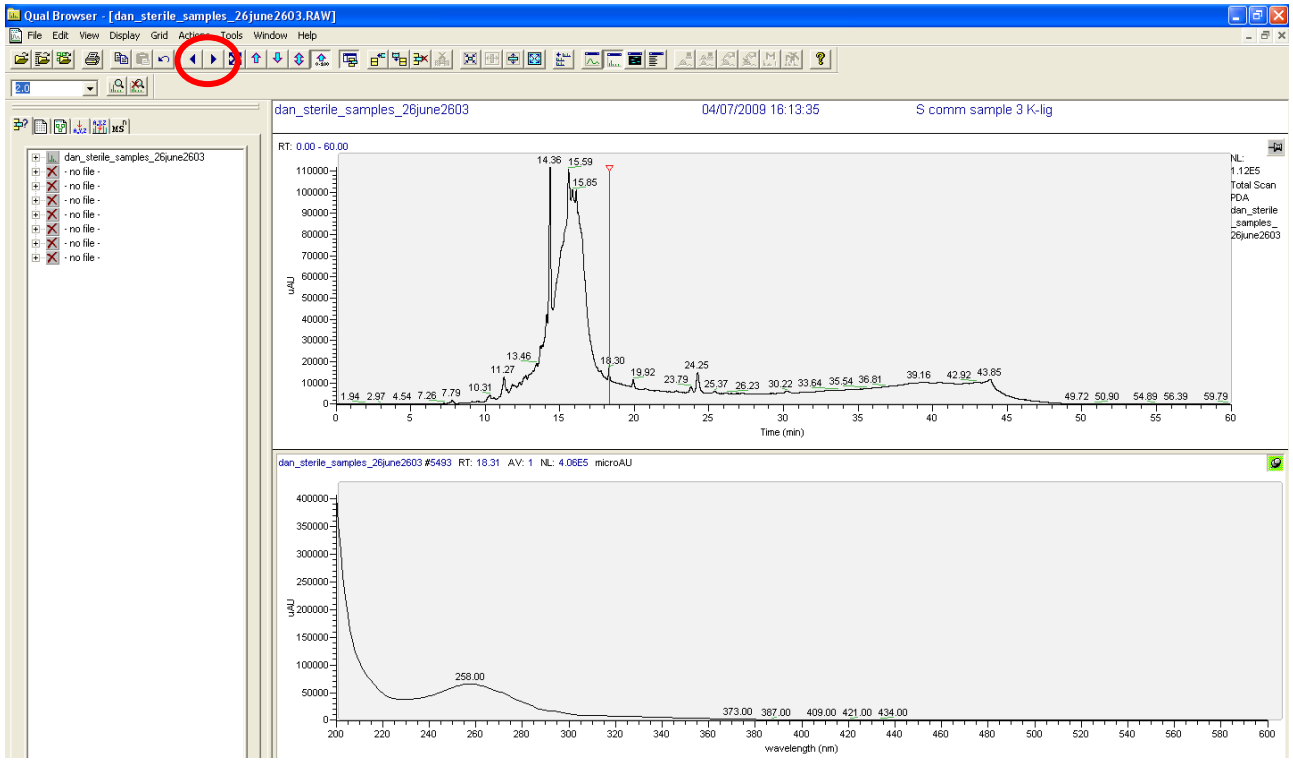

Checking that the pin (icon on the right hand side) of the bottom trace is highlighted

Right click on the bottom trace and select “Ranges”

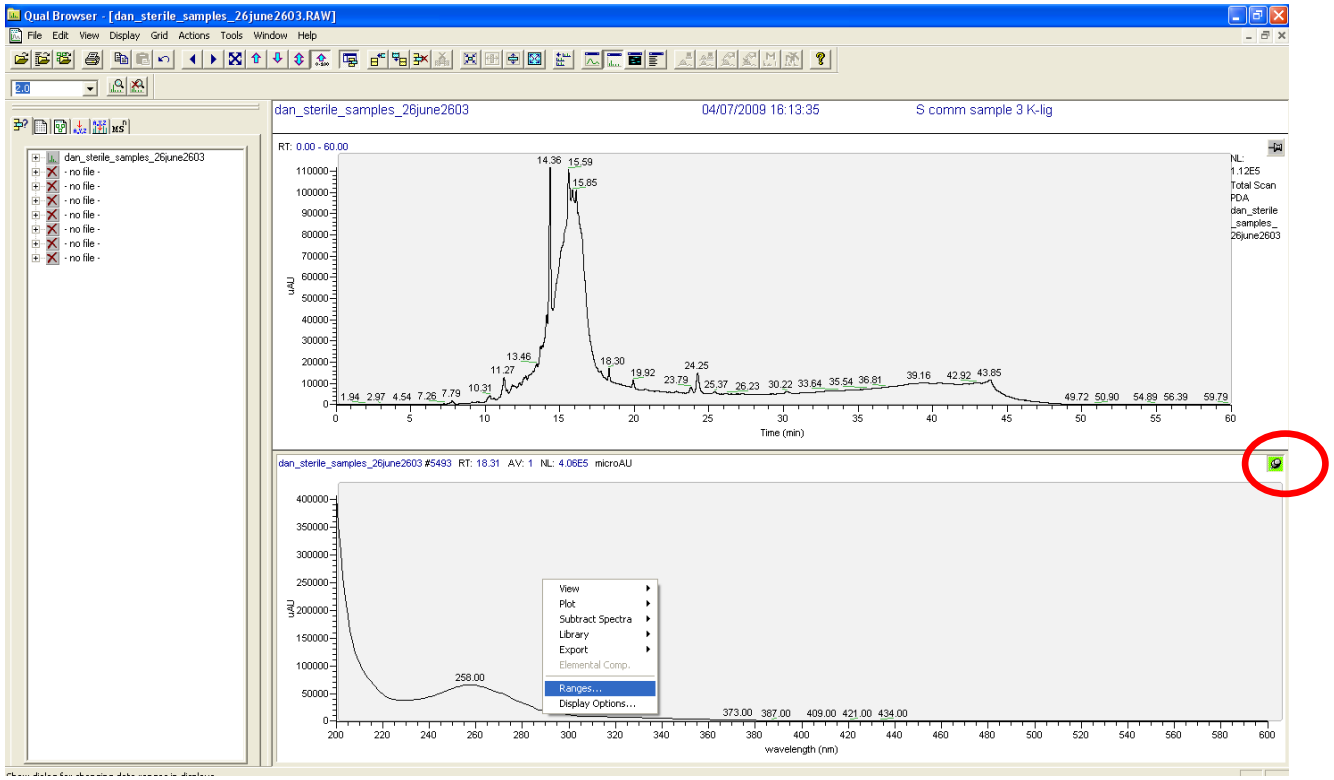

In the window that opens, select Filter and “MS”, then the filter (choose the positive ion – this will normally give you better MS spectra) – then click ok

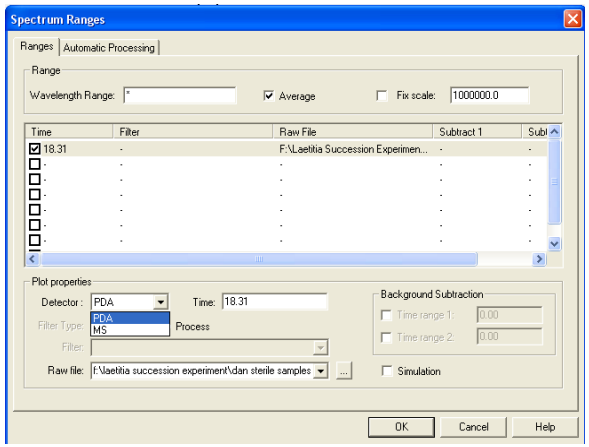

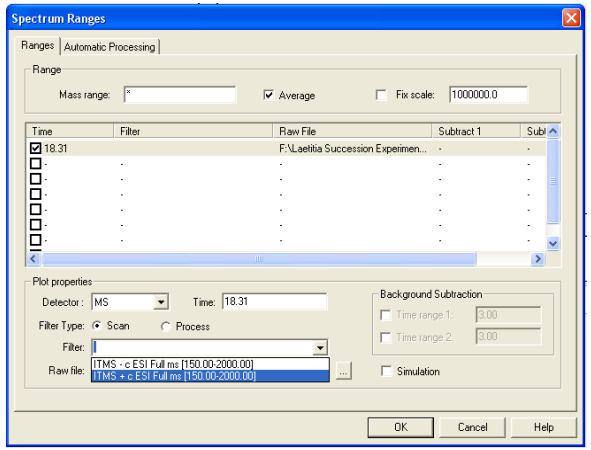

This should then show the MS in the bottom window

Sometimes the spectra is not very good and you need to use the arrows again to move the cursor slightly. If you manually use the mouse to move the cursor, the bottom pane will resort back to the UV absorbance and you will need to repeat the right click – ranges etc.

As you move the cursor, the retention time will change on the screen.

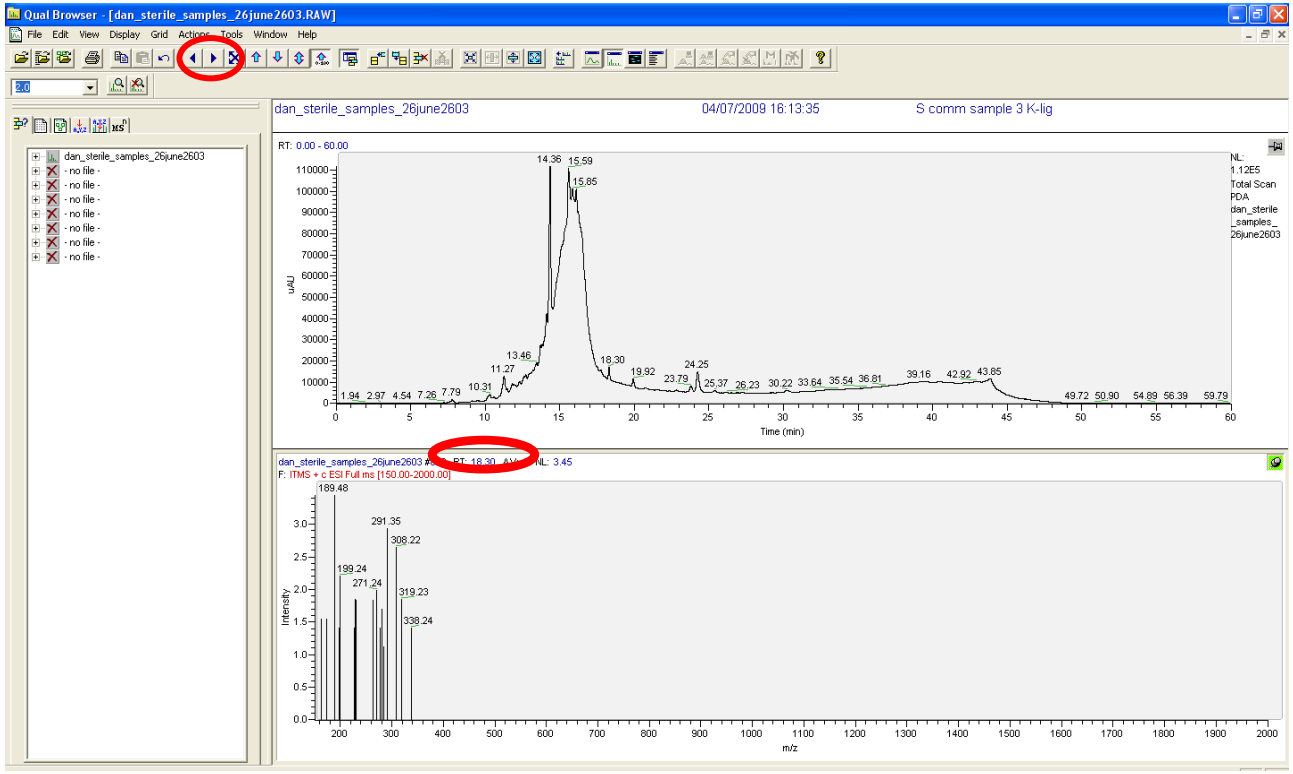

If you need to expand the spectra to get the peak labels you can do this by positioning your cursor below the x-axis of the MS, press the left mouse button and keep it pressed down while dragging across the region you want to expand

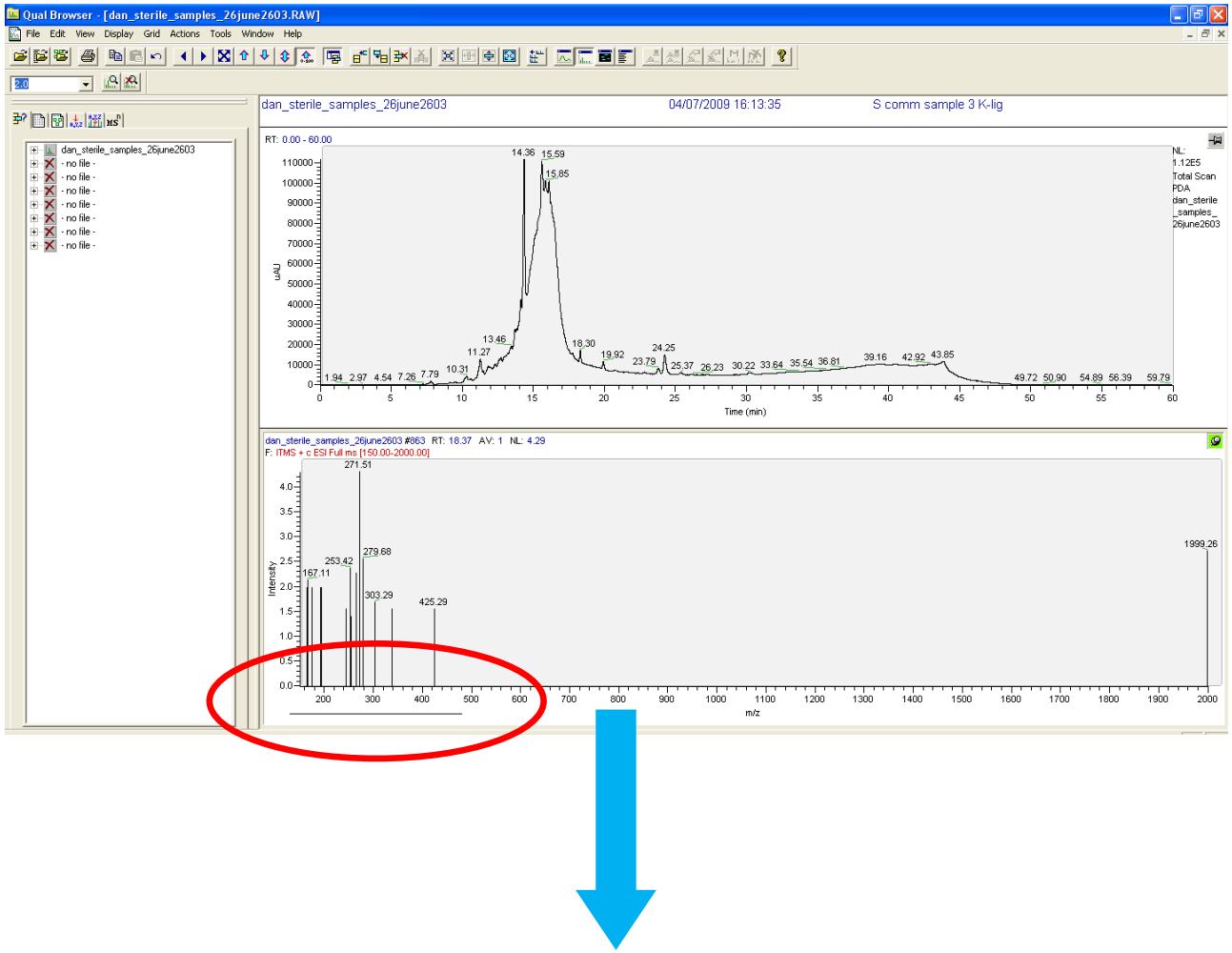
Qual Browser - [dan_sterile_samples_26june2603.RAW]
File Edit View Display Grid Actions Tools Window Help
dan_sterile_samples_26june2603
04/07/2009 16:13:35
S comm sample 3 K-lig
RT: 0.00 - 60.00
uAU
Time (min)
NL: 1.12E5 Total Scan PDA dan_sterile_samples_26june2603
dan_sterile_samples_26june2603 #863 RT: 18.37 AV: 1 NL: 4.29
F: ITMS + c ESI Full ms [150.00-2000.00]
Intensity
m/z
271.51
279.68
253.42
167.11
303.29
425.29
1999.26

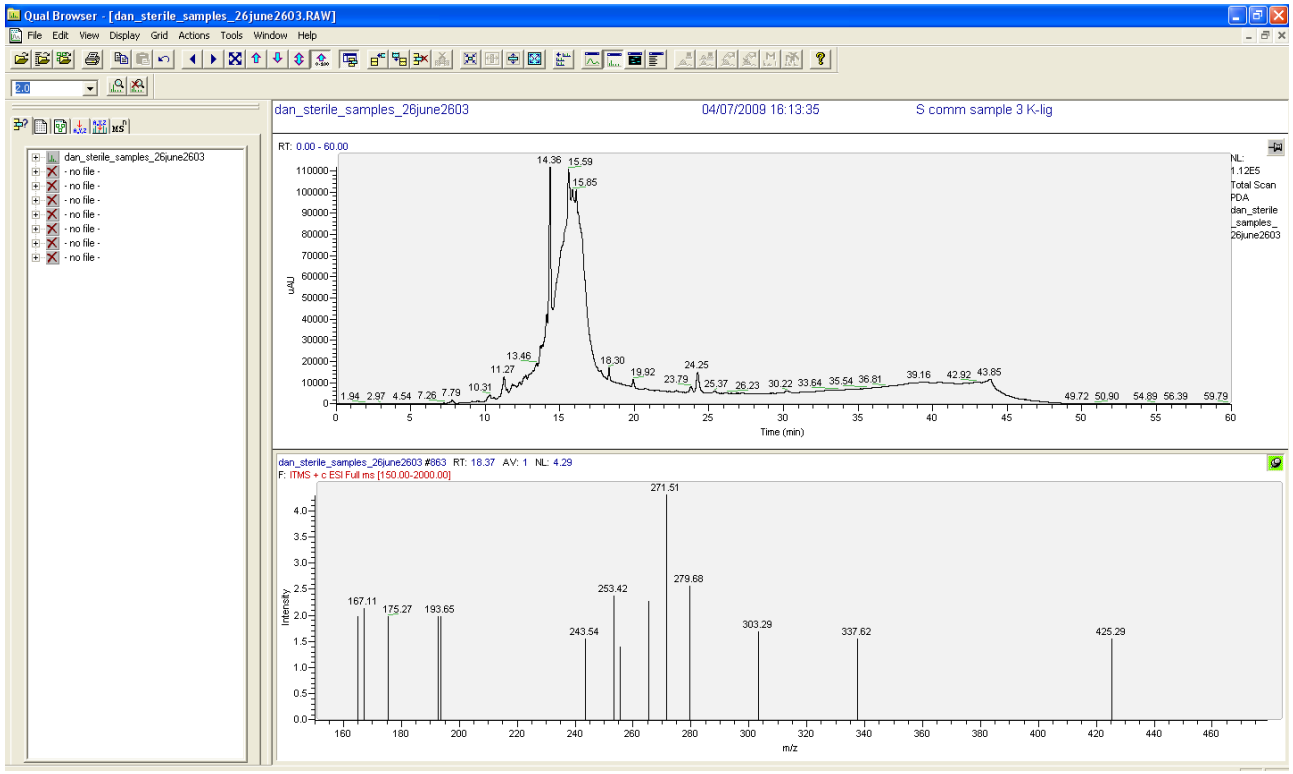
Qual Browser - [dan_sterile_samples_26june2603.RAW]
File Edit View Display Grid Actions Tools Window Help
dan_sterile_samples_26june2603
04/07/2009 16:13:35
S comm sample 3 K-lig
RT: 0.00 - 60.00
uAU
Time (min)
NL: 1.12E5 Total Scan PDA dan_sterile_samples_26june2603
dan_sterile_samples_26june2603 #863 RT: 18.37 AV: 1 NL: 4.29
F: ITMS + c ESI Full ms [150.00-2000.00]
Intensity
m/z

To return to the full spectra, use the four headed arrow on the menu bar

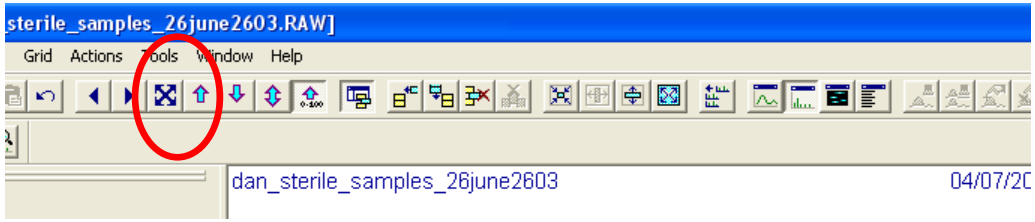

Appendix 3. A list of value added chemicals predicted based on the low molecular weight from the solvent extraction samples of each fungal after 21 days of incubation in wheat straw SSF (LC-MS analysis).
PC: *Phanerochaete chrysosporium*; SL:*Serpula lacrymans*; SC: *Schizophyllum commune*; PP:*Postia placenta*; MW: molecular weight.
a: M : b: $(M+H)^+$; c: (M+Na)+; d: (M+K)+
+ the valuable compounds released by fungi which are not present on the un-inoculated sample (control)

No	Treatment		PC3D21				SL3D21				SC1D21				PP3D21				control			
		MW	*Phanerochaetae chrysosporium*				*Serpulla lacrymans*				*Schizophyllum commune*				*Postia placenta*				(un-inoculated straw)			
			a	b	c	d	a	b	c	d	a	b	c	d	a	b	c	d	a	b	c	d
1	Guaiacol	124												+				+				
2	Creosol	138											+				+					
3	Kojic Acid	142															+					
4	Cinnamic Acid	148															+					
5	Coumaryl alcohol	150	+	+	+	+	+	+	+	+	+		+		+	+	+	+	+		+	+
6	Vanillin	152		+	+	+	+	+	+	+					+	+	+	+	+	+	+	
7	Vanillyl alcohol	154		+	+	+	+	+	+	+						+	+	+		+	+	+
8	Syringol	154		+	+	+	+	+	+	+						+	+	+		+	+	+
9	Protocatehuic acid	154		+	+	+	+	+	+	+						+	+	+		+	+	+
10	3-Hydroxy kojik acid	158		+	+	+	+	+	+	+									+	+	+	+
11	Eugenol	164	+	+	+	+	+	+	+						+	+	+	+	+	+	+	+
12	Iso-eugenol	164	+	+	+	+	+	+	+	+					+	+	+	+	+	+	+	+
13	Coumaric acid	164	+	+	+	+	+	+	+						+	+	+	+	+	+	+	+
14	Hydroxycinnamic acid	164	+	+	+	+	+	+	+						+	+	+	+	+	+	+	+
15	Acetoguaiacone (acetovanillone)	166	+	+	+	+	+	+	+	+	+	+				+	+	+	+		+	+

16	Propylguaiacol	166	+	+	+	+	+	+	+	+	+	+				+	+	+	+		+	+
17	3-guaiacyl propanol	166	+	+	+	+	+	+	+	+	+	+				+	+	+	+		+	+
18	Guaiacyl acetate	166	+	+	+	+	+	+	+	+	+	+				+	+	+	+		+	+
19	Apocynol	168		+	+	+	+	+	+	+	+				+	+	+	+		+	+	+
20	Homovanillyl alcohol	168		+	+	+	+	+	+	+	+									+	+	+
21	Vanillyl alcohol methyl eter	168		+	+	+	+	+	+	+	+									+	+	+
22	Vanillic acid	168		+	+	+	+	+	+	+	+									+	+	+
23	Syringyl creosol	168		+	+	+	+	+	+	+	+									+	+	+
24	Gallic acid	170	+	+	+	+	+	+	+	+		+		+	+	+	+	+		+	+	+
25	3-Hydroxy kojik acid methyl ether	172										+	+			+	+	+	+	+	+	+
26	Coniferyl aldehide	178	+	+	+	+	+	+	+	+			+		+	+	+	+	+	+	+	+
27	Propioguaiacone	180		+	+	+	+	+	+	+	+		+		+	+	+	+	+	+	+	+
28	Conyferyl alcohol	180		+	+	+	+	+	+	+	+		+		+	+	+	+	+	+	+	+
29	Dihydroxyc-cinnamic acid (caffeic acid)	180		+	+	+	+	+	+	+	+		+		+	+	+	+	+	+	+	+
30	Methyl vanillate	182		+	+	+	+	+	+	+					+	+	+	+		+	+	
31	Homovanillic acid	182		+	+	+	+	+	+	+					+	+	+	+		+	+	
32	Syringaldehide	182		+	+	+	+	+	+	+					+	+	+	+		+	+	
33	1-Guaiacylethyl methyl ether	182		+	+	+	+	+	+	+					+	+	+	+		+	+	
34	a-Guaiacyl propanol	182		+	+	+	+	+	+	+					+	+	+	+		+	+	
35	5-Methoxy protocatehuic acid	184					+	+	+	+					+	+	+	+		+	+	+
36	Syringil alcohol	184					+	+	+	+					+	+	+	+		+	+	+

37	4-Methoxy-3-hydroxyphenyl glycol	184					+	+	+	+					+	+	+	+		+	+	+
38	2- Hydroxy-2H-Pyran-4.6-dicarboxylic acid	186					+	+	+	+			+		+	+	+	+	+	+	+	+
39	3-hydroxy-5methoxy-2-pyran-4-one	186					+	+	+	+			+		+	+	+	+	+	+	+	+
40	Syringyl eugenol	194	+	+	+	+	+	+	+	+					+	+	+	+	+	+	+	+
41	Ferulic acid	194	+	+	+	+	+	+	+	+					+	+	+	+	+	+	+	+
42	Acetosyringone	196	+	+	+	+	+	+	+	+	+				+	+	+	+	+	+	+	+
43	alpha-Carboxyvanillin	196	+	+	+	+	+	+	+	+	+				+	+	+	+	+	+	+	+
44	Hydroxypropiovanillone	196	+	+	+	+	+	+	+	+	+				+	+	+	+	+	+	+	+
45	Syringic acid	198	+	+	+	+	+	+	+	+					+	+	+	+	+	+		+
46	4-Hydroxy-3-methoxy mandelic acid	198	+	+	+	+	+	+	+	+					+	+	+	+	+	+		+
47	X1	202	+	+	+	+	+		+	+					+	+	+	+	+	+		+
48	Sinapaldehyde	208	+	+	+	+	+		+	+		+			+	+	+	+	+	+	+	+
49	Sinapyl alcohol	210	+	+	+	+	+	+	+	+					+	+	+	+	+	+	+	+
50	Methylsyringate	212	+	+	+	+	+	+	+	+					+	+	+	+		+	+	+
51	α-Hydroxy ferulic acid	212	+	+	+	+	+	+	+	+										+	+	+
52	Carboxivanillic acid	212	+	+	+	+	+	+	+	+										+	+	+
53	X2	214	+	+	+	+	+	+	+	+	+	+	+						+	+	+	+
54	X3	222		+	+	+		+	+	+										+	+	+
55	Sinapic acid	224	+	+	+	+	+	+	+	+	+									+	+	+
56	Alpha-hydroxypropiosyr	225	+	+	+	+	+	+	+	+									+	+	+	+

	ingone																					
57	Hydroxytrimesic acid	226	+	+	+	+	+	+	+	+									+	+	+	+
58	X4	236	+	+	+	+	+	+	+	+		+								+	+	+
59	X5	244	+	+	+	+	+	+	+	+									+	+	+	+
60	X6	244					+	+	+	+												
61	X7	256	+	+	+	+	+	+	+	+				+					+	+	+	+
62	X8	258	+	+	+	+	+	+	+	+	+								+	+	+	+
63	X9	272		+	+		+	+	+	+					+	+	+	+	+	+	+	
64	Diguaiacyl stilbene	272		+	+		+	+	+	+					+	+	+	+	+	+	+	
65	Guaiacyl-o-guaiacylstilbene	272		+	+		+	+	+	+					+	+	+	+	+	+	+	
66	Enol ether	272		+	+		+	+	+						+	+	+	+	+	+	+	
67	Bicreosol	274	+	+	+	+	+	+	+	+					+	+	+	+				
68	α-Oxodihydrodiguaiacylstilbene	274	+	+	+	+	+	+	+	+					+	+	+	+	+	+		+
69	X10	274	+	+	+	+	+	+	+	+					+	+	+	+				
70	X11	274	+	+	+	+	+	+	+	+					+	+	+	+				
71	Guaiacylveratrylstilbene	286		+	+		+	+	+	+					+	+	+	+		+	+	
72	Bicreosol methane	288		+			+	+	+	+					+	+	+	+	+	+		+
73	α-Oxodihydrodiguaiacylstilbene	288		+			+	+	+	+					+	+	+	+	+	+		+
74	X12	290									+											
75	X13	290									+											
76	Bivanillin	302	+	+	+	+	+	+	+	+					+	+	+	+		+		+
77	Bivanillyl alcohol	306					+	+	+	+					+	+	+	+	+		+	+

78	α-α-dihydrodiguaiacyl stilbene	306					+	+	+	+					+	+	+	+	+		+	+
79	SV stilbene	312	+	+		+																
80	Syringylveratrylstilbene	316	+			+	+	+	+	+					+	+	+	+	+			+
81	DeDi stilbenzene	326					+	+	+	+					+	+	+	+				
82	Pinoresinol	358					+	+	+	+					+	+	+	+			+	

Appendix 4. The amount of fatty acid 18:2n6c (µ g^{-1} of straw) produced by all the fungal species for 35 days
PC : *Phanerochaete chrysosporium*; SL: *Serpula lacrymans*; PP: *Postia placenta*; SC: *Schyzophyllum commune*; D: days

	CONTROL	PCD7	PCD14	PCD21	PCD28	PCD35	SLD7	SLD14	SLD21	SLD28	SLD35	PPD7	PPD14	PPD21	PPD28	PPD35	SCD7	SCD14	SCD21	SCD28	SCD35
16:0	194.91	354.54	258.66	271.16	163.72	139.18	247.35	184.72	87.22	136.19	120.20	253.46	318.11	311.92	312.46	413.75	280.84	252.92	114.99	96.88	36.93
16:1n7	0.00	7.65	3.97	0.00	0.00	3.54	5.15	0.00	0.00	0.00	0.00	6.87	12.88	6.30	0.00	24.48	0.00	0.00	0.00	0.00	0.00
17:0	32.34	44.29	31.10	49.39	29.31	20.49	39.49	28.91	16.33	31.14	25.48	42.69	94.00	69.33	70.74	44.74	35.35	38.37	17.48	19.17	0.00
16:3	0.00	0.00	0.00	0.00	0.00	0.00	0.00	0.00	0.00	0.00	0.00	0.00	0.00	0.00	0.00	23.47	0.00	0.00	0.00	0.00	0.00
18:0	31.74	33.71	33.46	29.84	10.24	8.76	31.34	28.28	15.87	20.11	12.99	41.44	41.31	37.86	39.08	30.27	30.79	39.26	6.21	0.00	0.00
18:1n9t	18.56	0.00	7.14	27.94	0.00	0.00	0.00	104.49	36.96	17.30	27.57	70.61	52.19	73.37	53.19	122.95	0.00	0.00	0.00	0.00	0.00
18:1n9c	76.75	146.53	106.90	76.22	64.59	75.00	126.82	0.00	8.49	31.28	6.40	25.56	72.98	53.66	77.37	161.18	196.61	172.49	95.22	56.90	25.14
18:2n6t	0.00	0.00	0.00	0.00	0.00	0.00	0.00	0.00	0.00	0.00	0.00	0.00	0.00	0.00	0.00	0.00	0.00	0.00	0.00	0.00	0.00
18:2n6c	103.64	541.37	317.94	289.85	181.45	167.46	239.15	283.97	186.92	345.78	286.76	188.49	271.37	354.84	506.15	493.57	288.93	297.47	200.98	122.05	66.35
18:3n6	8.83	0.00	0.00	0.00	0.00	0.00	0.00	0.00	0.00	0.00	0.00	0.00	0.00	0.00	0.00	0.00	0.00	0.00	0.00	0.00	0.00
18:3n3	36.61	42.89	26.07	34.81	0.00	11.77	41.39	23.35	3.66	10.17	12.02	67.43	50.12	41.03	50.25	28.83	77.09	53.77	13.25	7.94	0.00
20:0	5.55	34.14	37.78	38.65	23.16	10.49	11.36	14.53	2.95	11.22	7.89	33.54	52.95	35.64	43.63	22.67	14.49	18.60	7.52	6.57	0.00
20:1n9	0.00	0.00	0.00	0.00	20.70	0.00	0.00	5.08	0.00	4.13	5.31	0.00	3.36	3.73	6.56	3.19	0.00	0.00	0.00	0.00	0.00
20:2n6+21	0.00	58.82	41.01	90.46	37.49	21.26	0.00	19.10	0.00	0.00	0.00	2.27	11.36	16.94	3.73	0.00	0.00	0.00	0.00	0.00	0.00
20:3n6	0.00	9.21	6.49	9.83	0.00	0.00	10.58	16.57	0.00	12.60	13.10	0.00	0.00	0.00	0.00	0.00	0.00	0.00	0.00	0.00	0.00
20:4n6	5.48	0.00	5.98	0.00	0.00	0.00	0.00	35.10	6.98	9.71	0.00	38.30	20.06	19.44	10.80	8.77	0.00	0.00	0.00	0.00	0.00
20:3n3	37.56	75.02	75.32	97.09	42.79	18.79	42.03	56.69	9.08	13.14	30.09	35.81	31.32	47.22	34.68	31.69	59.05	66.30	26.90	34.44	0.00
22:0	37.66	89.96	101.01	140.01	68.98	67.66	62.07	0.00	22.29	41.92	29.14	18.33	81.73	28.64	42.36	30.86	35.65	47.74	24.51	26.61	0.00
22:1n9	0.00	21.13	11.08	2.93	0.00	4.81	0.00	0.00	0.00	0.00	0.00	36.29	124.64	149.88	170.95	33.81	0.00	0.00	0.00	0.00	0.00
20:5n3	0.00	0.00	0.00	0.00	0.00	0.00	0.00	5.07	0.00	0.00	0.00	0.00	0.00	8.12	0.00	61.83	0.00	0.00	0.00	0.00	0.00
22:2n6	0.00	0.00	21.99	33.38	6.56	20.17	15.86	6.53	4.42	0.00	6.56	28.08	43.83	96.99	68.56	0.00	9.66	0.00	0.00	0.00	0.00
23:0	24.94	84.27	60.10	81.35	70.60	32.93	44.31	0.00	0.00	5.39	23.06	88.43	126.93	150.41	121.90	65.38	22.32	130.12	43.84	78.65	34.84
24:0	0.00	0.00	0.00	49.17	0.00	0.00	0.00	0.00	0.00	0.00	0.00	104.70	17.19	37.11	124.61	67.95	30.85	36.15	0.00	15.58	0.00
24:1n9	33.88	75.99	56.07	122.58	187.14	92.74	61.88	45.81	18.59	22.36	46.17	25.90	49.02	130.72	41.76	141.98	0.00	0.00	0.00	22.47	0.00
22:6n3	7.82	0.00	4.95	7.00	0.00	15.95	0.00	0.00	0.00	0.00	0.00	74.76	72.66	56.60	135.50	0.00	0.00	0.00	0.00	0.00	0.00